

Journal of Polymer Science

Part A-1: Polymer Chemistry

Contents

S. S. DIXIT, A. B. DESHPANDE, and S. L. KAPUR: Polymerization of Acrylonitrile with $VCl_4-Al(C_2H_5)_3$ Catalyst System in Presence of Acetonitrile	1167
S. KATAYAMA, H. HORIKAWA, and N. MASUDA: Anionic Copolymerizations of Acrylonitrile with β -Propiolactone	1173
K. HASHIMOTO and H. SUMITOMO: Anionic Copolymerization of <i>p</i> -Anisaldehyde with Dimethylketene	1189
J. J. KEARNEY, H. G. CLARK, V. STANNETT, and D. CAMPBELL: Methyl Methacrylate in Sulfur Dioxide: Solvated Radical Polymerization	1197
L. TAIMR and J. G. SMITH: Polyesters Containing Bicyclo[2.2.2]octane and Bicyclo[3.2.2]nonane Rings	1203
M. A. OSMAN and C. S. MARVEL: Polyesters from 12-Hydroxymethyltetrahydroabietic Acid and 12-Hydroxymethyltetrahydroabietanol	1213
H. H. G. JELLINEK and P. HRDLOVIC: Chain Scission of Butyl Rubber by Nitrogen Dioxide. II. Photo-Oxidation as Function of Nitrogen Dioxide, Oxygen Pressure, and Temperature	1219
P. HRDLOVIC, J. PAVLINEC, and H. H. G. JELLINEK: Degradation of Polymers and Morphology: Photo-Oxidative Degradation of Isotactic Polystyrene in Presence of Sulfur Dioxide as Function of Polymer Crystallinity	1235
H. YUKI and Y. OKAMOTO: Nuclear Magnetic Resonance Studies of Isoprenyllithium Derived from 1,1-Diphenyl- <i>n</i> -butyllithium-3,4- <i>d</i> ₂ and Isoprene	1247
D. A. MCCOMBS, C. S. MENON, and J. HIGGINS: Photocondensation Polymers: Polybenzopinacols. II. Photolytic Coupling of Aromatic Diketones	1261
E. H. CATSIFF, M. N. GILLIS, and R. H. GOBRAN: Poly(ethylene Sulfide). II. Thermal Degradation and Stabilization	1271
M. N. GILLIS, E. H. CATSIFF, and R. H. GOBRAN: Poly(ethylene Sulfide). III. Oxidative Degradation	1293
M. NOVÁK: Dissociation-Association Sorption on Ion Exchangers. I. Experimental Study of Dependence of Equilibrium Function of Acidity in Ion Exchanger on Activity of Hydrogen Ions in Aqueous Phase	1315
A. R. LYONS and E. CATTERALL: Organometal-Initiated Polymerization of Vinyl Ketones. III. Polymerization of Methyl Isopropenyl Ketone Initiated by the Triethylaluminum-Methyl Isopropenyl Ketone Complex	1335
J. M. AUGL and J. V. DUFFY: Soluble Imide-Quinoxaline Copolymers	1343

(continued inside)

ห้องสมุด คณะวิทยาศาสตร์

Board of Editors: H. Mark • C. G. Overberger • T. G. Fox

Advisory Editors:

R. M. Fuoss • J. J. Hermans • H. W. Melville • G. Smets

Editor: C. G. Overberger

Associate Editor: E. M. Pearce

Advisory Board:

T. Alfrey, Jr.	N. D. Field	R. W. Lenz	C. C. Price
W. J. Bailey	F. C. Foster	Eloisa Mano	B. Rånby
John Boor, Jr.	H. N. Friedlander	C. S. Marvel	J. H. Saunders
F. A. Bovey	K. C. Frisch	F. R. Mayo	C. Schuerch
J. W. Breitenbach	N. G. Gaylord	R. B. Mesrobian	W. H. Sharkey
W. J. Burlant	W. E. Gibbs	Donald Metz	V. T. Stannett
G. B. Butler	A. R. Gilbert	H. Morawetz	J. K. Stille
S. Bywater	M. Goodman	M. Morton	M. Szwarc
W. L. Carrick	J. E. Guillet	J. E. Mulvaney	A. V. Tobolsky
H. W. Coover, Jr.	George Hulse	S. Murahashi	E. J. Vandenberg
W. H. Daly	Otto Kauder	G. Natta	Herbert Vogel
F. Danusso	J. P. Kennedy	K. F. O'Driscoll	L. A. Wall
F. R. Eirich	W. Kern	S. Okamura	O. Wichterle
E. M. Fettes	J. Lal	P. Pino	F. H. Winslow

Contents (continued)

H. KOTHANDARAMAN and M. SANTAPPA: Polymerization of Acrylamide and Acrylic Acid Photoinitiated by Diazidotetramminecobalt(III) Azide.....	1351
V. I. JELISEJEVA and E. M. MOROZOVA: Polymerization of Aminoalkyl Methacrylates in a Thin Layer in the Presence of Atmospheric Oxygen.....	1365
M. ALBECK, M. KÖNIGSBUCH, and J. RELIS: Electroinitiated Polymerization of Vinyllic Monomers in Polar Systems. I. Contribution of the Electrolysis of Methanol to Free-Radical Polymerization.....	1375
M. M. O'MARA: Pyrolysis-Gas Chromatographic Analysis of Poly(vinyl Chloride). II. <i>In Situ</i> Absorption of HCl during Pyrolysis and Combustion of PVC.....	1387

(continued on inside back cover)

The Journal of Polymer Science is published in four sections as follows: Part A-1, Polymer Chemistry, monthly; Part A-2, Polymer Physics, monthly; Part B, Polymer Letters, monthly; Part C, Polymer Symposia, irregular.

Published monthly by Interscience Publishers, a Division of John Wiley & Sons, Inc., covering one volume annually. Publication Office at 20th and Northampton Sts., Easton, Pa. 18042. Executive, Editorial, and Circulation Offices at 605 Third Avenue, New York, N. Y. 10016. Second-class postage paid at Easton, Pa. Subscription price, \$325.00 per volume (including Parts A-2, B, and C). Foreign postage \$15.00 per volume (including Parts A-2, B, and C).

Copyright © 1971 by John Wiley & Sons, Inc. All rights reserved. No part of this publication may be reproduced by any means, nor transmitted, nor translated into a machine language without the written permission of the publisher.

Polymerization of Acrylonitrile with $VCl_4-Al(C_2H_5)_3$ Catalyst System in Presence of Acetonitrile

SUNIT S. DIXIT, A. B. DESHPANDE, and S. L. KAPUR,
National Chemical Laboratory, Poona 8, India

Synopsis

The polymerization of acrylonitrile with the homogeneous catalyst system of VCl_4-AlEt_3 in acetonitrile at 40°C has been investigated. The rate of polymerization is found to be first-order with respect to monomer and inversely proportional to the catalyst concentration. The overall activation energy for this catalyst system is 10.97 kcal/mole. The inverse proportionality of rate of polymerization with the catalyst concentration is attributed to the permanent complex formation between the catalyst complex and acrylonitrile, and a reaction scheme is proposed.

Introduction

Ziegler-Natta catalyst systems¹ as such or in the modified form have been used for the polymerization of certain polar monomers. The mechanism of polymerization and the structure of polymer, however, differ from that of coordinate anionic polymerization. Vanadium-containing catalyst systems²⁻⁵ are more effective for the polymerization of polar monomers than titanium-containing catalyst systems at room temperature. The mechanism of polymerization in vanadium-containing systems is coordinate anionic, like the titanium-based catalyst systems of $TiCl_4-AlEt_3$.

Further, polar solvents as additives are known⁴ to be effective modifiers of Ziegler-Natta catalyst systems, and in their presence the stereospecificity, molecular weight, and rate of polymerization improve considerably. But for some work on the polymerization of acrylonitrile⁶ with VCl_3-LiBH_4 or Ti, V, or Cr alcoholates or acetylacetonates with $AlEt_3$ in a dimethylformamide medium,⁷ there no data have been reported on the polymerization of polar monomers with Ziegler-Natta catalysts in a polar medium. The $TiCl_4-AlEt_3$ catalyst system⁸ in presence of a mixture of *n*-heptane and acetonitrile polymerizes acrylonitrile, but the exact mechanism is not reported. It is also known that transition metal halides and organo-metallic components of Ziegler-Natta catalyst systems react independently with polar solvents such as dimethyl-formamide or tetrahydrofuran and produce complexes which are not useful for polymerization reactions.

Our work⁴ has shown that VCl_4 with $Al(C_2H_5)_3$ forms a complex in the presence of an excess of acetonitrile and polymerizes acrylonitrile by a free radical mechanism. It has been suggested that free radicals are produced

from acetonitrile, and the rate of polymerization was observed to be inversely proportional to the catalyst concentration. A complete kinetic study of the system has been carried out, and a scheme is proposed for the reaction of polymerization. These results are presented and discussed in this communication.

Experimental

The reagents and solvents were purified and stored as mentioned in an earlier communication from this laboratory for the polymerization of methyl methacrylate with VCl_4-AlEt_3 in acetonitrile.⁹

Polymerization was conducted in a tightly stoppered 50-ml Erlenmeyer flask and the reactants were added in the order: solvent, VCl_4 , $AlEt_3$, and monomer. The procedure for the polymerization followed was the same manner as that reported earlier.^{2-4,9}

Acrylonitrile was purified¹⁰ by successive washings with dilute H_2SO_4 , dilute Na_2CO_3 solution, and water. After drying thoroughly with $CaCl_2$, it was distilled at atmospheric pressure and stored over $CaCl_2$, since otherwise the monomer absorbs water which cannot be removed by distillation. Immediately before use the monomer was filtered and fractionated under nitrogen. Purified and distilled DMF was used for viscosity measurements. Intrinsic viscosities of polyacrylonitrile were determined at 30°C, and the molecular weights were calculated by the relationship:¹¹

$$[\eta] = 29.6 \times 10^{-5} \bar{M}_v^{0.74}$$

Results and Discussion

As reported earlier^{4,9} VCl_4 reacts with an excess of acetonitrile to form a dark red complex. On addition of $AlEt_3$ to this complex, the color changes from dark red to dark green and then to dark brown, indicating some reactions *in situ*. However, the entire solution remained homogeneous. On addition of acrylonitrile to this complex, the brown color faded and changed to dark green and immediately the polymer precipitated out at a Al/V ratio of 1.

The dependence of active sites in the catalyst on Al/V ratio was examined by increasing $AlEt_3$ concentration and keeping the VCl_4 concentration constant. The rate of polymerization was maximum at Al/V ratio of 1; with further increase in Al/V, the rate of polymerization and molecular weights decreased (Fig. 1). At the same ratio of Al/V of 1, the per cent yield of polymer increased with time up to 120 min (Fig. 2) and later remained almost constant. However, molecular weights were unchanged with increase in reaction time, even up to 480 min. Under these steady-state reaction conditions, the initial rate of polymerization for 2 hr was measured with increasing concentrations of catalyst and monomer.

It was observed that the rate of polymerization increased linearly up to a monomer concentration of 5.44 mole/l. (Fig. 3) and thereafter decreased with further increase in the concentration of the monomer. Molecular

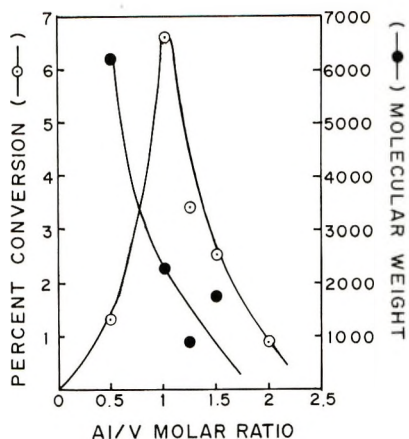


Fig. 1. Effect of Al/V ratio in $VCl_4-Al(C_2H_5)_3$ catalyst system on (○) per cent conversion and (●) molecular weight. Acrylonitrile, 4.5 ml; reaction time, 120 min; aging time, 20 min; temperature, 40°C; $[CVl_4]$, 0.05 mole/l., total volume, 25.0 ml.

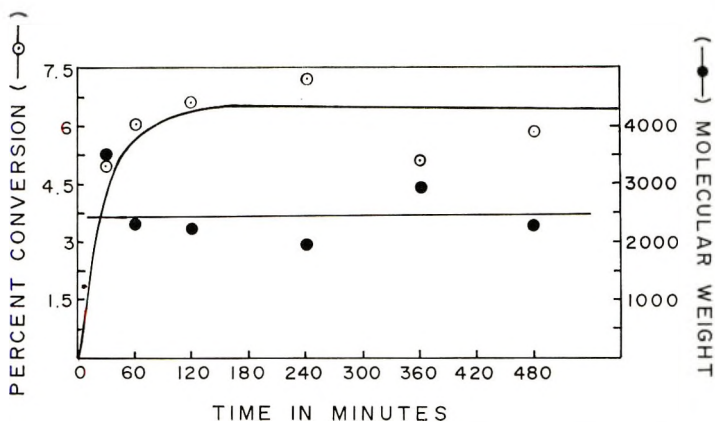


Fig. 2. Effect of reaction time in $VCl_4-Al(C_2H_5)_3$ catalyst system on (○) per cent conversion and (●) molecular weight. [Acrylonitrile], 4.5 ml; $[VCl_4]$ 0.05 mole/l.; $[Al(C_2H_5)_3]$, 0.05 mole/l.; Al/V = 1.0; aging time, 20 min; temperature, 40°C.

weights decreased with increasing monomer concentration, indicating chain transfer reaction with the monomer. The rate of polymerization also decreased with varying catalyst concentration (Fig. 4), and it was inversely proportional to catalyst concentration. Molecular weights too decreased with increase in the catalyst concentration, showing the chain termination of polymerization reaction by the catalyst itself.

The decrease in the rate of polymerization by the catalyst itself is rather unusual and is considered a remote possibility. Stivala et al.,¹² in their general scheme for the mechanism of coordinate anionic polymerization with Ziegler-Natta catalyst, suggested that catalyst could play a dual role of initiation and termination, but this has not been experimentally observed.

In the present studies, free radicals are responsible for the polymerization of acrylonitrile. Earlier we proposed^{4,9} a reaction scheme whereby free radicals are produced not from a free-radical initiator as such, but from the complex of VCl_4 and $AlEt_3$ with acetonitrile. The same reaction system

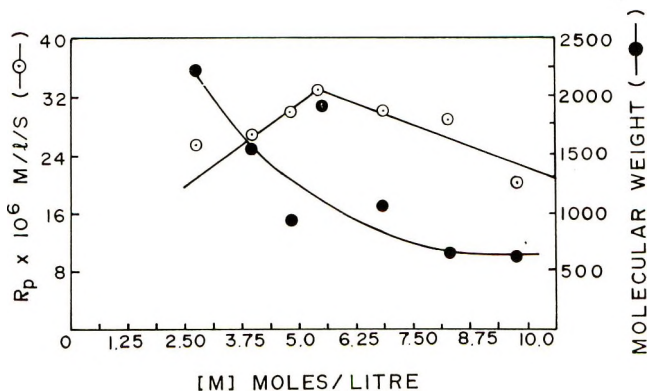


Fig. 3. Effect of monomer concentration in VCl_4 - $Al(C_2H_5)_3$ catalyst system on (○) R_p and (●) molecular weight. $[VCl_4]$, 0.05 mole/l.; $[Al(C_2H_5)_3]$, 0.05 mole/l.; $Al/V = 1.0$; reaction time, 120 min; aging time, 20 min; temperature, 40°C.

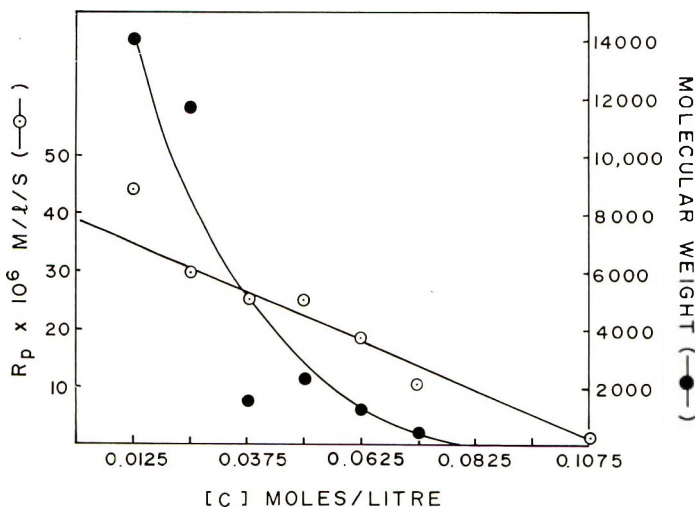
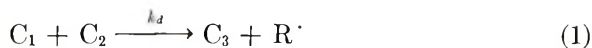


Fig. 4. Effect of catalyst concentration in VCl_4 - $Al(C_2H_5)_3$ catalyst system on (○) R_p and (●) molecular weight. [Acrylonitrile], 4.5 ml (2.72 mole/l.); $Al/V = 1.0$; reaction time, 120 min; aging time, 20 min; temperature, 40°C.

was also found effective for the polymerization of methyl methacrylate, and the mechanism of polymerization was apparently observed as coordinate anionic. The NMR structure of the poly(methyl methacrylate) obtained in presence and absence of hydroquinone, however, indicated that both anionic coordinate sites and free radicals are present in the reaction system.

These studies suggest that the complex formed from $VCl_4-Al(C_2H_5)_3$ in presence of acetonitrile may not be effective for the polymerization of acrylonitrile. It is suggested that with the increasing catalyst concentration, complex formation of acetonitrile with VCl_4 and $Al(C_2H_5)_3$ increases, and the formed complex reacts further with acrylonitrile, yielding a permanent complex. Such complex formation between polar monomers like acrylonitrile and one of the catalyst components of the Ziegler-Natta catalyst system such as $AlEtCl_2-AN/VOCl_3$ is already known.¹³ In view of the decrease in the rate of polymerization and molecular weight with catalyst concentration, it may be concluded that the rate of formation of permanent complex between acrylonitrile and catalyst complex is greater than the rate of polymerization of acrylonitrile with free radicals. This is illustrated by the reaction (1)-(4)



where C_1 , C_2 , C_3 , and $R \cdot$ refer to VCl_4 , $AlEt_3$, catalyst complex formed in acetonitrile, and radicals, respectively, and k_d is the rate constant for the reaction. Then



where k_i , k_p and k_{comp} are the rate constants for initiation, propagation, and the formation of a new complex. C_4 is the permanent complex formed between the catalyst complex and the monomer.

Hence with increasing concentration of the catalyst, the rate of complexing of monomer with catalyst complex R_{comp} is greater than the rate of polymerization R_p , i.e.,

$$k_{comp} > k_p$$

Thus R_p is proportional to the reciprocal of catalyst concentration at constant concentration of monomer.

The overall activation energy of polymerization calculated from the plot of $\log R_p$ versus $1/T$ in the range of temperature 20–40°C was 10.97 kcal/mole. This is slightly higher than that for the same reaction systems in absence of acetonitrile.

It follows that acrylonitrile undergoes free-radical polymerization at low concentration of catalyst but at higher concentrations of catalyst the formation of a permanent complex between catalyst complex and acrylonitrile is responsible for the drop in the rate of polymerization.

Examination of the permanent complex formed by physical methods such as ESR, NMR may be helpful in attaining a proper understanding of the nature and mechanism of its formation. The use of this system in the poly-

merization of other monomers may throw light on the complexity of the reaction.

References

1. U. Giannini, G. Bruckner, E. Pellino, and A. Cassata, in *Macromolecular Chemistry Brussels-Louvain 1967* (*J. Polym. Sci. C*, **22**), G. Smets, Ed., Interscience, New York, 1968, p. 157.
2. S. S. Dixit, A. B. Deshpande, L. C. Anand and S. L. Kapur, *J. Polym. Sci. A-1*, **7**, 1973 (1969).
3. S. S. Dixit, A. B. Deshpande, and S. L. Kapur, *J. Polym. Sci. A-1*, **8**, 1289 (1970).
4. S. S. Dixit, A. B. Deshpande, and S. L. Kapur, *J. Polym. Sci. B*, **8**, 211 (1970).
5. L. C. Anand, A. B. Deshpande, and S. L. Kapur, *Chem. Ind. (London)*, **1966**, 1457.
6. W. J. Linn (E. I. du Pont de Nemours and Co. Inc.), U.S. Pat. 2,961,433 (1960); *Chem. Abstr.*, **55**, 9952g (1961).
7. G. Natta and G. Dall'Asta (Montecatini), Ital. Pat. 570,434 Dec. 1957; *Chem. Abstr.*, **53**, 15640g (1959).
8. T. M. Gritsenko, V. S. Yakubovich, and V. I. Kartsovnik, *Polym. Sci., USSR*, **3**, 252 (1962).
9. S. S. Dixit, A. B. Deshpande, and S. L. Kapur, *J. Polym. Sci. A-1*, in press.
10. C. H. Bamford and A. D. Jenkins, *Proc. Roy. Soc. (London)*, **A216**, 515 (1953).
11. T. Nakaya, Y. Maki, and M. Imoto, *Makromol. Chem.*, **113**, 131 (1968).
12. L. Reich and S. S. Stivala, *J. Polym. Sci. A*, **1**, 203 (1963).
13. J. Furukawa and Y. Iseda, *J. Polym. Sci. A-1*, **8**, 1147 (1970).

Received October 6, 1970

Anionic Copolymerizations of Acrylonitrile with β -Propiolactone

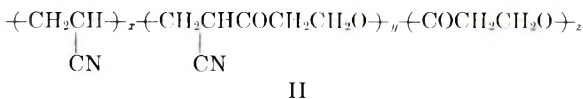
SHITOMI KATAYAMA, HIDEICHI HORIKAWA, *Faculty of Science and Technology, Akita University, Akita, Japan*, and NOBORU MASUDA, *Denki Onkjo Company, Ltd., Tokyo, Japan*

Synopsis

Anionic copolymerizations of acrylonitrile (monomer 1) with β -propiolactone (monomer 2) and the structures of the resulting copolymers were studied. The copolymerization with sodium cyanide in *N,N*-dimethylformamide gave copolymers of the structure I containing acid anhydride linkage in the molecular chains, with the monomer reactivity ratios, $r_1 = 1.20$, $r_2 = 0.00$.



The copolymerization with potassium hydroxide gave either copolymers of the structure II ($r_1 = 0.00$, $r_2 = 3.64$ at 30°C ; $r_1 = 0.00$, $r_2 = 5.00$ at 40°C) in *N,N*-dimethylformamide or only β -propiolactone homopolymer in toluene.



INTRODUCTION

In this paper anionic copolymerizations of acrylonitrile with β -propiolactone were performed following the authors' previous paper¹ on radical copolymerizations of β -propiolactone with acrylonitrile and with styrene. A series of intensive studies on the cationic copolymerization of β -propiolactone with styrene were performed by Yamashita and his co-workers,²⁻⁶ but they did not mention the reactivity ratios of the characteristic properties of the resulting copolymers. Shimosaka and his co-workers studied the copolymerization of β -propiolactone with acrylonitrile in the presence of anionic organometallic catalysts,⁷ but they also did not report reactivity ratios or the characteristic properties of the resulting copolymers.

In this paper the authors studied the anionic copolymerizabilities of β -propiolactone with acrylonitrile either in the presence of sodium cyanide or potassium hydroxide and discussed the monomer reactivity ratios and the structures and characteristic properties of the resulting copolymers.

EXPERIMENTAL

Acrylonitrile, β -propiolactone, and *N,N*-dimethylformamide (DMF) were purified by the same method as in our previous paper.¹ Commercially available best quality sodium cyanide was dried at room temperature under vacuum for one week before use. Dry tablets of potassium hydroxide were used as catalyst without treating. Toluene was treated with sodium metal and distilled.

The polymerization conditions are listed in Table I. Most of the polymerization techniques are similar to those of our previous paper with some additions, i.e., all the polymerizations were carried out in a nitrogen atmosphere either in a flask with stirring or in a glass ampoule without stirring. The monomer mixture of the compositions f_1 (mole fraction of acrylonitrile) and f_2 (mole fraction of β -propiolactone) was placed in the reaction vessel, followed by the addition of the solvent and then the catalyst. In polymerization in a flask, the contents were agitated during the whole process, the inner nitrogen pressure being kept a little above atmospheric pressure. In polymerization in a glass ampoule, the ampoule was sealed in a nitrogen atmosphere and placed in a constant temperature bath for polymerization without agitation. Polymers obtained in *N,N*-dimethylformamide were precipitated in water, washed with methanol, and dried *in vacuo* at the room temperature for several days. Polymers obtained in toluene were washed with benzene and then methanol.

Separation of poly- β -propiolactone homopolymer from polymer mixtures was carried out by the same method as in our previous paper,¹ namely, reprecipitation of the DMF solution in chloroform and extraction with refluxing chloroform. Polymer characterization and analyses were also by the

TABLE I
Polymerization Conditions^a

No.	Poly- merization	Catalyst	Solvent		Poly- meriza- tion tem- perature, °C	Poly- meriza- tion time, hr
			Type	Vol- ume, ml		
I ^b	Flask	DMF (15 ml) sat- urated with NaCN	DMF	350	-60	1
II	Flask	KOH (0.5 g)	DMF	300	40	20
III	Ampoule	KOH (0.6 g)	DMF	320	30	240
IV	Ampoule	KOH 0.6 g	Toluene	320	25	480

^a All quantities are for 1 mole of the total monomers.

^b The polymerization was stopped by the addition of 37.5 ml DMF containing 3% sulfuric acid.

same method as well, i.e., compositions of the polymers by elementary analyses, melting point by the disappearance of the optical birefringence, solution viscosity in DMF at 30°C, potassium bromide tablets of polymer powder for infrared spectra, and powder for x-ray diffraction.

RESULTS AND DISCUSSION

Polymerizability

As shown in Figure 1, copolymers were obtained with sodium cyanide in DMF (expt. I) at the initial monomer composition of $f_1 > 0.7$, and the polymer yield increased with increasing f_1 . On the other hand with potassium hydroxide in DMF (expts. II and III), polymerization took place throughout the whole f_1 range with the minimum polymer yield at $f_1 = 0.8$. The rate of polymerization of the copolymerization II (at 40°C) is ten times that of the copolymerization III (at 30°C). This seems to be a rather unexpected result, but is a remarkable fact due to the reactivity of β -propiolactone. The reactivity and polymerizability of β -propiolactone increase considerably with a small increase of temperature even without catalyst,⁸⁻¹⁰ and with catalyst increase very markedly.¹¹⁻¹³ The polymer-

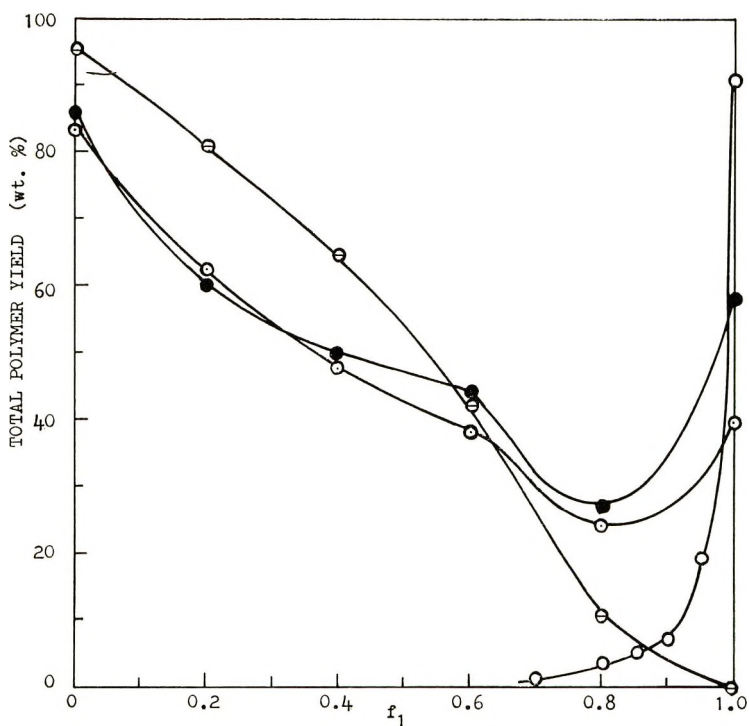


Fig. 1. Total polymer yield vs. monomer composition: (○) I, with sodium cyanide in DMF; (●) II, with potassium hydroxide in DMF at 40°C; (⊙) III with potassium hydroxide in DMF at 30°C; (⊖) IV, with potassium hydroxide in toluene at 30°C.

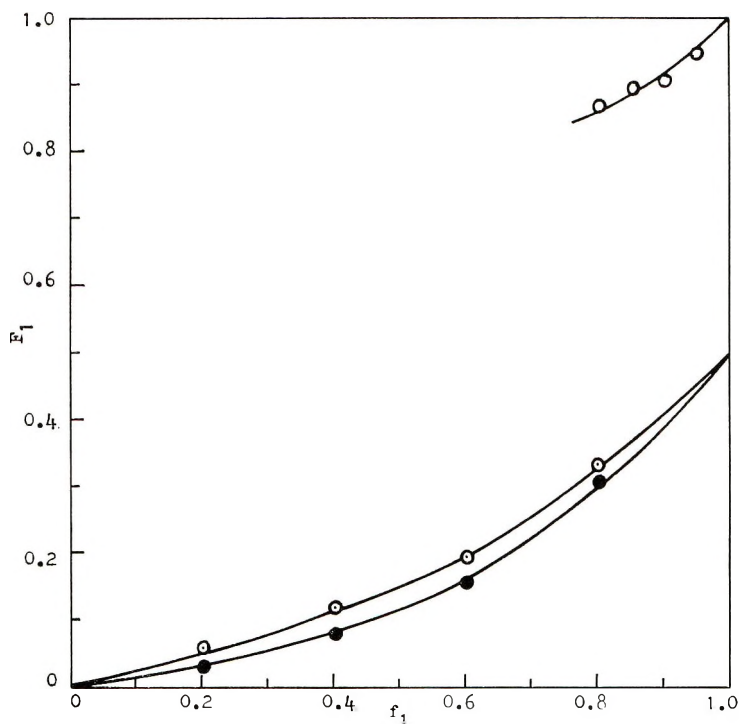


Fig. 2. Polymer composition vs. initial monomer composition: (○) I, sodium cyanide in DMF; (●) II, with potassium hydroxide in DMF at 40°C; (◊) III, with potassium hydroxide in DMF at 30°C.

ization with potassium hydroxide in toluene (expt. IV) gave only poly- β -propiolactone homopolymer in almost quantitative theoretical yield.

As shown in Figure 2 and Table II, the monomer reactivity ratios for the copolymerization with sodium cyanide are $r_1 = 1.20$ and $r_2 = 0.00$; from this, together with the zero yield on homopolymerizations of β -propiolactone, it may be concluded that β -propiolactone cannot react with the ring-opened β -propiolactone end of the propagating copolymer molecule but only with acrylonitrile end. For the copolymerizations with potassium hydroxide in DMF, the monomer reactivity ratios are $r_1 = 0.00$, $r_2 = 3.64$ at 30°C and $r_1 = 0.00$, $r_2 = 5.00$ at 40°C. In this case, though $r_1 = 0.00$, acrylonitrile can homopolymerize, so that the rate constant k_{11} is not zero but

TABLE II
Monomer Reactivity Ratios

No.	r_1	r_2	$r_1 r_2$
I	1.20	0.00	0.00
II	0.00	5.00	0.00
III	0.00	3.64	0.00
IV	0.00	∞	—

$k_{11} \ll k_{12}$. Let's take r and k as the reactivity ratio and the rate constant of the copolymerization at 30°C (run III) and r' and k' as those for the copolymerization at 40°C (run II); then,

$$r_2 = k_{p22}/k_{p21} = 3.64$$

$$r_2' = k_{p22}'/k_{p21}' = 5.00 \quad (1)$$

$$r_2/r_2' = 0.728 \quad (2)$$

$$r_2'/r_2 = 1.37 \quad (3)$$

Thus, eq. (2) shows the ratio of the relative length of the $-(M_2M_1)_x$ -sequence of the polymer II over that of the polymer III, and eq. (3) shows the ratio of the relative sequence length of the ring-opened β -propiolactone units, $-(M_2M_2)_y$ - of the polymer II over that of the polymer III. Thus polymer III has more alternating units and less $-(M_2M_2)_y$ - units than polymer II. The actual sequence length of the alternating units of the polymer III should be much longer than the polymer II, since the degree of polymerization of the polymer III is higher (as shown in Fig. 3) due to the smaller rate of termination than that of the polymer II which is lowered due to the higher rate of termination.

The monomer reactivity ratios on the copolymerization with potassium hydroxide in toluene should be $r_1 = 0.00$ and $r_2 = \infty$, since only poly- β -propiolactone homopolymer was obtained. The fact that acrylonitrile could not homopolymerize or copolymerize at all in toluene indicates that solvent plays an important role on this copolymerization and on the structures of the resulting copolymers.

Solution Viscosity and Melting Point

As shown in Figure 3, except for the polymerization in toluene by which only poly- β -propiolactone homopolymer was obtained, the solution viscosities of polymers increased with the increasing f_1 . The viscosity of the polymers obtained with potassium hydroxide in N,N -dimethylformamide at 30°C (No. III) was higher than that of the polymer (No. II) polymerized at 40°C. This means that in this copolymerization the temperature increase increases the rate of termination k_t . From this fact and the already mentioned r_2 values at 30°C and 40°C, it may be concluded that polymer III has longer alternating units than polymer II. In the case of the polymerization in toluene, acrylonitrile worked to decrease the degree of polymerization of the resulting poly- β -propiolactone homopolymer though it did not decrease the theoretical yield. A nonpolar solvent like benzene or toluene gives high molecular weight poly- β -propiolactone, while a solvent with higher dielectric constant or with unshared electron pair, like tetrahydrofuran or acetonitrile gives poly- β -propiolactone of lower molecular weight, though the yield is not lowered.^{12,14} In the above case of the polymerization in toluene, acrylonitrile functioned as a solvent. DMF is also this kind of solvent, as the copolymer resulting from copolymerizations in DMF

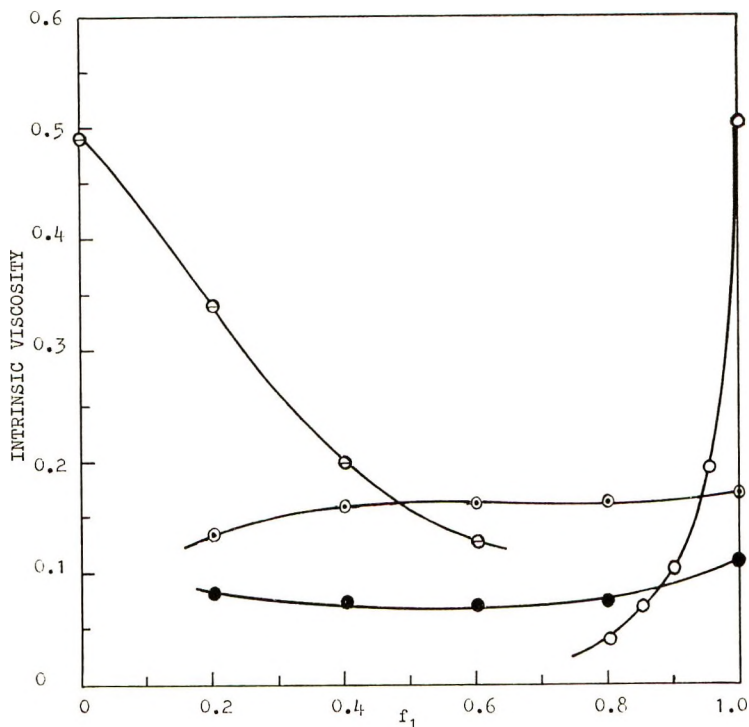


Fig. 3. Solution viscosity vs. monomer feed: (O) I, with sodium cyanide; (●) II, with potassium hydroxide in DMF at 40°C; (⊙) III with potassium hydroxide in DMF at 30°C; (⊖) IV, with potassium hydroxide in toluene at 30°C.

(polymers II and III) are of lower molecular weight, since the main sequence of the copolymer chain consists of the ring-opened β -propiolactone units.

As shown in Figure 4, the melting points of the copolymers obtained with sodium cyanide catalyst decreased with increasing f_1 and F_1 . On the other hand, the copolymers obtained with potassium hydroxide in DMF (II and III) had increasing melting points with increasing f_1 and F_1 . This difference indicates the difference of the chemical structures between the copolymer I and the copolymers II or III. The gently sloping increase of the melting point of copolymer III is due to the shorter sequence of the ring-opened β -propiolactone units in the copolymer molecule, while the melting point of copolymer II increased with a rapid slope, due to the longer sequence of the β -propiolactone units. The authors reported that a block copolymer with long sequences of each comonomer unit has an almost constant melting point in the richer F_1 range and another corresponding melting point in the richer F_2 range so that at one F_1 value the melting point of the block copolymer increases discontinuously to another melting point.¹⁵⁻¹⁷ The melting point of poly- β -propiolactone polymerized in toluene (IV) is constant regardless of f_1 and its molecular weight being higher than those of poly- β -propiolactone homopolymer obtained by the polymerizations in

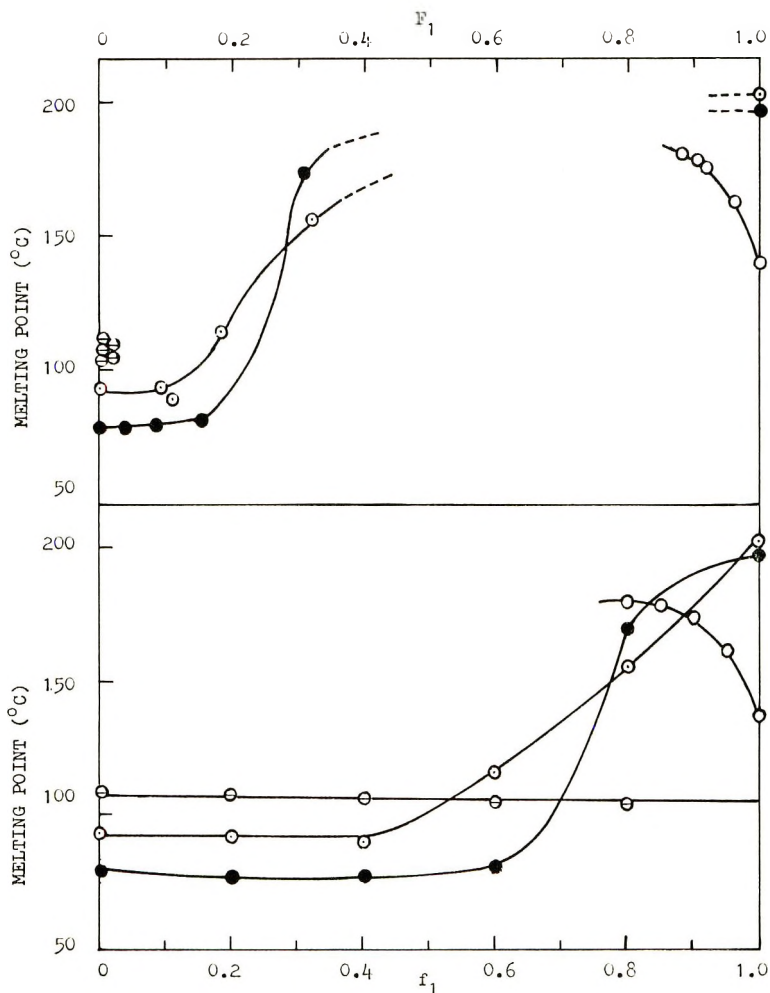


Fig. 4. Melting point vs. monomer feed and polymer composition: (○) I, with sodium cyanide; (●) II, with potassium hydroxide in DMF at 40°C; (⊙) III, with potassium hydroxide in DMF at 30°C; (⊕) IV, with potassium hydroxide in toluene at 30°C.

DMF (II and III). Asahara and Katayama^{12,13} reported that the melting point of poly- β -propiolactone does not necessarily depend upon its molecular weight but rather upon the method of polymerization and the after-treatment.

Separation of poly- β -propiolactone Homopolymer from Copolymers

As shown in Table III, the copolymers polymerized with sodium cyanide (I) were almost completely insoluble in chloroform without any extract, which indicates that the polymers are pure copolymers without any blending of poly- β -propiolactone homopolymer. The copolymers polymerized

with potassium hydroxide in DMF (II) were much extracted by chloroform to give residues with higher F_1 values. It should be noted that the extract contains not a little amount of acrylonitrile fraction, which indicates that the extract is not poly- β -propiolactone homopolymer but either a copolymer with ring-opened β -propiolactone units or at least a mixture of the copolymer and poly- β -propiolactone homopolymer. In Table III, data¹ on the radical copolymerizations are listed again with additional data on F_1 of the soluble part for reference. We recall that poly- β -propiolactone homopolymer was obtained together with copolymer on the radical copolymerization in *N,N*-dimethylformamide¹ as is shown in Table III and that the poly- β -propiolactone homopolymer was produced by the competing ionic polymerization. It should then be questioned why then the competing ionic polymerization in the solution radical polymerization did not give an ionic copolymer while an ionic copolymer was obtained by the copolymerization with potassium hydroxide in *N,N*-dimethylformamide.

TABLE III
Changes of Polymer Composition after Reprecipitation
and Extraction by Chloroform

poly- mer no. ^a	Original polymer F_1	Polymer after reprecipitation			Polymer after extraction		
		Insoluble		Soluble F_1	Insoluble		Soluble F_1
		Wt %	F_1		Wt %	F_1	
I	>0.88	>98	—	—	>99	—	—
II	0.319	28.7	0.754	0.107	29.1	0.761	0.0972
	0.158	8.55	0.732	0.0933	8.4	0.728	0.0937
	0.047	Trace	—	—	Trace	—	—
R _b	0.815	89.6	0.803	0.871	94.4	0.801	0.977
	0.700	77.7	0.783	0.387	69.6	0.715	0.665
R _s	0.672	74.9	0.910	0.00	75.6	0.916	0.00
	0.484	58.9	0.798	0.00	59.3	0.817	0.00
	0.295	52.3	0.502	0.02	61.4	0.420	0.00
	0.087	Trace	—	—	Trace	—	—

^a R_b is the radical polymerization without solvent¹ and R_s is the radical solution polymerization in *N,N*-dimethylformamide (DMF).

Actually only poly- β -propiolactone homopolymer was obtained in the presence of acrylonitrile without radical initiator in DMF, which means the resulting anion at the terminal of propagating poly- β -propiolactone could not react with acrylonitrile. Then the anion should be a carboxylate anion that can not react with acrylonitrile. Polymerization with potassium hydroxide produces an oxy anion which can react with both β -propiolactone and acrylonitrile. The extracts from the copolymers polymerized radically without solvent were oligomers rich in acrylonitrile units. The reason why such oligomers were not extracted from the copolymers by the radical solution polymerization may be that oligomers may be formed as the bulk polymerization proceeds on to make the reaction system solidify, trapping

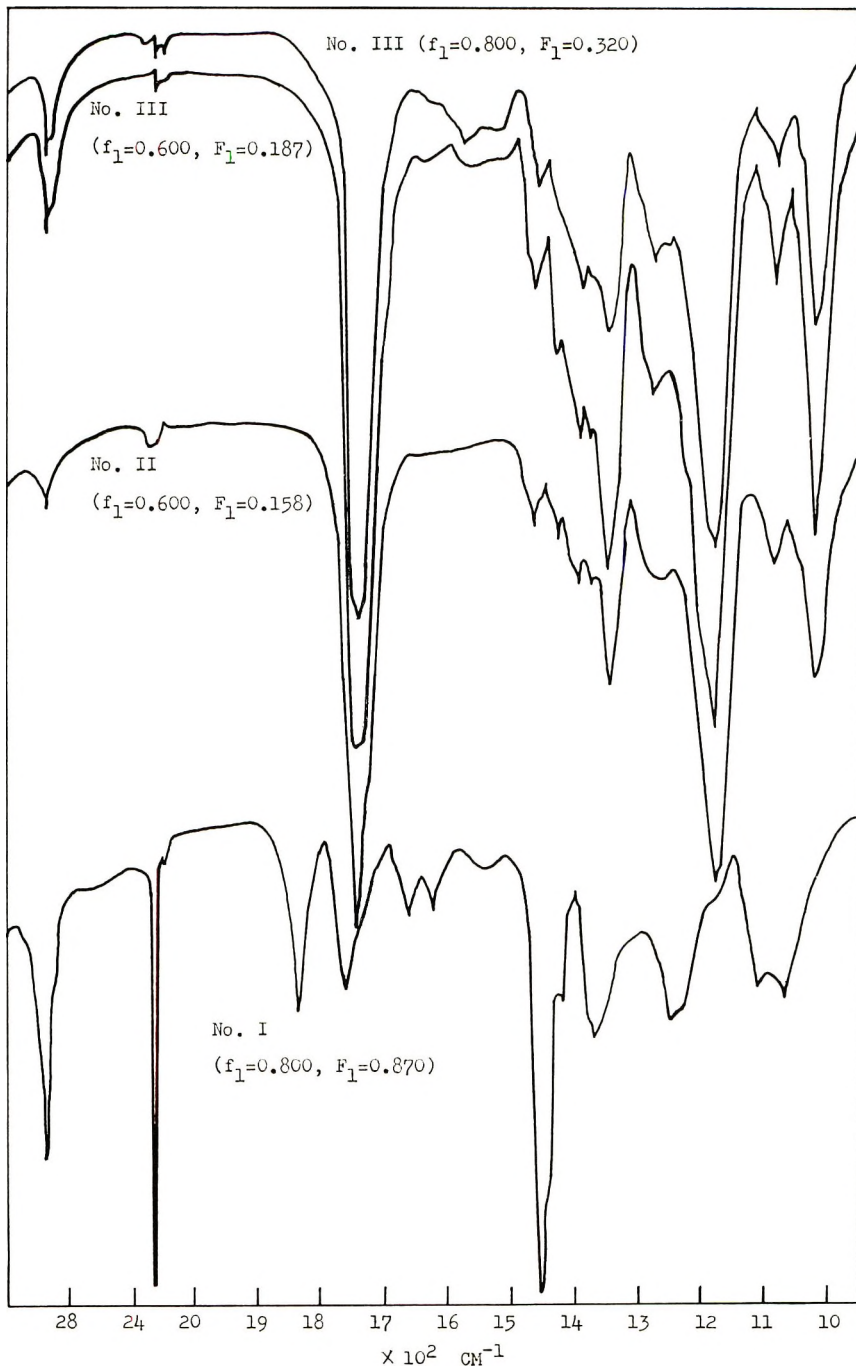


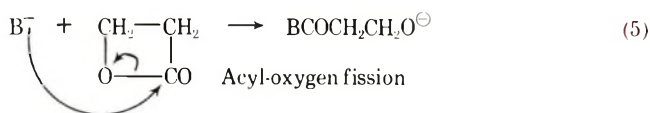
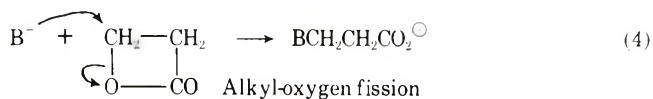
Fig. 5. Infrared absorption spectra of copolymers: (I) with sodium cyanide; (II) with potassium hydroxide in DMF at 40°C; (III) with potassium hydroxide in DMF at 30°C.

propagating oligomers to stop further propagation, while on the solution polymerization such a trapping does not take place.

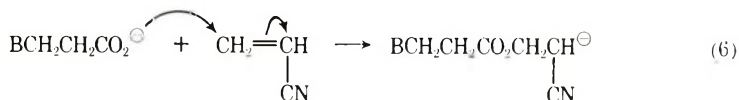
Structures of Copolymers

As shown in Figure 5, the infrared absorption spectrum of the copolymer polymerized with sodium cyanide (I) showed acid anhydride bands at 1820 and 1745 cm^{-1} (C=O stretching) and an ether band at 1070 cm^{-1} (C—O stretching). On the other hand, the copolymers polymerized with potassium hydroxide in DMF (II and III) showed ester bands, of which the C=O stretching absorption at 1740 cm^{-1} and the C—O stretching at 1180 cm^{-1} were marked. It is quite interesting that polymers II and III of different F_1 and F_2 values have almost the same infrared spectra. As we described in our previous paper,¹ the marked decrease of the intensity of the cyano group in the infrared spectra of both polymers II and III is due to the carbonyl group attached at the α -carbon of the nitrile unit. Bellamy described this phenomenon in detail: "The introduction of an oxygenated group into the molecule results in a quenching of the $\text{C}\equiv\text{N}$ absorption intensity to a remarkable extent, and its effect is greater when the oxygen-containing group is attached to the same carbon atom as the nitrile.¹⁸ The CH stretching and $\text{CH}_{1,2}$ deformation bands can be observed both in the nitrile and ring-opened β -propiolactone units in the copolymers, so that clear differences in the infrared spectra of polymers II and III are not observed.

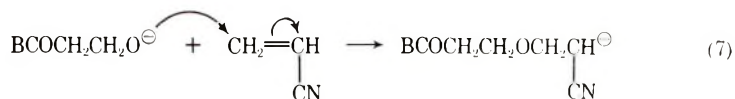
On the ring-opening of β -propiolactone by the attack of an anion B^- , there are two types of ring-opening mechanisms [eqs. (4) and (5)]:



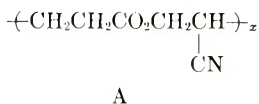
If the resulting carboxylate anion in eq. (4) reacts with acrylonitrile, an ester linkage should be formed [eq. (6)].



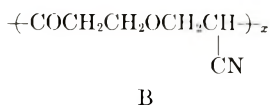
If the resulting oxy anion in eq. (5) reacts with acrylonitrile, a ketonic carbonyl and an ether linkage should be formed [eq. (7)].



If each reaction (4) or (5) is repeated by the attack of each resulting anion on β -propiolactone, poly- β -propiolactone units should be formed. If the resulting carbanion in the reaction (6) attacks β -propiolactone by the reaction (4) and then reactions (4) and (6) are repeated, the resulting copolymer should contain the unit A:



In the same manner, if the reactions (5) and (7) are repeated, the resulting copolymer should contain the structure (B)

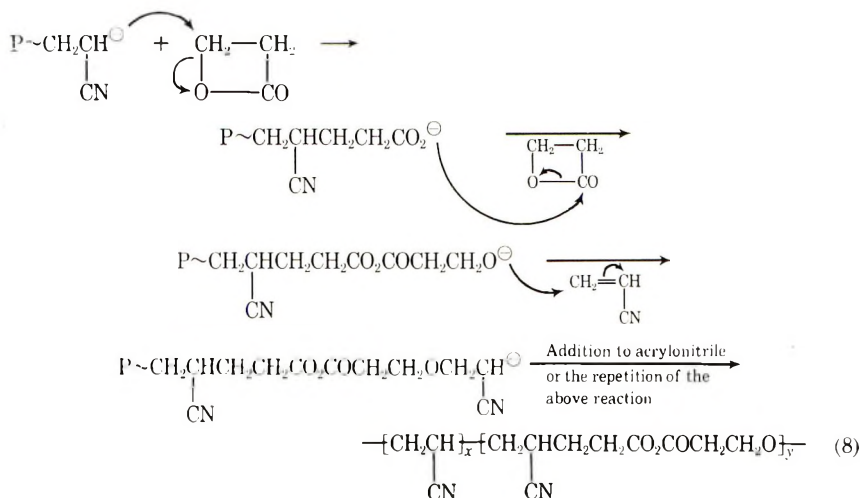


The structure of the copolymer polymerized with sodium cyanide (I) is, however, neither structures A nor B, since it has neither ester linkage or ketonic carbonyl linkage but acid anhydride and ether linkages, which indicates that there should be another copolymerization mechanism. From this fact that the monomer reactivity ratios, $r_1 = 1.20$ and $r_2 = 0.00$ without homopolymerization of β -propiolactone, the following conclusions may be reached concerning the structure of copolymer I.

(a) The carbanion of acrylonitrile unit at the propagating copolymer terminal can react with both acrylonitrile and β -propiolactone. The carbanion attacks β -propiolactone as shown in eq. (4) to give a carboxylate anion terminal, forming a methyne-methylene linkage. The reaction (5) does not take place, for if it did, the resulting copolymer would have a ketonic carbonyl linkage which was not observed in the infrared absorption spectra.

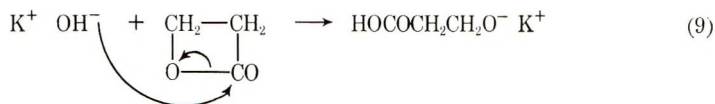
(b) The resulting carboxylate anion cannot react with acrylonitrile, for if it could, the resulting copolymer would have an ester linkage. The carboxylate anion reacts with β -propiolactone giving an oxy anion terminal and an acid anhydride linkage. The attack of the carboxylate anion on β -propiolactone by the mechanism (4) does not take place, for if it did the resulting copolymer would have ester linkages.

(c) The resulting oxy anion reacts with acrylonitrile to give an ether linkage, but cannot react with β -propiolactone. If the oxy anion were to react with β -propiolactone by the mechanism (4) and the resulting carboxylate anion were to react with β -propiolactone, a poly- β -propiolactone homopolymer $\text{-(CH}_2\text{CH}_2\text{CO}_2\text{COCH}_2\text{CH}_2\text{O)-}_z^-$ would be formed, which is contrary to the experimental result. If the oxy anion were to react with β -propiolactone by the mechanism (5), the resulting copolymer would have ester linkages. Thus the copolymerization mechanism may be summarized as shown in eq. (8).

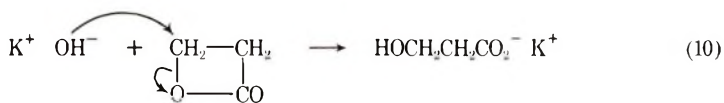


The copolymers polymerized with potassium hydroxide in DMF (II and III) probably have the structure B linked with poly- β -propiolactone unit sequence, for a carboxylate anion cannot react with acrylonitrile though it reacts with β -propiolactone at this temperature.¹⁹⁻²¹

The catalytic initiation may be as shown in eq. (9).



There may be two questions about the reaction: namely there may be another initiation mechanism as shown in the eq. (10), and the resulting carboxyethoxy anion in eq. (9) may be converted into the hydroxypropionate anion, which is the same anion as that in reaction (10).



β -Propiolactone (0.72 g) was added to a mixture of 0.56 g of potassium hydroxide either without solvent or in 5 ml of DMF or toluene. The mixtures without solvent and with DMF were kept at 30°C for 30 min. The mixture with toluene was kept at 60°C for 45 min, since the rate of the reaction was slow compared with those of the other two mixtures. The infrared absorption spectra of the mixtures are shown in Figure 6. The mixture reacted without solvent showed the OH stretching band of a carboxylic acid at 2400-2700 cm^{-1} , although the C=O stretching of the carboxylic acid is the same as that of the ester which constitutes poly- β -propiolactone, and a weak band of a carboxylate anion at 1570 cm^{-1} . The mixture reacted in DMF also shows the OH stretching band at 2400-2700 cm^{-1} but the band at 1570 cm^{-1} is not observed. The mixture reacted in

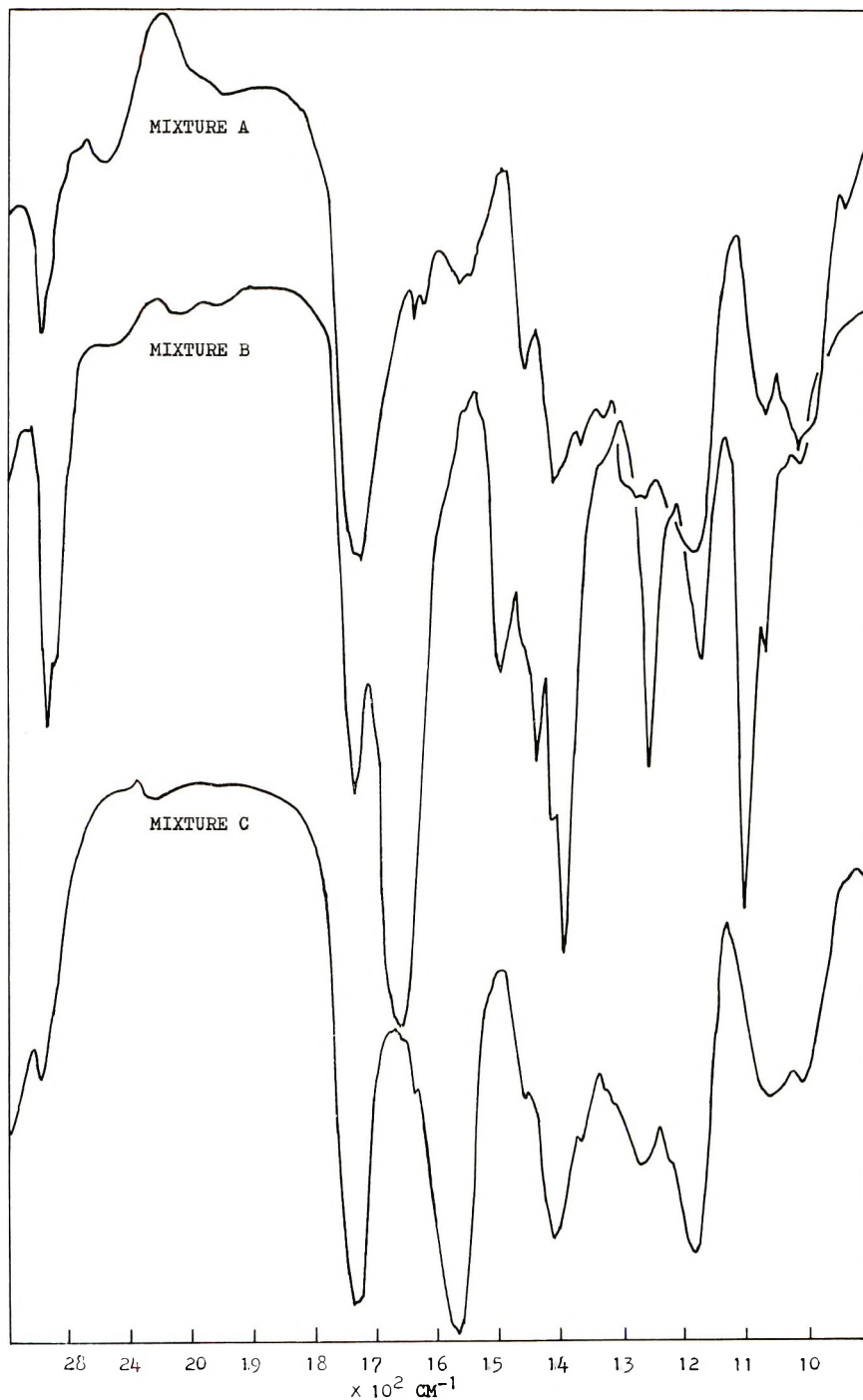
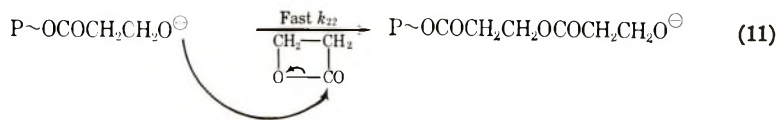
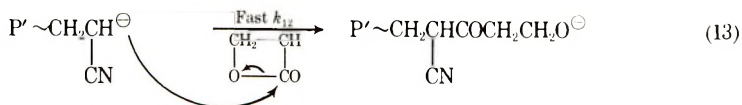
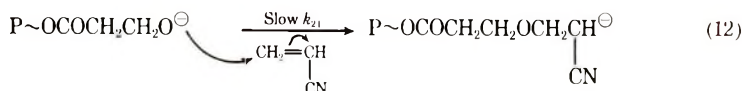


Fig. 6. Infrared absorption spectra of the reacted mixtures of β -propiolactone with potassium hydroxide: (A) without solvent; (B) with DMF; (C) with toluene.

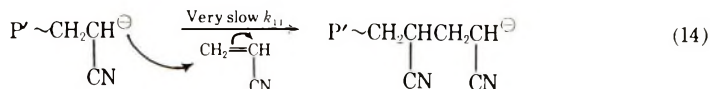
toluene does not show the band at 2400–2700 cm^{-1} but shows a strong absorption of carboxylate anion at 1570 cm^{-1} . These facts indicate that the initiation in DMF is by the mechanism (9) and the resulting oxy anion is stable. The initiation in toluene is by the mechanism (10), giving a carboxylate anion. The initiation without solvent is by both mechanisms. The above result is rather similar to the solvent effect on the reaction of β -propiolactone with amines studied by Gresham and his co-workers,²² i.e., acetonitrile gives aminoacid as the main product, water gives amide, and without solvent a mixture is obtained. It may be assumed that in a system where the basicity is strengthened, acyl-oxygen fission of β -propiolactone takes place, while in a neutral or acidic system or a system where the basicity is lowered, alkyl-oxygen fission takes place. In our previous paper¹ β -propiolactone homopolymerized in DMF with and without the presence of acrylonitrile. The propagation therein should be by the carboxylate anion, which is produced by the alkyl-oxygen fission of β -propiolactone since the polymerization system is not basic enough without strong base. Toluene does not work to make potassium hydroxide basic enough, so that only alkyl-oxygen fission takes place to give a carboxylate anion which polymerizes only β -propiolactone. Now the propagation of the copolymerization with potassium hydroxide in DMF will be as shown in eqs. (11)–(14), continued from the initiation (9).



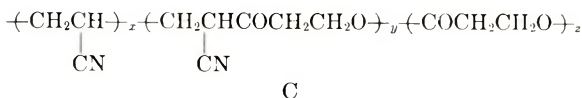
or



or



The above reaction mechanism leads to a copolymer of the structure C:



As shown in Figure 7, the copolymer polymerized with sodium cyanide has a rather broad x-ray diffraction peak at 16.8° which is the same peak

as that of polyacrylonitrile. Since F_2 is small, the alternating unit of the structure shown in eq. (8) cannot constitute a sequence long enough to give the corresponding crystalline region. The copolymers polymerized with potassium hydroxide in DMF at 30°C have four peaks, i.e., at 21.0° and 30.2° which are due to the poly- β -propiolactone unit of the structure (14),

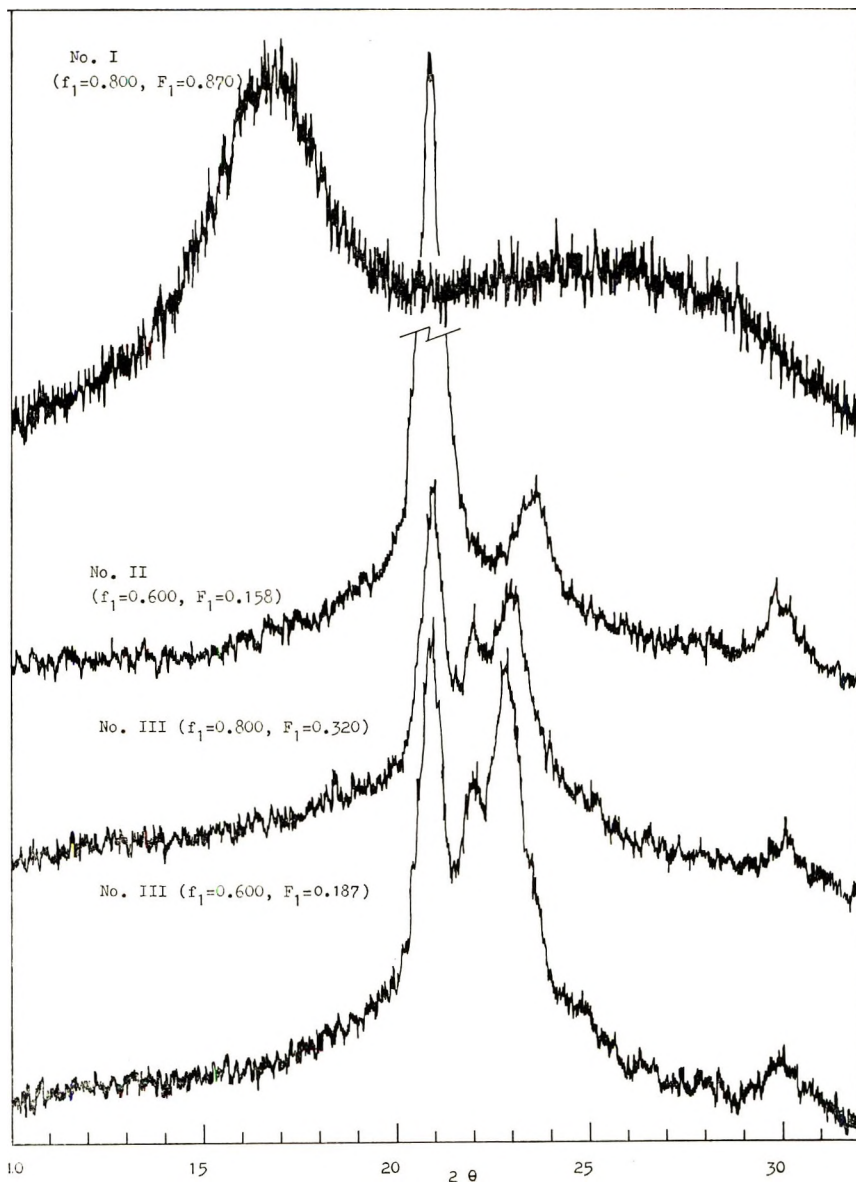


Fig. 7. X-Ray diffraction patterns of copolymers: (I) with sodium cyanide; (II) with potassium hydroxide in DMF at 40°C; (III) with potassium hydroxide in DMF at 30°C. $\text{CuK}\alpha$ source.

and at 22.1° and 23.0° which are new peaks that cannot be observed with poly- β -propiolactone or polyacrylonitrile homopolymers. These new peaks should be due to the alternating unit of the structure C. The lack of the peak at 16.8° indicates that the sequence of polyacrylonitrile unit in the structure C is too short to give the corresponding crystalline region. The copolymer polymerized with potassium hydroxide in DMF at 40°C has almost the same diffraction pattern as that of poly- β -propiolactone homopolymer. Copolymer III ($F_1 = 0.187$) and copolymer II ($F_1 = 0.158$) are very similar in chemical compositions, though the former has peaks due to the mentioned alternating unit while the latter has not. The alternating sequence of the copolymer II should be too short to constitute crystallites.

References

1. S. Katayama, N. Horikawa, and N. Masuda, *J. Polym. Sci. A-1*, in press.
2. T. Tsuda, S. Shimizu, and Y. Yamashita, *Kogyo Kagaku Zasshi*, **67**, 2145 (1964).
3. T. Tsuda and Y. Yamashita, *Makromol. Chem.*, **86**, 304 (1965).
4. Y. Yamashita, K. Ito, K. Umehara, and T. Tsuda, *J. Polym. Sci. B*, **4**, 241 (1966).
5. T. Tsuda and Y. Yamashita, *Kogyo Kagaku Zasshi*, **70**, 553 (1967).
6. K. Ito, T. Inoue, and Y. Yamashita, *Makromol. Chem.*, **117**, 279 (1968).
7. Y. Shimosaka, T. Tsuruta, and J. Furukawa, *Kogyo Kagaku Zasshi*, **66**, 1498 (1963).
8. I. S. Ioffe, F. K. Sukholinov, A. N. Leporskii, and L. B. Bukhman, *Zh. Prikl. Khim.*, **36**, 629 (1963).
9. R. K. Hoffman and B. Warshowsky, *Appl. Microbiol.*, **6**, No. 5, 723 (1958).
10. *β -Propiolactone*, Daiseru Company, Ltd., Japan, 1967, p. 16.
11. T. Asahara and S. Katayama, *Seisan Kenkyu*, **14**, 122 (1962), Japan.
12. T. Asahara and S. Katayama, *Kogyo Kagaku Zasshi*, **69**, 725 (1966).
13. T. Asahara and S. Katayama, *Kogyo Kagaku Zasshi*, **69**, 2179 (1966).
14. S. Okamura, T. Higashimura, and A. Tanaka, *Kogyo Kagaku Zasshi*, **65**, 707 (1962).
15. H. Horikawa, S. Katayama, and N. Sato, paper presented at 17th Annual Meeting, Japan Chemical Society, 1968; *Abstracts*, [21 C 11] p. 161 (1968).
16. S. Katayama, H. Horikawa, T. Sato, and Y. Takahashi, paper presented at 22nd Meeting, Japan Chemical Society, 1969; *Abstracts*, [01221] p. 2082 (1969).
17. S. Katayama, Y. Obuchi, and H. Horikawa, *Kogyo Kagaku Zasshi*, **73**, 1720 (1970).
18. L. J. Bellamy, *The Infrared-red Spectra of Complex Molecules*, Wiley, New York, 1958, p. 266.
19. T. Shiota, Y. Goto, and K. Hayashi, *J. Appl. Polym. Sci.*, **11**, 753 (1967).
20. H. Horikawa, S. Katayama, and T. Mori, paper presented at 21st Annual Meeting, Japan Chemical Society, 1968; *Abstracts*, [16216] p. 2788 (1968).
21. H. Horikawa, Y. Takahashi, and S. Katayama, paper presented at 21st Annual Meeting, Japan Chemical Society, 1968; *Abstracts*, [16217] p. 2789 (1968).
22. T. L. Gresham, J. E. Jansen, F. W. Shaver, R. A. Bankert, and F. T. Fiedorek, *J. Amer. Chem. Soc.*, **73**, 3168 (1951).

Received August 6, 1970

Revised October 7, 1970

Anionic Copolymerization of *p*-Anisaldehyde with Dimethylketene

KAZUHIKO HASHIMOTO and HIROSHI SUMITOMO, *Faculty of
Agriculture, Nagoya University, Chikusa, Nagoya, Japan*

Synopsis

Anionic copolymerization of *p*-anisaldehyde (ANA) with dimethylketene (DMK) was made with use of benzophenone-dilithium complex as an initiator at -78°C in a high vacuum. In spite of a copolymerization in such a good polar solvent as tetrahydrofuran, the composition of the copolymer was nearly exactly 1:1 over a quite wide range of the monomer feed. From the analytical data of the product after the hydrogenolysis of the copolymer with lithium aluminum hydride, the copolymer was found to have a structure resulting from the alternating addition of the C=O double bond of ANA to the C=C double bond of DMK. No copolymerizations of ANA with phenyl isocyanate and methyl isocyanate take place under the same conditions.

Introduction

In the preceding papers¹⁻³ anionic copolymerizations of β -cyano-propionaldehyde (NC—CH₂—CH₂—CHO, CPA) with various monomers having heterocumulative double bonds such as dimethylketene [(CH₃)₂C=C=O, DMK],¹ phenyl isocyanate (C₆H₅N=C=O, PhI),² and methyl isocyanate (CH₃N=C=O, MeI)³ were found to give random copolymers. The microstructures of these copolymers as determined by NMR analysis were discussed.

p-Anisaldehyde (CH₃O—C₆H₄—CHO, ANA) is an interesting monomer obtained from anise oil and also prepared by the oxidation of anethol. Copolymerization of ANA with DMK was briefly mentioned by Natta et al. in their paper.⁴ The present paper is concerned with more detail studies on anionic copolymerization of ANA with DMK, in comparison with that of CPA with DMK.

Experimental

The material and methods employed here was essentially the same as those described previously.^{1-3,5} ANA was distilled *in vacuo* after drying over Molecular Sieves. Hydrogenolysis of the resulting copolymer with lithium aluminum hydride was performed in boiling tetrahydrofuran (THF). The number-average molecular weight of the copolymer \bar{M}_n was determined by using vapor pressure osmometry on a Hewlett-Packard instrument, Model 302 in benzene at 37°C . The infrared spectra were

measured with a Hitachi grating infrared spectrophotometer, Model 215. NMR analyses were made in deuterated chloroform with a JNM-4H-100 spectrometer. Mass spectra were run on a Hitachi RMS-4 mass spectrometer.

Results and Discussion

The results of copolymerization of ANA with DMK initiated by benzophenone–dilithium complex ($\text{Li}_2\text{-BzPh}$) at -78°C are shown in Table I.

Copolymerization proceeded in a homogeneous phase, and the rate decreased with increasing mole fraction of ANA in the monomer mixture. No homopolymerization of ANA occurred, while DMK homopolymerized to give polyester under the present conditions. In spite of the fact that copolymerization was carried out in such a good polar solvent as THF, the composition of the copolymer obtained here was nearly exactly 1:1 over a quite wide range of the monomer feed, as also shown in Figure 1.

The resulting copolymer obtained was a white powder which was soluble in THF and chloroform and partially insoluble in benzene and dimethylformamide. In Table II are given the results of elution fractionation of the copolymer, including softening points and molecular weights of the fractions.

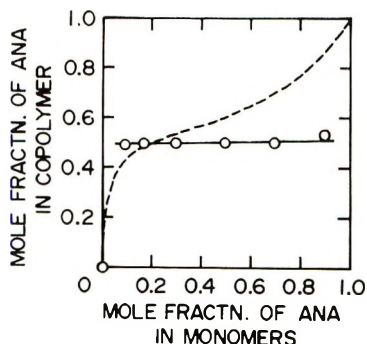


Fig. 1. Composition of copolymer as a function of monomer composition in the system of ANA and DMK: (O), experimental value; (---) composition curve calculated from $r_1 = 0.6$, $r_2 = 0.04$ in the system of CPA (M_1) and DMK (M_2).¹ Conditions: $\text{Li}_2\text{-BzPh}$; THF; -78°C .

It was found that each fraction had a nearly equimolar composition, but the softening point of the benzene-insoluble fraction was higher than that of benzene-soluble fraction. The x-ray diffraction diagram revealed that the crystallinity of the original copolymer was not high but that of the benzene-insoluble fraction increased after treatment at a temperature near its softening point.

Natta et al.⁴ mentioned the butyllithium-initiated ANA–DMK copolymerization in a nonpolar solvent such as toluene. Their copolymer seemed to be much less soluble than that obtained here from the $\text{Li}_2\text{-BzPh}$ –THF

TABLE I
Anionic Copolymerization of *p*-Anisaldehyde with Dimethylketene^a

Expt.	Monomer		Mole fraction of ANA	Li ₂ BzPh, mole-% to monomer)	Time, min	Polymer yield, % ^b	Mole fraction of ANA in copolymer ^c
	ANA, g	DMK, g					
128	24.32	0	1.00	0.10	960	0	—
118	27.40	0.94	0.93 ₇	0.05	20	0.9	—
114	12.32	0.75	0.89 ₄	0.05	6	5.7	0.53 ₄
109	9.50	2.17	0.69 ₄	0.05	2	7.4	0.50 ₆
119	9.10	2.62	0.64 ₁	0.05	6	26.2	0.51 ₉
108	6.93	3.65	0.49 ₄	0.05	8	47.7	0.49 ₉
129	4.00	4.93	0.29 ₅	0.01	0.5	3.3	0.49 ₇
110	4.00	4.94	0.29 ₄	0.05	1	71.3	0.46 ₄
113	1.09	2.75	0.16 ₇	0.01	0.5	4.5	0.49 ₇
130	1.25	6.52	0.09 ₆	0.01	0.5	3.7	0.48 ₇
60	0	1.72	0	0.30	1440	36.6	0

^a At <10⁻⁴ mm Hg, -78°C; solvent, THF; volume ratio of solvent to monomer, 5.

^b Calculated for the total weight of the monomers.

^c Estimated from the peak intensity in the NMR spectrum.

TABLE II
Results of Elution Fractionation of ANA-DMK Copolymers

Sample ^a	Mole fraction of ANA in copolymer	Benzene-soluble			Benzene-insoluble	
		Weight, %	Softening point, °C	\bar{M}_n^b	Weight, %	Softening point, °C
114	0.53 ₄	81.0	128-144	—	19.0	144-198
109	0.50 ₆	83.2	146-175	—	16.8	162-203
108	0.49 ₃	70.4	149-160	5210	29.6	177-190
110	0.46 ₃	100	147-153	13770	0	—
113	0.49 ₇	100	141-151	9220	0	—
130	0.48 ₇	100	136-145	7810	0	—

^a Sample numbers refer to products of experiments listed in Table I.

^b By vapor pressure osmometry in benzene at 37°C.

system. The more polar solvent may give the lower molecular weight and the less crystalline copolymer.

The infrared spectrum of the resulting copolymer shown in Figure 2 has both characteristic absorption bands due to the ANA unit (at 2840, 1610, 1510, and 830 cm^{-1}) and to the DMK unit (at 1465, 1385, and 1360 cm^{-1}). Absorption bands attributed to the ester group also appear at 1735, 1250, and 1120 cm^{-1} .

The NMR spectrum of the copolymer is shown in Figure 3. In the spectrum methyl protons of DMK unit give two peaks at τ values of 9.35 and 9.05, quite differing from methyl protons of the polyester type homopolymer of DMK.¹ The peaks appearing at 6.37, 4.20, and 2.8-3.5 τ are attributed to methoxy, methine, and aromatic protons of ANA unit, respectively. There is an intensity ratio of 6:3:1:4 among the peaks due to methyl, methoxy, methine, and aromatic protons, which means that the copolymer consists of equivalent numbers of ANA and DMK units. Taking account of the chemical shift of the only one peak due to methine proton, the copolymer is thought to exclusively consist of sequence I formed through the alternative addition of the C=C double bond of DMK to the C=O double bond of ANA. It is also supported by the fact that methyl

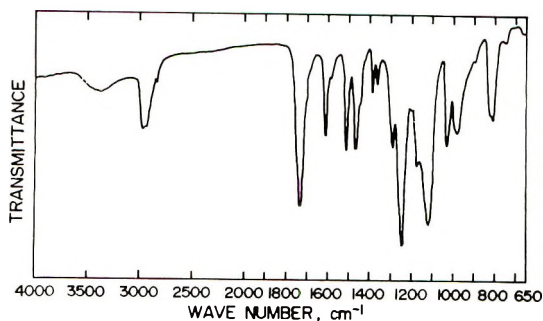
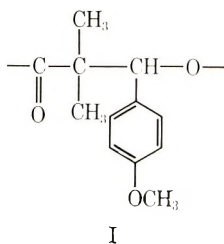


Fig. 2. Infrared spectrum of ANA-DMK copolymer. Sample 113, KBr disk.



peaks are observed at a higher magnetic field under the influence of the neighboring aromatic group in the ANA-DMK copolymer than in CPA-DMK copolymer previously reported.¹

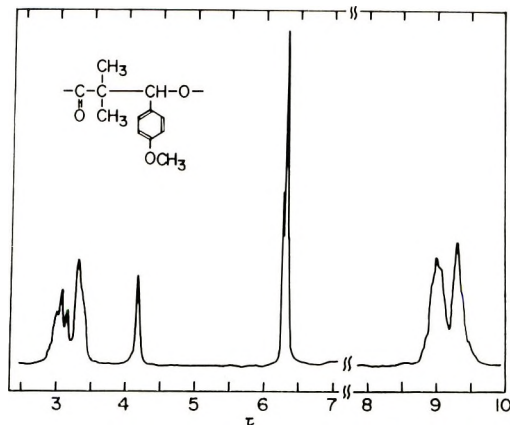
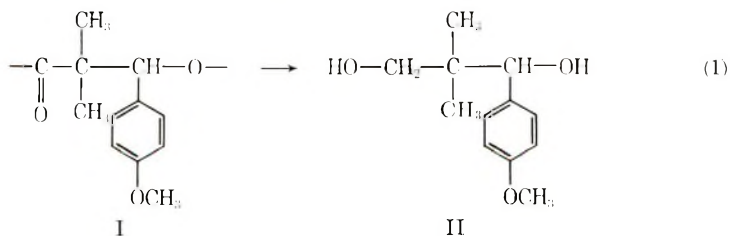


Fig. 3. NMR spectrum of ANA-DMK copolymer. Sample 113; 15% deuterated chloroform solution; 70°C.

Hydrogenolysis of the ANA-DMK copolymer with lithium aluminum hydride in boiling THF resulted in the formation of a colorless viscous oil in a good yield (97%). If the copolymer sample possesses the alternating structure I, the hydrogenolysis product should be 2,2-dimethyl-1-(*p*-methoxy)phenyl-propanediol-1,3 (II).



ANAL. Calcd for C₁₂H₁₈O₃: C, 68.54%; H, 8.63%, mol. wt., 210.26. Found: C, 68.24%; H, 8.65%.

In the mass spectrum of the reduction product was observed a parent peak at *m/e* = 210, which agreed with the molecular weight of compound II.

The infrared spectrum of the product (Fig. 4) exhibits characteristic absorption bands at 3300–3400, and 1035 cm^{-1} assignable to $\nu_{\text{O-H}}$ and $\nu_{\text{C-O}}$ of hydroxyl group, respectively, instead of the absorption at 1735 cm^{-1} due to $\nu_{\text{C=O}}$ of the ester group.

NMR analysis was also applied to this compound. In the NMR spectrum given in Figure 5, the peaks at τ values of 9.21 and 9.18, 6.22, and 3.18 and 2.80 are assignable respectively to methyl, methoxy, and aromatic protons. The methine peak of ANA unit shifted from 4.20 τ to 5.47 τ after the hydrogenolysis. The AB-pattern peak at 6.54 τ is attributed to the methylene group formed by the reduction of the ester group. A new broad peak at 6.86 τ is thought to come from the hydroxyl proton in view of the facts that the chemical shift depended on the concentration of the solution (for example, 6.2–6.4 τ in 10% deuterated chloroform solution) and the peak almost disappeared after the addition of a small amount of heavy water.

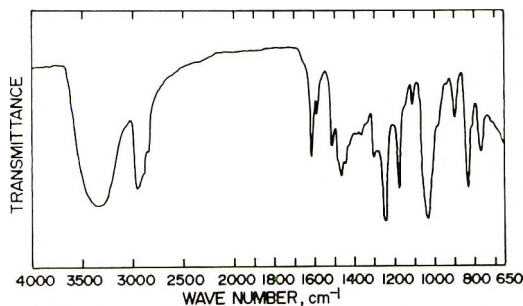
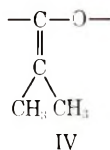
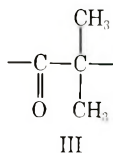


Fig. 4. Infrared spectrum of hydrogenolysis product of ANA-DMK copolymer (liquid).

In conclusion, the copolymer obtained in the present system was confirmed to consist of the alternative sequence I. In other words, the DMK unit enters the copolymer through opening of the C=C double bond. It is to be noted that the CPA-DMK copolymer rich in DMK, previously described,¹ was a random copolymer containing the structural unit III followed by the unit IV.



In the NMR spectrum of the ANA-DMK copolymer seen in Figure 3, an especially large shift of one of the two methyl peaks to a higher magnetic field, owing to the influence of the neighboring phenyl group, is observed. The difference between the chemical shifts may be increased by the slow movement of the macromolecules in the solution.

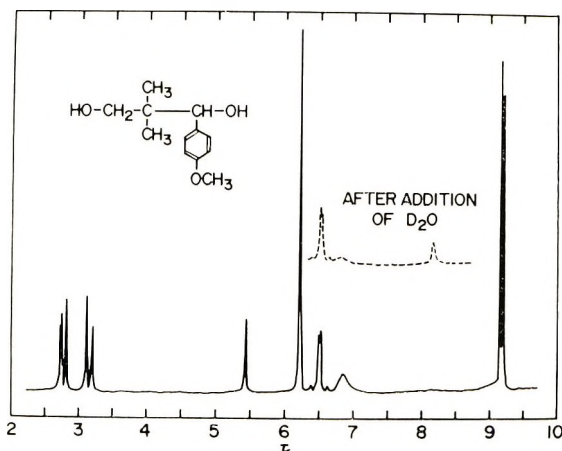


Fig. 5. NMR spectrum of hydrogenolysis product of ANA-DMK copolymer. In 3% deuterated chloroform solution; 25°C.

Anionic copolymerizations of ANA with MeI and PhI under the present conditions yielded only homopolymers of the isocyanates, differing from those of CPA (Table III).^{2,3}

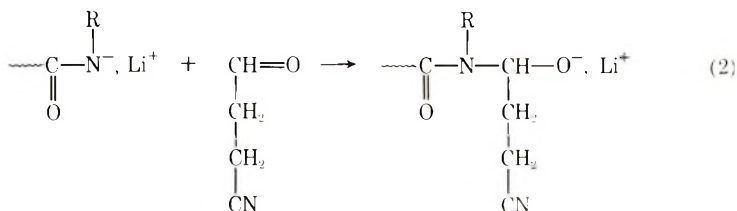
TABLE III
Anionic Copolymerizations of *p*-Anisaldehyde with Isocyanates^a

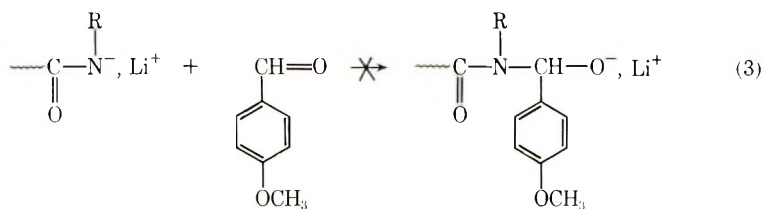
Expt.	Monomer		Mole fraction of ANA	Time, min	Polymer yield, % ^b	Product
	ANA, g	Isocyanate, g				
106	6.80	MeI 2.87	0.49 ₉	8	2.7	MeI homopolymer
107	6.83	PhI 6.01	0.49 ₉	0.5	2.3	PhI homopolymer

^a At <10⁻⁴ mm Hg, -78°C; initiator, Li₂-BzPh, 0.10 mole-% (on monomer); solvent, THF; volume ratio of solvent to monomer, 5.

^b Calculated for the total weight of the monomers.

It is likely that the ambident anion from isocyanates may be able to add CPA [eq. (2)] but not ANA [eq. (3)] in competition with the isocyanates under the present conditions:





where R is CH₃ or C₆H₅. Such lower reactivity of ANA monomer may be due to the resonance effect of the phenyl group on the C=O double bond.

References

1. K. Hashimoto and H. Sumitomo, *Polymer J. (Japan)*, **1**, 190 (1970).
2. K. Hashimoto and H. Sumitomo, *J. Polym. Sci. A-1*, in press.
3. K. Hashimoto and H. Sumitomo, *J. Polym. Sci. A-1*, **9**, 107 (1971).
4. G. Natta, G. Mazzanti, G. F. Pregaglia, and G. Pozzi, *J. Polym. Sci.*, **58**, 1201 (1962).
5. H. Sumitomo and K. Hashimoto, *J. Polym. Sci. A-1*, **7**, 1331 (1969).

Received October 14, 1970

Methyl Methacrylate in Sulfur Dioxide: Solvated Radical Polymerization

J. J. KEARNEY, H. G. CLARK,* V. STANNETT,†

and D. CAMPBELL,‡ *Camille Dreyfus Laboratory,*

Research Triangle Institute, Research Triangle Park, North Carolina 27709

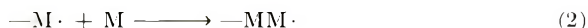
Synopsis

Methyl methacrylate may be polymerized by free-radical initiators in liquid sulfur dioxide without incorporating sulfur dioxide in the polymer chain, even though methacrylate radicals add sulfur dioxide readily as indicated by electron spin resonance studies. An explanation for this anomalous result is advanced, and evidence for the participation of sulfur dioxide in the transition state of the addition reaction is presented.

INTRODUCTION

Methyl methacrylate (MMA) is known to polymerize in sulfur dioxide (S) as solvent to produce a homopolymer containing only traces of sulfur. During the course of an investigation of the behavior of MMA in terpolymerizations with isoprene and S,¹ it became desirable to study the homopolymerization in greater detail. The results of this study indicate that the growing methacrylate chain exists as a solvated free radical. Solvated radicals have been postulated previously²⁻⁴ to explain polymerization kinetics although some earlier studies had indicated that solvents do not participate in free-radical propagation.⁵ In the present case clear evidence of radical solvation is obtained without the complexities of monomer association complexes.

Acrylonitrile and other vinyl monomers with strong electron-withdrawing substituents also give homopolymers in S as solvent. The usual assumption is that radicals derived from such monomers do not add S but do add their own monomer, i.e.,



* Present address: Biomedical Engineering Department, Duke University, Durham, North Carolina.

† Present address: Chemical Engineering Department, North Carolina State University, Raleigh, North Carolina.

‡ Present address: Department of Physics, Royal Military College of Science, Shrivvenham, England.

The electron spin resonance studies of Kuri and Ueda, however,⁶ indicate that S adds readily to the methacrylate radical. Verification of the ESR observations would make it of considerable interest to explain the reported polymer composition.

EXPERIMENTAL

Polymerization

Methyl methacrylate (M) obtained from the Rohm and Haas Corporation was distilled under high vacuum. Anhydrous sulfur dioxide (S) was obtained from the Matheson Company. It was distilled from lecture bottles into the polymerization ampoules without other purification. M and S were degassed separately at 10^{-5} torr and sufficient M was distilled into S maintained at liquid nitrogen temperature to make a 20% solution. The sample tubes were sealed off, brought to room temperature and irradiated with ^{60}Co γ -radiation at the desired temperatures. Sufficient radiation dose was used to give approximately 10–15% conversion of M to polymer, except in the case of polymers prepared at -50°C , where the polymerization rate was very low and conversions of 3–5% were obtained. After irradiation the tubes were quenched in liquid nitrogen, cut open, and methanol added. After the mixture warmed to room temperature it was filtered and allowed to air dry.

Carbon, hydrogen, and sulfur analyses, performed by the Galbraith Laboratories, Knoxville, Tennessee, showed no sulfur; results agreed with the theoretical values for poly(methyl methacrylate).

Nuclear Magnetic Resonance (NMR) Spectra

NMR data for the polymers were obtained with a Varian A-60 spectrometer in deuterated chloroform at 75°C .

Electron Spin Resonance (ESR) Spectra

ESR spectra were run on poly(methyl methacrylate) in the apparatus depicted in Figure 1, which has provisions for the addition of monomers as gases. Powdered polymer was dried and compacted in a pellet press at pressures below 500 psi. The pellets could be cut and shaped but were brittle and porous by superficial inspection. The pellets were cut into pieces small enough to fit in the 5 mm quartz tube. The tube was evacuated to 10^{-5} torr and sealed off. M and S vapors evaporated from degassed samples were added to the quartz tube from side arms having glass break seals. The apparatus could be evacuated through a tube connected to the measuring tube which was fitted with a greaseless O-ring stopcock. Vapors of S and M were added by breaking the appropriate glass seal with a bar magnet and vapors removed through the stopcock without removing the sample from the spectrometer chamber.

The poly(methyl methacrylate) sample was irradiated by inverting the apparatus and thus allowing the sample to fall from the measuring tube to

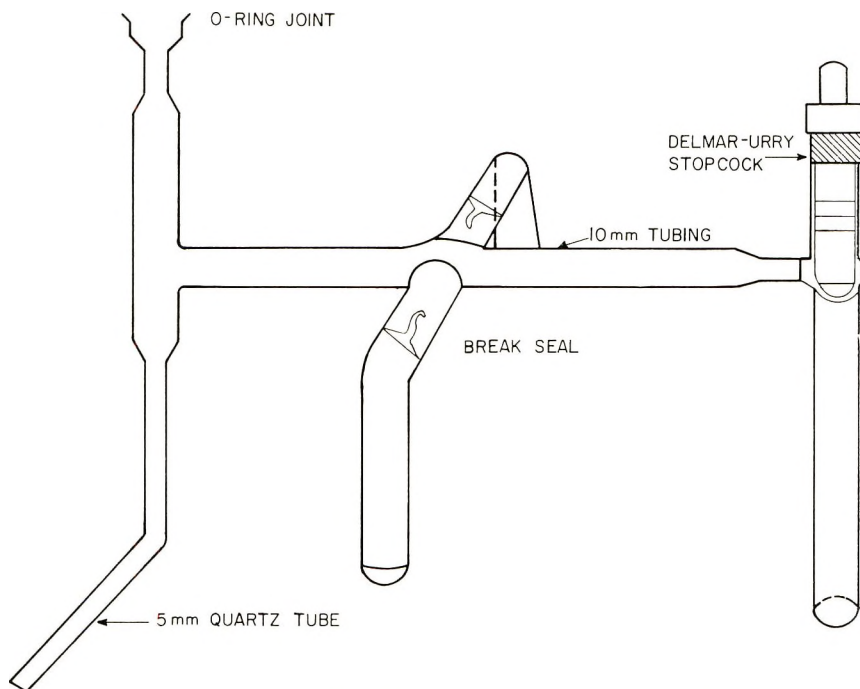


Fig. 1. Apparatus for determining electron spin resonance spectra.

the Pyrex tube to which it was connected. The Pyrex tube was placed against the ^{60}Co source and the quartz tube shielded from irradiation. When irradiation was completed, the apparatus was inverted and the sample shaken down into the quartz tube ready for measurement of the ESR spectra.

RESULTS AND DISCUSSION

After irradiation with ^{60}Co the highly porous poly(methyl methacrylate) gave the same ESR signal as growing methyl methacrylate chain radicals. When S was admitted to the evacuated sample the signal changed rapidly to one characteristic of a sulfonyl radical. The system was then evacuated; the signal being observed continuously during the evacuation. There was no return of the methacrylate spectrum, only a very slow decline of the sulfonyl radical signal. The signals are shown in Figure 2.

The experiment was repeated, and M vapor was admitted after the sulfonyl radical was formed. There was no change in the spectrum shape; there was only a gradual decay in the intensity.*

* High pressures of S or M led to rapid decay of the ESR signal presumably because the polymer was plasticized increasing the mobility of the radicals leading to an accelerated decay of the signal from the sulfonyl radical. As a check on this hypothesis, isoprene vapor was added to a sample of the methacrylate radical. A more complex signal was rapidly obtained (Fig. 2c) indicating that isoprene could both diffuse to the site and undergo addition.

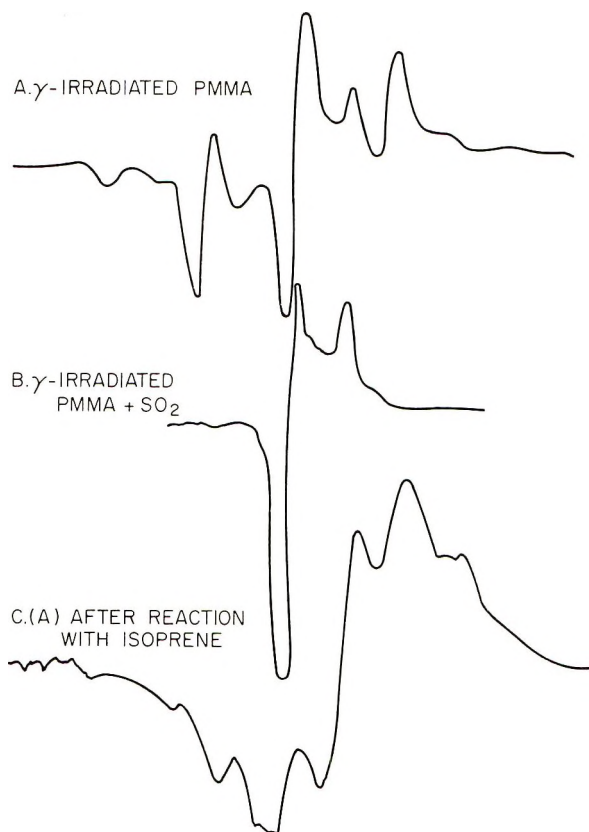
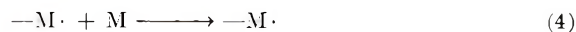


Fig. 2. ESR spectra of PMMA.

It was possible that S vapor could diffuse more readily than M to the radical site in a solid polymer. This might account for the failure of M vapor to alter the shape of the signal from the sulfonyl radical. However the results obtained with isoprene argue strongly against this possibility.

These observations indicate that the growing chain of poly(methyl methacrylate) in sulfur dioxide exists predominately as a solvated radical, $-\text{MS}\cdot$, and the addition of monomer must either involve a reversal of solvation followed by addition, [eqs. (3) and (4)] or that polymerization must proceed via an insertion mechanism, [eq. (5)]. This latter is the equivalent of saying that the S of solvation participates in the transition state during addition, but no specific geometry or type of bonding is implied.



It has been suggested that if the transition state of a radical chain propagation involves a solvent molecule that change in the stereochemistry of the resulting polymer should be expected. On the other hand, the work of

Fox and Schnecko⁵ shows that free-radical polymerization of M in a variety of solvents has no significant effect on the polymer stereochemistry and the steric triad composition is determined only by polymerization temperature. Thus at a given temperature if polymerization follows eq. (3) and (4),

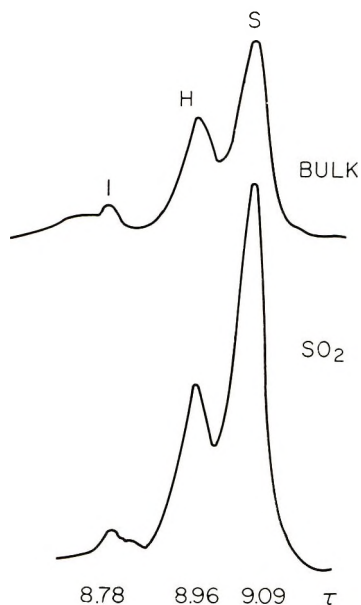


Fig. 3. NMR spectra of PMMA.

NMR analysis of polymer prepared in S solution should be the same as for polymer prepared in bulk.

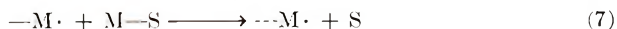
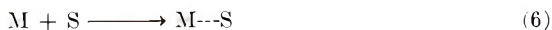
NMR spectra as shown in Figure 3 actually show significantly greater syndiotactic triad content of the solution polymers. Table I gives values

TABLE I
Steric Triads of Methyl Methacrylate Polymers

Polymerization temp, °C	Solvent	Triad, %	
		<i>H</i>	<i>S</i>
25	SO ₂	26	64
25	None	30	55
-35	SO ₂	29	71
-35	None	35	64

for triad content calculated by the method of Bovey.⁷ An alternate mechanism for changes in stereochemistry through solvent interaction might be for the monomer to form a complex with the solvent. The altered geometry of the incoming monomer would influence the orientation in which it

could add to the radical. This mechanism could be expressed by the combination of eqs. (3), (6), and (7):



where $M\cdots S$ is a monomer-solvent complex and fit both ESR and NMR data. It seems most unlikely, however, that this mechanism is pertinent to the present case. S is known to form charge transfer complexes with donor molecules such as butene, vinyl ethers, and dienes, but monomers with electron-withdrawing substituents such as acrylonitrile and methyl methacrylate are generally considered to have donor properties which are too low to form such complexes. An examination of the ultraviolet spectra of M and S and their mixtures in heptane solution did show slight shifts in wavelength of the absorption maximum and extinction coefficient, which may indicate very weak interaction at the limits of the ability to detect in unpressurized systems which are used.

A third mechanism for altering the stereochemistry of the polymer would be for monomer residues in the growing chain to solvate without involving the radical center. Altered geometry of the chain caused by solvent interactions could then influence the geometry of the incoming monomer, similar to the proposal of Szwarc.⁸ Again, there is no reason for believing that S should have a greater effect on the poly(methyl methacrylate) chain than the other solvents which have been evaluated by Fox.

It therefore appears that, during the free-radical polymerization of M in S as solvent, the growing radical is solvated with S and that S is involved in the transition state for chain propagation.

The authors wish to thank the Division of Isotope Development of the Atomic Energy Commission for support of this work under Contract AT(40-1)-2513, Task No. 13.

References

1. J. J. Kearney, V. Stannett, and H. G. Clark, in *Macromolecular Chemistry Prague 1965* (*J. Polym. Sci. C*, **16**), O. Wichterle and B. Sedláček, Eds., Interscience, New York, 1968, p. 3441.
2. C. F. Bamford, M. S. Blackie, and C. H. Finch, *Chem. Ind. (London)*, **1962**, 1763.
3. G. F. Sar tee, R. H. Marchessault, H. G. Clark, J. J. Kearney, and V. Stannett, *Makromol. Chem.*, **73**, 177 (1964).
4. I. Rosen, P. H. Burleigh, and J. F. Gillespie, *J. Polym. Sci.*, **54**, 31 (1961).
5. T. G. Fox and H. W. Schnecko, *Polymer*, **3**, 575 (1962).
6. Z. Kuri and H. Ueda, *J. Polym. Sci.*, **50**, 349 (1961).
7. F. A. Bovey and G. V. D. Tiers, *J. Polym. Sci.*, **54**, 173 (1960).
8. M. Szwarc, *Chem. Ind. (London)*, **1958**, 1589.

Received September 21, 1971

Polyesters Containing Bicyclo[2.2.2]octane and Bicyclo[3.2.2]nonane Rings

LUDEK TAIMR* and JAMES G. SMITH, *Department of Chemistry, University of Waterloo, Waterloo, Ontario, Canada*

Synopsis

Polyesters containing bicyclo[2.2.2]octane and bicyclo[3.2.2]nonane rings are prepared from 1,4-bis(carboethoxy)bicyclo[2.2.2]octane, 1,4-bis(hydroxymethyl)bicyclo[2.2.2]octane and the 1,5-disubstituted bicyclo[3.2.2]nonane analogs. These polyesters are compared to the related polymers containing 1,4-phenylene and *trans*-1,4-cyclohexylene rings in terms of their melting point, thermal stabilities and oxidative stabilities. The lower symmetry of the bicyclo[3.2.2]nonane ring produces lower-melting polymers than the other ring systems. The remaining three rings are approximately equivalent in their effect on the melting point of a polymer provided that no more than one bicyclo[2.2.2]octane ring is present per polymer repeat unit. Two such rings produce a higher-melting polymer than any other combination. Both the thermal and oxidative stabilities of the polyesters is improved by the presence of the bicyclo rings. This is attributed to the rings providing an approximation of a ladder polymer.

One of the most important properties of a linear polymer is its melting point. Its importance and ease of determination have stimulated numerous attempts to correlate this property with the chemical structure of the repeat unit. Bunn¹ has reviewed the structural factors affecting the melting point and suggests that interchain forces, flexibility (or rigidity) of the polymeric repeat units, and the symmetry of this unit are the most important.

Within a given class of polymers, the interchain forces may be considered approximately constant and the interplay of rigidity and symmetry becomes apparent. While several studies have been reported on polyamides, polyesters have been of less interest probably due to their generally lower melting points and consequent lower commercial interest. Korshak's study² of the aliphatic polyesters is the most extensive and, of course, the poly(methylene terephthalates),^{2,3} the polyesters of *p*-xylylene glycol^{4,5} and 1,4-cyclohexanedimethanol⁵ are additional examples.

Our present study stems from this last example in which the combination of symmetry and rigidity of the *trans*-1,4-cyclohexanedimethanol ring was considered responsible for the high melting points observed for the derived polyesters. It seemed appropriate to examine the effect of other

* Postdoctoral fellow from the Institute of Macromolecular Chemistry of the Czechoslovak Academy of Sciences, Prague, Czechoslovakia.

rigid cyclic compounds whose structure closely resembled that of 1,4-cyclohexanedimethanol.

The bicyclo[2.2.2]octane ring system seemed admirably suited for this purpose. A diol such as 1,4-bis(hydroxymethyl)-bicyclo[2.2.2]octane has a rigid symmetrical structure of similar steric size to that of 1,4-cyclohexanedimethanol with the added advantage that ring inversion which can convert the *trans*-diaxial conformer of the latter diol to the *trans*-diequatorial form cannot occur. Furthermore, polyesters from bicyclo[2.2.2]octane-1,4-dicarboxylic acid can be prepared, whereas *trans*-1,4-cyclohexanedicarboxylic acid is known to isomerize during preparation of polyesters.⁶

As an additional point of interest, the related polymers containing bicyclo[3.2.2]nonane rings were also prepared. In this series, the rigidity of the ring remained the same, but the symmetry was reduced. As models show, functional groups attached to the bridgehead carbons of the bicyclo[2.2.2]octane ring are arranged at 180° to one another; in the bicyclo[3.2.2]nonane ring, these same groups form an angle of approximately 150°.

Some information already exists on polymers from the bicyclo[2.2.2]octane derivatives.^{7,8} This is contained in the patent literature and is directed towards high-melting polymers of potential commercial value. Some overlap between the present study and these earlier reports do exist and a few discrepancies have been noted. These have been discussed elsewhere.⁹

EXPERIMENTAL

With the exception of the bridgehead derivatives of bicyclo[2.2.2]octane and bicyclo[3.2.2]nonane, all polymer intermediates were obtained from commercial sources. The bicyclo derivatives were synthesized by well-documented procedures.^{10,11}

All the polymers examined in this study were prepared in approximately 1-g quantities with the use of titanium tetrabutoxide as catalyst except for poly(ethylene terephthalate), for which a zinc acetate-antimony pentoxide catalyst was employed. Polymers melting below 200°C were prepared by a melt-phase polymerization,¹² while polymers which melted above 200°C were prepared by the solid-phase polymerization procedure.¹³ In both cases, the polymerization time was 2-3 hr and the temperature 260-280°C. The heat source was an electrically heated, temperature controlled, drilled aluminum block, and the reaction vessel was a test tube equipped with a head with outlets for nitrogen and vacuum.

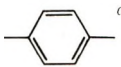
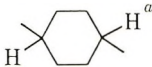
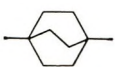
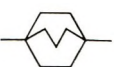
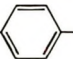
Since it was desired to compare the melting points with those of related polyesters,⁵ the polymer samples were crystallized in acetone and their melting points determined in the manner previously described. To obviate the possibility of annealing during solid-phase polymerization producing an artificially high melting point,¹⁴ two consecutive melting points were run on the same sample of each polyester prepared in this fashion.

Inherent viscosities were determined in 60:40 phenol-tetrachloroethane solvent. Thermal stabilities were measured under nitrogen on a duPont 950 thermogravimetric analyzer at a heating rate of 15°C/min on 9 ± 1 mg samples. Oxidative stabilities were assessed on the same instrument by measuring the weight loss as a function of time in an oxygen atmosphere at 340°C, again for a 9 ± 1 mg sample.

RESULTS AND DISCUSSION

Table I compares the melting point of polymers which differ only in the nature of the ring present in the diol portion of the repeat unit, i.e. 1,4-phenylene, *trans*-1,4-cyclohexylene, 1,4-bicyclo[2.2.2]octane and 1,5-bicyclo[3.2.2]nonane. It is readily seen that the first three rings all have approximately the same effect on the melting point. No added increment in melting point is obtained on replacing any rigid, symmetrical ring system with the bicyclo[2.2.2]octane ring.

TABLE I
Melting Point of Polyesters: Comparison of the
Diol Ring Structure D, HOCH₂-D-CH₂OH

Diacid	Mp of polyester, °C			
				
HO ₂ C-(CH ₂) ₄ -CH ₂ I	78-81	122-124	99-101 (0.36) ^b	80-82 (0.40)
HO ₂ C-(CH ₂) ₆ -CO ₂ I	79-82	94-96	74-77 (0.60)	NX ^c
HO ₂ C-(CH ₂) ₇ -CO ₂ H	63-66	45-50	34-37 (0.36)	NX
HO ₂ C-(CH ₂) ₈ -CO ₂ H	88-93	72-78	63-65 (0.55)	NX
HO ₂ C-  -CO ₂ H	263-272	312-318 (0.33)	304-307 (0.18)	150-170 (0.18)

^a Data are from Kibler et al.⁴

^b Inherent viscosity η_{inh} in parentheses.

^c Non crystallizable gum.

A strict structural comparison of ring system would require that the bicyclo[2.2.2]octane I ring be compared to the *cis*-1,4-cyclohexylene ring in the boat conformation II. However, it is most unlikely that the *cis*-1,4-



cyclohexanedimethanol is constrained in the boat conformation by the polymer chain and much more likely that it adopts the chair conformation with its lower symmetry. For this reason, the comparison is made between the two rings of similar symmetry and rigidity, *trans*-1,4-cyclohexylene and bicyclo[2.2.2]octane.

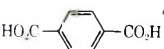

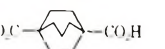

Considering only those polyesters derived from aliphatic dicarboxylic acids, the polymers containing *trans*-1,4-cyclohexanedimethanol melt uniformly higher than those containing the other ring systems. The slightly compressed conformation available to the *trans*-diol moiety⁵ probably accounts for this, since such a possibility is not available to the rigid bicyclo[2.2.2]octane ring.

In general, the flexible acid segment controls the polymers' melting points which all tend to be low. Even decreasing the symmetry of the diol unit by using a bicyclo[3.2.2]nonane ring reduces the melting point only slightly. However, considerable difficulty in crystallizing these polymers does reflect their lower tendency to form ordered arrangements.

If the acid segment is itself rigid (terephthalic acid), the polyester melting point takes a sharp increase and the symmetry of the diol segment now exerts considerable influence on the melting point. Note that the terephthalate/1,5-bis-hydroxymethylbicyclo[3.2.2]nonane polymer melts at a much lower temperature than any of the other three ring analogs.

Turning to the polymers prepared from the "bicyclo acids" (Table II), a somewhat different behavior can be observed. If the aliphatic diol contains an even number of carbon atoms, there is again little difference between an aromatic ring and a bicyclo[2.2.2]octane ring insofar as the melting point is concerned. However, polyesters prepared from diols with an odd number of carbon atoms and terephthalic acid melt at a higher temperature than the analogous polyesters with a bicyclo[2.2.2]octane ring replacing the aromatic one. Interestingly enough, a similar behavior was noticed⁵ in the comparison of polyesters from *p*-xylylene glycol and *trans*-1,4-cyclohexanedimethanol.

TABLE II
Melting Point of Polyesters: Comparison of the
Diacid Ring Systems, HO₂C—R—CO₂H

Diol unit	Mp of polyesters, °C		
			
HO—(CH ₂) ₂ —OH	258–262	b	b
HO—(CH ₂) ₃ —OH	225	140–143 (0.44) ^c	NX ^d
HO—(CH ₂) ₄ —OH	225	233–238 (0.56)	127–130 (0.57)
HO—(CH ₂) ₅ —OH	136–140	54–56 (0.22)	NX ^d
HO—(CH ₂) ₆ —OH	157	144–147 (0.54)	50–55 (0.56)
	312–318	310–315 (0.40)	188–192 (0.26)

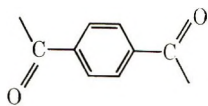
^a Data are from Smith et al.³

^b Polymer did not form under the usual preparative conditions.

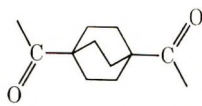
^c Inherent viscosity η_{inh} in parentheses.

^d Noncrystallizable gum.

The higher melting point of the terephthalate polymers can be rationalized by considering the entire acid unit as a rigid symmetrical structure III



III

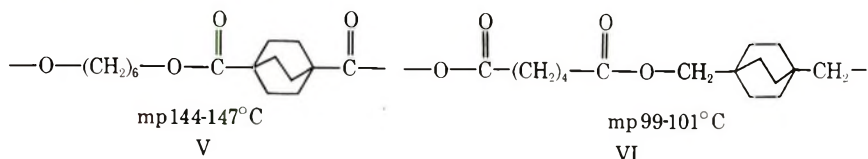


IV

due to the overlap of the π -orbitals of the aromatic ring and the carbonyl groups.^{15,16} Such cannot be generally true of the bicyclo ring; although the ring itself is a rigid unit, the carbonyl groups would appear to be free to rotate. However, the fact that some polymers containing the bicyclo acid have melting points equivalent to their terephthalate analog would indicate that a preferred orientation of the bridge head carbonyl groups probably exists. This can be attributed to the dipole-dipole repulsion of the two carbonyl groups which would tend to orient them as shown in IV, an arrangement resembling that of the terephthalate unit.

Obviously, this dipole repulsion is a weaker orienting effect than that operating in the aromatic system. When the bicyclo rings are coupled through an odd-carbon diol it evidently ceases to be fully effective and a lower melting polymer is generated.

A similar explanation accounts for the difference in melting point of the pair of polymers V and VI. Each unit has the same number and kind of



structural units, the difference being the arrangement of the $-\text{CH}_2-\text{O}-\overset{\text{O}}{\parallel}{\text{C}}-$ link. If the carbonyl group of this link is attached to a rigid symmetrical ring, the melting point is appreciably higher than if attached to a flexible polymethylene segment. The dipole-dipole repulsions of the carbonyl groups are sufficient to orient these groups provided the intervening unit is itself rigid. In the case of the polymethylene chain, the orienting influence is counteracted by the flexible connecting chain.

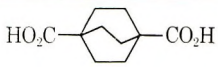
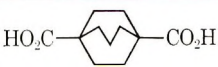
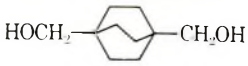

Again, as Table II shows, the less symmetrical bicyclo[3.2.2]nonane ring produces lower melting polymers. But here the effect is quite pronounced in all the examples which were obtained crystalline.

Table III shows the effect of combining two rigid bridged ring systems in a polymer repeat unit.

The inherent viscosities of these polymer compositions would indicate that the melting ranges obtained are somewhat less than the equilibrium melting temperatures.¹⁷ Unfortunately, the limited amounts of monomers precluded an optimization of polymerization conditions. However, the differences observed in these melting temperatures is sufficiently large that certain conclusions can be made. The four different repeat units can be considered to be of equivalent rigidity and differ only in the symmetry of the diol and/or diacid components. A combination of two bicyclo[2.2.2]-

octane rings produces a polymer of remarkably high melting point considering that it is completely free of any aromatic component. Replacement of one of these rings by a less symmetrical bicyclo[3.2.2]nonane ring produces a sharp drop in melting point. Note that it is immaterial whether the ring of the diol or of the diacid segment is replaced; either polymer has about the same melting point. Naturally, a combination of two bicyclo[3.2.2]nonane rings again produces a sharp drop in melting point, a further reflection of the importance of symmetry.

TABLE III
Melting Point of Bridged Polyesters Having Different
Diol and Diacid Units

Diol unit	Diacid unit			
				
	Mp, °C	η_{inh}	Mp, °C	η_{inh}
	380-390	0.25	225-227	0.24
	244-246	0.21	172-177	0.27

A few polymers derived from triptycene have been reported.¹⁸ Among this group, the terephthalate-bis(hydroxymethyl)triptycene polymer melts at 350-380°C compared with 304-307°C for the terephthalate-bis(hydroxymethyl)bicyclo[2.2.2]octane polymer. The structural difference between these two polymers is essentially the three benzene rings fused to the bicyclo[2.2.2]octane ring. The additional rigidity conferred upon the repeat unit by this structure, must account for the higher melting point of the triptycene polymer.






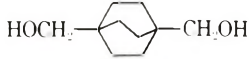

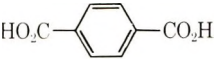

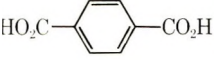

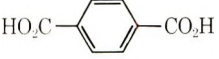


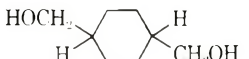
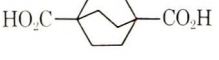
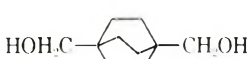
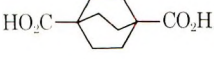
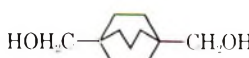

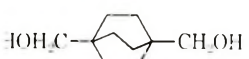


Thermal Stability

Because of the limited amounts of the polyesters available, the thermal stability has been measured by thermogravimetric analysis under nitrogen. These stabilities are summarized in Table IV in terms of the temperatures at which the polymer sample has lost 10% and 50% of its original weight.

The polymers fall in three groups on the basis of these stabilities. The first group, which is characterized by the presence of a single ring in the unit, shows decomposition temperature (T_{10} and T_{50}) of ca. 400°C and 420-430°C.

The second group, with two rings in the repeat unit of which one may be a bridged ring, shows a somewhat higher stability. Here T_{10} and T_{50} values of 420-430°C and 440-450°C are observed. Polymer units based on 1,4-cyclohexanedimethanol appear somewhat less stable than their bridged analogs.

TABLE IV
 Thermal Stability of the Polymers

Diacid unit	Diol unit	Decomposition temp, °C ^a	
		T ₁₀	T ₅₀
	HOCH ₂ —CH ₂ OH	404	428
	HOCH ₂ —(CH ₂) ₂ —CH ₂ OH	395	419
	HOCH ₂ —(CH ₂) ₄ —CH ₂ OH	398	422
	HOCH ₂ —(CH ₂) ₄ —CH ₂ OH	400	421
	HOCH ₂ —(CH ₂) ₂ —CH ₂ OH	392	412
HO ₂ C—(CH ₂) ₄ —CO ₂ H		398	433
HO ₂ C—(CH ₂) ₄ —CO ₂ H		412	447
		414	430
		438	461
		430	444
		422	445
		452	480
		455	477
		455	482
		457	477

^a Temperatures at which 10% (T₁₀) and 50% (T₅₀) of the initial sample weight has been lost.

The third group, showing the greatest thermal stabilities, are those containing two bridged rings in the same repeat unit. In this case, the T_{10} and T_{50} values are 455°C and 480°C.

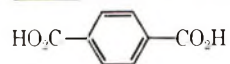
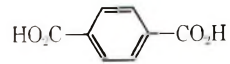

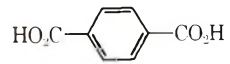
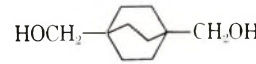
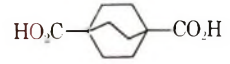
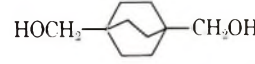
This behavior is most simply interpreted by considering that the insertion of rings, and especially bicyclo rings, into a polymer chain brings the structure to a closer approximation of an ideal ladder polymer. As the concentration of rings in the chain rises, the chances of thermal decomposition cleaving the appropriate bonds in the polymer chain to produce volatile fragments decreases.

Oxidative Stability

The relative oxidative stability of these polymers was also assessed by a thermogravimetric method. Here the weight loss as a function of time was measured in an atmosphere of oxygen (and in nitrogen) at 340°C. The temperature was chosen to minimize thermal decomposition yet be a sufficiently high temperature to obtain reasonable instability in oxygen.

As the values summarized in Table V show, an oxygen atmosphere does accelerate the loss of weight of all polymers studied. The effect of two bridged rings in improving the thermal stability is also apparent in these isothermal weight loss determinations. Even the weight loss in oxygen is reduced by the presence of these rings.

TABLE V
Oxidative Stability of Polymers at 340°C

Diacid unit	Diol unit	Atmosphere	Decomposition time, min ^a		
			t_{10}	t_{25}	t_{50}
	HOCH ₂ —CH ₂ OH	N ₂	50	154 ^b	—
		O ₂	2	4	12-14
		N ₂	14	23	39
		O ₂	3	5	11
		N ₂	73	163 ^b	—
		O ₂	7	21	80
		N ₂	310 ^b	780 ^b	—
		O ₂	8	27	100

^a Time required for the sample to lose 10% (t_{10}), 25% (t_{25}) or 50% (t_{50}) of its original weight.

^b Weight loss was essentially linear and these values were estimated by extrapolation.

In the case of the 1,4-cyclohexanedimethanol polymer, the tertiary hydrogens present on the ring have been considered¹⁹ the most easily oxidizable portion of the repeat unit. While this sensitive spot is absent in the polymers containing the bridged rings, it is more reasonable to attribute

the improved oxidative stability once again to the approximation of a ladder structure by inserting these bicyclo[2.2.2]octane rings in the chain.

The authors wish to acknowledge the financial support of the Defence Research Board of Canada. The authors are indebted to Drs. Alan Bell and Charles J. Kibler of the Tennessee Eastman Co., Kingsport, Tennessee who arranged for the determination of the inherent viscosities of the polymer samples and to Mr. R. Needham who determined the stabilities of many of the polymer samples.

References

1. C. W. Bunn, *J. Polym. Sci.*, **16**, 323 (1955).
2. V. V. Korshak and S. V. Vinogradova, *Polyesters*, Pergamon Press, New York-London, 1965, pp. 313-332.
3. J. G. Smith, C. J. Kibler, and B. J. Sublett, *J. Polym. Sci. A-1*, **4**, 1851 (1966) and references cited therein.
4. V. V. Korshak and S. V. Vinogradova, *Bull. Acad. Sci. U.S.S.R., Div. Chem. Sci.* (1959), 138 (Engl. transl.).
5. C. J. Kibler, A. Bell, and J. G. Smith, *J. Polym. Sci. A*, **2**, 2115 (1964).
6. J. C. W. Chien and J. F. Walker, *J. Polym. Sci.*, **45**, 239 (1960).
7. W. H. Watson, U.S. Pat. 3,256,241 (June 14, 1966).
8. M. J. Hogsd and W. H. Watson, U.S. Pat. 3,337,498 (August 22, 1967).
9. L. Taimr and J. G. Smith, *J. Polym. Sci. A-1*, **9**, 239 (1971).
10. J. D. Roberts, W. T. Moreland, Jr., and W. Fraser, *J. Amer. Chem. Soc.*, **75**, 637 (1953).
11. L. Taimr and J. G. Smith, *Can. J. Chem.*, **48**, 1219 (1970).
12. W. R. Sorenson and T. W. Campbell, *Preparative Methods of Polymer Chemistry*, 2nd ed., Interscience, New York, 1968, pp. 131-134.
13. C. J. Kibler, A. Bell, and J. G. Smith, U.S. Pat. 2,901,466 (December 22, 1955).
14. D. L. Nealy, T. G. Davis and C. J. Kibler, paper presented to the Division of Polymer Chemistry, American Chemical Society Meeting, Houston, Texas, February 1970.
15. E. F. Izard, *J. Polym. Sci.*, **9**, 35 (1952).
16. C. W. Bunn, *J. Polym. Sci.*, **16**, 323 (1955).
17. K. Veberreiter, G. Kanig, and A. S. Brenner, *J. Polym. Sci.*, **16**, 53 (1955).
18. E. Hoffmeister, J. E. Kropp, T. L. McDowell, R. H. Michel, and W. L. Rippie, *J. Polym. Sci. A-1*, **7**, 55 (1969).
19. E. V. Martin and C. J. Kibler, in *Man-Made Fibers*, Vol. 3, H. F. Mark, S. M. Atlas, and E. Cernia, Eds., Interscience, New York, 1968, p. S3.

Received July 6, 1970

Revised November 6, 1970

Polyesters from 12-Hydroxymethyltetrahydroabietic Acid and 12-Hydroxymethyltetrahydroabietanol

MAGED A. OSMAN and C. S. MARVEL, *Department of Chemistry, The University of Arizona, Tucson, Arizona 85721*

Synopsis

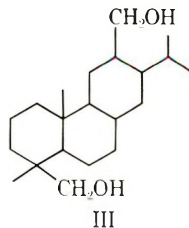
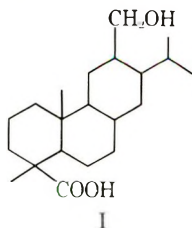
The polyester of 12-hydroxymethyltetrahydroabietic acid was prepared by the self-condensation of the hydroxy acid (I) and from its methyl ester (II). The condensation reaction was studied and different catalysts investigated. The inherent viscosity of the polymers were measured and their DTA diagrams taken. A polyurethane as well as different polyesters of the diol (III) with methylene di-*p*-phenyl diisocyanate, terephthalic, adipic, suberic, and sebacic acids were synthesized. Mixed polyesters and polyamide ester were also prepared. The properties of the above described polymers were investigated and their behavior on DTA reported.

INTRODUCTION

The oleoresin is the basis of the extensive naval stores industry throughout the world. Rosin is the most important of this group of products which also includes tar, pitch, turpentine, pine oil, and other terpenes. World production of rosin during the last decade was over two billion pounds per year, about half of which originated from the United States. The resin acids amount to 90% of the rosin and thus provide a good natural resource of raw material. Some trials¹⁻⁷ to obtain useful polymers from these products have been reported.

RESULTS AND DISCUSSION

Three rosin derivatives were investigated viz., 12-hydroxymethyltetrahydroabietic acid⁸ (I), methyl 12-hydroxymethyltetrahydroabietate⁹ (II), and 12-hydroxymethyltetrahydroabietanol¹⁰ (III).*



* These products were supplied by Dr. Glen Hedrick of the Naval Stores Research Laboratory, Olustee, Florida.

TABLE I
 Self-Condensation of I

Catalyst	Temp, °C	Time, hr	η_{inh}^a
—	280	66	0.08
—	300	20	0.09 ^b
H ₃ PO ₄	260	20	0.05
H ₃ PO ₄	230	44	0.04
Mg	240	44	0.08

^a The viscosity measurements were carried out in an Ostwald viscometer at $31 \pm 1^\circ\text{C}$. Solutions of 0.25% polymer in benzene were used.

^b Sample a, Table IV.

The self-condensation of compound I was carried out in melt according to the standard method described in the literature.^{11a} Table I shows the results obtained.

During the condensation a white solid sublimed on the walls of the condensation tube. In a typical experiment the monomer was heated under nitrogen at 250°C for 2 hr and vacuum was then slowly applied until 7 mm Hg was reached after 1 hr. The melt was heated under these conditions for 1 hr more, then the pressure reduced to 0.05 mm Hg and the temperature kept at 280°C for a further 43 hr. Benzene was used to extract the sublimate, and the benzene-insoluble fraction, which amounted to 10% of the starting material, was found by infrared and melting point data to be the original hydroxy acid (I). The benzene extract was evaporated, the residue redissolved in tetrahydrofuran and precipitated in water. This substance was found to be a low molecular weight polymer of $\eta_{inh} = 0.03$ and amounted to 41% of the starting material. Its infrared spectrum showed the presence of the expected functional groups, (ester, acid, alcohol). The unsublimed material, amounting to 45%, had an inherent viscosity of 0.08, and the infrared spectrum showed the presence of the expected functional groups of polyester. The number of endgroups^{11b} was determined, and the corresponding amount of freshly distilled methylene di-*p*-phenyl diisocyanate (IV) was added. Reaction with the diisocyanate was carried out both in melt at 230°C and also in refluxing toluene. In both cases no increase in viscosity was observed. It was concluded that chain-growth termination was not due to the loss of the functional groups in side reactions but probably due to steric factors.

The polyester of I was a hard, glass-clear product, whose films were brittle. It was soluble in benzene, tetrahydrofuran, methylene chloride, chlorobenzene, partially soluble in dimethylformamide and petroleum ether, but insoluble in methanol. Sample a showed two DTA peaks at 164°C and 218°C .

The same polymer was obtained from the self-condensation of the methyl ester (II) by the melt method. Table II shows the results obtained.

A polyurethane (sample c, Table IV) was obtained by refluxing the diol (III) with the diisocyanate (IV) for 24 hr in dry dimethylformamide under

TABLE II
 Self-Condensation of II

Catalyst	Temp, °C	Time, hr	η_{inh}^a
—	200	3	No polymerization
Mg	230	22	No polymerization
<i>p</i> -Toluenesulfonic acid	280	64	0.04 (benzene)
Tetraisopropyl titanate	220	68	0.14 (THF) ^b

^a The viscosity of 0.25% polymer solution was measured in an Ostwald viscometer at $31 \pm 1^\circ\text{C}$. Sample b showed two peaks in the DTA diagram, one at 168°C and one at 240°C .

^b Sample b, Table IV.

 TABLE III
 Polyesters of III with Aliphatic Dicarboxylic Acids

Acid	Method used	Catalyst	Temp, °C	Time, hr	η_{inh}^a
Adipic	Solution	Methanesulfonic acid	110 (Toluene)	71	0.40
Suberic	Solution	"	110 (Toluene)	71	0.24 ^b
Suberic	Melt	"	250	25	0.16
Dimethyl sebacate	Melt	Tetraisopropyl titanate	270	40	0.18 ^c

^a The viscosities of 0.25% solutions in benzene were measured in an Ostwald viscometer at $31 \pm 1^\circ\text{C}$.

^b Sample e, Table IV.

^c Sample f, Table IV.

 TABLE IV
 Analyses

Sample	C, %		H, %		N, %		O, %	
	Calcd	Found	Calcd	Found	Calcd	Found	Calcd	Found
a	79.19	79.15	10.76	10.69			10.05	10.18
b	79.19	78.72	10.76	10.76			10.05	10.05
c	73.69	75.05	7.90	8.56	4.77	4.99	13.63	10.84
d	76.95	76.82	8.91	8.91			14.14	14.41
e	75.60	75.76	10.50	10.52			13.89	13.63
f	76.18	76.16	10.72	10.80			13.10	13.15
g	72.64	73.31	7.50	7.84			19.85	18.59
h	71.08	70.84	10.10	10.19	4.25	3.19	14.57	14.45

nitrogen. The polyurethane was soluble in DMF and precipitated in methanol. Its inherent viscosity in dimethylformamide at 31°C was 0.14. It showed two DTA peaks, one at 80°C and one at 163°C .

The polyterephthalate of (III) was prepared in two different ways. When III was condensed with dimethyl terephthalate in melt (230°C) for 24 hr, using tetraisopropyl titanate as a catalyst, a polymer having $\eta_{inh} = 0.17$ (benzene) was obtained. Condensing III with terephthaloyl chloride

(crystallized from dry hexane) in refluxing chlorobenzene under nitrogen for 4 hr gave a polymer (d, Table IV) with $\eta_{inh} = 0.2$ (benzene) which showed peaks at 50°C and 160°C in the DTA diagram. When the latter condensation was carried out in melt (240°C/0.01 mm Hg, 10 hr), the polymer showed $\eta_{inh} = 0.13$ in benzene. Films of this polyester were also brittle. In order to get more plastic polyesters, the diol (III) was condensed with adipic acid, suberic acid and dimethyl sebecate respectively. Table III shows the results obtained.

Films of the polyadipate were still brittle. It showed peaks at 72°C and 165°C in the DTA diagram. Solutions of the polysuberate and polysebacate were found to be promising as adhesives. The polysuberate (polymer e) showed peaks at 51°C and 107°C and the polysebacate (polymer f) at 52°C and 157°C in the DTA diagram. These polyesters are colorless, glassy, soft plastic materials which can be cut by a knife, soluble in benzene and could be precipitated in methanol.

Polyesters and polyamide esters were also prepared:



One mole of III was condensed with two moles of terephthaloyl chloride in refluxing chlorobenzene and the diacid chloride so obtained was reacted with ethylene glycol. The polyester (g) was precipitated in methanol and gave $\eta_{inh} = 0.10$ (benzene). When the chlorobenzene was driven off from a sample of polymer solution and the polymer melt heated for 24 hr at 250°C/0.01 mm Hg, the viscosity of the polymer could be raised to 0.14 (benzene). Sample g showed peaks at 74°C and 173°C in the DTA diagram.

Condensation of III with adipoyl chloride under the same conditions described above gave an acid chloride which was used for interfacial polymerization with hexamethylenediamine. The polyamide ester (h, Table IV) so obtained gave $\eta_{inh} = 0.28$ measured in *m*-cresol and showed one peak at 55°C in the DTA diagram.

EXPERIMENTAL

Monomers

12-Hydroxymethyltetrahydroabiatic acid (I). This acid was sparingly soluble in ether, ethanol, benzene, acetone, and chlorobenzene but soluble in tetrahydrofuran, acetic acid, and nitrobenzene. The purity was checked by TLC on silica gel with tetrahydrofuran as eluent.

Methyl 12-Hydroxymethyltetrahydroabietate (II). This compound was soluble in ethanol, tetrahydrofuran, and benzene and crystallized from acetone. Its purity was tested by TLC (silica gel/THF).

12-Hydroxymethyltetrahydroabietanol (III). This product was sparingly soluble in ether, benzene, and acetone but soluble in ethanol and tetrahydrofuran. The purity was checked by TLC (silica gel/THF).

Condensation in Melt

When the condensation was carried out in melt, the reactants were melted under dry nitrogen, brought to the desired temperature within 4–5 hr, then pressure gradually reduced until a pressure of 0.05–0.02 mm Hg was reached. The melt was heated under these conditions until the condensation was completed.

Condensation in Solution

In this method the reactants were heated in a refluxing solvent which forms an azeotrope with water. The refluxing solvent passed through a layer of CaH_2 to remove the water before returning to the reaction vessel.

Mixed Polyterephthalate of III with Ethylene Glycol

Terephthaloyl chloride (0.02 mole) was dissolved in 20 ml of dry chlorobenzene and 0.01 mole of III added. Dry nitrogen was passed through and the reaction mixture cautiously warmed until the evolution of HCl started. The solution was refluxed for 1.5 hr to complete the reaction, then 0.01 mole of ethylene glycol (distilled over Na) was added and the mixture refluxed for a further 4 hr under nitrogen. The solution was diluted to 10% and the polymer precipitated in methanol.

Mixed Polyamide Ester

Adipoyl chloride (0.02 mole), 40 ml of tetrachloroethylene, and 0.01 mole of III were gradually brought to reflux under dry nitrogen. The mixture refluxed for 1.5 hr, then cooled down to room temperature. A solution of 4.4 g of hexamethylenediamine in 50 ml of water was poured cautiously onto the previously prepared diacid chloride. The polymer formed on the interface was continuously removed and washed with aqueous ethanol.

This is a partial report of work done under contract with the Western and Southern Utilization Research and Development Divisions, Agricultural Research Service, U.S. Department of Agriculture, and authorized by the Research and Marketing Act of 1946. The contract is supervised by Dr. Glen Hedrick of the Naval Stores Research Laboratory.

References

1. J. R. Sowa and C. S. Marvel, *J. Polym. Sci. B*, **4**, 431 (1966).
2. R. Liepins and C. S. Marvel, *J. Polym. Sci. A-1*, **4**, 2003 (1966).
3. W. Fukuda and C. S. Marvel, *J. Polym. Sci. A-1*, **6**, 1050 (1968).
4. W. Fukuda and C. S. Marvel, *J. Polym. Sci. A-1*, **6**, 1281 (1968).
5. W. Fukuda, M. Saga, and C. S. Marvel, *J. Polym. Sci. A-1*, **6**, 1523 (1968).
6. M. Saga and C. S. Marvel, *J. Polym. Sci. A-1*, **7**, 2135 (1969).
7. M. Saga and C. S. Marvel, *J. Polym. Sci. A-1*, **7**, 2365 (1969).
8. K. K. Sugathan, W. A. Rohde, and G. W. Hedrick, *J. Chem. Eng. Data*, in press.
9. J. B. Lewis and G. W. Hedrick, *Ind. Eng. Chem. Product Res. Develop.*, **9**, 304 (1970).

10. B. A. Parkin Jr., H. B. Summers, R. L. Settine, and J. W. Hedrick, *Ind. Eng. Chem., Product Res. Develop.*, **5**, 257 (1966).

11. W. R. Sorenson and T. W. Campbell, *Preparative Methods of Polymer Chemistry*, 2nd ed., Interscience, New York, 1968, (a) p. 130 ff.; (b) pp. 154-55.

Received October 23, 1970

Chain Scission of Butyl Rubber by Nitrogen Dioxide. II. Photo-Oxidation as Function of Nitrogen Dioxide, Oxygen Pressure, and Temperature

H. H. G. JELLINEK and P. HRDLOVIC, *Department of Chemistry,
Clarkson College of Technology, Potsdam, New York 13676*

Synopsis

Studies of chain scission of butyl rubber (1.75% by weight of isoprene) have been extended. Experiments showing chain scission as function of various oxygen and nitrogen pressures, temperatures, and near-ultraviolet light intensity are presented. The experimental data agree with the mechanisms assumed in previous work or with elaborations of such mechanisms to include additional factors (ultraviolet radiation etc.). NO_2 retards chain scission in presence of near-ultraviolet light. Photo-oxidation in presence of relatively high and low nitrogen dioxide pressures, respectively, show experimental curves of opposite curvature; these data have also been evaluated in terms of mechanism. Arrhenius equations are presented for experiments related to the different reaction mechanisms.

Chain scission of butyl rubber by nitrogen dioxide in absence and presence of air was investigated previously.¹ In the present paper, the studies have been extended, including the effect of near ultraviolet radiation in presence of a range of nitrogen dioxide and oxygen pressures; these reactions have also been investigated over a range of temperatures (25–65°C).

It is known that ultraviolet radiation causes instantaneous isomerization and cyclization of diene polymers in the form of films and also in solution.^{2,3} Main-chain scission was observed in presence of sensitizers such as halogen nitrosopropane.⁴ Chien⁵ suggested that initiation in the case of photo-oxidation takes place via charge transfer complexes between oxygen and substrate. Recently, a paper on photo-oxidation of rubber was presented by Morand.⁶

EXPERIMENTAL

Apparatus

The high-vacuum (10^{-5} – 10^{-6} mm Hg) all-glass apparatus was described in previous papers.^{1,7} Intrinsic viscosity was measured in Ubbelohde dilution viscometers in benzene solutions at $25 \pm 0.02^\circ\text{C}$.

Materials

Butyl rubber was the same material as used previously¹ (Enjay Chem. Corp., Butyl 268, 1.75% by weight of isoprene). The polymer was purified by twice precipitating with methanol from 2% (w/v) benzene solutions.¹ The purified product was stored in a refrigerator (4°C) under nitrogen before use. After prolonged storage time, some aging took place. NO₂ was obtained from Matheson Comp. All solvents were of reagent-grade quality.

Procedure

Polymer films were prepared by casting 0.9 ml of a 3% (w/v) solution of butyl rubber in benzene onto flat glass plates (ca. 1.8 cm × 7.0 cm). These plates were then placed into boxes over dried silica gel and put into a desiccator. Fresh polymer solution was used for each casting. The solvent was slowly evaporated under standardized conditions (ca. 12 hr). The films were then dried in high vacuum for 24 to 30 hours at 50°C. Film thickness was on the average 20 μ.

Nitrogen dioxide pressure was obtained in the same way as described previously¹ by using the vapor pressure-temperature relationship. The NO₂ pressures were low enough so that practically 100% NO₂ was present (the percentage of N₂O₄ due to the equilibrium between NO₂ and its dimer is negligible). The NO₂ vapor pressures were as follows, at various temperatures, -56.5°C, 1.0 mm Hg of NO₂; -61.5°C, 0.5 mm Hg; -68.0°C, 0.2 mm Hg.

Temperatures were measured with a thermometer placed in the trap containing liquid NO₂. Its calibration was checked by the melting point of chloroform (-63.5°C). The equilibrium vapor pressure was established in the entire high-vacuum system, including a 3-liter storage flask, keeping liquid NO₂ at the respective temperature in the trap for 2 hr before closing it to the rest of the system. The reaction vessels were connected throughout the experiments to the 3-liter vessel, hence the NO₂ pressure remained constant. The vessels were thermostatted (±0.1°C), and arranged along the circumference of a circle with the light source in its center. The glass plates carrying the cast films were located exactly parallel and vertical to the light source by means of a telescopic device. Experiments were also performed in which 1 atm of dry air was introduced into the system. The ultraviolet light source was a Hanovia medium-pressure lamp (654 A 36); the reaction vessels were made of Pyrex glass (#7742) which cuts out all light below about 2800 Å. Films were at once degassed after exposure in order to avoid dark reactions due to absorbed gases.

Number-average chain lengths, \overline{DP}_n , were obtained from viscosity-average chain lengths as described previously.¹ In all cases, the films showed a weight increase of about 5% after exposure. It may be noted here that it is quite difficult to remove last traces of benzene from butyl rubber.

RESULTS

Figure 1 shows the degree of degradation α

$$\alpha = (1/\overline{DP}_{n,t}) - (1/\overline{DP}_{n,0})$$

as a function of reaction time t for constant NO₂ pressure (1 mm Hg) and various oxygen pressures at 35°C. Figure 2 gives the temperature relationship (35–65°C) of α versus t for 1 mm Hg of NO₂ and 13 mm of O₂.

Near-ultraviolet light alone does not lead to chain scission of butyl rubber in high vacuum near room temperature; neither could any changes in infrared spectra be detected under such conditions.

Figure 3 shows a comparison of α versus t in the presence and absence of ultraviolet radiation with 1 mm Hg of NO₂ at 35°C (no O₂). The irradiated films actually show less degradation than those exposed in presence of NO₂ only. An initially rapid degradation is followed in either case by a slower degradation rate.

The temperature dependence of α versus t in presence of 150 mm O₂ or 1 atm of dry air, respectively, and near-ultraviolet radiation (without NO₂) is presented in Figure 4.

Figure 5 gives results for degradation in presence of ultraviolet radiation, 1 atm of air, and various NO₂ pressures at 35°C. A curve for deg-

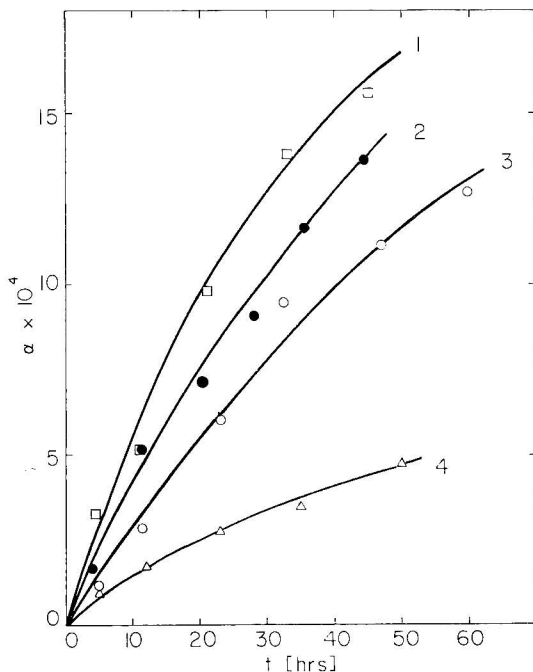


Fig. 1. Plots of α as a function of time for 1 mm Hg of nitrogen dioxide at 35°C and various oxygen pressures: (1) 125 mm Hg; (2) 69 mm Hg; (3) 39 mm Hg; (4) 13 mm Hg. The curves have been calculated according to eq. (7); the points are experimental data.

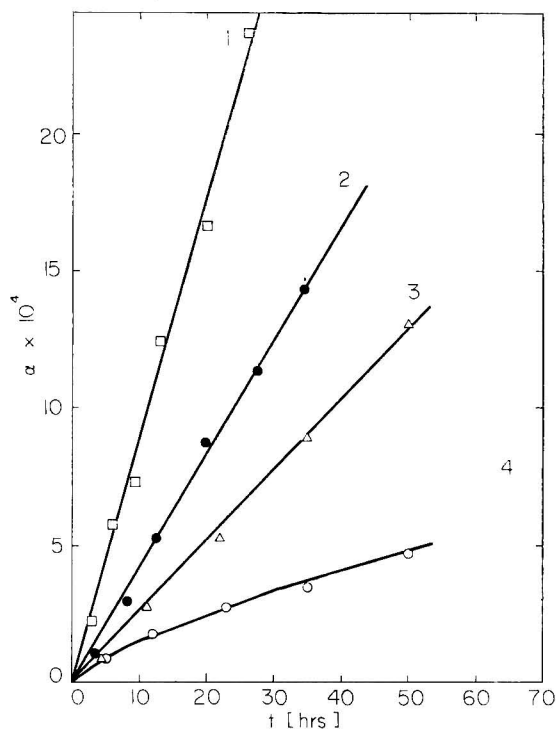


Fig. 2. Plots of α vs. time for 1 mm Hg of NO_2 , 13 mm Hg of O_2 for various temperatures: (1) 65°C; (2) 55°C; (3) 45°C; (4) 35°C.

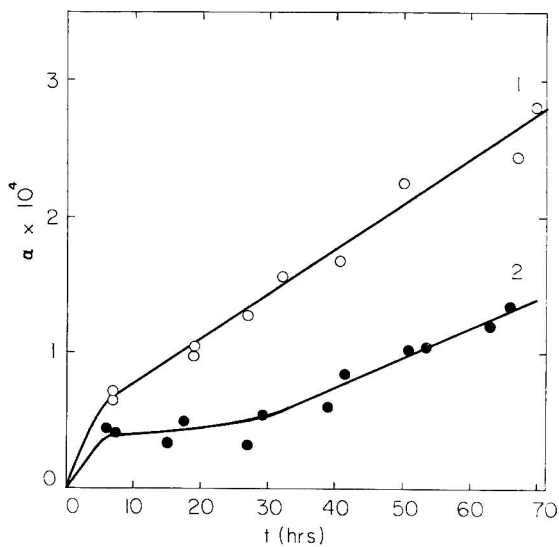


Fig. 3. Plots of α vs. t for 1 mm Hg of NO_2 at 35°C with and without near-ultraviolet irradiation (no O_2): (1) without, (2) with irradiation.

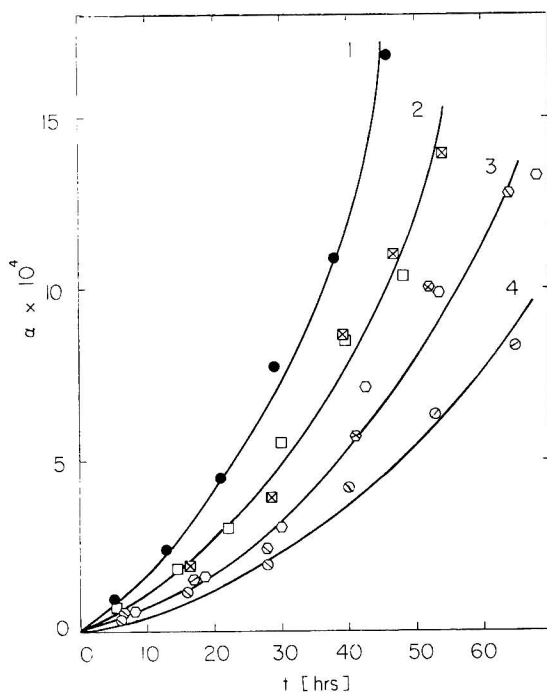


Fig. 4. Plots of α vs t for 150 mm Hg of O₂ or 1 atm. of dry air and near-ultraviolet irradiation at various temperatures: (1) 55°C, 150 mm Hg; (2) 45°C, (□) 150 mm Hg, (⊗) 1 atm. of dry air; (3) 35°C, (○) 150 mm Hg, (⊗) 1 atm. dry air; (4) 25°C, 150 mm Hg.

radiation without ultraviolet radiation, 1 atm of air and 1 mm of NO₂ is also shown. The temperature (35°C, 45°C, 65°C) dependence for degradation of films exposed to 0.2 mm Hg of NO₂, 1 atm of air, and ultraviolet radiation is depicted in Figure 6.

DISCUSSION

Degradation by NO₂ and O₂

A mechanism for the degradation of butyl rubber in presence of these two gases was presented in the previous paper.¹ However, the reaction was then only investigated as function of NO₂ pressure at constant oxygen pressure. Here, results are presented as function of oxygen pressure and temperature for constant NO₂ pressure (Fig. 1). The mechanism suggested previously¹ consists of three parts: contribution to chain scission (1) by O₂, (2) by NO₂, (3) by NO₂ and O₂ (synergistic action). Evaluation of this mechanism leads to,¹

$$\alpha = K_{\text{exp}}t + (K_{\text{exp}}''/K_{\text{VI}}^3)(1 - e^{-K_{\text{VI}}t}) \quad (1)$$

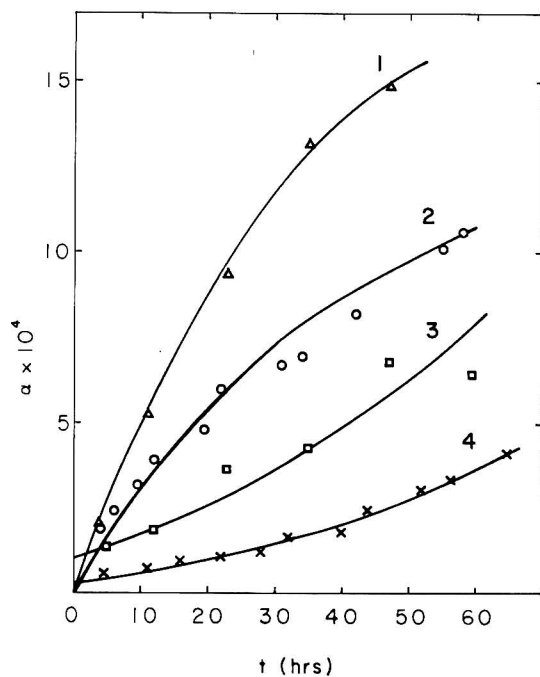


Fig. 5. Plots of α vs. t for 1 atm of dry air at 35°C, ultraviolet irradiation (except curve 1) and various NO_2 pressures: (1) dark reaction, 1 mm Hg NO_2 ; (2) 1 mm Hg NO_2 ; (3) 0.5 mm Hg NO_2 ; (4) 0.2 mm Hg NO_2 .

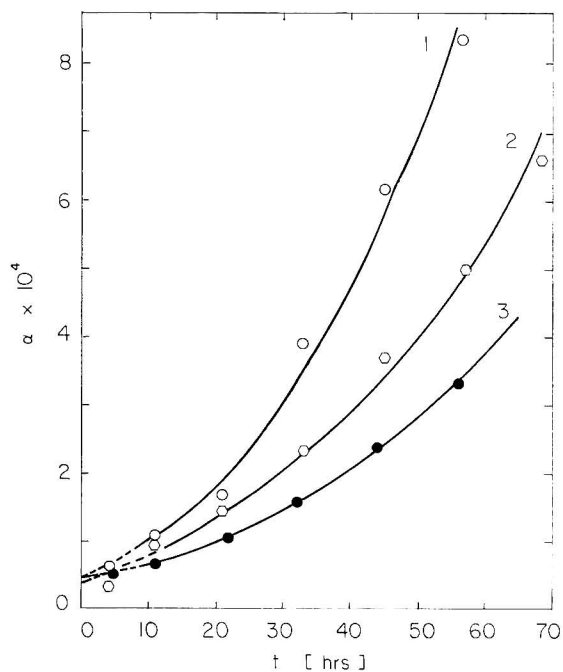


Fig. 6. Plots of α vs. t for 1 atm of dry air, 0.2 mm Hg of NO_2 , and near ultraviolet irradiation at various temperatures: (1) 55°C; (2) 45°C; (3) 35°C.

where

$$K_{\text{exp}}'' = k_{11}k_{12}k_{14}[\text{NO}_2]K_V/\{(k_{13} + k_{14})[n]_0\} \quad (2)$$

$$K_V = K_{\text{IV}}k_5[n']_0^{1/2}[\text{O}_2]^{3/2} \quad (3)$$

and

$$K_{\text{IV}} = \{k_4(k_{16}[\text{O}_2] + k_{17})/k_{15}k_{17}\}^{1/2} \quad (4)$$

where $[n']_0$ is the initial molar concentration of isoprene units and $[n]_0$ is the initial total unit concentration. Hence

$$K_{\text{exp}}''^2 = A[\text{NO}_2]^2 + B[\text{O}_2]^4 + B'[\text{O}_2]^3 \quad (5)$$

$$K_{\text{VI}} = k_7 + k_8 + k_{11}[\text{NO}_2] - k_9k_3/(k_9 + k_{10}[\text{O}_2]) \quad (6)$$

and

$$K_{\text{exp}} = k_1k_3[n']_0[\text{NO}_2]/\{[n]_0(k_2 + k_3[\text{NO}_2])\}$$

K_{exp}'' and K_{VI} were derived from the experimental data as follows. If $\alpha' = \alpha - K_{\text{exp}}t$, one obtains,

$$d\alpha'/dt = (K_{\text{exp}}''/K_{\text{VI}}^2) - K_{\text{VI}}\alpha' \quad (7)$$

A plot of $d\alpha'/dt$ versus α' should give a straight line, whose slope is K_{VI} and whose intercept on the ordinate is $K_{\text{exp}}''/K_{\text{VI}}^2$. Figure 1 (curves are calculated) shows that eq. (7) is satisfactorily obeyed. Further, Figures 7a and 7b (K_{exp}'' and K_{VI} , respectively, plotted versus O₂ pressure) are in agreement with the expressions for K_{VI} and K_{exp}'' . In principle, K_{exp} can be obtained from eq. (1), once K_{VI} and K_{exp}'' , respectively, are known. However, the accuracy of the experiments is not sufficient for this purpose; K_{exp} appears to be quite small and often negative values are obtained due to experimental error. Thus the value $K_{\text{exp}} = 3.24 \times 10^{-6}$ hr⁻¹ directly obtained from experiments with NO₂ alone was taken here. The corresponding value obtained in the previous paper is 3.50×10^{-6} hr⁻¹. The discrepancy is due to the different age of the original sample at the time of the two different investigations and possibly to a small personal error. It is assumed throughout that $[n']_0 = [n']_t$. Table I contains the relevant rate constants. (All rate constants are given including pressure units, as the volume during reaction was constant and Henry's law is assumed.)

The reaction was also studied as a function of temperature for a NO₂ pressure of 1 mm Hg and an O₂ pressure of 13 mm Hg (Fig. 2). K_{exp} has a value of 3.24×10^{-6} hr⁻¹ at 35°C. The experiments for higher temperatures than 35°C can be written as follows (straight lines, Fig. 2),

$$\alpha = K_{\text{exp}}t + (K_{\text{exp}}''/K_{\text{VI}}^2)t \quad (8)$$

In the case of the experiment at 35°C, $K_{\text{exp}}''/K_{\text{VI}}^2 = 1.5 \times 10^{-5}$, which is larger than K_{exp} . At higher temperatures, only the first term needs to be considered, as the Arrhenius plot gives a straight line including the K_{exp} value for 35°C. This is shown in Figure 8 (curve 1). The relevant rate

TABLE I
Rate Constants K_{exp}'' and K_{VI} at Various Oxygen Pressures and 1 mm Hg of NO_2 at 35°C ; $K_{\text{exp}} = 3.24 \times 10^{-6} \text{ hr}^{-1}$

O_2 , mm Hg	$K_{\text{exp}}'' \times 10^8$, hr^{-1}	$K_{\text{VI}} \times 10^2$, hr^{-1}
13	0.57	1.95
39	1.11	1.77
69	1.66	1.92
125	6.70	3.3
126	5.60	3.3
1 atm air	5.70	3.2
1 atm air ^a	3.44	2.4

^a Data of Jellinek and Flajsman.¹

constants K_{exp} at 35 , 45 , 55 , and 65°C , respectively, are 3.24×10^{-6} , 2.60×10^{-5} , 4.24×10^{-5} and 8.93×10^{-5} . The Arrhenius equation is

$$K_{\text{exp}} = 4.1 \times 10^5 e^{-14,900/RT} \text{ hr}^{-1} \quad (9)$$

It is of interest to note that the energy of activation for 1 mm Hg of NO_2 is exactly twice that for 0.2 mm Hg of NO_2 ;¹ this may be due to the energy of activation for dissolving NO_2 in the polymer.

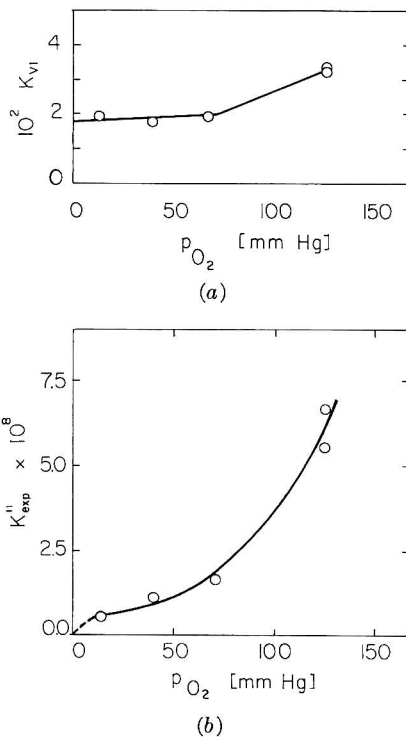


Fig. 7. Plots of (a) K_{VI} and (b) K''_{exp} vs. O_2 pressure in mm Hg; at 35°C , derived from Fig. 1.

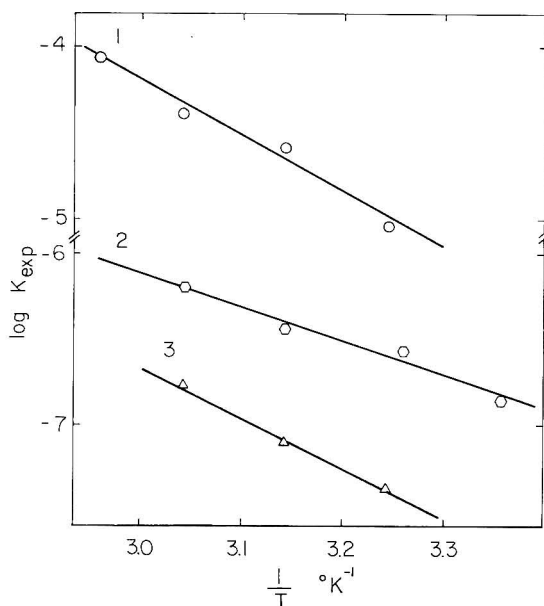
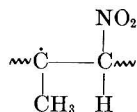


Fig. 8. Arrhenius plots pertaining to data from other Figures: (1) from Fig. 2; (2) from Fig. 4; (3) from Fig. 6.

The degradation by 1 mm Hg of NO₂ is compared in Figure 3 in presence and absence of near-ultraviolet light at 35°C. The degradation is slower when ultraviolet radiation is present. The mechanism in absence of ultraviolet radiation and oxygen was given in the previous paper.¹ NO₂ reacts directly with a double bond, forming a radical



which is located in a cage. α for this case is given by,¹

$$\alpha = \frac{k_1 k_3 [n']_0 [\text{NO}_2] t}{[n]_0 (k_2 + k_3 [\text{NO}_2])} = K_{\text{exp}} t \quad (10)$$

The curves in Figure 3 show marked indications of weak links; these are specially apparent in the degradation in the presence of ultraviolet light. The rate constants and the average number of weak links for each original chain for degradation in presence of NO₂ only, were found to be

$$K_{\text{exp}} = 3.24 \times 10^{-6} \text{ hr}^{-1}$$

the weak link rate constant is

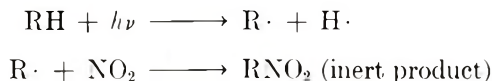
$$K_{\text{exp}}' = 2.3 \times 10^{-1} \text{ hr}^{-1}$$

The average number of weak links for each original chain molecule is $m = 1.8 \times 10^{-1}$. (In the previous paper,¹ $K_{\text{exp}} = 3.50 \times 10^{-6} \text{ hr}^{-1}$, $m = 1.44$

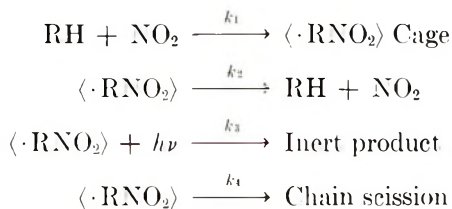
$\times 10^{-1}$, $K_{\text{exp}}' = 2.88 \times 10^{-1} \text{ hr}^{-1}$.) The curve (see Fig. 3) is calculated [eq. (10)] and the points are experimental data.

The mechanism in the presence of ultraviolet light is as follows. Direct attack of photons on the butyl rubber molecule is very small indeed as chain scission is not apparent for quite a considerable time in vacuum at 35°C . Hence, the ultraviolet light must act directly on the structure bonding the NO_2 molecule. Such a mechanism (NO_2 pressure is constant) can be formulated as follows.

Reaction with double bond (negligible on exposure to near-ultraviolet radiation):



Reaction with double bond (see previous paper¹):



In this particular case, the steady-state concentration of the cages will be attained only after a long time, as there are no free radicals present. The rate of chain scission is given by,

$$-d[n']/dt = k_4[\text{Cage}] \quad (11)$$

and

$$\begin{aligned} \frac{d[\text{Cage}]}{dt} &= k_1[n']_0[\text{NO}_2] - k_2[\text{Cage}] - k_3[\text{Cage}] - k_4[\text{Cage}] \quad (12) \\ &= k_1[n']_0[\text{NO}_2] - k_3[\text{Cage}] \end{aligned}$$

Integration of eq. (12) gives,

$$[\text{Cage}] = (k_1/k_3)[n']_0[\text{NO}_2](1 - e^{-k_3 t}) \quad (13)$$

The average number of chain scissions for each original chain remains very small throughout the whole degradation process considered here, hence only initial stages of chain scission are involved; eq. (13) reduces to,

$$[\text{Cage}] = k_1[n']_0[\text{NO}_2]t \quad (14)$$

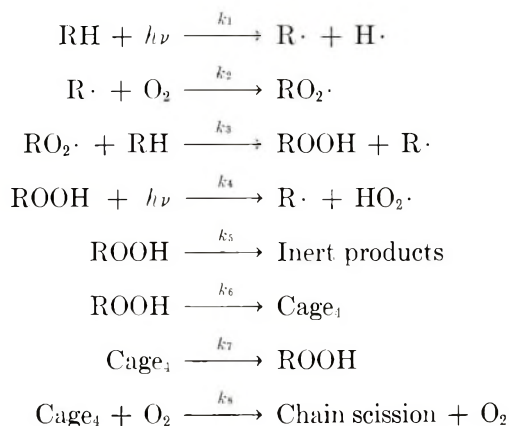
Finally,

$$\alpha = \frac{k_1 k_4 [n']_0 [\text{NO}_2] t^2}{[n]_0} = K_{\text{exp}} t^2 \quad (15)$$

Hence, $\alpha^{1/2}$ plotted versus t should give a straight line or α versus t a parabola, which is actually the case. The parameters for the relevant curve

in Figure 3 found in this way are: $K_{\text{exp}} = 1.88 \times 10^{-8} \text{ hr}^{-2}$, K_{exp}' (weak links) = $2.6 \times 10^{-1} \text{ hr}^{-1}$, and $m = 1.5 \times 10^{-1}$. The curve in Figure 3 has been calculated, the points represent experimental data.

Photo-oxidation results are shown in Figure 4. A tentative mechanism is suggested here, which accounts satisfactorily for the experimental results:



Detailed calculations are given in the Appendix, α for this case is given by,

$$\alpha_2 = K_{\text{exp},2} t^2 \quad (16)$$

Figure 9 shows $\alpha_2^{1/2}$ plotted versus t , which gives satisfactory straight lines. The rate constants $K_{\text{exp},2}$ derived from the slopes at 25, 35, 45, and 55°C are, respectively, 1.37×10^{-7} , 2.92×10^{-7} , 3.60×10^{-7} , and $6.40 \times 10^{-7} \text{ hr}^{-2}$.

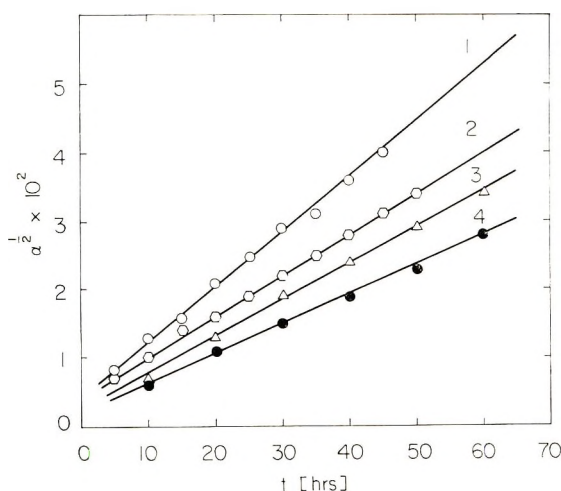


Fig. 9. Plots of $\alpha^{1/2}$ vs. t for data from Fig. 4. Numbering is the same as in Fig. 4.

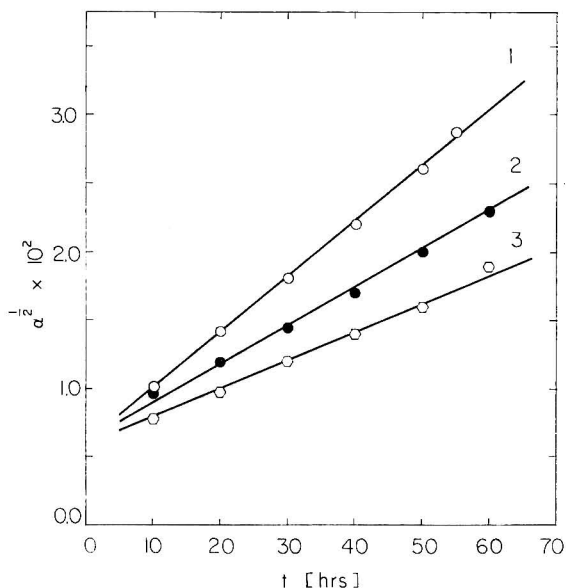


Fig. 10. Plots of $\alpha^{1/2}$ vs. t for data given in Fig. 6. Numbering is the same as in Fig. 6.

The fact that the straight lines in Figure 9 do not pass through the origin of the coordinate system is due to weak links, hence $\alpha_2 = \alpha_{n,2} + \alpha_w$ (where α_n and α_w stand for normal and weak links, respectively).

Figure 8, curve 2, shows the corresponding Arrhenius plot, which yields eq. (17):

$$K_{\text{exp},2} = 3.2 \times 10^{-2} e^{-9200/RT} \text{ hr}^{-2} \quad (17)$$

Addition of NO_2 to the photo-oxidation process adds only one additional step to the photo-oxidation reaction, which accounts for the retardation of the reaction by small amounts of NO_2 (see Fig. 6). This additional reaction is,



α as function of t for this mechanism is given by

$$\alpha_3 = K_{\text{exp},3} t^2 \quad (18)$$

(Details are given in the Appendix.)

The data in Figure 6 have been evaluated by eq. (18). The results are shown in Figure 10, which are very satisfactory. Here again weak links are apparent and

$$\alpha_3 = \alpha_{n,3} + \alpha_w.$$

The rate constants $K_{\text{exp},3}$ as function of temperature (Figs. 6 and 10) at 0.2 mm Hg NO_2 , 1 atm of air, at 35, 45, and 55°C are 4.20×10^{-8} , 7.80×10^{-8} , and $1.63 \times 10^{-7} \text{ hr}^{-2}$, respectively.

The corresponding Arrhenius plot is shown in Figure 8 (curve 3) and

$$K_{\text{exp},3} = 1.5 \times 10^{-2} e^{-10,400/RT} \text{ hr}^{-2}$$

The NO₂ pressure in Figure 6 is quite small. However, the experimental curves change from convex to concave towards the time axis with increasing NO₂ pressures (see Fig. 5). Apparently, an additional reaction becomes prominent. This reaction is the one treated above, where NO₂ reacts directly with the double bonds in the polymer molecules [eq. (15)]. Because of the appreciable NO₂ pressure involved, the experimental term cannot any more be approximated by the initial terms of its series. Hence the expression for α_1 becomes,

$$\alpha_1 = (k_1 k_3 [n']_0 / k_3 [n]_0) [\text{NO}_2] [t + (1/k_3)(1 - e^{-k_3 t})] \quad (19)$$

The term in t can be neglected, hence the total α_1 is given by,

$$\alpha_1 = K_{\text{exp},3} t^2 + K_1 [\text{NO}_2] (1 - e^{-k_3 t}) \quad (20)$$

For sufficiently high NO₂ pressures, α reduces to the second term in eq. (20), while for relatively small NO₂ pressures, it is given by the first term. Intermediate pressures have to be evaluated by the complete expression for α_1 [eq. (20)]. The experiments in Figure 5 have been evaluated as follows. The two runs (Fig. 5, curves 4 and 3), having low NO₂ pressure, have been evaluated by using the first term in eq. (20); curve 2 was obtained by the second term only. The curves in Figure 5 are calculated. The rate constants at 35°C, 1 atm air, ultraviolet radiation, are listed in Table II.

TABLE II

NO ₂ , mm Hg	K_{exp} , hr ⁻²	$K_1[\text{NO}_2]$	k_3 , hr ⁻¹
0.2	5.49×10^{-8}	—	—
0.5	1.96×10^{-7}	—	—
1.0	—	5.34×10^{-6}	2.55×10^{-2}

APPENDIX

Photo-Oxidation

Equations for photo-oxidation are as follows.

Rate of chain scission:

$$-d[n']/dt = k_8 [\text{O}_2] [\text{Cage}_4] \quad (\text{A-1})$$

Steady-state cage concentration:

$$[\text{Cage}_4] = (k_6/k_7) [\text{ROOH}] \quad (\text{A-2})$$

Rate of hydroperoxide formation:

$$d[\text{ROOH}]/dt \cong k_3 [n']_0 [\text{RO}_2\cdot] - k_4 [\text{ROOH}] \quad (\text{A-3})$$

Steady-state concentrations of radicals ($k_1[n']_0 = \phi I_{\text{abs}}$, where ϕ denotes quantum yield and I_{abs} is absorbed light intensity):

$$[\text{R}\cdot] = \{k_1[n']_0 + k_1[\text{ROOH}] + k_3[\text{RO}_2\cdot][n']_0\}/k_2[\text{O}_2] \quad (\text{A-4})$$

$$\cong (k_1[n']_0 + k_1[\text{ROOH}])/k_2[\text{O}_2]$$

$$[\text{RO}_2\cdot] = k_2[\text{O}_2][\text{R}\cdot]/k_3[n']_0 \quad (\text{A-5})$$

$$= (k_1[n']_0 + k_1[\text{ROOH}])/k_3[n']_0$$

Introducing eq. (A-5) into eq. (A-3) gives,

$$d[\text{ROOH}]/dt = k_1[n']_0 \quad (\text{A-6})$$

Integration yields:

$$[\text{ROOH}] = k_1[n']_0 t \quad (\text{A-7})$$

Finally

$$\alpha_2 = ([n']_0 k_1 k_6 k_8 [\text{O}_2] / [n]_0 2 k_7) t^2 = K_{\text{exp},2} t^2 \quad (\text{A-8})$$

Photo-Oxidation in Presence of NO_2

The steady-state concentrations for this case are,

$$[\text{R}\cdot] \cong (k_1[n']_0 + k_1[\text{ROOH}]) / (k_2[\text{O}_2] + k_9[\text{NO}_2]) \quad (\text{A-9})$$

$$[\text{RO}_2\cdot] = k_2[\text{O}_2][\text{R}\cdot] / k_3[n']_0$$

$$= k_2[\text{O}_2](k_1[n']_0 + k_1[\text{ROOH}]) / k_3[n']_0 (k_2[\text{O}_2] + k_9[\text{NO}_2]) \quad (\text{A-10})$$

Hence,

$$\frac{d[\text{ROOH}]}{dt} = (k_1 k_2 [\text{O}_2] [n']_0 - k_1 k_9 [\text{ROOH}] [\text{NO}_2]) / (k_2 [\text{O}_2] + k_9 [\text{NO}_2]) \quad (\text{A-11})$$

or

$$\frac{d[\text{ROOH}]}{dt} = A - B[\text{ROOH}] \quad (\text{A-12})$$

Integration gives,

$$[\text{ROOH}] = (A/B)(1 - e^{-Bt}) \quad (\text{A-13})$$

For initial stages only,

$$[\text{ROOH}] = At \quad (\text{A-14})$$

and

$$\alpha_3 = [n']_0 k_1 k_2 k_6 k_8 [\text{O}_2]^2 t^2 / 2 [n]_0 k_7 (k_2 [\text{O}_2] + k_9 [\text{NO}_2]) \quad (\text{A-15})$$

For $[\text{NO}_2] = 0$, eq. (A-15) becomes identical with eq. (A-8).

The authors wish to express their appreciation to the Bureau of State Services, PHIS, Division of Air Pollution, 1-RO-1-AP00486, for financial support.

References

1. H. H. G. Jellinek and F. Flajsman, *J. Polym. Sci. A-1*, **8**, 711 (1970) (Part I).
2. M. A. Golub and C. L. Stephens, in *Macromolecular Chemistry, Prague 1965* (*J. Polym. Sci. C*, **16**), O. Wichterle and B. Sedláček, Eds., Interscience, New York, 1967, p. 765; *J. Polym. Sci. A-1*, **7**, 63 (1968).
3. M. A. Golub, *Macromolecules*, **2**, 550 (1969).
4. J. F. Robek, *J. Appl. Polym. Sci.*, **9**, 2121 (1965); in *Macromolecular Chemistry, Prague 1965* (*J. Polym. Sci. C*, **16**), O. Wichterle and B. Sedláček, Eds., Interscience, New York, 1967, p. 949.
5. J. C. W. Chien, *J. Phys. Chem.*, **69**, 4317 (1965).
6. J. Morand, *Rubber Chem. Technol.*, **39**, 537 (1966).
7. H. H. G. Jellinek and F. Flajsman, *J. Polym. Sci. A-1*, **7**, 1153 (1969).

Received September 1, 1970

Revised November 9, 1970

Degradation of Polymers and Morphology: Photo-Oxidative Degradation of Isotactic Polystyrene in Presence of Sulfur Dioxide as Function of Polymer Crystallinity

P. HRDLOVIC,* J. PAVLINEC,* and H. H. G. JELLINEK, *Department of Chemistry, Clarkson College of Technology, Potsdam New York 13676*

Synopsis

The photo-oxidative chain scission of isotactic polystyrene films has been studied as a function of the degree of crystallinity, SO₂ and NO₂ pressures, and temperature. The rate of chain scission increases in the presence of SO₂ with extent of crystallinity. It is assumed to be faster due to strain in and near the folds in the crystalline areas than in the amorphous regions. In the presence of NO₂, chain scission increases up to about 8% crystallinity but subsequently becomes constant with further increase in crystallinity. It is suggested that the diffusion rates of oxygen and nitrogen dioxide into the films decrease with increasing crystallinity. These two processes compensate each other.

The photo-oxidation of isotactic polystyrene in presence of SO₂ has been studied recently.^{1,2} However, the effect on polymer films of morphology or of the degree of crystallinity was not investigated. Generally, the effect of morphology on oxidative degradation in presence of various gases and near-ultraviolet light has not been studied as yet.

In this work, the photo-oxidative degradation of isotactic polystyrene films, prepared in a variety of ways, producing different degrees of crystallinity, has been studied in presence of sulfur dioxide and nitrogen dioxide, respectively. Pronounced effects on the rates of degradation as a function of crystallinity have been observed which will be described and discussed in this paper.

EXPERIMENTAL

Apparatus

The high-vacuum apparatus (10^{-5} – 10^{-6} mm Hg) has been described in a previous paper.¹ It was equipped with a linear McLeod gauge. Six reaction vessels were arranged in a circular fashion around the ultraviolet light source (Hanovia 654-36). The vessels were made of Pyrex glass

* Permanent address: Polymer Institute, Slovak Academy of Sciences, Bratislava, Czechoslovakia.

(#7740) cutting out all light below 2800 Å; they were provided with three-way stopcocks each and arrangements for mounting the films, cast on microscope slides, exactly vertical and parallel to the light source. Films could thus be removed one at a time from each reaction vessel. The whole assembly was immersed in a thermostatted water bath, constant within $\pm 0.1^\circ\text{C}$. Each film was evacuated after exposure to prevent continuance of the reaction due to absorbed gases. SO_2 and NO_2 were obtained from Matheson Inc.

Purification of Polymer

The purification of isotactic polystyrene was described in a previous paper.¹ It was freed from about 20% (w/w) atactic polymer by dissolving in methyl ethyl ketone and precipitation. It was further purified by repeated precipitation.

Intrinsic viscosities were measured at $30 \pm 0.02^\circ\text{C}$ for the SO_2 experiments in benzene solution ($[\eta] = 1.88$ dl/g) and in chloroform solutions for the NO_2 experiments ($[\eta] = 2.01$ dl/g). All chemicals were of reagent-grade quality.

Film Preparation

The casting procedures for preparing films was described previously.¹ Three different procedures were used for the production of films. These were cast from 2% (w/v) chloroform solutions, after filtration through fritted glass filters (41-60 ASTM). The films were formed on microscope glass slides or on clean mercury surfaces. The thickness of the films was roughly 20-25 μ .

Amorphous films, designated A, were obtained by quick evaporation of solvent ($20-22^\circ\text{C}$, 2.2 cm^3 solvent, surface area ca. 19 cm^2 , evaporation time ca. 40 min).

Partly crystalline films, C_I, were formed by slow evaporation of solvent, otherwise the conditions were the same as for films A, except for the evaporation times, ca. 12 hr or longer. In the previous work¹⁻³ only films of type C_I were investigated.

More highly crystalline films, C_{II}, were obtained by annealing amorphous films, A, in a nitrogen atmosphere at 170°C . The films remained on the glass slides during this procedure (softening point of isotactic polystyrene ca. 230°C).

Still more crystalline films, C_{III}, were produced after annealing in vacuum, heating from 30°C to 165°C , keeping the films at this temperature for 2 hr and then cooling them slowly to room temperature.

A film of still higher degree of crystallinity, C_{IV}, can be obtained by a variation of this procedure. Amorphous film prepared on a mercury surface was placed between two microscope glass plates and heated in high vacuum slowly to $165-180^\circ\text{C}$; it was kept at this temperature for 2-5 hr and then was cooled to room temperature within about 30 min.

RESULTS

Observations under the Polarizing Microscope

Films prepared by the various procedures outlined above revealed different degrees of crystallinity under the polarizing microscope. The amorphous films, A, have only very few fibrils (Fig. 1). The C_I and C_{II} films contain several networks of crystallinity (fibrils) (Fig. 2). Figure 3 represents C_{III} films having 30% crystallinity. Kargin et al.⁴ made similar observations for isotactic polystyrene obtained from solution. The well known spherulite structure formed by crystallization from melts was not observed in this work.

Specific Gravity of Films

Specific gravities were measured on films 1 cm² in area by adding NaCl solution⁵ to degassed water (free floating method⁶) at 20 ± 0.02°C. The degrees of crystallinity were evaluated according to the equation,⁷

$$\alpha_d = \frac{d_c(d - d_A)}{d(d_c - d_A)} \quad (1)$$

where α_d is the degree of crystallinity, d_c and d_A the specific gravities (20°C/4°C) of 100% crystalline and amorphous films, respectively; d is the specific gravity of the films of intermediate degrees of crystallinity ($d_c = 1.111$ g/cm³ from crystallographic data). The specific gravity of the amorphous films A, obtained in this work, has been taken as $d_A = 1.061$ g/cm³. The most recent value for d_A containing 10% of atactic isomer is 1.057 g/cm³.⁸ d_A Values range from 1.053 to 1.056 g/cm³ and 1.04 to 1.065

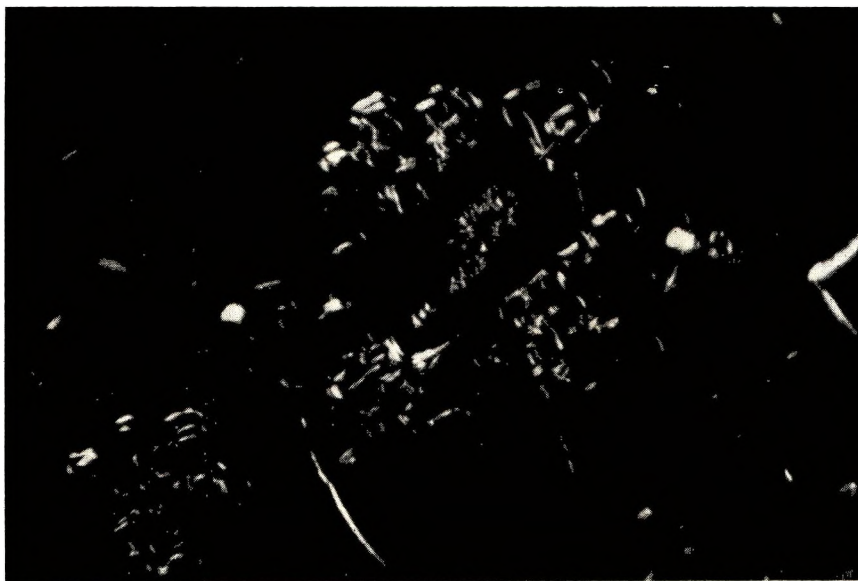


Fig. 1. Film representing A samples. Polarizing microscope, 100×.

g/cm^3 .^{9,10} Interesting density data were given by Hay,¹¹ who observed that after annealing at 170°C for 20 hr, the sample had a density of $1.070 \text{ g}/\text{cm}^3$, while after annealing for 3 hr at 165°C , the density was $1.081 \text{ g}/\text{cm}^3$. The difference in densities is rather similar to those ones for C_{II} and C_{III} films, respectively. It is quite reasonable to assume that the A films ob-

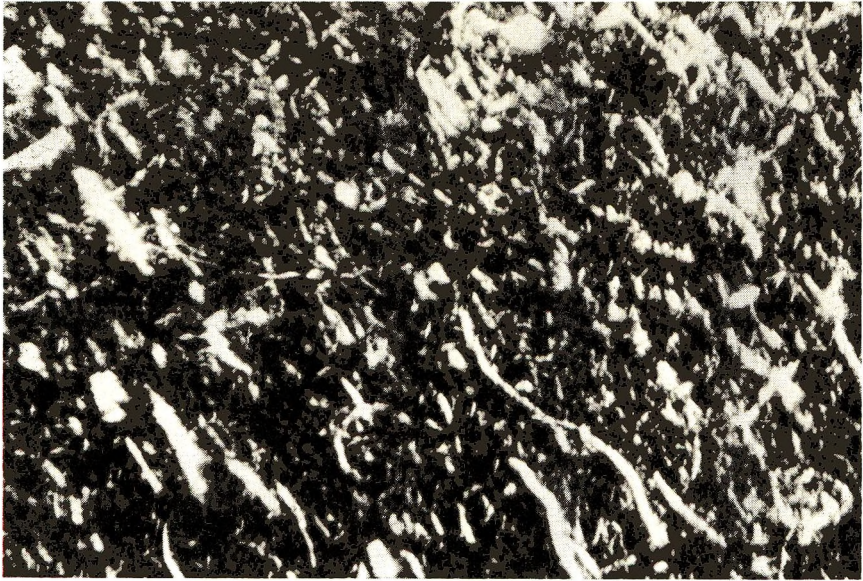


Fig. 2. Film representing C_I samples. Polarizing microscope, $100\times$.

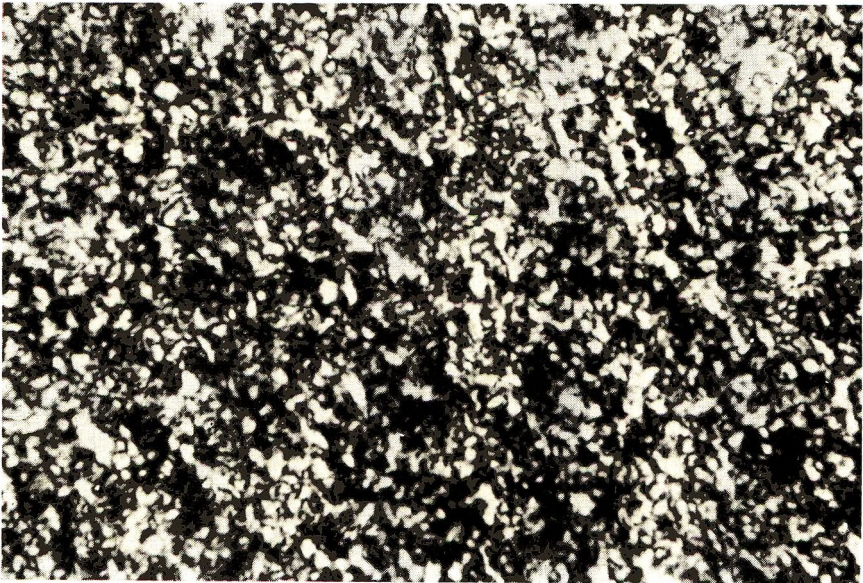


Fig. 3. Film representing C_{III} samples. Polarizing microscope, $400\times$.

tained in this work are practically completely amorphous, as the films are soluble in benzene at 6°C.

Degradation was carried out in presence of 150 mm Hg of oxygen or 1 atm of air, respectively, constant light intensity ($\lambda > 2800 \text{ \AA}$), and various SO₂ pressures or 10 mm Hg of NO₂ (35°C only) at 30, 45, 57, and 60°C (SO₂ only) using films of various degrees of crystallinity.

TABLE I
Solubilities and Specific Gravities of Isotactic
Polystyrene Films as Function of Crystallinity

Sam- ple	Soluble in 48 hr, wt-%	Solubility in benzene, as temperature, °C, at which			Specific gravity (20°C/4°C)	Crystal- linity, wt-% ^a
		Haziness disappears	Main part dissolves	100% dissolves		
A	98.7	—	—	45.0	1.0610	0
C _I ^b	68.0	47.5	50.0	51.5	1.0630 (on Hg surface) 1.0635 (on glass surface) 1.065 (highest density) ^c	4.2 4.7 8.3
C _{II}	2.5	—	49.0	51.5	1.0715	23
C _{III}	2.0	58.5	62.0	72.0	1.0746	30
C _{IV}	—	Insoluble in boiling benzene			1.0788	38

^a Specific gravity 1.061 of amorphous films (A) taken as standard for zero per cent crystallinity.

^b C_I films were used in all previous work^{1,2}.

^c Densities change somewhat with locations on the film surface; this was the highest average density found.

Table I gives the solubilities, specific gravities and percentages of crystallinity of the various films. The specific gravity has a standard deviation of ± 0.0015 ; it varies somewhat at different locations of the films.

Results of Experiments in Presence of SO₂

The experimental degradation rate constants are given in Table II and their α (degree of degradation) versus t plots in Figures 4 and 5. The conversion of the viscosity-average to number-average chain length has been described in the previous paper.¹ The C_{II} films, prepared under nitrogen, show an initially fast reaction. This is probably due to the fact that some hydroperoxidation took place, as the nitrogen gas contained a small amount of oxygen.

Sample A was investigated as function of temperature, (Table III).

The rate constants in Table III are identical within experimental error, hence an energy of activation cannot be derived; the magnitude could possibly be as large as about 500 cal/mole (see Fig. 6).

C_I films gave previously¹ for 0.84 mm Hg of SO₂

$$K_{\text{exp},C_I} = 2.83 \times 10^{-6} e^{-4500/RT} \text{ sec}^{-1}$$

or, for 1 mm Hg of SO₂,

$$K_{\text{exp},C_I} = 3.37 \times 10^{-6} e^{-4500/RT} \text{ sec}^{-1}$$

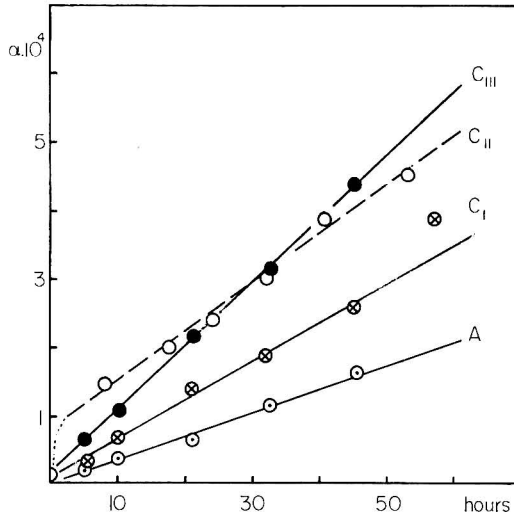


Fig. 4. Plots of α vs. reaction time: (A) amorphous, (C_I) 8% (C_{II}) 23%; (C_{III}) 38% w/w crystallinity. 30°C, 1 mm Hg of SO₂, 150 mm Hg of O₂, ultraviolet light ($\lambda > 2800\text{\AA}$).

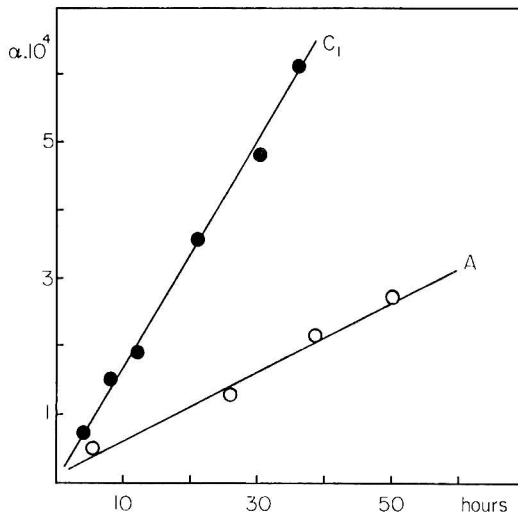


Fig. 5. Plots of α vs. time: (A) amorphous, (C_I) 8% w/w crystallinity. 57°C, 3.5 mm Hg of SO₂, 150 mm Hg of O₂, ultraviolet light ($\lambda > 2800\text{\AA}$).

TABLE II
Experimental Degradation Rate Constants for Isotactic Polystyrene
as Function of Degree of Crystallinity for Various Pressures of SO₂
(150 mm Hg of O₂ and Ultraviolet Light, $\lambda > 2800 \text{ \AA}$)

Sample	Temperature, °C	$10^9 K_{\text{exp}}, \text{sec}^{-1}$	SO ₂ pressure, mm Hg
A	30	0.93	1.0
C _I	30	1.7, ^a 1.6 ^b	1.0
C _{II}	30	2.0	1.0
C _{III}	30	2.6	1.0
A ^c	57	1.4	3.5
C _I ^c	57	4.6	3.5

^a Not considering the experimental point for 57 hr (see Fig. 4).

^b From Arrhenius equation, data of Jellinek and Kryman¹.

^c Films were prepared on mercury surface.

TABLE III
Degradation of Amorphous Films A as a Function of Temperature^a

Temperature, °C	$10^{10} K_{\text{exp}}, \text{sec}^{-1}$
30	9.3
45	9.5
60	9.7
	Avg. 9.5

^a At 1 mm Hg of SO₂, 150 mm Hg of O₂, ultraviolet light intensity constant throughout the whole work, $\lambda > 2800 \text{ \AA}$, K_{exp} chain scission rate constant.

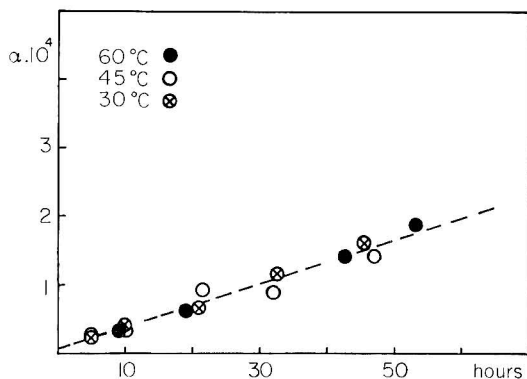


Fig. 6. Plots of α vs. time and temperature for C_I: (⊗) 30°C; (○) 45°C; (●) 60°C. 1 mm Hg of SO₂, 150 mm Hg of O₂, ultraviolet light ($\lambda > 2800 \text{ \AA}$).

Results for Experiments in Presence of NO₂

Figure 7 shows α plotted versus exposure time. The rate constants K (at 10 mm Hg of NO₂, 1 atm of air, 35°C, $\lambda > 2800 \text{ \AA}$, viscosity-average converted to number average chain length¹) are 2.2×10^{-9} , 3.4×10^{-9} , 3.4×10^{-9} and $3.4 \times 10^{-9} \text{ sec}^{-1}$ for samples A, C_I, C_{II}, and C_{IV}, respectively.

DISCUSSION

Experiments with Sulfur Dioxide

The crystallinities and densities obtained for the various films are in good agreement with results found in the literature.⁷⁻¹¹

A reaction mechanism was presented in a paper by Jellinek and Pavlinec² which accounts satisfactorily for all data known at that time concerning the degradation of isotactic polystyrene films (C_1) as a function of SO_2 and O_2 pressures and near ultraviolet light. Evaluation of this mechanism leads to ($[SO_2] < [O_2]$),

$$\alpha \cong K_{\text{exp}} t \cong \frac{k_{10}k_{12}}{k_5k_{11}} (k_1[O_2] + k_2[SO_2])t \quad (2)$$

Here K_{exp} is the experimental chain scission rate constant and the k are the rate constants for various steps in the mechanism. Photo-excited SO_2^* molecules are the reactive species; this was not indicated in the previously described mechanism;² this changes the k_2 value but not the overall eq. (2).

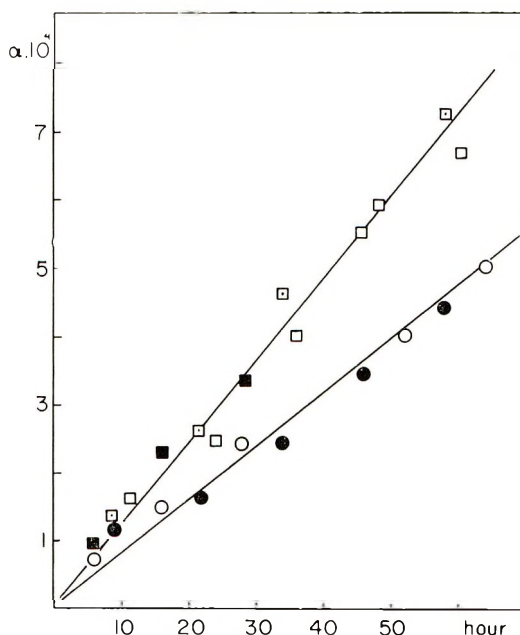


Fig. 7. Plots of α vs. time for isotactic polystyrene exposed to 10 cm Hg of NO_2 , 1 atm. air, ultraviolet light ($\lambda > 2800 \text{ \AA}$).

The increase in the experimental rate constants with percentage crystallinity of the films is shown in Figure 8. It can be represented by a straight line except for a slight discrepancy of the C_1 samples or by a curve slightly concave towards the crystallinity axis. The straight line is preferred here.

First, it was ascertained whether the cause for this increase in the rate constants is simply a concentration effect; it was assumed that SO₂ is only taken up by the amorphous part and not by the crystalline part of the films. The available amorphous film values can be calculated by means of the specific gravities and the SO₂ concentrations can be derived. The results are indicated by the dotted line in Figure 8. Apparently, the increase in the rate constants is not due to such a simple concentration effect.

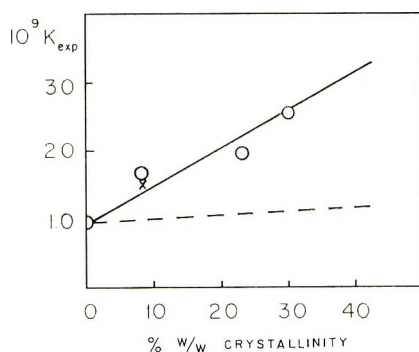


Fig. 8. Experimental rate constants as function of percentage of crystallinity: (---) rate constants as function of SO₂ concentration in amorphous parts of films only, zero concentration in crystalline parts.

Next, the assumption was made, that the rate constants in the amorphous parts are different from those for the main-chain scission near or in the "fold" regions of the chains in the crystalline parts. It is known from work¹² on polyethylene that the fold regions are quite susceptible to chain scission. This case is similar to that of a chain containing weak links. However, in the present case, the "weak" links are quite numerous. As the percentage of total links broken in the film is quite small, the number of normal and weak links in the amorphous part and in the folds, respectively, remain practically constant during degradation. One obtains on this basis for the degradation process an expression as follows,

$$\alpha_A + \alpha_{CR_{100\%}} = \alpha_{total} = K_{exp}t = [aK_A + (1 - a)K_{CR_{100\%}}]t \quad (3)$$

where α_A and $\alpha_{CR_{100\%}}$ are the degrees of degradation in the amorphous and 100% crystalline films, respectively, the K are the respective rate constants, and a is the weight percentage of amorphous material in a film. The value for $K_{CR_{100\%}}$ can be calculated; however, this value is fictitious as long as it is not known whether the curve in Figure 8 remains straight from 40% to 100% crystallinity. The value can be used to calculate rate constants or percentage of crystallinities for the range from 0 to 38% crystallinity, however. The rate constants K_A and $K_{CR_{100\%}}$ are, according to the mechanism, given by eq. (4),

$$K_A \text{ or } K_{CR_{100\%}} = (k_{10}k_{12}/k_{11}k_3)(k_1[O_2] + k_2[SO_2])t \quad (4)$$

The question arises as to the cause for the differences of the rate constant K_{exp} for the amorphous and crystalline parts in a film, respectively. It is not unlikely that the main chain links in or near the fold are weakened in contrast to those in the amorphous regions. Thus, in the latter regions, "normal" chain scission takes place, whereas in or near the folds, the energy of activation for chain scission is increased (this is indicated by the experimental results). The steady-state cage concentration must be larger in the fold than in the amorphous regions, and the frequency of escape of macroradicals from the cages² leading from potential to actual chain scission is increased. Differently expressed, the k_{12} and k_{10}/k_{11} values are larger for the fold than for the amorphous regions. This view is in general agreement with the usual assumption relating to degradation of crystalline polyethylene by nitric acid.¹²

Jellinek and Lipovac¹³ found the thermal oxidative degradation of isotactic polystyrene at elevated temperatures to be diffusion-controlled. This must also be the case here. However, SO_2 is quite soluble in benzene and also in polystyrene and is, therefore, not subject to diffusion control.

Experiments with Nitrogen Dioxide

Nitrogen dioxide behaves differently from sulfur dioxide. In the latter case, chain scission rate constants increase practically linearly with increase in weight percentage of crystallinity; however, main chain scission constants for films exposed to nitrogen dioxide increase at first until about 8% w/w of crystallinity are reached, but then become constant. It was observed in case of butyl rubber, degraded in presence of near u.v. radiation ($\lambda > 2800 \text{ \AA}$) and 15 cm of oxygen, that addition of NO_2 actually decreased the random chain scission rate constants.¹⁴ However, in case of isotactic polystyrene this does not happen.³

It may be again tentatively assumed, in accordance with work of various authors,¹² that main chain links in the "fold" regions of the crystalline parts degrade faster than main chain links in the amorphous regions. It is known from work by Jellinek and Lipovac¹³ that thermal oxidative degradation of isotactic polystyrene is diffusion-controlled at elevated temperatures. Hence, the supply of oxygen in the present instance will certainly also be diffusion-controlled. As the diffusion coefficient for O_2 (25°C, $D \approx 10^{-8} \text{ cm}^2/\text{sec}$) into polystyrene is larger than that for NO_2 (35°C, $D \approx 10^{-10} \text{ cm}^2/\text{sec}$), the NO_2 supply must also be diffusion-controlled. The diffusion rates into the polymer films will decrease with increasing crystallinity. At the same time, the chain scission rates increase with increasing crystallinity. These two processes may almost compensate each other after a certain low degree of crystallinity (ca. 8 wt-%) is reached. This would account for the observed functional relationship between the overall experimental random chain scission rate constants and weight percentages of crystallinity.

This work was made possible by a grant from NASA, Grant NO. NGR-33-007-074.

References

1. H. H. G. Jellinek and J. F. Kryman, paper presented at Pacific Conference on Chemistry and Spectroscopy, Anaheim, California, Oct. 8-9, 1969; in *Photochemistry of Macromolecules*, Plenum Press, New York, 1970, p. 85.
2. H. H. G. Jellinek and J. Pavlinec, in *Photochemistry of Macromolecules*, Plenum Press, New York, 1970, p. 91.
3. H. H. G. Jellinek and F. Flajsman, *J. Polym. Sci. A-1*, **7**, 1153 (1969).
4. V. A. Kargin and T. A. Koretskaya, *Polym. Sci., USSR*, **10**, 1244 (1968).
5. Landolt Boernstein, *Physical Chemical Tables*, 5th ed. Vol. 5, Part I, p. 392; *Handbook of Chemistry and Physics*, 38th ed., Chemical Publishing Co., Cleveland, p. 2070.
6. A. Weissberger, *Physical Methods of Organic Chemistry*, Vol. I, Interscience, New York, 1947, pp. 69-107.
7. M. L. Miller, *The Structure of Polymers*, Reinhold, New York, 1966, pp. 505, 521.
8. B. J. Challag and D. W. Van Krevelan, *J. Polym. Sci., A-2*, **6**, 1791 (1968).
9. O. G. Lewis, *Physical Constants of Linear Homopolymers*, Springer-Verlag, Berlin-Heidelberg-New York, 1968.
10. J. Brandrup and E. H. Immergut, *Polymer Handbook*, Interscience, New York, 1966, VI-75.
11. J. N. Hay, *J. Polym. Sci. A*, **3**, 433 (1965).
12. I. M. Ward and T. Williams, *J. Polym. Sci. A-2*, **7**, 1585 (1969).
13. H. H. G. Jellinek and S. N. Lipovac, *Macromolecules*, P [II], **3**, 237, (1970)
14. H. H. G. Jellinek and P. Hrdlovic, *J. Polym. Sci.*, in press.

Received June 30, 1970

Revised November 17, 1970

Nuclear Magnetic Resonance Studies of Isoprenyllithium Derived from 1,1-Diphenyl-*n*- butyllithium-3,4- d_5 and Isoprene

HEIMEI YUKI and YOSHIO OKAMOTO, *Department of Chemistry,
Faculty of Engineering Science, Osaka University, Toyonaka, Osaka, Japan*

Synopsis

The equimolar reactions of 1,1-diphenyl-*n*-butyllithium-3,4- d_5 (RLi) with isoprene (I) and isoprene-1,4- d_4 (Id) were carried out in benzene- d_6 quantitatively to give isoprenyllithiums, RILi and RIdLi, respectively. From the NMR spectrum of the RILi it was proposed that the isoprene unit had *cis*-1,4, *cis*-4,1 and some unknown structures in benzene- d_6 . When RILi was prepared in the presence of about one equivalent of THF to RILi, the anion was considered to include an isoprene unit in *cis*-1,4, *trans*-1,4, *cis*-4,1, and probably 3,4 structures. The same anion was obtained even if an equimolar THF was added afterward to the RILi prepared in benzene- d_6 . The RLi was reproduced by the reverse reaction from RILi, when a large excess of THF was added or the temperature of the solution was elevated. The results obtained were correlated with those of anionic polymerizations of isoprene by lithium initiators.

INTRODUCTION

In a previous paper,¹ we reported the NMR study of 1,1-diphenyl-*n*-butyllithium-3,4- d_5 (RLi) in benzene-tetrahydrofuran (THF) systems. One equivalent of isoprene (I) was added to this anion in benzene- d_6 quantitatively to form an isoprenyllithium, RILi. In the present study, the structures of RILi and RIdLi (Id = isoprene-1,4- d_4) were investigated by NMR spectroscopy. Recently, Schue, Worsfold, and Bywater² reported the NMR spectra of oligomer anions of isoprene derived from *tert*-butyllithium- d_9 (*t*-BuLi- d) and isoprene in benzene. Our results were a little different from theirs.

EXPERIMENTAL

Materials

1,1-Diphenyl-*n*-butyllithium-3,4- d_5 (RLi) was prepared from ethyllithium- d_5 and 1,1-diphenylethylene in benzene- d_6 .¹

Isoprene-1,4- d_4 was obtained by pyrolysis of isoprene sulfone- d_4 , which had been synthesized by repeated exchange reactions of isoprene sulfone³ with deuterium oxide in the presence of a small amount of potassium carbonate.⁴ The deuterated isoprene was dried over a mixture of calcium

hydride and Molecular Sieves 4A. The content of deuterium in Id was more than 96% by NMR spectroscopy.

Isoprene was dried over calcium hydride and Molecular Sieves 4A.

THF and THF- d_6 were dried over lithium aluminum hydride and then distilled onto Na-K alloy and benzophenone. From a blue solution, the solvents were distilled just before use.

Reaction of RLi with Isoprene

The reaction was carried out in an NMR sample tube, which had been dried by heating with a gas burner under high vacuum. Each of isoprene and THF was transferred to the tube in vapor phase using a vacuum system of a known volume. Their amounts were estimated from the depression of pressure. RLi was then added into the tube by using a syringe under dry argon and the tube was sealed off. The mixture was allowed to react in several minutes at room temperature and then was stored at -20°C .

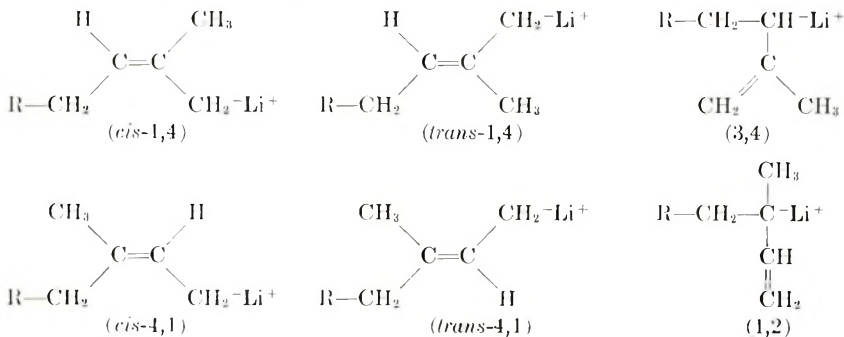
NMR Spectrum

The spectra were taken with JNM-4H-100 and/or JNM-C-60HL spectrometers (JEOL) at 100 MHz and 60 MHz, respectively, using benzene as an internal standard. The upfield shift from benzene was shown as positive δ .

RESULTS

NMR Spectrum in Benzene- d_6

When RLi was added to an equimolar amount of isoprene in benzene, a deep red color owing to RLi turned yellow due to the formation of RLiI in a few minutes at room temperature. Contrary to the rapid reaction between RLi and isoprene in benzene, the addition of RLiI to isoprene was so slow that besides the NMR spectrum of RLiI, that of unreacted isoprene was observed for a while after the formation of RLiI at room temperature when isoprene was used in only a slight excess. The spectrum of the remaining isoprene was the same as that of this monomer in benzene without RLiI. The NMR spectra of RLiI and RLiI₂ measured in benzene- d_6 at room temperature and above 60°C are shown in Figures 1 and 2, respectively. As the structures of RLiI the following six can be considered:



The peak areas of the spectra in Figures 1 and 2 indicated that the anion was composed mainly of two structures which were 1,4 and/or 4,1. Consequently, as the main configuration of RLi the *cis*-1,4 anion was presumed, because the polyisoprene formed by lithium catalysts in benzene has a high *cis*-1,4 structure.⁵⁻⁸ The second was assumed to be *cis*-4,1, because it is preferable that the anion newly formed in the existence of THF is considered as a *trans*-1,4 anion, as described later.

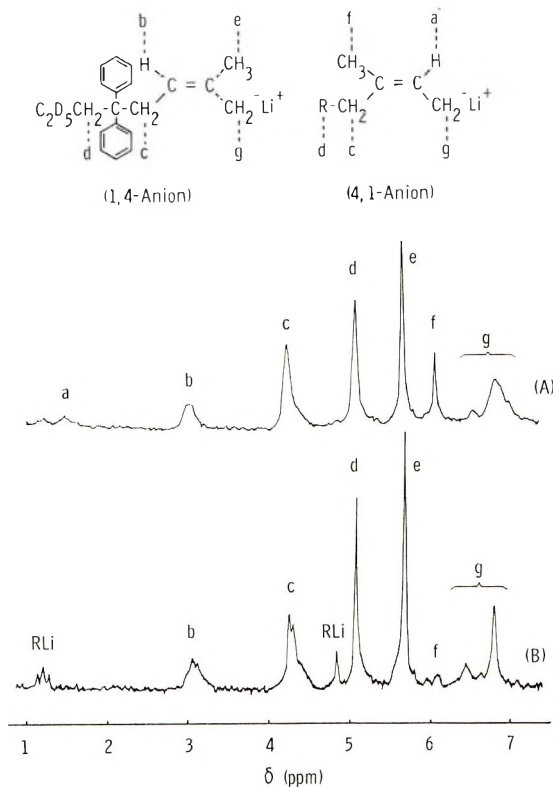


Fig. 1. NMR spectra of RLi in benzene-*d*₆ at 100 MHz: (A) 22°C; (B) 60°C.

The assignments of the peaks in the NMR spectra are shown in the Figures. If RLi was assumed to be composed only of *cis*-1,4 and *cis*-4,1 structures, there seemed to be some discrepancies among the peak intensities in the spectra. The sum of the areas of the peaks *a* and *b* was smaller than one half of the area of the peak *c*, and the areas of the peaks *c* and *d* were not equal, but should have been equal, if the assumption stated above was correct. As a possible cause of these discrepancies there may be some unknown anion other than *cis*-1,4 and *cis*-4,1 anions, and their signals may overlap on the peaks other than *a* and *b* in the spectra.

The peak *g* in Figure 1 was rather complex and broad. This may be caused by the formations of some aggregates which consisted of different compositions of the isoprenyllithiums.^{9,10}

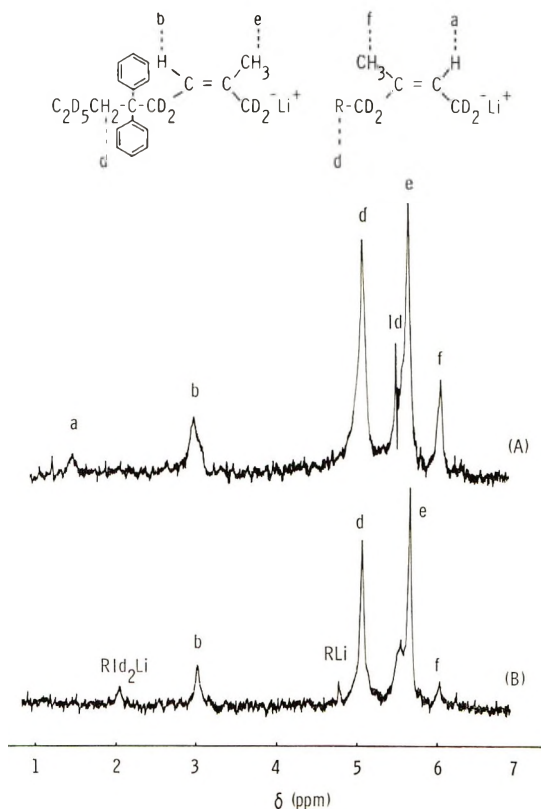


Fig. 2. NMR spectra of RLi in benzene-*d*₆ at 100 MHz: (A) 24°C; (B) 68°C. Peak *Id* in (A) was due to the methyl group of the unchanged isoprene).

The relative area of each peak in Figures 1 and 2, and the microstructure of the anion determined from the areas are summarized in Table I. The missing fraction arising after subtracting those of the 1,4 and 4,1 anions from unity was assumed to be attributed to the unknown units. On a raise in temperature, the relative intensities of the peaks *a* and *f* decreased, whereas that of *e* increased (B in Figs. 1 and 2). At the same time, peaks attributable to RLi and RLi₂ appeared in the spectra, indicating that the reaction of RLi with isoprene was reversible and a dimer of isoprene was formed from RLi and a monomer reproduced. The chemical shifts of the RLi in these spectra were just the same as those measured in the absence of RLi.¹ The microstructure of RLi above 60°C could not simply be determined from the ratio of peak areas because of the existence of RLi₂ as described above. Therefore, the microstructure was calculated by assum-

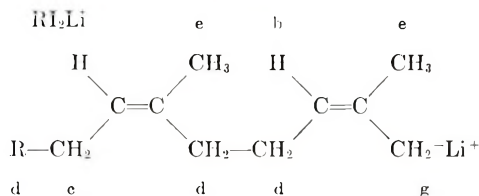
TABLE I
 Intensities of the Peaks in the NMR Spectra of RLi and RLiLi in Benzene- d_6

Fig. no.	Temp, °C	Intensity of peak ^a						Total intensity	Microstructure			
		H_a	H_b	H_c	H_d	H_e	H_f		H_g	<i>cis</i> -1,4, %	4,1, %	3,4, %
1	22	0.2	0.7	1.9	2.1	2.3	0.8	2.0	10.0	70	20	10
1	60	0.1	0.8	1.9	2.1	2.7	0.3	2.1	10.0	80	10	10
2	24	0.2	0.7	—	2.1	2.4	0.6	—	6.0	70	20	10
2	68	0.1 ^b	0.7	—	2.3	2.6	0.3	—	6.0	70	10	20
—	23	0.2	0.7	2.0	2.2	2.3	0.8	1.8	10.0	70	20	10
—	83	0.1 ^b	0.7	1.8	2.5	2.9	0.4	1.6	10.0	70	10	20

^a See Figs. 1 and 2.

^b Calculated as a third of the intensity of H_f .

ing that the RI_2Li had a *cis-cis* structure, and the following assignments could be adopted for its NMR spectrum:



The relative areas of the peaks in the spectrum of RI_2Li (Table I) at high temperature were obtained by subtracting the areas considered to be due to the RI_2Li . The area due to RI_2Li was estimated from that of the reproduced RI_2Li .

When water was added to RI_2Li , the peak due to $-\text{CH}_2-\text{Li}^+$ disappeared, the peak *b* shifted to 2.2 ppm. The peaks *c*, *d*, and *e* also shifted but slightly. The NMR spectra of the resultant protonated compound of the anion indicated that the anion had been composed of equimolar amounts of RLi and isoprene.

NMR Spectrum in the Presence of THF

The NMR spectra were measured on RI_2Li and RI_2Li , each of which was prepared in benzene- d_6 by the reaction of RLi with equimolar amount of isoprene or isoprene- d_4 in the presence of a small amount of THF. The spectra are shown in Figures 3 and 4, respectively. The spectra were rather complicated because of the existence of the peaks due to THF. A similar

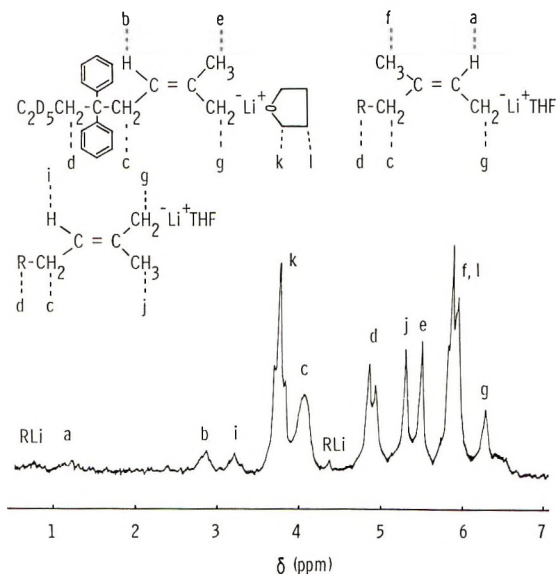


Fig. 3. NMR spectrum of RI_2Li in the presence of a small amount of THF in benzene- d_6 at 100 MHz (THF/ RI_2Li = 0.56; 23°C).

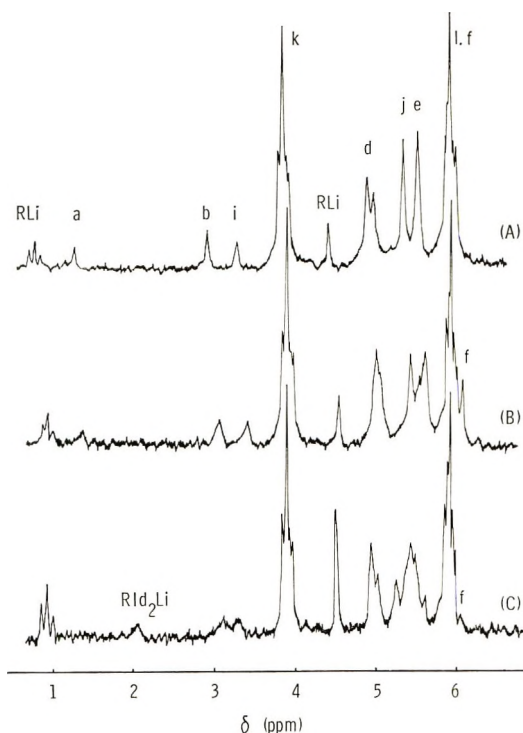


Fig. 4. NMR spectra of RLi in the presence of a small amount of THF in benzene- d_6 at 100 MHz (THF/ RLi = 0.83): (A) 23°C, (B) 50°C, (C) 63°C.

spectrum was also obtained when THF was added afterward to RLi in benzene- d_6 .

The spectrum of RLi in benzene- d_6 in the presence of about one mole of THF- d_8 per the anion is shown in Figure 5. Except the unknown peaks i and j , every peak in the spectrum was found to correspond to those of the spectrum A in Figure 2 with slight downfield shifts. Therefore, the RLi in Figure 5 contained at least the *cis*-1,4 and *cis*-4,1 structures. The spectra in Figures 3 and 4 were assigned similarly as to the signals raised from the *cis*-1,4 and *cis*-4,1 anions. The spectra were found to be composed of the signals from these two anions, those from THF, and the unknown signals i and j .

The peak i is considered to be due to an olefinic proton because of its chemical shift at rather low magnetic field. It appears as an insufficiently resolved triplet in Figure 3 and as a singlet in Figures 4 and 5, similar to the peaks a and b . This indicates that the proton causing the peak i must have been coupled with a methylene group in RLi , and hence the proton may belong to the 1,4 and 4,1 anions. The 1,2 anion is not likely to be considered, because of steric hindrance. The relative intensities of the peaks b and i and of the peaks j and e changed as a ratio of THF to RLi was varied; i.e., the relative intensities of the peaks i and j increased with

TABLE II
 Intensities of the Peaks in the NMR Spectra of RLi and RLiLi in the Presence of
 a Small Amount of THF in Benzene- d_6 at 23°C

Fig. no.	THF		Intensity of peaks ^a										Total intensity ^b	Microstructure		
	RLi		H _a	H _b	H _i	H _k	H _c	H _d	H _j	H _e	H _{f,g}	cis- 1,4, %		trans- 1,4, %	4,1, %	3,4, %
3	0.56		0.2	0.3	0.3	2.5	1.7	2.0	1.2	1.3	5.1	30	30	20	20	
4	0.83		0.1	0.4	0.3	3.4	—	1.9	1.3	1.5	3.9	40	30	10	20	
4 ^c	0.83		0.1	0.3	0.3	3.2	—	2.0	1.4	1.5	3.6	30	30	10	30	
5	1.1		0.1	0.3	0.4	—	—	2.1	1.3	1.3	0.5	30	40	10	20	
—	1.3		0.1	0.3	0.4	5.2	—	2.0	1.4	1.4	5.6	30	40	10	20	

^a See Figs. 3 and 5.

^b Total intensity after subtracting that of THF.

^c Measured at 50°C.

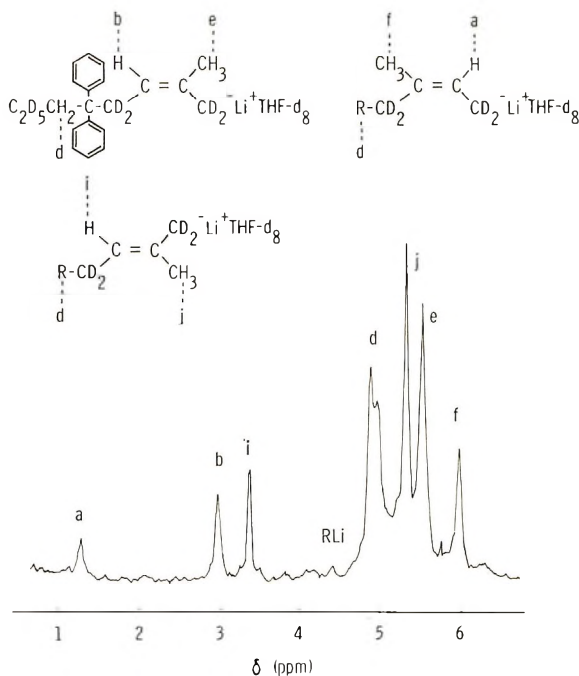


Fig. 5. NMR spectrum of $RLiLi$ in the presence of a small amount of $THF-d_8$ in benzene- d_6 at 60 MHz ($THF-d_8/RLiLi = 1.1$; $23^\circ C$).

increasing ratio of $THF/RLiLi$ as observed in Figures 3 and 5. As in the anionic polymerization of isoprene by alkyl lithium in hydrocarbon solvent, the content of the *cis*-1,4 structure decreased with an increase in the ratio of THF to alkyl lithium,^{5,7} we attributed the peaks *i* and *j* to the *trans*-1,4 anion. No additional peak was observed around the peak *a*, indicating the absence of the *trans*-4,1 anion.

The assignments of the peaks are shown in Figures 3 and 5. The relative intensities of the peaks in the spectra are collected in Table II. In these cases there may also be unknown anions. The ratio of THF to $RLiLi$ was, therefore, checked after the $RLiLi$ was protonated, in order to avoid the error caused from the overlaps among the peaks due to THF and the unknown anions.

The microstructures of the isoprene unit in $RLiLi$ and $RLiLiLi$ are also shown in Table II. The missing fraction was estimated and assumed as that of the unknown anions similarly as in Table I. When the ratio $THF/RLiLi$ was increased, the portion attributable to the 4,1 structure decreased and the ratio of *trans*-1,4 to *cis*-1,4 structure increased. At high temperature, the peaks due to the 4,1 anion decreased and those due to $RLiLi$ increased in time (Fig. 4). Contrary to Figures 1 and 2, the peaks due to 1,4 anion were broadened with increasing temperature.

When about half the volume of benzene- d_6 in a $RLiLi$ solution was replaced by $THF-d_8$, a great deal of $RLiLi$ was produced, and the liberated iso-

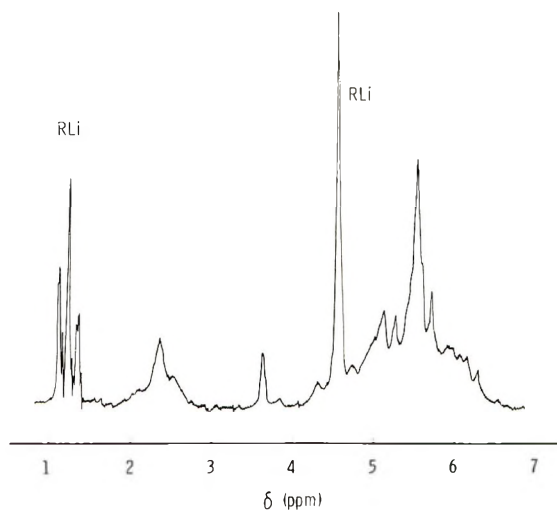


Fig. 6. NMR spectrum of RLi in a mixture of benzene- d_6 and THF- d_8 at 60 MHz (benzene- d_6 /THF- d_8 = 1.0; THF- d_8 was added to RLi in benzene- d_6 ; 23°C).

prene seemed to be consumed in the polymerization. The NMR spectrum is shown in Figure 6. The peak due to the $\text{CH}_2=$ group in the isoprene unit was found at 2.35 ppm, where the peak due to the $\text{CH}_2=$ group of the 3,4-structure in polyisoprene appeared in the measurement in benzene.⁴

DISCUSSION

The NMR spectrum of the RLi in benzene- d_6 was rather different from that of isoprenyllithium ($t\text{-BuLi}$) in benzene reported by Bywater et al.² who prepared the sample by the reaction of *tert*-butyllithium- d_9 with isoprene. In our spectrum the resonance peaks of the isoprene unit were found at higher field than those in the spectrum of $t\text{-BuLi}$. This must be attributed to the anisotropic effect induced by the ring current of the benzene rings in the R group. Since polyisoprenyllithium is known to

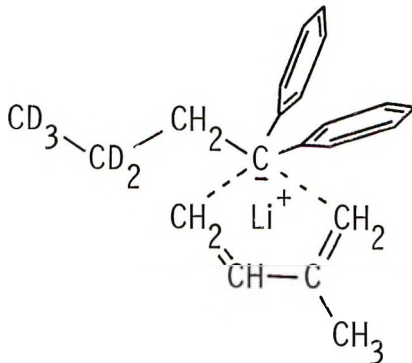
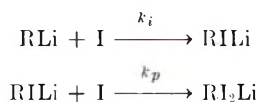


Fig. 7. Transition complex of RLi with isoprene.

again with one another to give the *cis*-1,4 and other anions, probably 3,4 anion. This is caused by the difference in the steric effect of the methyl groups in the 1,4 and 4,1 anions; the methyl group in the latter must occupy a sterically unfavorable position, and the coordination shown in Figure 7 is likely to be disturbed.

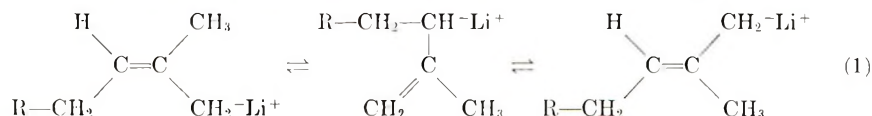
It was reported that a dimer anion was produced to some extent in the reaction between equimolar amounts of butyllithium and isoprene.¹⁹ In the reaction between equimolar amounts of RLi and isoprene the concentration of RLi rapidly diminished to zero at room temperature, suggesting a very fast reaction between these two compound and the almost quantitative formation of the RLi. The fast reaction was evidenced by the change in the NMR spectrum.

The reaction of RLi with isoprene was much faster even in the presence of a small amount of THF than that of the reaction of RLi with isoprene, i.e., $k_i \gg k_p$.

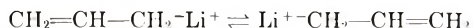


The RLi is considered to involve steric hindrance and a resonance stabilization much larger than RLi, and accordingly the difference in the reactivity may be ascribed to the difference in the state of association, i.e., in the concentration of active species.

The addition of a small amount of the THF could, however, induce the isomerization of RLi. This indicated an equilibrium between the *cis*-1,4 and *trans*-1,4 anion, probably through the 3,4-anion [eq. (1)].



The NMR spectrum of allyllithium in diethyl ether showed a well separated doublet and quintet typical of a spectrum of the AX₄ type,¹⁷ indicating a rapid exchange reaction [eq. (2)].

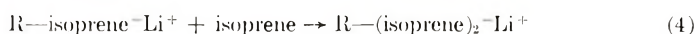
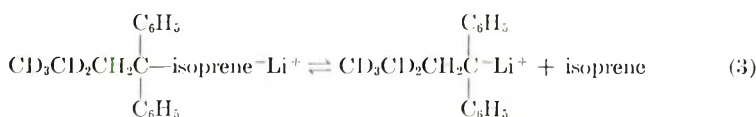


Bywater et al.² reported that the isomerization of *cis*-1,4 to *trans*-1,4 structures occurs even at -40°C if a large quantity of THF is present. In Figure 4 the peaks due to the methine and methyl groups were rather broadened at high temperatures, implying that the isomerization reactions became rather rapid between the *cis*-1,4 and *trans*-1,4 anions.

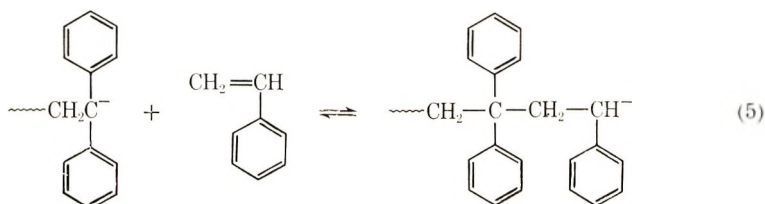
In Tables I and II unknown anions were assumed. Because of the low accuracy of the NMR measurement the data are not sufficiently reliable, but the existence of unknown anions may not be ignored. The 3,4 anion is the most likely anion to exist besides the 1,4 and 4,1 anions, although direct evidence indicating its existence was not observed in the NMR spectra.

The transition complex shown in Figure 7 becomes less important in the presence of THF, since the THF strongly coordinates lithium cation,^{1,5,20} and a part of the 1,4 anion may be formed, probably through the 3,4-anion. The reactivity of isoprene must therefore depend on the presence of THF. A higher reactivity of isoprene was observed in benzene than in THF in the alkylolithium-initiated copolymerizations of this monomer with 1,1-diphenylethylene²¹ and styrene.²²

A large amount of THF led to the decomposition not only of the aggregation of RLi in benzene but also of this salt into RLi and isoprene. The large steric hindrance due to the two benzene rings in RLi must be responsible for the reversible reaction of RLi formation. The readdition of liberated isoprene took place more easily to RLi which had been dissociated from the aggregation than to RLi because of the lower steric hindrance of the former.



The equilibrium reaction (5) in THF including a diphenylethylene anion and styrene has been reported.²³



The 3,4 anion of RLi has a configuration similar to that of the styryl anion, the product of reaction (5).

The authors wish to thank Yoshio Terawaki and Hiroshi Okuda for the measurements of the NMR spectra.

References

1. Y. Okamoto and H. Yuki, to be published in *J. Organometal. Chem.*
2. F. Schue, D. J. Worsfold, and S. Bywater, *J. Polym. Sci. B*, **7**, 821 (1969).
3. R. F. Frank, C. E. Adams, J. R. Blegen, R. Deanin, and P. V. Smith, *Ind. Eng. Chem.*, **39**, 887 (1947).
4. Y. Tanaka, M. Kobayashi, H. Tadokoro, paper presented at the 17th Polymer Symposium of the Polymer Society of Japan, Matsuyama, October 1968.
5. A. V. Tobolsky and C. E. Rogers, *J. Polym. Sci.*, **40**, 73 (1959).
6. R. S. Stearns and L. E. Forman, *J. Polym. Sci.*, **41**, 381 (1959).
7. D. J. Worsfold and S. Bywater, *Can. J. Chem.*, **42**, 2884 (1964).
8. H. L. Hsieh, *J. Polym. Sci. A*, **3**, 181 (1965).
9. M. A. Weiner and R. West, *J. Amer. Chem. Soc.*, **85**, 485 (1963).
10. G. E. Hartwell and T. L. Brown, *J. Amer. Chem. Soc.*, **88**, 4625 (1966).

11. H. Sinn, C. Lundborg, and O. T. Onsager, *Makromol. Chem.*, **70**, 222 (1964).
12. M. Morton and L. J. Fetters, *J. Polym. Sci. A*, **2**, 3311 (1964)
13. M. Morton, L. J. Fetters, R. A. Pett, and J. F. M. Meier, *Macromolecules*, **3**, 327 (1970).
14. H. L. Hsieh, *J. Polym. Sci. A*, **3**, 173 (1965).
15. Y. Tanaka and S. Otsuka, *Kobunshi Kagaku*, **25**, 177 (1968).
16. S. Toppet, G. Slinckx, and G. Smets, *J. Organometal. Chem.*, **9**, 205 (1967).
17. C. S. Johnson, Jr., M. A. Weiner, J. S. Waugh, and D. Seyferth, *J. Amer. Chem. Soc.*, **83**, 1306 (1961).
18. V. R. Sandal, S. V. McKinley, and H. H. Freedman, *J. Amer. Chem. Soc.*, **90**, 495 (1968).
19. F. Schue and S. Bywater, *Bull. Soc. Chim. France*, **1970**, 271.
20. R. Waack, M. A. Doran, and P. E. Stevenson, *J. Amer. Chem. Soc.*, **88**, 2109 (1966).
21. H. Yuki and Y. Okamoto, *Bull. Chem. Soc. Japan*, **42**, 1644 (1969).
22. A. V. Tobolsky and C. E. Rogers, *J. Polym. Sci.*, **38**, 205 (1959).
23. E. Ureta, J. Smid, and M. Szwarc, *J. Polym. Sci. A-1*, **4**, 2216 (1966).

Received September 1, 1970

Photocondensation Polymers: Polybenzopinacols. II. Photolytic Coupling of Aromatic Diketones

D. A. McCOMBS, C. S. MENON, and JERRY HIGGINS,* *Department of Chemistry, Illinois State University, Normal, Illinois 61761*

Synopsis

Photolytic condensations of *p,p'*-dibenzoyldiphenyl sulfide, *p,p'*-dibenzoyldiphenyl ether, *p,p'*-dibenzoyldiphenylmethane, and *p,p'*-dibenzoyldiphenylethane with a 100-W long-wavelength ultraviolet lamp gave polypinacols having inherent viscosities ranging from 0.12 to 0.45. Treatment of the same monomers under similar conditions with a 450-W ultraviolet lamp produced polypinacols having inherent viscosities ranging from 0.04 to 0.37.

INTRODUCTION

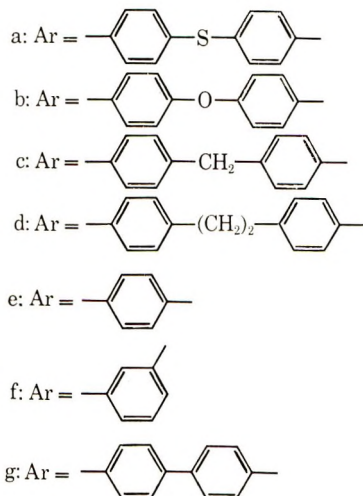
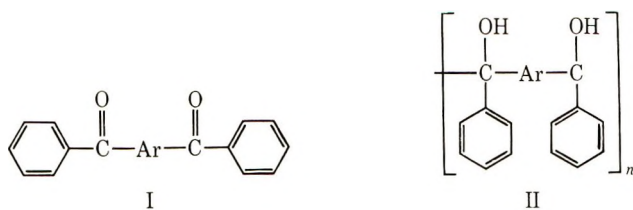
Previously,¹ we described the preparation of three aromatic polypinacols (IIb, IIe, and IIf) by photocondensation† of the corresponding aromatic diketones Ib, Ic, and If. These polymers had low inherent viscosities (0.06–0.14) and contained a considerable amount of reduced rather than coupled product. We now wish to report the preparation of three new polymers IIa, IIc, and IId by a modification of our original procedure. In addition, the procedure described in this paper has been used to prepare polymer IIb having a significantly increased inherent viscosity over that previously reported.

RESULTS AND DISCUSSION

The photocondensations of monomers Ia–Id in benzene–isopropanol solutions with a 100-W, long-wavelength ultraviolet lamp was effected by a slightly modified version of the procedure reported previously. Irradiations of the diketone monomers were done in 1:1 benzene–isopropanol solutions at reflux in an open system under a stream of nitrogen for a period of 24 hr rather than in a closed vessel under a nitrogen atmosphere over a period of several days.

* To whom correspondence should be addressed.

† In order to distinguish photochemically induced chain-reaction polymerizations from stepwise photochemical polymerizations, we define a photocondensation polymerization as any stepwise polymerization which requires the absorption of one or more photons per step.



An analogous procedure to that described above was used with a 450-W ultraviolet lamp fitted with a Pyrex filter. The use of a 450-W lamp resulted in a reduction of the reaction times from 24 hr to 2 hr, but the inherent viscosities of the polymers were somewhat lower than those produced with the 100-W lamp (Table I). These lower molecular weights could be due to cleavage of carbon-carbon bonds. Breakage of carbon-carbon bonds during a photochemical process in sunlight has been reported.² Perhaps the high-intensity irradiation with the 450-W lamp may give rise to some cleavage to give lower molecular weights than the 100-W lamp.

TABLE I

Polymer	100-W UV lamp ^a		450-W UV lamp ^b	
	Mp, °C	η_{inh}^c	Mp, °C	η_{inh}^c
IIa	155-165	0.10	130-145	0.04
IIb	165-180	0.30	165-170	0.24
IIc	160-170	0.25	135-160	0.21
IId	170-185	0.45	165-170	0.37

^a A 100-W Blak-Ray B100-A ultraviolet lamp used for polymerizations.

^b A 450-W Ace Glass No. 3514 ultraviolet lamp and Pyrex filter used for polymerizations.

^c Polymer concentrations ranged from 0.1 to 0.4 g/100 ml.

Variations of the benzene-isopropanol ratios in the solvent did not seem to have any effect on the viscosities of the polymers. However, the monomer solubilities were greatly affected. The monomers were soluble in benzene but practically insoluble in isopropanol. Also, with smaller ratios of iso-

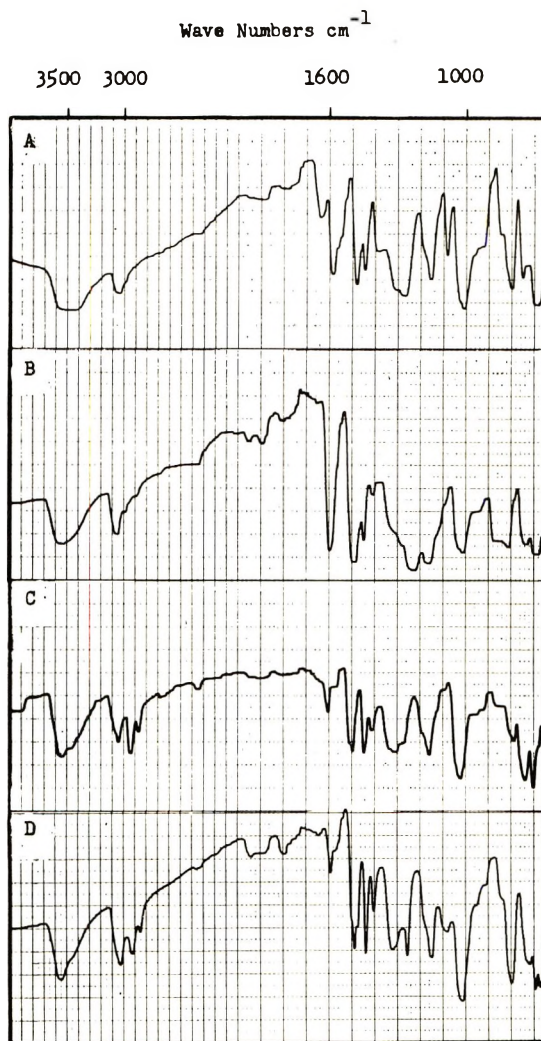


Fig. 1. Infrared spectra of polymers (KBr discs): (A) polymer IIa; (B) polymer IIb; (C) polymer IIc; (D) polymer IIId.

propanol to benzene, longer irradiation periods were required for reductive carbonyl coupling. Thus, a 1:1 ratio of benzene to isopropanol was found to be quite satisfactory.

Contrary to the results obtained in the closed systems, the polymers formed in the above procedures did not contain benzhydryl hydrogens, as

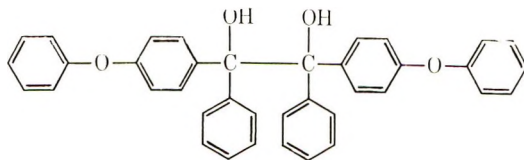
determined by NMR. This absence of reduction products may have been a result of increased monomer concentrations in these reaction mixtures.

Monomers Ie–Ig failed to give polymers under the above conditions. With the exceptions of small —OH stretching bands centered at about 3500 cm^{-1} , the infrared spectra of the products were identical to those of the corresponding monomers. The presence of a considerable carbonyl stretch in the infrared spectrum of polymer IIa at (1640 cm^{-1}) (Fig. 1) suggests that the reductive coupling of the corresponding monomer was incomplete under these conditions. By comparing the ultraviolet spectra in 95% ethanol solution of monomers Ie–Ig with that of benzophenone, it was found that the high intensity $\pi \rightarrow \pi^*$ absorption band showed bathochromic shift in going from benzophenone, $\lambda_{\text{max}} 255\text{ m}\mu$, to If, $\lambda_{\text{max}} 257\text{ m}\mu$, Ie, $\lambda_{\text{max}} 269\text{ m}\mu$, and Ig, $\lambda_{\text{max}} 306.2\text{ m}\mu$. Although the $n \rightarrow \pi^*$ absorption band was well resolved from the $\pi \rightarrow \pi^*$ for benzophenone, the same $n \rightarrow \pi^*$ absorption bands for Ie and If showed only as shoulders of the $\pi \rightarrow \pi^*$ bands and for Ig the $n \rightarrow \pi^*$ was completely buried under the $\pi \rightarrow \pi^*$ band. As these low-lying $\pi \rightarrow \pi^*$ triplet states do not lend to efficient hydrogen abstraction,³ monomers Ie–Ig failed to give polymers, apparently for this reason.

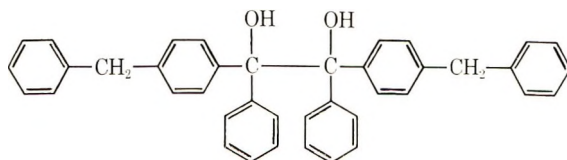
Polymers IIb–IId form brittle films and may be drawn into brittle fibers from the melt. However, prolonged heating above 110°C causes considerable decomposition, as determined by infrared and viscosity studies.

Model Compound Study

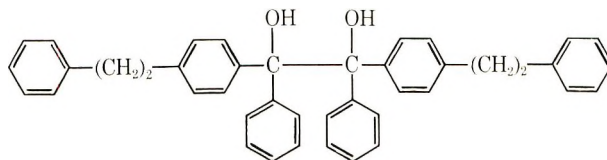
In order to aid in the identification of polymers IIb–IId, model pinacols IIIa and IIIc were prepared by photocoupling *p*-benzoyldiphenyl ether and *p*-benzoyldiphenylethane. Pinacol IIIb proved to be very difficult to prepare by photochemical coupling, since the starting ketone, *p*-benzoyldiphenylmethane, was difficult to purify. Photocoupling of this ketone proceeded very slowly so the ketone was coupled with magnesium and iodine by a modification of the procedure described by Gomberg and Bachmann⁴ for the coupling of benzophenone. Here, too, yields were low and the resulting pinacol IIIb was purified with great difficulty.



IIIa



IIIb



IIIc

Spectral data (NMR and infrared) obtained for model compounds IIIa–IIIc and those obtained for the corresponding polymers were consistent with the formulated structures (Fig. 2). The model pinacol for polymer IIa was not synthesized since only limited success was achieved in the preparation of this polymer. No attempt was made to separate the stereoisomers of the model pinacols.

EXPERIMENTAL

Instruments

The ultraviolet lamps used in this study were a 100-W Blak-Ray B100-A long-wavelength lamp and an Ace Glass No. 3515 450-W lamp. The

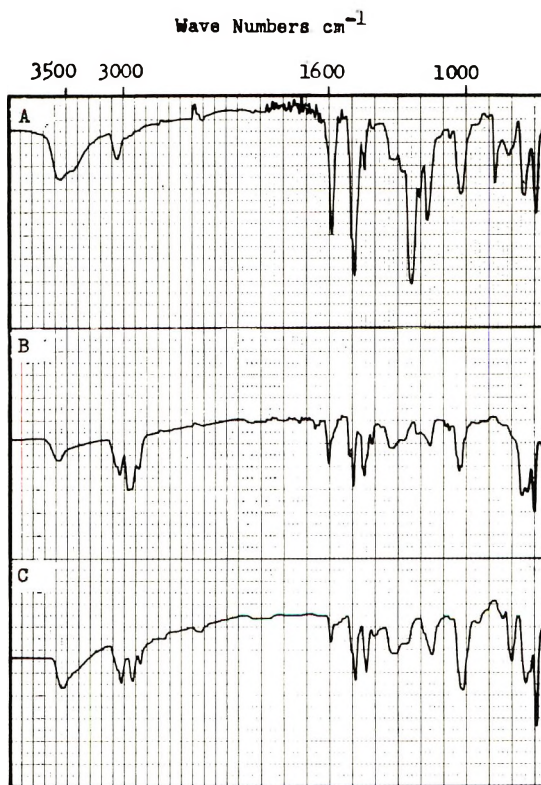


Fig. 2. Infrared spectra of model pinacols: (A) pinacol IIIa (KBr disc); (B) pinacol IIIb (neat); (C) pinacol IIIc (KBr disc).

reaction vessel used with the 450-Watt lamp was an Ace Glass No. 6523 photochemical reaction vessel fitted with a pyrex immersion well. Nuclear magnetic resonance (NMR) spectra were obtained with a Hitachi Perkin-Elmer R20 instrument. Infrared spectra were taken on Beckman IR-8 and Perkin-Elmer Model 700 instruments.

Preparation of Monomers

Preparation of *p,p'*-Dibenzoyldiphenyl Sulfide (Ia). To a mixture of 33 g (0.18 mole) of diphenyl sulfide, 67 g (0.5 mole) of anhydrous aluminum chloride, and 150 ml of carbon disulfide was slowly added 59 g (0.42 mole) of benzoyl chloride with stirring. After the addition was complete, the reaction mixture was refluxed for 4 hr, cooled, and stirred into a 10% solution of HCl in ice water. The liquid layer was decanted and the white solid was washed with concentrated hydrochloric acid, 10% sodium carbonate solution, and finally with water. The crude product was then dried *in vacuo* and recrystallized from carbon tetrachloride to a constant melting point of 168–169°C (lit.⁵ mp 169°C). The yield of product was 48 g (69%).

Preparation of *p,p'*-Dibenzoyldiphenylmethane (Ic). To a vigorously stirring mixture of 105 g (0.75 mole) of benzoyl chloride and 100 g (0.75 mole) of anhydrous aluminum chloride was quickly added 30 g (0.18 mole) of diphenylmethane. The reaction mixture was allowed to stir at 80–90°C for an additional 20 min before being hydrolyzed in 10% hydrochloric acid, washed with 10% sodium hydroxide solution, and then with water. The crude product was recrystallized to a constant melting point of 145–147°C (lit.⁶ mp 147.5–148.5°C). The yield of product was 8 g (12%).

Preparation of *p,p'*-Dibenzoyldiphenylethane (Id). To a mixture of 105 g (0.75 mole) of benzoyl chloride and 100 g (0.75 mole) of anhydrous aluminum chloride was slowly added 25 g (0.14 mole) of 1,2-diphenylethane. The resulting mixture was then stirred an additional 90 min at 80–90°C before being poured into dilute hydrochloric acid in ice water. The precipitate was digested with 10% hydrochloric acid, washed with 10% sodium hydroxide, and with water. The crude product was recrystallized from benzene to a constant melting point of 175–176°C (lit.⁶ mp 174.5–176°C). The yield of product was 28 g (52%).

Preparation of *p,p'*-Dibenzoylbiphenyl (Ig). To a mixture of 91 g (0.65 mole) of benzoyl chloride and 125 g (0.94 mole) anhydrous aluminum chloride was added 29 g (0.19 mole) of biphenyl. The reaction mixture was stirred and kept at 80–90°C until evolution of hydrogen chloride ceased and was then hydrolyzed in cold, dilute hydrochloric acid. The resulting solid was digested with 10% hydrochloric acid, washed with 10% potassium hydroxide solution, and with water. The crude product was recrystallized from dioxane to a constant melting point of 219–220°C (lit.⁷ mp 218°C). The yield of product was 30 g (41%).

Preparation of Model Compounds

Preparation of *p*-Benzoyldiphenyl Ether. To a mixture of 34 g (0.20 mole) of diphenyl ether and 33 g (0.25 mole) of anhydrous aluminum chloride in 275 ml of carbon disulfide was slowly added 14 g (0.10 mole) of benzoyl chloride. The mixture was then refluxed for 120 min before being hydrolyzed in a 10% solution of hydrochloric acid in ice water. After evaporation of the carbon disulfide, the oily layer was taken up in benzene, washed with 10% sodium hydroxide solution, washed with 10% hydrochloric acid solution, and with water. The benzene layer was dried over anhydrous magnesium sulfate and the solvent was removed leaving a yellow oil which crystallized upon standing 3 days. The crude product was recrystallized from hexane to a constant melting point of 68–69°C (lit.⁸ mp 69.2–69.4°C). The yield of product was 11.5 g (38%).

Preparation of *p*-Benzoyldiphenylmethane. To a mixture of 360 g (2.1 mole) of diphenylmethane and 28 g (0.2 mole) of benzoyl chloride was slowly added 41 g (0.31 mole) of anhydrous aluminum chloride with vigorous stirring. After the evolution of hydrogen chloride gas had ceased, the mixture was stirred into a 10% solution of hydrochloric acid in ice water. The organic layer was taken up in benzene and washed with 10% sodium hydroxide solution, 10% hydrochloric acid, 10% sodium bicarbonate, and with water. The benzene layer was dried over anhydrous magnesium sulfate, benzene solvent removed, and distilled at reduced pressure. The fraction boiling at 230–240°C at 5–6 mm pressure (lit.⁹ bp 230–235°C/5 mm Hg) was collected. The yield of product was 10 g (18%).

Preparation of *p*-Benzoyldiphenylethane. Into a solution of 50 g (0.28 mole) of diphenylethane and 35 g (0.25 mole) of benzoyl chloride in 150 ml of carbon disulfide was added with stirring 50 g (0.38 mole) of anhydrous aluminum chloride. The mixture was refluxed for 30 min, cooled, and hydrolyzed in cold, dilute hydrochloric acid. After evaporation of the carbon disulfide, the oily layer was taken up in benzene, washed with 10% sodium hydroxide solution and with water. The benzene layer was dried over magnesium sulfate, benzene solvent removed, and distilled at reduced pressure. The fraction boiling at 175°C/0.2 mm pressure (lit.¹⁰ bp 260–280°C/15 mm Hg) was collected. The oil crystallized upon standing and was then recrystallized from hexane yielding 28.5 g (40%) of ketone melting at 81–82°C.

Preparation of 1,2-Bis(*p*-phenoxyphenyl)-1,2-diphenyl-1,2-ethanediol (IIIa). A solution of 6.0 g (0.022 mole) of *p*-benzoyldiphenyl ether in 200 ml of a 1:1 benzene–isopropanol mixture and two drops of glacial acetic acid was heated to refluxing temperature, purged with nitrogen, and irradiated under a stream of nitrogen for 24 hr with a 100-W ultraviolet lamp. The solvent was removed and the gummy product was reprecipitated from hexane to a constant melting point of 110–113°C. The yield of product was 3 g (50%).

ANAL. Calcd for $C_{35}H_{30}O_4$: C, 82.88%; H, 5.49%; Found: C, 82.83%; H, 5.45%.

Preparation of 1,2-Bis(*p*-benzylphenyl)-1,2-diphenyl-1,2-ethanediol (IIIb). To a mixture of 1.8 g (0.075 g-atom) of powdered magnesium, 15 ml of dry ether, and 18 ml of dry benzene was slowly added 4.6 g (0.036 g-atom) of iodine. After this mixture had been refluxed for 15 min, a solution of 6.3 g (0.032 mole) of *p*-benzoyldiphenylmethane in 10 ml of benzene was added. The resulting mixture was refluxed an additional hour and poured into 75 ml of water. A 30-ml portion of 10% hydrochloric acid was added to dissolve the precipitate and a small amount of sodium bisulfite was added to remove excess iodine. The organic layer was washed with water, dried over anhydrous magnesium sulfate, and treated with decolorizing charcoal. The solvent was removed and the resulting solid was reprecipitated twice from hexane and twice from pentane. The yield was 0.5 g (8%), mp 100–110°C.

ANAL. Calcd for $C_{40}H_{34}O_2$: C, 87.87%; H, 6.27%. Found: C, 87.89%; H, 6.31%.

Preparation of 1,2-Bis[*p*-(2'-phenylethyl)phenyl]-1,2-diphenyl-1,2-ethanediol (IIIc). A solution of 6 g (0.026 mole) of *p*-benzoyldiphenylethane in 200 ml of a 1:1 benzene-isopropanol mixture and two drops of glacial acetic acid was heated to refluxing temperature, purged with nitrogen, and irradiated under a stream of nitrogen at reflux with a 100-W ultraviolet lamp for 24 hr. The solvent was removed and the solid residue was washed with hexane and reprecipitated from benzene-hexane solvent. The yield of product was quantitative, mp 180–181°C.

ANAL. Calcd for $C_{42}H_{38}O_2$: C, 87.76%; H, 6.66%. Found: C, 87.65%; H, 6.70%.

Preparation of Polymers

Photocondensations of Diketones with a 100-W Ultraviolet Lamp

Photocondensation of *p,p'*-Dibenzoyldiphenyl Sulfide (Ia). In a 250-ml round-bottomed flask fitted with a reflux condenser, magnetic stirrer, and nitrogen flow adapter was placed a solution of 6 g (0.016 mole) of *p,p'*-dibenzoyldiphenyl sulfide in 200 ml of a 1:1 mixture of benzene and isopropanol and 2 drops of glacial acetic acid. This solution was purged with nitrogen at reflux temperature and irradiated at reflux under a slow stream of nitrogen for 24 hr. The solvent was removed and the crude product was washed with isopropanol and dried *in vacuo* at 80°C overnight. The yield was essentially quantitative, mp 155–165°C. The inherent viscosity was 0.10 (dioxane).

ANAL. Calcd for $(C_{26}H_{20}O_2S)_n$: C, 78.78%; H, 5.09%; S, 8.09%. Found: C, 77.68%; H, 5.17%; S, 7.70%.

Photocondensation of *p,p'*-Dibenzoyldiphenyl Ether (Ib). The procedure employed for the photocondensation of *p,p'*-dibenzoyldiphenyl ether was exactly analogous to that described above for *p,p'*-dibenzoyldiphenyl sulfide except that 6 g (0.017 mole) of *p,p'*-dibenzoyldiphenyl ether was used as the monomer. The yield was quantitative, mp 165–180°C. The inherent viscosity was 0.30 (dioxane).

ANAL. Calcd for $(C_{26}H_{20}O_2)_n$: C, 82.10%; H, 5.30%. Found: C, 81.75%; H, 5.59%.

Photocondensation of *p,p'*-Dibenzoyldiphenylmethane (Ic). The procedure employed for the photocondensation of *p,p'*-dibenzoyldiphenylmethane was exactly analogous to that described above for *p,p'*-dibenzoyldiphenyl sulfide except that 6 g (0.016 mole) of *p,p'*-dibenzoyldiphenylmethane was used. The yield was quantitative, mp 160–170°C. The inherent viscosity was 0.25 (dioxane).

ANAL. Calcd for $(C_{27}H_{22}O_2)_n$: C, 85.67%; H, 5.86%. Found: C, 83.96%; H, 5.64%.

Photocondensation of *p,p'*-Dibenzoyldiphenylethane (Id). The procedure employed for the photocondensation of *p,p'*-dibenzoyldiphenylethane was exactly analogous to that used for *p,p'*-dibenzoyldiphenyl sulfide above except that 6 g (0.013 mole) of *p,p'*-dibenzoyldiphenylethane was used as the monomer. The yield was essentially quantitative, mp 170–185°C. The inherent viscosity was 0.45 (dioxane).

ANAL. Calcd for $(C_{28}H_{24}O_2)_n$: C, 85.69%; H, 6.16%. Found: C, 85.01%; H, 6.01%.

Photocondensations with a 450-W Ultraviolet Lamp

Photocondensation of *p,p'*-Dibenzoyldiphenyl Sulfide (Ia). A refluxing solution of 5 g (0.013 mole) of *p,p'*-dibenzoyldiphenyl sulfide in 250 ml of a 1:1 benzene–isopropanol mixture was purged with nitrogen and irradiated for 2 hr under a stream of nitrogen. The solvent was removed, and the lumpy residue was crushed in cyclohexane, collected, and dried *in vacuo* at 78°C overnight. The yield was 3.0 g (60%), mp 130–145°C. The inherent viscosity was 0.04 (dioxane).

Photocondensation of *p,p'*-Dibenzoyldiphenyl Ether (Ib). The procedure employed for the photocondensation of *p,p'*-dibenzoyldiphenyl ether was exactly analogous to that described above for *p,p'*-dibenzoyldiphenyl sulfide except that 5 g (0.014 mole) of *p,p'*-dibenzoyldiphenyl ether was used as the monomer, and the reaction mixture was irradiated for 90 min. The yield was 3.9 g (78%), mp 165–170°C. The inherent viscosity was 0.26 (dioxane).

Photocondensation of *p,p'*-Dibenzoyldiphenylmethane (Ic). The procedure employed for the photocondensation of *p,p'*-dibenzoyldiphenylmethane was exactly analogous to that described for *p,p'*-dibenzoyldiphenyl sulfide except that 5 g (0.014 mole) of *p,p'*-dibenzoyldiphenylmethane was

used as the monomer. The yield was 3.8 g (76%), mp 135–160°C. The inherent viscosity was 0.21 (dioxane).

Photocondensation of 4,4'-Dibenzoyldiphenylethane (Id). The photocondensation procedure for 4,4'-dibenzoyldiphenylethane was exactly analogous to that used for 4,4'-dibenzoyldiphenyl sulfide except that 5 g (0.013 mole) of 4,4'-dibenzoyldiphenylethane was used as the monomer. The yield was 3.4 g (68%), mp 155–170°C. The inherent viscosity was 0.37 (dioxane).

We wish to acknowledge the helpful suggestions of Dr. J. H. Stocker. This work was supported by the Army Research Office-Durham, Durham, North Carolina.

References

1. J. Higgins, A. H. Johannes, J. F. Jones, R. Schultz, D. A. McCombs, and C. S. Menon, *J. Polym. Sci. A-1*, **8**, 1987 (1970).
2. A. Schönberg and A. Mustafa, *Chem. Rev.*, **40**, 181 (1947).
3. G. S. Hammond and P. A. Leermakers, *J. Amer. Chem. Soc.*, **84**, 207 (1962).
4. M. Gomberg and W. E. Bachmann, *J. Amer. Chem. Soc.*, **49**, 236 (1927).
5. W. Dilthey, L. Neuhaus, E. Reis, and W. Schonner, *J. Prakt. Chem.*, **124**, 81 (1930).
6. G. Wittig and M. Leo, *Ber.*, **61B**, 854 (1928).
7. L. M. Long and H. R. Henze, *J. Amer. Chem. Soc.*, **63**, 1939 (1941).
8. H. E. Ungnade, E. F. Kline, and E. W. Crandall, *J. Amer. Chem. Soc.*, **75**, 3333 (1953).
9. M. M. Delacre, *Bull. Soc. Chim. France*, **5**, 952 (1909).
10. Ng. Ph. Buu-Hoi, Ng. Hoan, J. Lecocq, and M. de Clercq, *Recl. Trav. Chim.*, **67**, 795 (1948).

Received October 6, 1970

Revised November 20, 1970

Poly(ethylene Sulfide). II. Thermal Degradation and Stabilization

E. H. CATSIFF, M. N. GILLIS, and R. H. GOBRAN, *Thiokol Chemical Corporation, Trenton, New Jersey 08607*

Synopsis

High molecular weight poly(ethylene sulfide) undergoes severe thermal degradation at the high temperatures (220–260°C) required for processing in injection-molding equipment. Thermal degradation of the polymer is accompanied by gas evolution and a decrease in melt viscosity. Stabilization of poly(ethylene sulfide) can be effectively accomplished by addition of small concentrations of certain 1,2-polyamines, preferably together with certain zinc salts as coadditives. Use of this stabilizer system inhibits thermal degradation to a remarkable extent, making it possible to mold the polymer at these high temperatures and obtain excellent physical and mechanical properties. Investigation of the thermal degradation process was carried out. The rate at which gases evolved from unstabilized poly(ethylene sulfide) resins of various molecular weights and preparative histories and from model compounds of the same organic backbone structure was measured at temperatures ranging from 220 to 260°C. Rate of gas evolution from the resins, irrespective of chain length or preparation, was found to be constant at 230°C. The evolved gases, analyzed by infrared spectroscopy and gas chromatography, contained ethylene. Nearly identical apparent activation energies were found for the gas evolution reaction from the resin and model compounds. The ΔE^* values were in good agreement with ΔE^* determined by other techniques, 58 ± 2 kcal/mole. This is about the energy requirement expected for the homolytic cleavage of a carbon-sulfur bond of the type present in a poly(ethylene sulfide) structure. The rate and analytical data indicate that the degradative mechanism at processing (molding) temperatures is primarily due to the organic structure of the polymer. A mechanism of thermal stabilization is proposed in which the polyamine and zinc salt, in presence of molten polymer at processing temperatures, form a two-centered electron transfer complex, capable of reacting with both radicals of the homolytically cleaved bond, "healing" the scission, so to speak.

Introduction

Poly(ethylene sulfide), specifically the high polymer prepared by the diethylzinc-water seed technique,¹ can be molded to a thermoplastic having exceptional properties suitable for engineering end-uses.² Due to the high melting point of the resin, 205–210°C, injection molding of the polymer must be carried out at temperatures ranging from 220°C to 260°C. Since the resin, as prepared, degrades rapidly at these temperatures, the presence of a stabilizer is necessary in the melt in order to make processing possible.

After an extensive screening study of additives, certain polyamines, alone or in combination with ZnO or zinc hydroxychloride, were found to

have an extraordinary effect in stabilizing the melt.^{3,4} The principal screening technique used was the Melt Indexer stability test, in which a charge of powdered resin, after blending with prospective stabilizers, was loaded into a Melt Indexer⁵ and subsequently extruded under a static pressure of 43 psi through a right cylindrical orifice 0.0825 in. in diameter and 0.315 in. long. The test temperature was initially 215°C, at which temperature the as-polymerized material was molten and degraded rapidly. As more effective stabilizers were found, test temperature was raised, until 235°C was eventually adopted. Results were plotted as flow rate (g/min) versus time after a standard warmup period. When the flow rate was plotted on a logarithmic ordinate, in many cases the data could be approximated by a straight line. For poorly stabilized melts, the rate of flow accelerated so rapidly that the entire charge was exhausted in a few minutes, but effective stabilizers reduced the degradation rate so that more than 30 min was required to empty the Melt Indexer barrel (for polymers of moderate to high apparent molecular weight). Where possible, the semi-logarithmic slope of the flow curve (expressed as per cent per minute rate increase) was used to measure the degree of chemical instability.

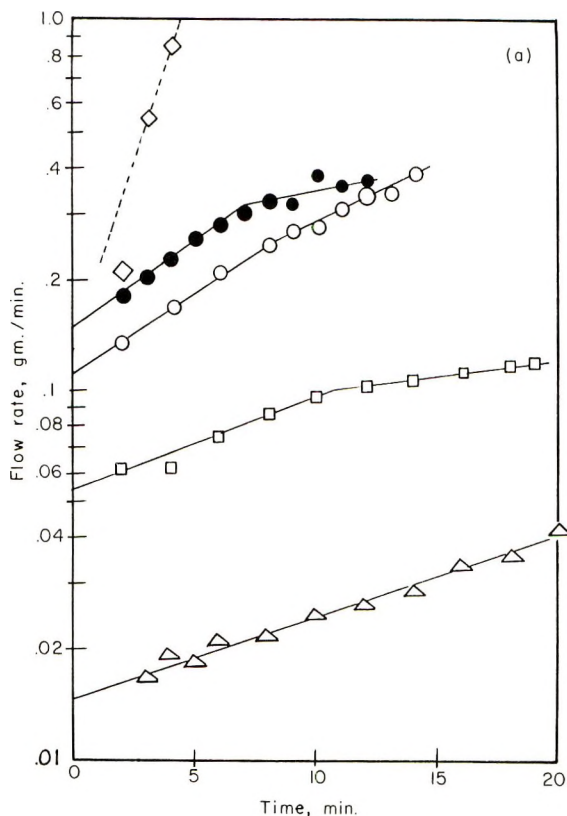


Fig. 1 (continued)

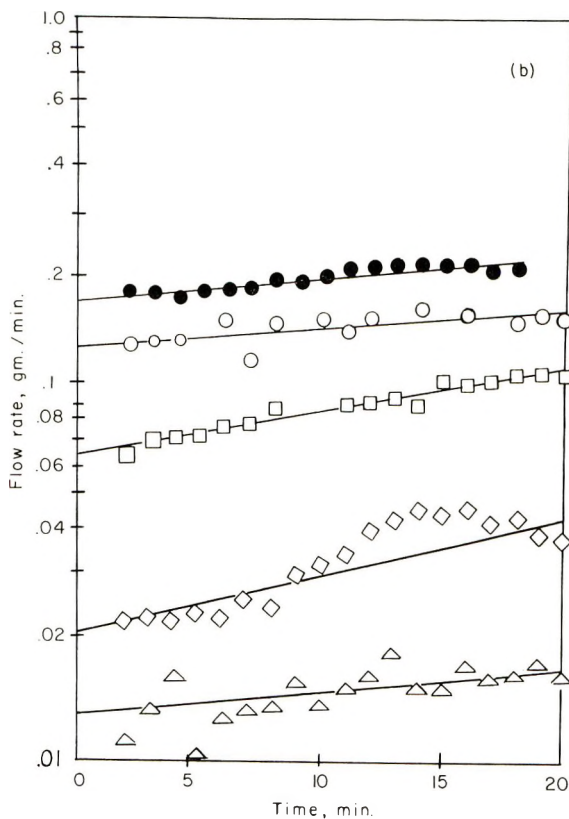


Fig. 1. Melt Indexer flow curves for standard poly(ethylene sulfide) at 235°C (a) with 2 phr BDPPPO and (b) with 2 phr BDPPPO and 1 phr zinc hydroxychloride. (●) lot A; (○) lot B; (□) lot C, 230°C; (△) Lot D; (◇) Lot D, zinc-free by extraction with 2-mercaptoethanol. Abscissa is time after warmup period.

Typical flow curves are shown in Figure 1. The type of data derivable from such curves is given in Table I. The stabilizing effect of suitable amines and the significant improvement brought about by added costabilizers are demonstrated by these data. The best amine we found was a bisdiamine, bis[*p*-(2,5-diazapentyl)phenyl] oxide (BDPPPO). A finely divided zinc hydroxychloride* was the best costabilizer found, although colloidal ZnO from commercial sources was also extremely effective. The apparent molecular weight referred to in Table I and elsewhere in this article is obtained from the apparent melt viscosity at 235°C calculated from the Melt Indexer flow rate extrapolated to the end of the warmup period, by using the essentially arbitrary relationship:⁶

$$\log M = 5.14 - 0.4167 \log G \quad (1)$$

* Approximate composition $Zn(OH)_{1.5}Cl_{0.5}$. Prepared by precipitation from aqueous $ZnCl_2$ solution with aqueous diethylenetriamine.

TABLE I
Melt Index Data of Poly(ethylene Sulfide) Prepared by the
Diethylzinc-Water Seed Technique

Stabilizer additives	Tem- perature, °C	Slope, %/min	Total flow time, min ^a	Apparent molecular weight ^b
Polymer of conventional molecular weight				
None	215	Very steep	5.4	—
BDPPO (2 phr)	235	9	14.1	300,000
BDPPO (2 phr) + zinc hydroxychloride (1 phr)	235	1.7	25.9	280,000
Polymer of high molecular weight				
None	215	c	26	640,000 ^c
None	235	—	3.5	—
BDPPO (2 phr)	235	6	30+	800,000
BDPPO (2 phr) + zinc hydroxychloride (1 phr)	235	1.8	30+	825,000

^a For 4-g sample; 4-min hold time.

^b Determined from zero-intercept melt viscosity.⁶

^c Two slopes: initial, 0-7 min, steep; second slope, 7-26 min, 6.5%/min. Molecular weight extrapolated from first slope.

where M is apparent molecular weight and G is flow rate (g/min) in our Melt Indexer.

In the work which follows, there was a dual purpose: (1) to define the nature of the breakdown occurring at elevated temperatures, and (2) to postulate a mechanism of stabilization. Certain additional facts should be added, which were known at the outset of this work: the zinc-containing catalyst residues in the polymer could be extracted; such zinc-free polymer did not respond to stabilization by BDPPO alone, but could be stabilized by a combination of amine and zinc hydroxychloride; the BDPPO-zinc hydroxychloride system was also effective in stabilizing polymer prepared by the use of some zinc-free initiators, e.g., NaCN in DMF and triethylenediamine (DABCO), but not all poly(ethylene sulfide)s could be so stabilized.

Gas Evolution Studies of Thermal Degradation Process

Study of the rate and products of thermal degradation of poly(ethylene sulfide) and of certain model compounds was undertaken. The primary experimental technique used was the quantitative determination of total gases evolved. Standard gas evolution apparatus was used for volumetric studies with modifications intended to reduce the dead volume and maximize the concentration of gas products in the (N₂) atmosphere at the end of an experiment for purposes of analysis. Polymer or model compound was weighed into a 25-ml flask, over glass beads, and the flask was connected to the volumetric apparatus. The system was evacuated at room temperature, filled with N₂, and the flask then immersed in a constant temperature bath. Readings were taken of the volume of gas in the system with time.

experiments, since the period of exposure to nonoxidative high-temperature conditions, in practical application, is limited to the period of molding, 6-15 min at most.

The factors which were feared capable of influencing the degree of instability were: (a) concentration of endgroups (related to polymer molecular weight), (b) type of endgroup, (c) presence of inorganic fragments in the polymer chain. Wragg⁹ found that model compounds of the type $\text{Bu-SCH}_2\text{CH}_2\text{SZnSCH}_2\text{CH}_2\text{SBu}$ (zinc mercaptide model salt), rapidly evolved ethylene and H_2S at 220°C and above. The products identified from the thermal breakdown of the zinc mercaptide model salt primarily implicated S-Zn scission.

The zinc mercaptide work is indeed evidence of S-Zn instability. However, two considerations must be borne in mind: (1) a S-Zn-S link has not been specifically postulated for the organic-inorganic fragments of our polymer (a monomercaptide zinc linkage has been considered more probable than a zinc dimercaptide); (2) the concentration of S-Zn-S bonds in the model is much greater (0.28 eq SZnS/100 g) than could possibly be present in the polymer: one SZnS group/molecule of 330,000 molecular weight corresponds to 3×10^{-4} eq SZnS/100 g.

In Table II, the initial rates of gas evolution are listed for poly(ethylene sulfide) polymers of various categories. There is no apparent effect of molecular weight, endgroups, or inorganic fragments on the rate of gas evolution from a poly(ethylene sulfide).^{*} The average value is about 10×10^{-5} mole gas/unit ES/min at 230°C. If this were ascribed to the above-calculated maximum possible concentration of SZnS groups, each such group would be evolving gas at the nearly-explosive rate of 0.55 mole/min.

The polymers from which Zn was extracted were virtually Zn-free and are believed to have mercaptan endgroups. The cyanide-initiated polymers should have nitrile and mercaptan or mercaptide endgroups with no possibility of Zn-S bonding.

In Table III rates of gas evolution are listed for the model compounds and for a typical "standard" polymer. Data for DTO is limited due to its low boiling point. TTU and DBT evolved gas at a single linear rate. Their rates are compared with the initial rate of gas evolution from the polymer; the ES unit was used as the mole substrate for the polymer.

At 230°C, under 1 atm N_2 , both DBT and TTU gave linear rates of gas evolution for as long as 6 hr. The infrared spectrum of the gas phase from DBT had a reproducible strong C-H absorption, unlike anything seen in

* Some polymers have been prepared (by use of other catalyst systems) which gave atypically low gas evolution rates, suggesting thermal stability. In the Melt Indexer, however, these polymers did not exhibit melt viscosity stability in the absence of added stabilizer. Apparently in these systems chain scission occurs but some secondary reaction inhibits gas evolution. Catalyst systems showing this phenomenon include NaCN in mixed toluene-DMF solution and triethylenediamine (DABCO) in DMF or in the mixed solvent. "Standard" diethylzinc-water-initiated polymer shows this phenomenon in the presence of some stabilizer candidates also.

TABLE II
Initial Rate of Gas Evolution from Poly(ethylene Sulfide)s
at 230°C under 1 Atmosphere N₂

Initiator	Apparent MW	Total gas generated, mole/ unit ES/min × 10 ⁵
ZnEt ₂ -H ₂ O ^a	140,000	10.0
ZnEt ₂ -H ₂ O ^a	330,000	8.7
ZnEt ₂ -H ₂ O ^a	500,000	5.8-15.5 ^b
ZnEt ₂ -H ₂ O ^{a,c}	210,000	11.04
ZnEt ₂ -H ₂ O ^{a,d}	210,000	15.5
NaCN-DMF	215,000	8.0
NaCN-DMF	570,000	6.2
NaCN-DMF	620,000	7.0-8.4 ^b

^a Seed technique.

^b Range of replicate experiments.

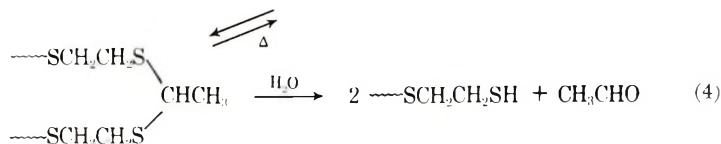
^c Zinc extracted by mercaptoethanol.

^d Zinc extracted by acetic acid.

the gas phases from polymer or TTU, which we have assigned to 1-butene. The ethylene absorption at 940 cm⁻¹ was relatively weak, so that quantitative monitoring of this wavelength would give a misleading impression of stability. The rate of gas evolution from DBT shows that thermal breakdown is taking place at a rate per mole comparable to TTU.

Comparative infrared spectra of the gaseous thermal breakdown products of standard polymer and the model compound TTU after 3.5 hr N₂ aging at 220°C are reproduced in Figure 2. These spectra represent also the general distribution of gas products observed in the gas phase after comparable reaction time at 230°C.

The presence of acetaldehyde (and perhaps CO₂) among the thermal breakdown gas products is most readily accounted for by molecular oxygen contamination. However, an alternate mechanism may be envisioned for acetaldehyde production during thermal breakdown in the absence of O₂. A reversible thiol-vinyl reaction is proposed, followed by hydrolysis [eqs. (3) and (4)]:¹⁰



Only water and sufficient acidity to catalyze thioacetal hydrolysis would need to be present as contaminants. Acetaldehyde would also be produced by hydrolysis of 2-methyl-1,3-dithiolane, a major product of thermal degradation of Zn mercaptide-initiated poly(ethylene sulfide).⁹ We did not search for such products, however, nor did we observe evidence of the formation of 1,4-dithiane, a sublimable solid. [A quantitative yield of

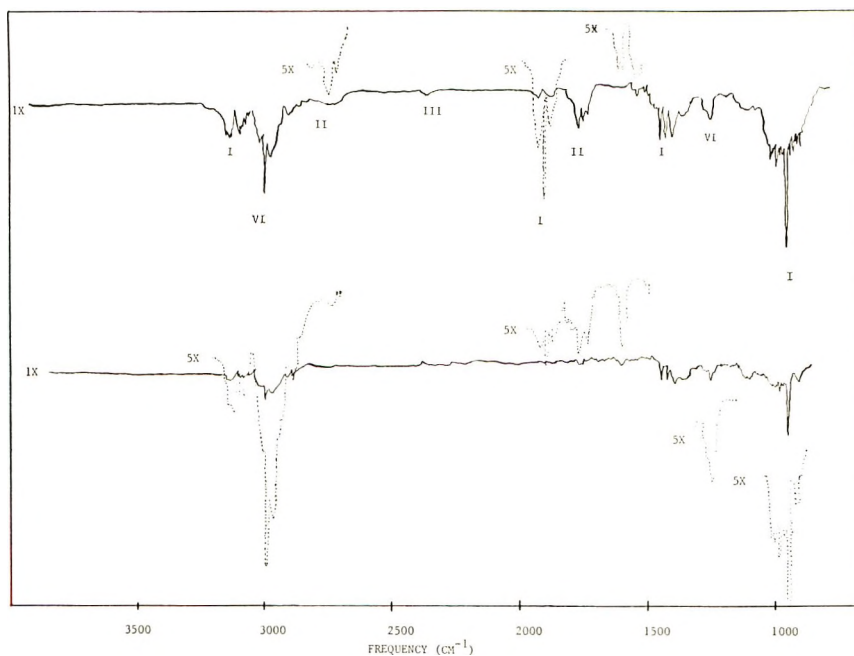


Fig. 2. Infrared spectra of gas phase after aging substrate 3.5 hr at 220°C under N_2 for (top) standard poly(ethylene sulfide) and (bottom) 3,6,9-trithiaundecane (TTU): (I) ethylene; (II) acetaldehyde; (III) CO_2 ; (VI) ethanethiol. 1X and 5X represent extent of scale expansion.

dithiane is obtained by $ZnCl_2$ -catalyzed decomposition of poly(ethylene sulfide) at high temperature. This presumably occurs via a sulfonium ion intermediate.] It appears that concentration of acetaldehyde relative to ethylene is greatest at short reaction times, e.g. 20 min, implying that only a limited amount of O_2 or H_2O is available. The gases present and their distribution are quite different from the array seen in the gas phase following oxidation at 150°C.⁸ The agreement in products obtained from the

TABLE III
Comparative Rates of Gas Evolution During Thermal Breakdown
of Model Compounds and Standard Polymer

Temperature, °C	Total gas, mole/mole substrate/min $\times 10^5$			
	DTO	TTU	DBT	Polymer ^a
180	<0.01	0.1		
223		7.5	4.6	6
230		18.3	17.8	8.7
236		19.7	17.2	25.9
240		57		39.4
245		41.7	78.6	25.2
250		97.5		76.1

^a Moles/unit ES/min $\times 10^6$.

polymer and model suggests that similar thermal breakdown mechanisms are operative in the model compound TTU and in the polymer above its melt temperature.

In a quasi-kinetic study by infrared absorption, gas phases were analyzed following thermal reaction at 230°C for different lengths of time. The spectrum obtained after 20 min agrees fairly well with the absorption due to ethylene in a reference spectrum. However between 1 and 3 hr, the multiple absorptions centering around 2995 cm^{-1} changed shape and increased in size, so that they resembled the absorptions due to ethanethiol in the gas phase; the growth of a companion peak at 1250 cm^{-1} supports the identification of ethanethiol. The transition in products being generated, occurring between 1 and 3 hr, may well correlate with the onset of rapid degradation in the polymer, generally occurring at about 115 min at 230°C.

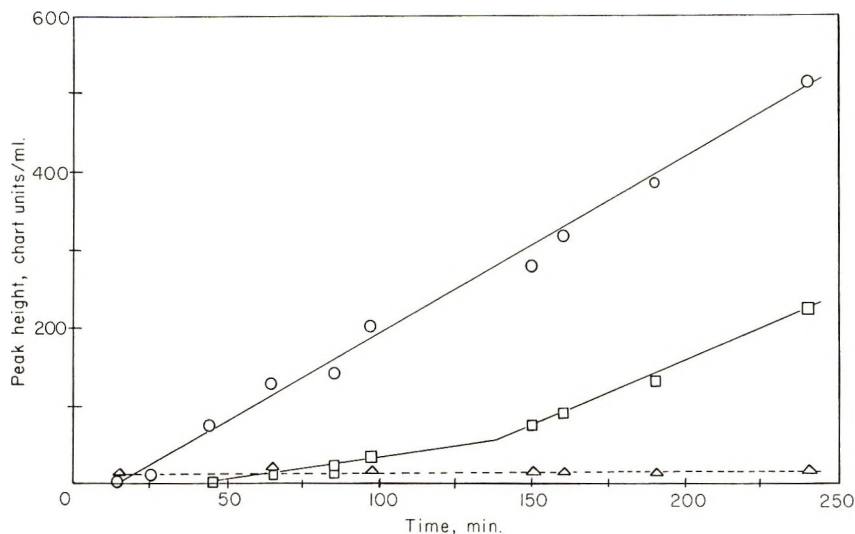


Fig. 3. Uncalibrated gas-chromatographic study of gaseous products from thermal treatment of standard poly(ethylene sulfide) at 230°C under N_2 : (O) ethylene; (\square) H_2S ; (\triangle) ethanethiol.

For gas chromatographic (GC) study of thermal decomposition gases, a column packing of Amberlite XAD-2 was found to give effective separation of nitrogen and ethylene gases at 45°C, with a flow rate of 75 ml/min helium. The major gas products, identified by their retention times, were H_2S , ethylene, and ethanethiol. H_2S , a weak absorber in the infrared, had not been heretofore identified by us among the gas products of polymer thermally degraded at these temperatures. It has been detected by Wragg⁹ and was known to be a product of pyrolysis of poly(ethylene sulfide) at 400°C.¹¹

The growth of (uncalibrated) peak height of the three gases with reaction time is depicted in Figure 3. Two important trends can be seen:

generation of ethylene apparently follows a constant rate throughout the course of the reaction; and H₂S undergoes an increase in rate at about the time usually observed as the onset of rapid degradation. The explanation for the constant content of ethanethiol is not clear.* Infrared spectra of the cooled gases were indicative of increased ethanethiol content as the degradation proceeded.

TABLE IV
Quantitative Determinations of Gases Evolved Thermally
at 230°C from Poly(ethylene Sulfide)

Reaction time at 230°C, min	Sample size, ml	Ethylene concn, μmole/ml	H ₂ S concn, μmole/ml	Ratio, H ₂ S/C ₂ H ₄
15	0.40	0.067	Not measurable	—
20	0.70	0.138	“ “	—
40	1.00	0.402	0.333	0.83
50	0.42	0.479	No data	—
55	0.40	0.603	0.334	0.55
65	0.26	1.60	1.28	0.80
70	0.46	1.91	1.74	0.91
80	0.56	2.87	2.74	0.96
95	0.82	4.10	4.48	1.09
105	0.84	4.90	5.78	1.18
115	1.06	5.09	6.25	1.23
145	0.80	8.05	13.5	1.68
155	2.96	7.78	15.8	2.04
170	1.94	12.58	28.8	2.28
185	1.46	19.2	49.9	2.60
215	2.42	13.89	50.4	3.63
235	2.70	13.41	66.0	4.92

For a more quantitative determination, peak-height response factors were determined for ethylene and hydrogen sulfide gases under the following conditions: column, 5 ft × 1/4 in. OD stainless steel column; packing, Amberlite XAD-2; column temperature, 47°C; helium flow rate, 67 ml/min. Ethylene response factor was 0.893×10^{-8} mole ethylene/chart unit; hydrogen sulfide response factor, 16.67×10^{-8} mole H₂S/chart unit. The Amberlite column is preferred for GC study of the gas products from poly(ethylene sulfide) breakdown under N₂ because of the separation of peaks for nitrogen, ethylene, and hydrogen sulfide, so that all three gases can be distinguished. However, as can be seen from the response factors, the sensitivity of the column toward H₂S is much poorer than the sensitivity to ethylene.

* The gas sample in this technique is taken from a cool region of the flask side-arm, where some droplets of condensate may be seen. The constant ethanethiol content may most readily be explained as resulting from the equilibrium vapor pressure of this condensate, so no conclusions may be drawn about the rate of generation of EtSH.

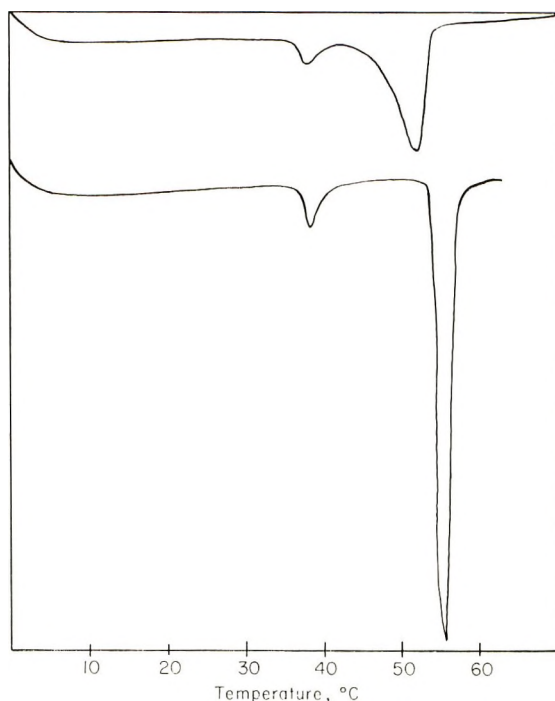


Fig. 4. DSC thermograms under N_2 of 5,8,11,14-tetrathiaoctadecane (DBT) at a scanning rate of $10^\circ C/min$: (bottom) unaged; (top) after 4 hr at $230^\circ C$ under N_2 .

A more favorable response factor for H_2S was obtained with a similar stainless steel column, when 15% tricresyl phosphate (TCP) was used as liquid phase on Firebrick support: column temperature, $30^\circ C$; He flow rate, 75 ml/min. H_2S response factor was 0.735×10^{-8} mole H_2S /chart unit. This column may therefore be considered preferable in degradation studies for more accurate measurement of H_2S evolution. It cannot, however, be used for ethylene, since the ethylene and N_2 peaks overlap under analytical conditions convenient for frequent determinations.

In the present study of polymer breakdown, the size of sample withdrawn was adjusted to the rate of gas evolution. Quantities of ethylene and H_2S present in each sampling of the gas phase, as determined by GC, are given in Table IV. Ethylene is not the only major gas product generated; hydrogen sulfide and ethylene are apparently evolved in roughly equimolar quantities during the period of the first (slower) rate, until approximately 120 min of reaction. Thereafter, H_2S evolution increases sharply. The total molar rate of gas evolution is not necessarily equal to the molar rate of melt scission. (An acceleration in rate of gas evolution has always been observed at about 115 min in the thermal degradation of polymer at $230^\circ C$).

As a further method of assessing the effect of thermal treatment on the molecular integrity of the poly(ethylene sulfide) backbone a differential

TABLE V
 Products from Thermal Breakdown

Substrate	Formula	Degradation products
DTO ^a	Et(SCH ₂ CH ₂) ₂ SEt	CH ₂ =CH ₂ , EtSH? (also diethyl disulfide and ethyl vinyl sulfide, liquid products at 150°C, determined by GC-MS)
TTU	Et(SCH ₂ CH ₂) ₂ SEt	CH ₂ =CH ₂ , EtSH, H ₂ S, C ₂ H ₆ ?
Polymer	-(SCH ₂ CH ₂) _x -	CH ₂ =CH ₂ , EtSH, H ₂ S
DBT	Bu(SCH ₂ CH ₂) ₃ SBu	Butene-1, H ₂ S, CH ₂ =CH ₂ , EtSH, Butane?

^a Limited data on thermal breakdown due to low boiling point.

scanning calorimetry (DSC) thermogram was obtained of recovered DBT (model compound) that had been heated 4 hrs/230°C/N₂. In Figure 4 this is compared with a thermogram of the original sample. Clearly, the model compound is fairly pure, as received, and undergoes significant thermal degradation. The apparent premelting observed about 15°C below the true melting point is also affected by thermal degradation. This premelting is scarcely a surprising phenomenon in a somewhat polar molecule of this length.

Also, gas chromatographic analysis was performed on the liquid products of DTO thermally degraded at 150°C. A GC-mass spectral analysis was also performed. This method has been described elsewhere.⁸ Results are incorporated in a comparative listing of the known products from the various models and from unstabilized polymer, given in Table V. Most identifications were made by using infrared and/or GC data of the known compound as reference. The generation of butene-1 from DBT was verified by both techniques. H₂S was identified by GC alone due to its weak absorption in the infrared. Ethylene from DTO (at 180°C) was identified by infrared spectroscopy alone.

The rate of scission may be calculated from a Melt Indexer curve by using the random-scission equation,* the number-average molecular weight being taken to be one-half the apparent (weight-average) molecular weight, as found by eq. (1) with the first constant set at 5.08 for 215°C.⁶ (This assumes that the molecular weight distribution of the polymer is the "most probable," which should be true after some degradation has already occurred.) A study of the gas evolution to scission relationship was made by comparing Melt Indexer data with gas evolution measurements. Rate of gas evolution of a high molecular weight standard polymer at 220°C, was 2.1×10^{-5} mole gas/unit ES/min. The rate of scission calculated from a Melt Indexer curve of the same polymer at 215°C was

* The equation for random scission of a polymer is $n = (1/\bar{M}_t) - (1/\bar{M}_0)$, where n is the number of moles of scissions per gram polymer in time t , \bar{M}_t is the number-average molecular weight of polymer at time t , and \bar{M}_0 is the initial number-average molecular weight of polymer.

1.6×10^{-5} mole scission/unit ES/min from 7 min until the end of the Melt Indexer experiment at 16 min. This suggests that one mole of gas was generated per scission. Data were given by Lee and Wragg¹² for melt-flow breakdown of DABCO-initiated poly(ethylene sulfide) at 230°C. For their Melt Indexer, the first constant of eq. (1) should be 4.993 at 230°C.¹³ The scission rate then turns out to be 4×10^{-5} mole scission/ES unit/min, which is of the same order of magnitude as for our $\text{ZnEt}_2\text{-H}_2\text{O}$ -initiated polymer.

Activation Energy of Thermal Breakdown

The rates of gas evolution from the thermal breakdown reaction of TTU, DBT, and standard polymer at several temperatures were used to determine the activation energy for the breakdown reaction. For the breakdown of the polymer, initial rates only were used. In Table VI, initial and rapid rates at each temperature, and the time of onset of the rapid rate, are listed for a standard polymer.

TABLE VI
Thermal Degradation of Poly(ethylene Sulfide)

Temperature, °C	Initial rate, mole gas generated/unit ES/min $\times 10^5$	Time of onset of rapid rate, min	Rapid rate, mole gas generated/unit ES/min $\times 10^6$
220	5.4	>210	—
224	9.05	154 (?)	12.5
225	6.36	260	9.7
231	8.7	110 ^a	20.9 ^b
236	25.9	110	56.9 (?)
240	39.4	84	80.0
244	25.2	85	34.2
250	76.1	58	99.1 ^c

^a Typical value; values at the other temperatures are from a single experiment each.

^b Average of 2 experiments: 18.9 and 22.8.

^c A third rate could be measured, starting at 123 min, 210×10^{-5} mole gas/unit ES/min. until the termination of the reaction at 140 min.

The Arrhenius plot of the rate data for the polymer is given in Figure 5a; rate data for DBT and TTU are plotted together in Figure 5b. For thermal breakdown of polymer, ΔE^* is in reasonable agreement with values (Table VII) determined independently by using two other techniques, thermogravimetric analysis (TGA) and dynamic differential calorimetry (DDC).¹⁴ Thus the rate-determining step of breakdown, in the temperature range tested, could be C-S bond scission, since the bond dissociation energy† is of a magnitude similar to ΔE^* .

† Values for dissociation energy of the carbon-sulfur bond in thioethers are given¹⁵ as: Me-SMe, 73.2 kcal; Et-SEt, 69.3 kcal; $\text{C}_6\text{H}_5\text{CH}_2\text{-SCH}_3$, 51 kcal. The carbon-sulfur bond in a poly(ethylene sulfide) structure $\sim\text{SCC}-\text{SC}\sim$ should have a bond strength more like that of a benzyl thioether, than of a diethyl thioether, since it is doubly activated, or weakened, by the proximity of another electron-withdrawing sulfur atom.

For the gas-producing thermal breakdown reaction of the model compounds, $\Delta E^* = 57.1$ kcal, within the range (55 ± 4 kcal) of values for ΔE^* of the breakdown of polymer. This agreement is strong indication that the thermal breakdown of polymer is due primarily to the instability, at the temperatures studied, of the carbon-sulfur bond in a poly(ethylene sulfide) structure. Therefore sufficient weakness exists in the organic

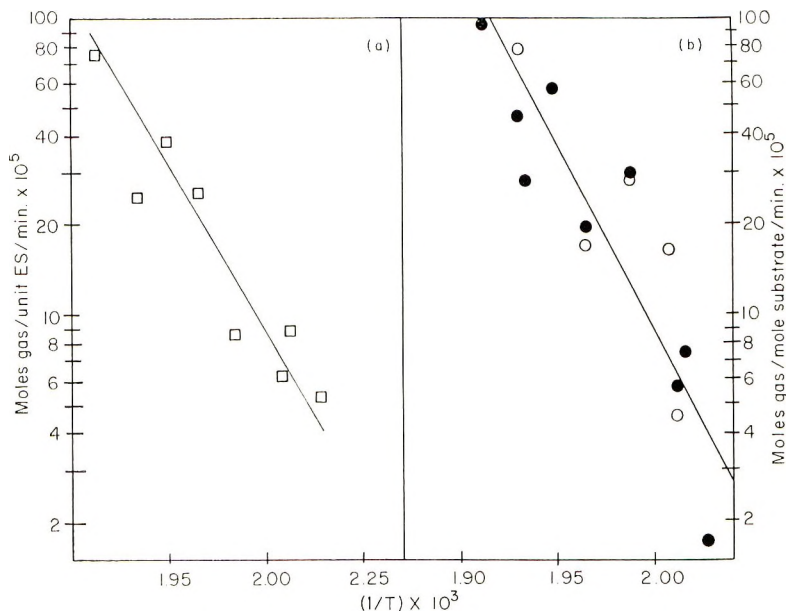


Fig. 5. Arrhenius plots of total gas-evolution rates under N_2 for (a) standard poly(ethylene sulfide), $\Delta E^* = 51.7$ kcal, and (b) model compounds: (O) 5,8,11,14-tetrathiaoctadecane (DBT); (●) 3,6,9-trithiaundecane (TTU), $\Delta E^* = 57.1$ kcal.

portion of the polymer, without invoking endgroup or metal-sulfur bond effects, to account for the thermal degradation of poly(ethylene sulfide) observed in the molding process. Furthermore, Zn or Cd mercaptide-initiated poly(ethylene sulfide) could not be stabilized by the BDPPO-zinc hydroxychloride combination, so the instability of the SZnS grouping cannot be the cause of the thermal dissociation of ZnEt₂-H₂O-initiated polymer, which could be so stabilized.

TABLE VII

Method	Apparent activation energy, kcal	Temperature range of test, °C
TGA	58.5	340-360
DDC	55	312-337
Gas evolution	51.7	220-250

Postulated Mechanism of Thermal Degradation of Poly(ethylene Sulfide)

We conclude that there is intrinsic instability of the carbon-sulfur bond in a sequence of $(-\text{CH}_2\text{CH}_2\text{S}-)$ units. While this instability could go unnoticed at temperatures of use (ambient to 150°C), it becomes an important, overriding consideration at temperatures of processing (200–250°C or higher). The evidence to support the existence of this intrinsic thermal instability is threefold.

(1) The rate of gas evolution, at 230°C under N_2 , is uniform for polymers having diverse molecular weights with zinc catalyst fragments intact or extracted, and for polymers prepared by a catalyst system other than diethylzinc-water. This rate has an average value of 10×10^{-5} mole gas evolved/unit ethylene sulfide/minute at 230°C. These data are also substantiated by the similarity in melt flow behavior of standard polymer and zinc-free (by extraction) standard polymer of similar molecular weight; and by similar calculated melt scission rates for standard diethylzinc-water-initiated polymer and for DABCO-initiated polymer.

(2) The activation energy for evolution of gas, obtained via the Arrhenius equation from the experimentally determined rates of gas evolution at several temperatures, is close to that required to cleave a C-S bond of the type found in the polymer. Activation energy (ΔE^*) for the gas evolution reaction also coincides with ΔE^* for polymer degradation determined by two other techniques.

(3) Similarities are found in the thermal degradation reactions of polymer and model compounds trithiaundecane (TTU), dithiaoctane (DTO), and dibutyl trimer (DBT) in identity of gaseous products formed, as well as in the activation energy ΔE^* , for the gas-producing breakdown reaction of models TTU and DBT and polymer.

To explain the observed phenomena of thermal breakdown, a random homolytic scission is proposed, followed by evolution of ethylene and probably H_2S from the cut ends. (While ethylene production is probably an exothermic step, we have not been able to explain H_2S evolution in this scheme.) This scheme is intended as a general mechanism for the initial (slower) stage of polymer degradation only. Formation of ethanethiol from ethyl-terminated model compounds is easily explainable by a scission of the type

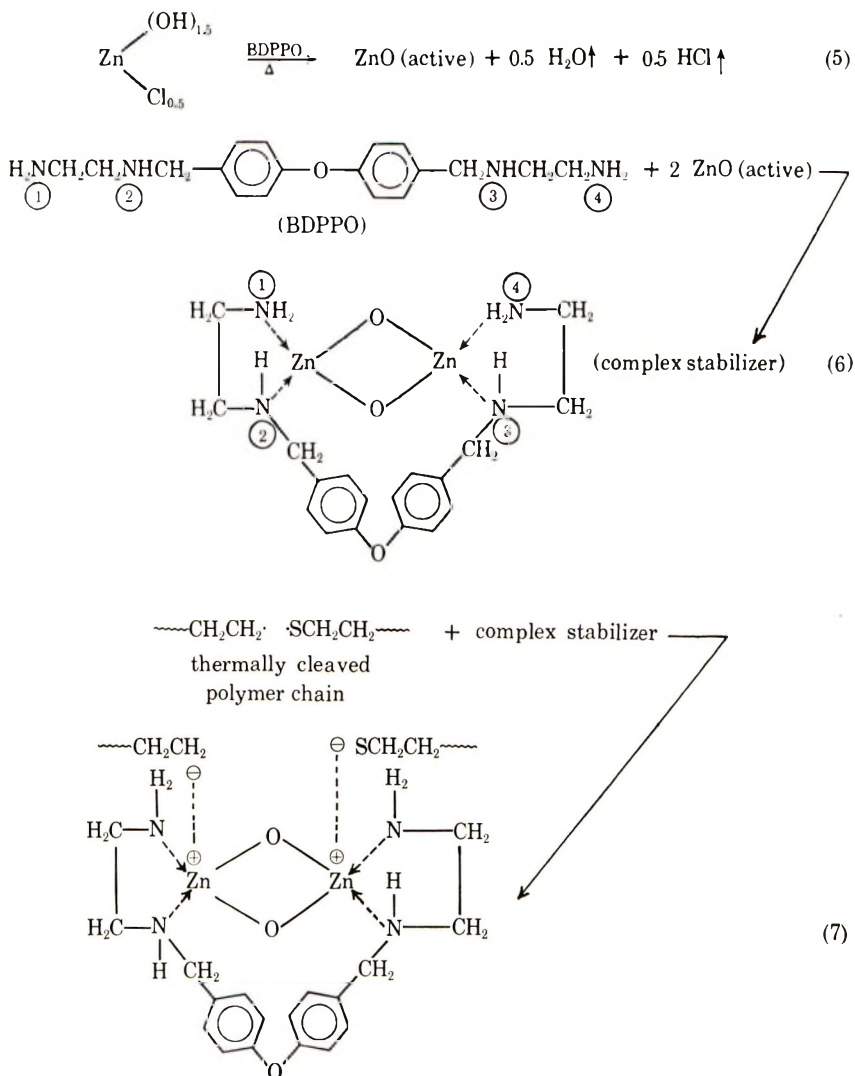


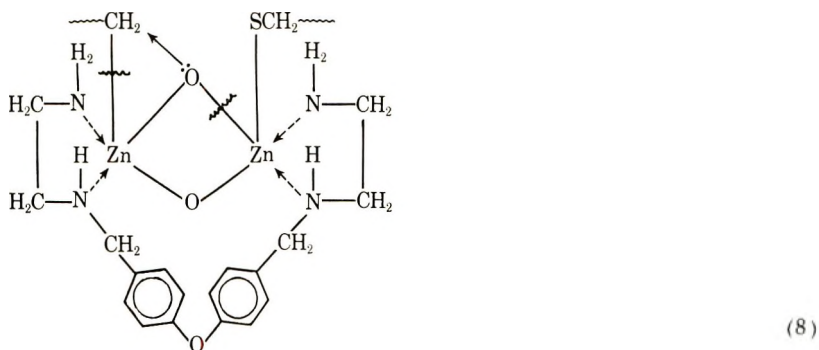
followed by hydrogen abstraction; however, ethanethiol generated from the polymer is more probably an addition product of H_2S and $\text{CH}_2=\text{CH}_2$. If so, this would tie in the observed increase (by infrared) of ethanethiol at about the time of onset of rapid degradation, with the observed increase (by GC) in H_2S generation at about the same time. The second, rapid stage of polymer degradation has been established only for polymers initiated by diethylzinc-water. Increased H_2S generation, therefore, may

be dependent upon method of polymer initiation. The extent of H_2S generation in the initial (slower) stage of polymer breakdown is not firmly established; the chromatographic column used for the quantitative study was ideal for separation of ethylene from N_2 , but comparatively insensitive to H_2S .

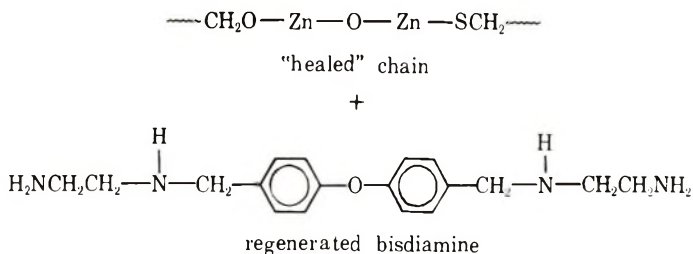
Stabilization of Poly(ethylene Sulfide) Against the Effects of Thermal Breakdown

There would seem to be an anomaly in claiming stabilization against uncatalyzed homolytic scission. However, the melt index flow curve of "standard" polymer stabilized with 2 phr BDPPPO + 1 phr zinc hydroxychloride is nearly flat. The apparent action of the thermal costabilizers is to "heal" the scission.





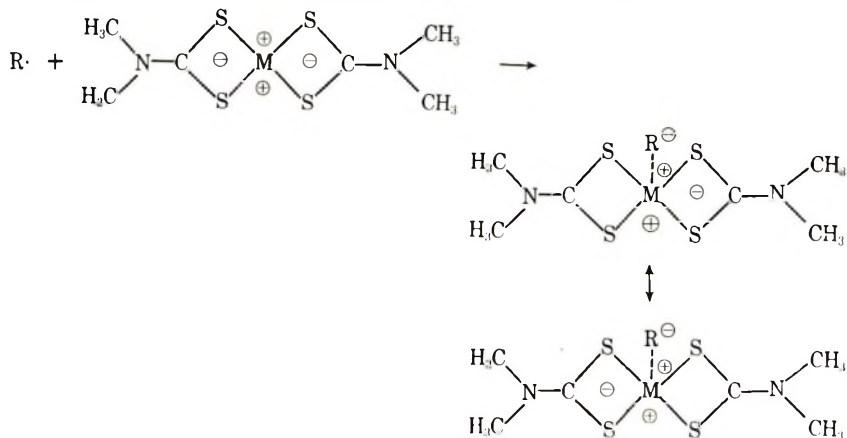
Cleavage and rearrangement



Assembling all the experimentally determined requirements for stabilization of poly(ethylene sulfide), a general structure emerges which may perhaps approximate that of the effective thermal stabilizer. In the specific case of BDPPPO and zinc hydroxychloride, the structure of the stabilizer may be something like that shown in eqs. (5) and (6).

The stabilization reaction may then proceed according to eq. (7), followed by an internal stabilization of the charges in the complex.*

* This stabilization reaction is proposed by analogy to the intermediate step of an electron-release reaction between free radicals and metal dithiocarbamates which has been proposed¹⁶ to explain the potent antioxidant effect of the latter:



A further step in the thermal stabilization reaction might be visualized as (S). If this latter step takes place slowly, the net effect of the bisdiamine is to serve to insert $-\text{ZnO}-$ units into the polymer backbone at the site of a break, but the stabilizer is effectively consumed.

We may postulate that the proposed structure might require some part of the polymer to complete formation of the effective thermal stabilizer. (A carbon-sulfur bridge structure might be visualized connecting the two zinc-diamine complex centers, rather than the simple oxide bridge.) Two observations support this possibility: (1) apparently reduced stabilizer effectiveness of a prereacted BDPPPO-zinc hydroxychloride system; (2) initial sharp drop in torque (and by inference, molecular weight) of polymer stabilized with BDPPPO-zinc hydroxychloride in Plasticorder studies under N_2 . (There are less effective thermal stabilizers which do not cause this sharp drop, although they permit a steady, fairly rapid decrease in torque.) Such a stabilizer structure could lead to, e.g., $\sim\text{CH}_2\text{OZnSCH}_2\text{-CH}_2\text{OZnSCH}_2\sim$, as the "healed" chain.

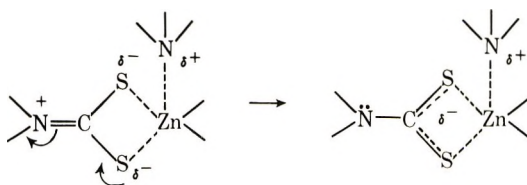
A general mechanism as described is consistent with the requirements and conditions that have been observed. (a) A double zinc salt would provide two electron-releasing centers, stabilizing both radicals of a homolytic scission. A single-, or stepwise-electron-releasing stabilizer such as a dithiocarbamate salt would be incapable of "healing" a scission. (b) The structure explains (1) the effectiveness of zinc hydroxychloride as a costabilizer and (2) the near interchangeability of finely divided ZnO and zinc hydroxychloride. (c) The Melt Indexer behavior of polymer in the presence of BDPPPO when zinc is present in the polymer, but no costabilizer is used, is made reasonable. A typical polymer of 0.08% zinc content contains 1.2×10^{-3} g-atoms of zinc/100 g; 2 g (2 phr) BDPPPO contain 6×10^{-3} mole amine; 1 phr zinc hydroxychloride contains 9.2×10^{-3} g-atoms zinc. Since the proposed complex requires 2 atoms of Zn per mole of the bisdiamine, the hydroxychloride supplies most of the zinc to the complex. In the absence of zinc hydroxychloride, the amine must obtain the zinc oxide from the catalyst residues in the polymer, an inadequate source. (d) Other metal salts, especially oxides, show varying degrees of effectiveness as costabilizers. CuO , CdCO_3 , and diphenyltin oxide (DPTO) were the best of those we examined. (e) In work on the Brabender Plasticorder, addition of BDPPPO-zinc hydroxychloride to an unstabilized, partially degraded polymer caused the prevention of further degradation, but not the repair of previous breakdown, nor any increase in molecular size (as measured by torque). The data are most consistent with a "healing" mechanism, effective only with freshly scissioned chains.

On the other hand, some contradictory evidence exists. Poly(ethylene sulfide)s initiated by Na naphthalene or Cd or Zn mercaptide appear to be unstabilizable by BDPPPO-zinc hydroxychloride.¹² We found that the metal mercaptide-initiated polymer appears to evolve gas at a rate comparable to the second (fast) rate of standard polymer. This may

indicate a different type of breakdown. Another apparent contradiction is the precipitation of benzene-dissolved diethylzinc-water-catalyzed poly(propylene sulfide) by small amounts of polyfunctional amines (especially BDPPPO) at room temperature. This phenomenon may be interpreted as signifying crosslinking of chains by the stabilizer, but in the melt the stabilizer does not crosslink standard poly(ethylene sulfide). At room temperature perhaps a chelation of the initiator fragments takes place causing polymer crosslinking; at temperatures in the region of 230°C, the amine may be capable of extracting the chelated zinc and thereby forming the effective thermal stabilizer.

A film-compensation technique was used to obtain infrared spectra of the amine-metal oxide (MO) additive combinations. Unaged films were examined of standard polymer containing 2 phr BDPPPO + 1 phr MO, where MO may be CuO, Cu₂O, ZnO, or SnO. These were compensated with a reference film of standard polymer. The most obvious effect was a shift in the location of the maximum absorption of a broad peak from ~3300 cm⁻¹ to ~3200 cm⁻¹ when zinc hydroxychloride was the MO used, but not with ordinary ZnO.

In the literature, absorption in the 3500–3300 cm⁻¹ region is assigned to NH stretching in primary and secondary amines.¹⁷ In coordination compounds involving primary amines these absorptions can be lowered by as much as 200 cm⁻¹. Similarly, in the reaction of piperidine with zinc dibutyldithiocarbamate (zinc DBDTC), Higgins and Saville¹⁸ found an absorption band at 3245 cm⁻¹, which they provisionally assigned to N-H vibration of the complexed amine, indicating a shift of -97 cm⁻¹ on complex formation. The intensity of the band was proportional to the concentration of piperidine when [Piperidine]:[Zinc DBDTC] < 1:1, indicating that a 1:1 complex formed. The structures postulated for the complex were:



By analogy, the shift we observed might be a measure of the zinc-nitrogen bonding in a complex molecule. Since the polymer films were subjected to heat only long enough to insure melting, it may be that slow-forming complex molecules did not have time to form from their individual components. Melt Indexer data can be interpreted as indicative of slow complex formation in the cases of MO = ZnO, CuO, Cu₂O, and perhaps SnO and SnO₂.

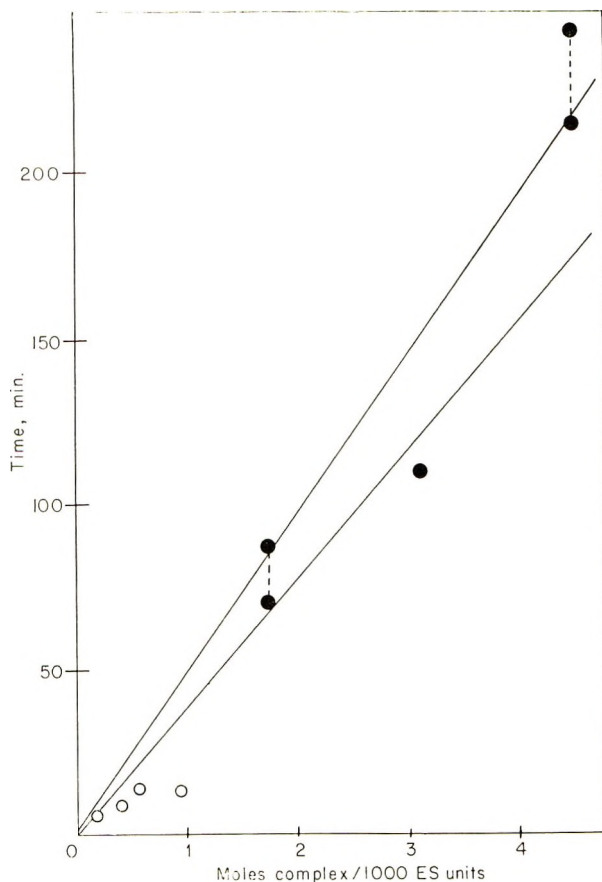


Fig. 6. Duration of thermal "protection" at 230°C of standard poly(ethylene sulfide) by hypothetical complex of BDPPPO·2ZnO: (●) Gas evolution data, time from temperature equilibration (20 min) to onset of rate 3 (marked increase in gas-evolution rate); (○) Melt Indexer data, time from warmup period (4 min) to flow instability point (marked increase in melt flow rate). Broken lines show range of uncertainty.

The hypothesis of a charge-transfer stabilizer complex in the presence of a randomly cleaving homolytic degradation implies that the duration of thermal stabilization is dependent on concentration of the complex. Therefore, gas evolution data were obtained on thermally stabilized polymer, for correlation with Melt Indexer stability. It was known that the bisdiamine (BDPPPO) used alone suppressed gas evolution of thermally degrading polymer to a near-zero rate, although melt stability was still rather poor. Several dosages of (2 parts BDPPPO/1 part zinc hydroxychloride) were added to standard polymer, giving the following gas evolution pattern at 230°C: (a) gas expansion with temperature equilibration of the reaction flask from $t = 0$ to $t = 20$ min; (b) gas evolution at a constant rate, called rate 1 (R_1), from $t = 20$ until $t = \sim 60$, where the rate is roughly proportional to the concentration of additive; (c) a slower

constant rate, called rate 2 (R_2), where the duration is proportional to the concentration of additive; and (d) a rate, more rapid than rate 2, called rate 3 (R_3), until the termination of the experiment. All the rates are much slower than the gas evolution of the unstabilized polymer. In the Melt Indexer, with a low concentration of this additive, the flow rate is fairly irregular and similarly displays an upward break or trend after a period that appears to depend on the dosage used.

The total time required for onset of gas evolution R_3 , less 20 minutes for initial temperature equilibration, is plotted versus the hypothetical complex concentration in Figure 6. The instability points of flow curves at 230°C are included in Figure 6 for comparison. Two possible straight-line fits are shown. Assuming that the ordinate of Figure 6 represents

TABLE VIII
Physical Properties of Stabilized Poly(ethylene Sulfide)
Molded After Various Hold Times at 216°C

Series	Hold time at 216°C prior to molding, min	Tensile strength, psi	Elongation at break, %	Apparent molecular weight of molded part
A	0 (control)	11,900	9.32	280,000
	5	11,740	8.23	260,000
	10	9,560	5.95	275,000
	30	9,450	5.57	270,000
	60	11,220	8.83	280,000
B ^a	0 (control)	11,310	8.06	280,000
	30	11,050	9.15	285,000
	60	11,430	7.71	280,000
	90	10,110	5.46	270,000
	120	11,310	7.99	260,000

^a Duplicating original conditions.

the time at which the stabilizer complex has been used up, the slopes indicate that the stabilizer complex is consumed at a rate of $2.1\text{--}2.6 \times 10^{-5}$ mole/ES unit/min. At this temperature, the rate of gas generation of unstabilized polymer is about 10×10^{-5} , so each mole of stabilizer suppresses the evolution of 4 or 5 moles of gas. This is order-of-magnitude agreement with the stoichiometry of the proposed mechanism which uses both ZnO groups to heal a scission. Obviously, if one ZnO will do the job or if more than one mole of gas is evolved/scission, the agreement is even better.

From Figure 6, it may be inferred that a standard poly(ethylene sulfide) stabilized with 2 phr BDPPPO and 1 phr zinc hydroxychloride will survive 2 hr at 230°C. Such polymer was injection-molded with hold times (at 216°C) in the machine barrel of 0 to 120 min. The molded parts were studied by tensile-elongation determinations, Melt Indexer stability, thermogravimetry, and dynamic differential calorimetry. None of these techniques revealed any breakdown in molecular weight or stability of the

polymer. As an example, physical properties of standard tensile-test bars molded after various hold times are given in Table VIII.

We are indebted to the Dunlop Research Centres, Sheridan Park, Ontario, Canada and Birmingham, England for a supply of the model compound DBT and for samples of poly(ethylene sulfide) initiated by a metal mercaptide, as well as for extensive discussions of this work. We also wish to acknowledge the many contributions of our present and former colleagues at Thiokol Chemical Corporation, in particular M. B. Berenbaum, S. W. Osborn, S. M. Ellerstein, G. F. Bulbenko, and R. Isaac, as well as I. L. Dewitt of the Elkton Division, who performed the GC-MS analyses and assisted in their interpretation.

References

1. R. H. Gobran and R. Larsen, *J. Polym. Sci. C*, **31**, 77 (1970) (Part I).
2. R. H. Gobran and S. W. Osborn, U.S. Patent 3,365,431 (to Thiokol Chemical Corp.) (Jan. 23, 1968).
3. G. F. Bulbenko, R. H. Gobran, A. J. Patarcity, E. A. Peterson, and S. W. Osborn, Can. Pat. 736,026 (to Thiokol Chemical Corp.) (June 7, 1966).
4. R. Larsen, Can. Pat. 778,848 (to Thiokol Chemical Corp.) (Feb. 20, 1968).
5. *ASTM Standards*, Vol. 27, Amer. Soc. for Testing and Materials, Philadelphia, 1965, ASTM D1238-62T, p. 447.
6. E. H. Catsiff, *J. Appl. Polym. Sci.*, **15**, 1641 (1971).
7. E. E. Reid, *Organic Chemistry of Bivalent Sulfur*, Vol. II, Chemical Publishing Co., New York, 1960, (a) p. 126; (b) p. 129.
8. M. N. Gillis, E. H. Catsiff, and R. H. Gobran, *J. Polym. Sci. A-1*, **9**, 1293 (1971).
9. R. T. Wragg, *J. Chem. Soc. B*, **1970**, 404.
10. E. R. Bertozzi, private communication.
11. E. J. Barsum and R. Isaac, paper presented at First Middle Atlantic Regional Meeting, American Chemical Society, Philadelphia, Feb. 3, 1966.
12. T. C. P. Lee and R. T. Wragg, *J. Appl. Polym. Sci.*, **14**, 115 (1970).
13. W. Cooper, private communication.
14. S. M. Ellerstein, private communication.
15. T. L. Cottrell, *The Strengths of Chemical Bonds*, 2nd ed., Butterworths, London, 1958, p. 203.
16. B. Saville, private communication.
17. L. J. Bellamy, *The Infrared Spectra of Complex Molecules*, Wiley, New York, 1958, p. 248 ff.
18. G. M. C. Higgins and B. Saville, *J. Chem. Soc.*, **1963**, 2812.

Received June 30, 1970

Revised November 20, 1970

Poly(ethylene sulfide). III. Oxidative Degradation

MARINA N. GILLIS, E. H. CATSIFF, and RIAD H. GOBRAN, *Thiokol Chemical Corporation, Trenton, New Jersey 08607*

Synopsis

Injection-molded poly(ethylene sulfide) containing polyamines and zinc salts as thermal stabilizers has excellent physical properties at room temperature, but discolors rapidly on air aging at 150°C, with embrittlement and general deterioration of properties. Degradative breakdown under these conditions is preponderantly thermo-oxidative in nature. The site of the polymer's thermo-oxidative instability was sought in oxidation experiments involving the resin as well as model compounds for the polymer's organic structure. Identification studies were carried out on the oxidation products of 3,6-dithiaoctane (a model compound). Rate of oxygen consumption by the model compound was measured by a pressure-bomb technique and by a volumetric method. Oxidation of the model compound was found to proceed indefinitely as long as the supply of oxygen was replenished. Rate of oxidation was nonaccelerating and independent of oxygen pressure within the range 1.7-3 atm O₂. The gaseous products of the oxidation of unstabilized (no polyamine) resin were found to be identical to the products from the oxidation of the model compound. A mechanism has been proposed taking into account the products isolated and identified, and the nonaccelerating nature of the oxidation. The poly(ethylene sulfide) structure is able to decompose hydroperoxides via formation of sulfoxides, preventing the acceleration of the oxidation reaction. While effecting this radical deactivation, the polymer chains are cleaved, with a resultant loss in molecular weight and physical properties. Some success has been met in the use of inorganic or metallo-organic additives as antioxidants. Among these are dithiocarbamate salts and selenocyanates. The effectiveness of these compounds has been demonstrated in the polymer, and a suggested rationale for stabilization is given.

Ethylene sulfide can be polymerized to a crystalline high molecular weight resin by anionic¹ or coordination-type catalysis.^{2,3} The first article in this series⁴ described a two-step polymerization method in which diethylzinc-water was used as catalyst for ethylene sulfide monomer to form an initial seed. This seed was used to further polymerize fresh monomer to the desired particle size and bulk density.

The injection molding of poly(ethylene sulfide), mp ~210°C, which requires molding temperatures in the range of 220-260°C, was successfully accomplished by the use of certain thermal stabilizers to prevent thermal degradation at these high temperatures. The second article in this series⁵ dealt with the thermal degradation problem and described the use of polyamines in presence of certain zinc salts as excellent stabilizers for poly(ethylene sulfide). Molded polymer containing this stabilizer system has

TABLE I
Comparative Aging Study of Stabilized Molded
Poly(ethylene Sulfide) in N₂ and Air at 121°C

Physical Properties	Unaged (Control)	Aged in N ₂		Aged in air	
		2 days	5 days	2 days	5 days
Maximum tensile, psi	10,300	10,700	10,800	6,200	2,500
Maximum elongation, %	6.4	5.0	5.1	1.9	0.7
Modulus of elasticity, psi	366,000	401,500	432,000	405,000	433,000
Notched Izod impact, ft-lb/in	1.08	1.03	0.97	0.15	0.01
Apparent molecular weight*	250,000	245,000	240,000	175,000	163,000
Density, surface layer, g/cc	1.343	1.348	1.352	1.364	1.375

* Calculated from melt viscosity measurements.⁵

excellent mechanical properties as an engineering thermoplastic as shown in Table I.

It was found, in parallel experiments, that the molded polymer maintained its properties when aged at 121°C under nitrogen with careful exclusion of trace oxygen. However, aging the polymer at the same

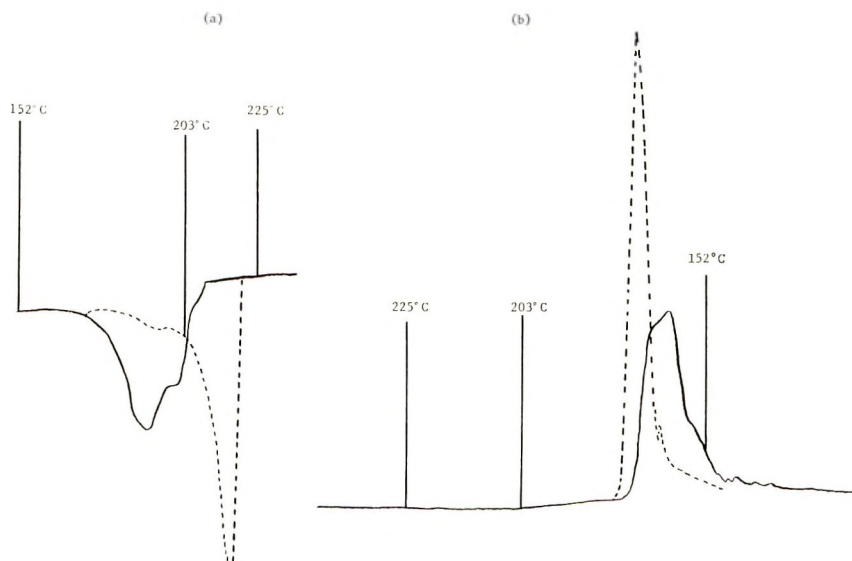


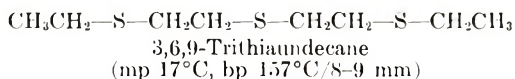
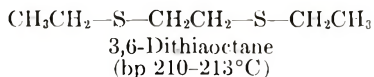
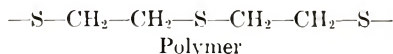
Fig. 1. Thermograms of the differential thermal analysis in N₂ of poly(ethylene sulfide) containing thermal stabilizer system 1% ZnO and 2% bis[p-(2,5-diazapentyl)phenyl] oxide for (a) heating cycle and (b) cooling cycle: (—) thermogram in N₂ of a sample which had undergone prior melting and crystallization in the DTA test chamber in an air atmosphere; (--) thermogram in N₂ of a sample which had undergone prior melting and crystallization in the DTA test chamber in a N₂ atmosphere. Molten sample held at 225°C in N₂ for 15 min prior to cooling.

temperature in an air atmosphere resulted in severe deterioration of properties, particularly the elongation and impact strength (Table I). This characteristic deterioration in properties is generally accompanied by surface cracking and the appearance of a 1715 cm^{-1} band in the infrared spectrum indicating carbonyl formation. Oxidative degradation at high temperatures affects only the surface layer of a molded specimen. It was found that after the oxidized surface layer was scraped, the original properties were again obtained. Also, the density of the oxidized layer was considerably higher than that of the original or nitrogen-aged polymer (Table I).

The effect of oxidative and nonoxidative environments was also studied by differential thermal analysis (DTA). Polymer containing the thermal stabilizer system showed the same sharp melting and crystallization peaks when the DTA measurements were repeated twice under N_2 atmosphere. When the measurements were carried out first in air, and then under N_2 , shifts and broadening of these peaks were observed indicating oxidative degradation. Superimposed thermograms of the second cycle (N_2) in each experiment are shown in Figures 1a and 1b.

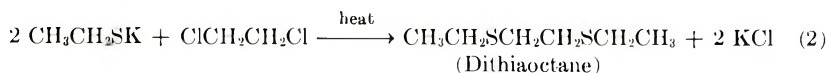
DITHIAOCTANE AND TRITHIAUNDECANE AS MODELS FOR POLYMER IN OXIDATIVE STUDIES

Due to the difficulties inherent in conducting experiments on the high molecular weight poly(ethylene sulfide), 3,6-dithiaoctane and 3,6,9-trithiaundecane were selected as suitable model compounds representing the repeat unit structure of the polymer but without the polymer's complicating features of catalyst fragments, end groups and crystallinity.



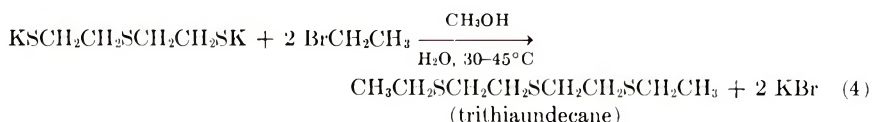
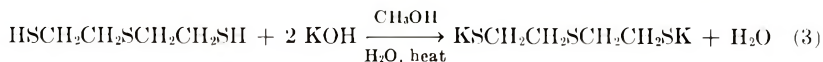
Before any oxidative studies were carried out, the thermal stability of dithiaoctane was established by heating it at 150°C for 40 hr under 30 psi N_2 pressure after careful removal of oxygen. Gas chromatographic analysis showed only traces of decomposition products. Also, there was no increase in pressure during the experiment indicating that no volatile decomposition products were formed. This experiment demonstrated the stability of dithiaoctane under nonoxidative conditions and justified its use as a model compound for the polymer in oxidative studies.

Dithiaoctane was synthesized according to reactions (1) and (2).⁶



The crude product obtained in about 80% yield was fractionally distilled until impurities detectable by gas chromatography were essentially removed.

3,6,9-Trithiaundecane was synthesized by reactions (3) and (4).⁶



The product, obtained in 58% yield, was repeatedly distilled until 99.7% purity (by gas chromatography) was achieved.

TECHNIQUES USED IN THE STUDY OF OXIDATION

The techniques used in following the oxidation of the model compound, dithiaoctane, were equally applicable to the higher model homolog, trithiaundecane, as well as to the high molecular weight poly(ethylene sulfide). The oxidation study was composed of two parts: (1) quantitative determination of oxygen uptake as a function of time and, (2) identification of oxidation products by various analytical techniques.

The oxygen uptake experiments were carried out in either a constant-volume, variable-pressure bomb apparatus, or a variable-volume, constant-pressure gas buret. All the oxidation experiments were carried out at a constant temperature of 150°C and generally without agitation. In a comparative experiment with the gas buret apparatus, the rate of oxidation of dithiaoctane at 150°C was 1.5 times as great when the system was agitated, compared to a nonagitated system. This shows that the effect of oxygen diffusion is not of major importance.

The bomb apparatus used consisted of a stainless-steel pressure bomb of the ASTM Norma-Hoffman type equipped with a pressure gauge and a Pyrex glass container as a sample holder. In a typical experiment, 25 ml dithiaoctane was charged into the glass container, the bomb was then assembled and pressurized with oxygen until the total air plus oxygen pressure reached 30 psig at room temperature. The bomb was then sealed and placed in a constant-temperature bath at 150°C. After thermal equilibrium was reached, the decrease in pressure was followed as a function of time and, when necessary, the consumed oxygen was replenished

after cooling the bomb to room temperature. Knowing the volume of the bomb, the pressure drop could be converted into apparent moles of oxygen consumed. Typically, 25 ml of dithiaoctane consumed the available oxygen in about 20 hr at 150°C. The bomb technique has several drawbacks: (a) the thermal lag in attaining temperature equilibrium, about 1 hr after immersion, masks the initial rate of oxidation; (b) the build-up of gas products makes it difficult to determine true oxygen consumption since only the net drop in pressure is measured; and (c) the metallic surface of the bomb might affect the mechanism of oxidation, but this was minimized by use of a glass container for the compounds under study. In spite of these problems, the bomb technique was useful in that it allowed for many experiments to be performed simultaneously. Analysis of the gaseous and liquid products of oxidation were carried out after the bomb had cooled to room temperature.

The gas buret used was a conventional apparatus. In a typical oxidation experiment, 10.0 g of dithiaoctane was weighed into a 25-ml round-bottomed flask containing glass beads. The beads were used to adjust the available volume in the flask so that the amount of oxygen introduced into the cold flask would not be too great for the buret when heat was applied. Air was excluded from the buret by raising the mercury level with the leveling bulb up to the three-way stopcock and sealing the stopcock. An ice bath was then applied to the reaction flask to freeze the dithiaoctane. Vacuum was next applied to evacuate the flask and tube up to the stopcock and O₂ was introduced in the evacuated system. The frozen dithiaoctane was allowed to melt at room temperature, and then the reaction flask was immersed in an oil bath at a constant temperature of 150°C. The stopcock was opened between buret and flask, and the oxygen in the heated flask was allowed to expand, filling the gas buret. As heating continued, the oxidation of dithiaoctane consumed oxygen, as manifested in a rising Hg level and decreased gas volume. This decreasing O₂ volume was read periodically. Gas in the buret was maintained at a pressure of 1 atm by continuously adjusting the mercury leveling bulb as the oxidation and O₂ consumption progressed so that the Hg levels in the manometer arm (open to the atmosphere) and the gas buret arm were always level. Since pressure was maintained constant at 1 atm, the gas volume consumed, measured in milliliters, could subsequently be converted to moles O₂. The total readable volume in the gas buret was 7 ml, corresponding approximately to the volume of O₂ consumed by the 10 g of dithiaoctane at 150°C in 4 hr.

The advantages of the gas buret system are that its glass surfaces presented no threat of contamination and it could be easily and thoroughly cleaned. Further, it was so designed that a trap with molecular sieves could be included if desired. The trap was used to absorb gaseous oxidation products when a true measurement of gas consumption was required. The trap was eliminated when a build-up of gaseous products for analytical purposes was preferred. Frequently parallel oxidation experiments were

carried out in presence and absence of the trap. After oxidation, analysis was performed on liquid and gas products.

Similar sampling and analytical techniques were used for both the bomb and gas buret experiments to identify the oxidation products. Gaseous samples were taken for infrared analysis by venting the gases into an evacuated gas cell having 7.5 cm path length. Infrared spectroscopic analysis was performed on a Perkin-Elmer model 221. Gas chromatographic analysis of liquid samples was carried out on an Aerograph Model 202. The liquid carrier was SE30 on Chrom W support. The temperature of the column was 150°C, the injector was kept at 220°C and the detector at 280°C. Helium flow rate was maintained at 67 ml/min. To isolate a desired product, a cooled cell was fitted over the exit port at the appropriate time. The concentrated fraction was then analyzed by infrared spectroscopy.

The mass spectrometric technique for analysis of liquid oxidation products consisted of trapping the effluent gas from the Aerograph instrument as a product was eluting, in an evacuated bulb which was cooled in liquid N₂, and then transferring the condensed sample by syringe into a CEC Mass Spectrometer Model 21-620A.

In the case of poly(ethylene sulfide), infrared analysis of the gaseous decomposition products was carried out similarly to that of the model compound. Analysis of the solid breakdown products, trapped in the intractable polymer, was carried out on a compression-molded polymer film of 0.1 mm thickness. Films were oxidized in an air-circulating oven, maintained at either 150 or 120°C, and then analyzed by infrared spectroscopy. Analysis by this film technique is analogous to the infrared analysis of liquid oxidation products from the model compound.

OXIDATION OF DITHIAOCTANE AT HIGH TEMPERATURES

Rate of Oxidation

Dithiaoctane consumed oxygen at an initial and apparently linear high rate at 150°C. After approximately 1 hr, the rate of oxygen uptake was reduced but continued to be linear up to at least 4 hr (Fig. 2). This non-accelerating oxygen consumption contrasts sharply with the autoaccelerating rate typical of polyethers as shown in Figure 2 for the dimethyl ether of tetraethylene glycol, $(\text{CH}_3\text{OCH}_2\text{CH}_2\text{OCH}_2\text{CH}_2)_2\text{O}$, under the same experimental conditions.

The linearity of oxygen uptake by the dithiaoctane model compound, furthermore, was constant on long-term oxidation up to 120 hr as long as the oxygen consumed was replenished. Figure 3 shows data for three oxidation experiments, each showing a leveling of oxygen uptake when the oxygen supply had been depleted. But by replenishing oxygen at the point that retardation would otherwise occur, the apparent oxygen consumption by the model compound was maintained at a constant rate.

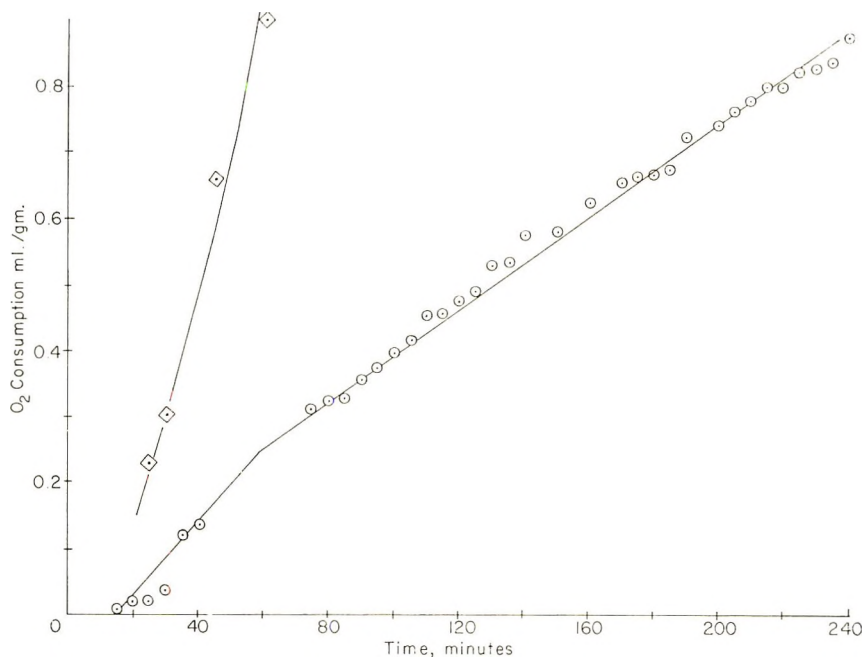


Fig. 2. Oxygen uptake at 150°C and 1 atm O₂ by thioether and ether model compounds: (◇) tetraethylene glycol dimethyl ether; (○) 3,6-dithiaoctane.

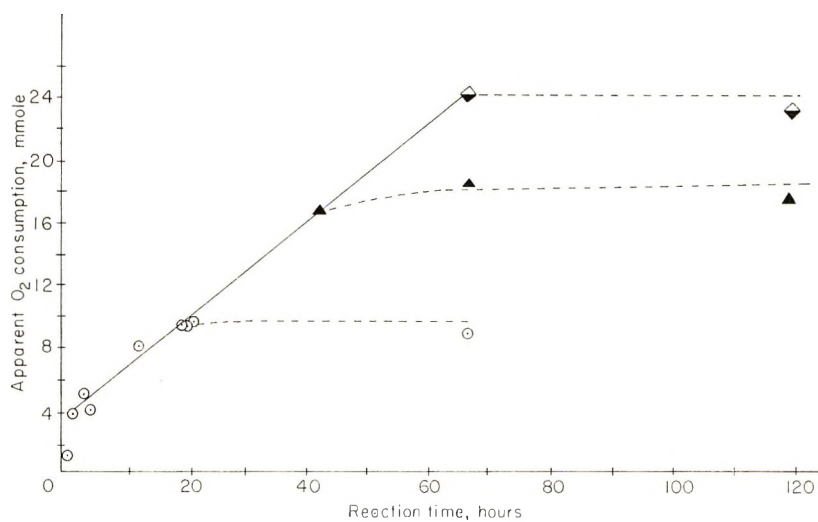


Fig. 3. Apparent uptake of O₂ by 25 g 3,6-dithiaoctane over long periods of time at 150°C: (○) oxygen charged once, 12×10^{-3} mole; (▲) oxygen charged twice, totalling 22×10^{-3} mole; (◆) oxygen charged three times, totalling 30×10^{-3} mole.

Bateman and Cunneen⁷ studied the oxidation of organic monosulfides at temperatures from 45 to 75°C. They observed that saturated monosulfides are inert towards oxygen at these temperatures. On the other hand, unsaturated sulfides react readily with oxygen at 75°C such that the initial rate is greater than that of comparable monoolefins. However, the rate of oxygen uptake by these unsaturated sulfides was reported to decrease giving way to autoinhibition at an early stage of oxidation. Such inhibition was not observed in our work with dithiaoctane or poly(ethylene sulfide) which was carried out at 150°C and in which oxygen was replenished when depleted.

It was also found in our study that the rate of apparent oxygen consumption is independent of oxygen pressure. Thus, from experiments carried out in pressure bombs, the rate of apparent oxygen uptake by dithiaoctane at 150°C was found to be approximately 2.4×10^{-3} mole of oxygen/hr/mole of DTO at both 1.7 and 3.1 atm of oxygen partial pressure. No

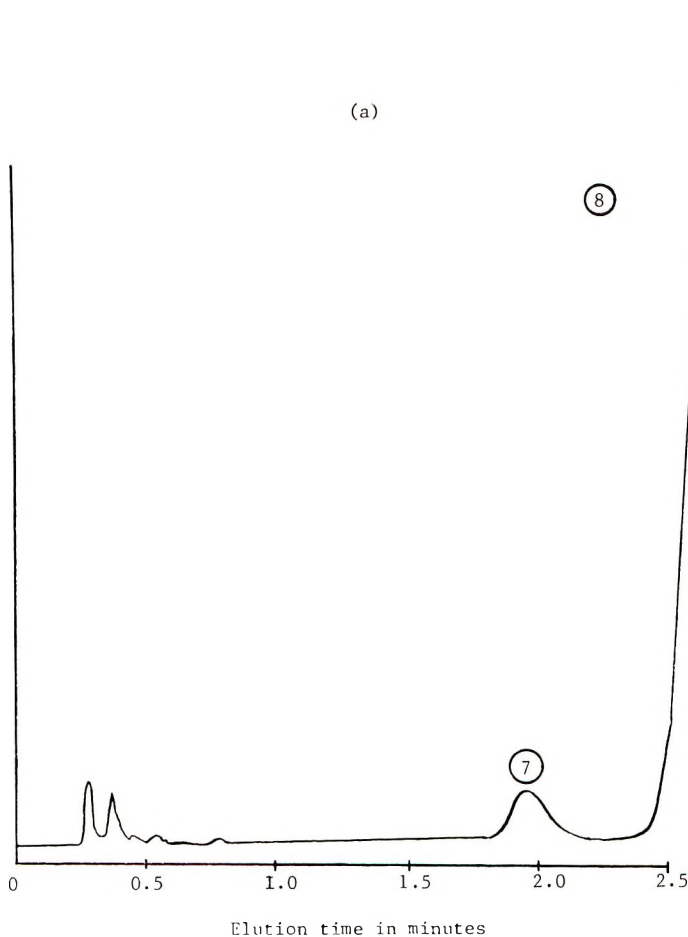


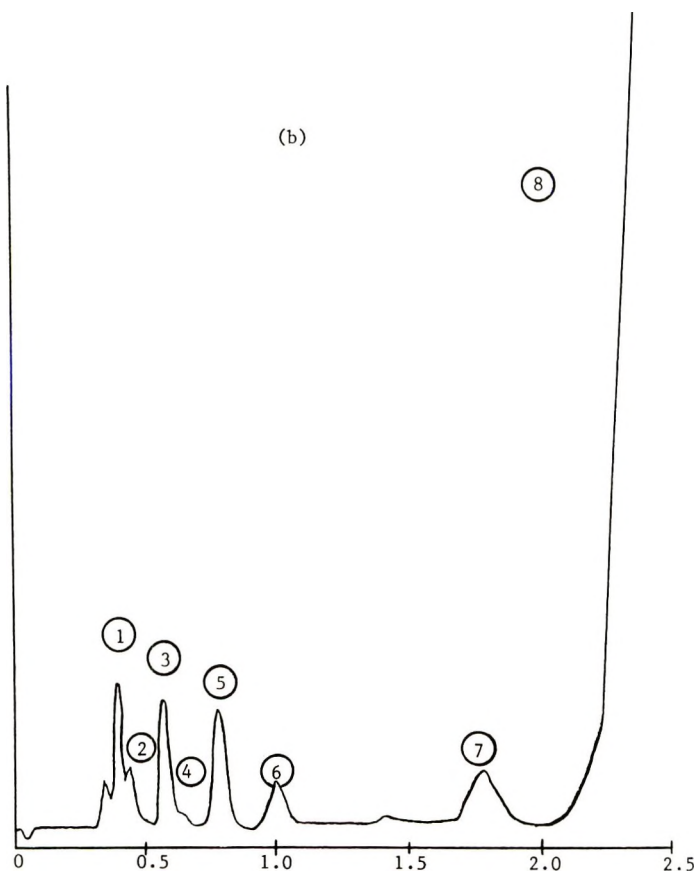
Fig. 4 (continued)

attempt was made in these experiments to absorb the gaseous degradation products and thus the apparent oxygen uptake is lower than the true value.

The constant rate of oxidation over the pressure range studied shows that the oxidation of organic monosulfides is not rate-dependent on oxygen concentration. This nondependency therefore precludes direct oxygen attack on the molecule as the rate-determining step of oxidation, thus eliminating such possibilities as the reaction of molecular oxygen with the monosulfide to form a monosulfoxide as the initial rate-determining oxidation step. An attack of the molecule (by some mechanism) to form a free radical site is therefore suggested as the rate-determining step, preceding the reaction with oxygen.

Identification of the Oxidation Products of Dithiaoctane

Liquid Products of Oxidation of Dithiaoctane. The distribution of liquid phase decomposition products of dithiaoctane was most readily



Elution time in minutes

Fig. 4 (continued)

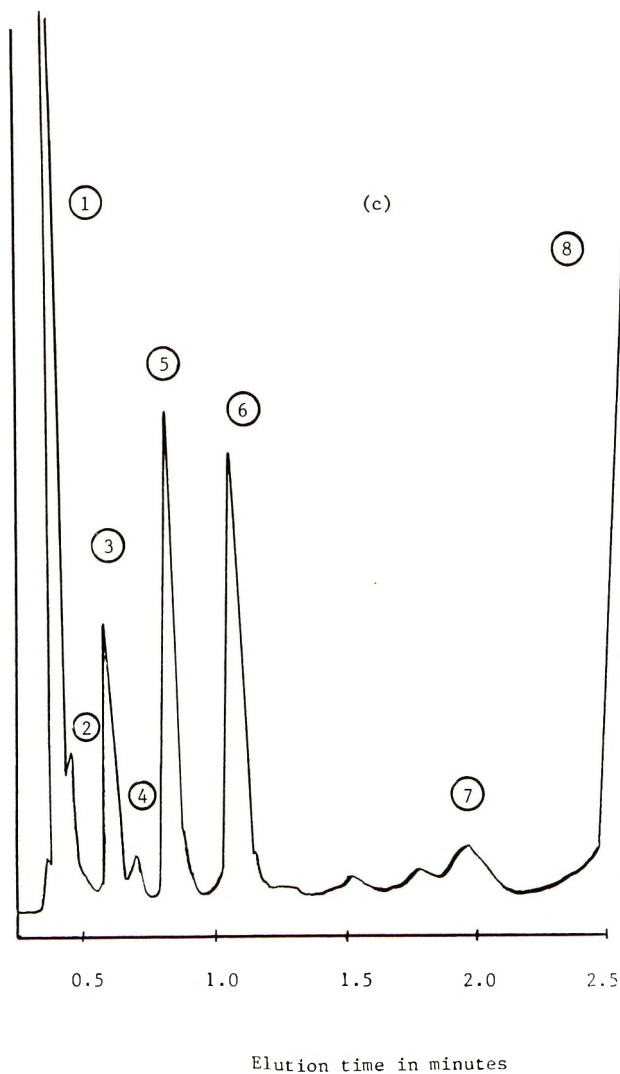


Fig. 4 (continued)

detected by gas chromatography. In Figure 4, a series of chromatograms is reproduced, representing oxidation reactions in the pressure bombs for varying lengths of time at 150°C. The product peaks are numbered so that their relative growth may be followed with time. Identification of the oxidation products was carried out by infrared (IR), gas chromatography (GC), and mass spectrometry as shown in Table II.

The infrared spectrum of oxidized dithiaoctane in Figure 5a was made with a cell having 0.10 mm path length, to approximate the intensity of absorptions usually obtained on oxidized polymer film, having 0.1 mm thickness.

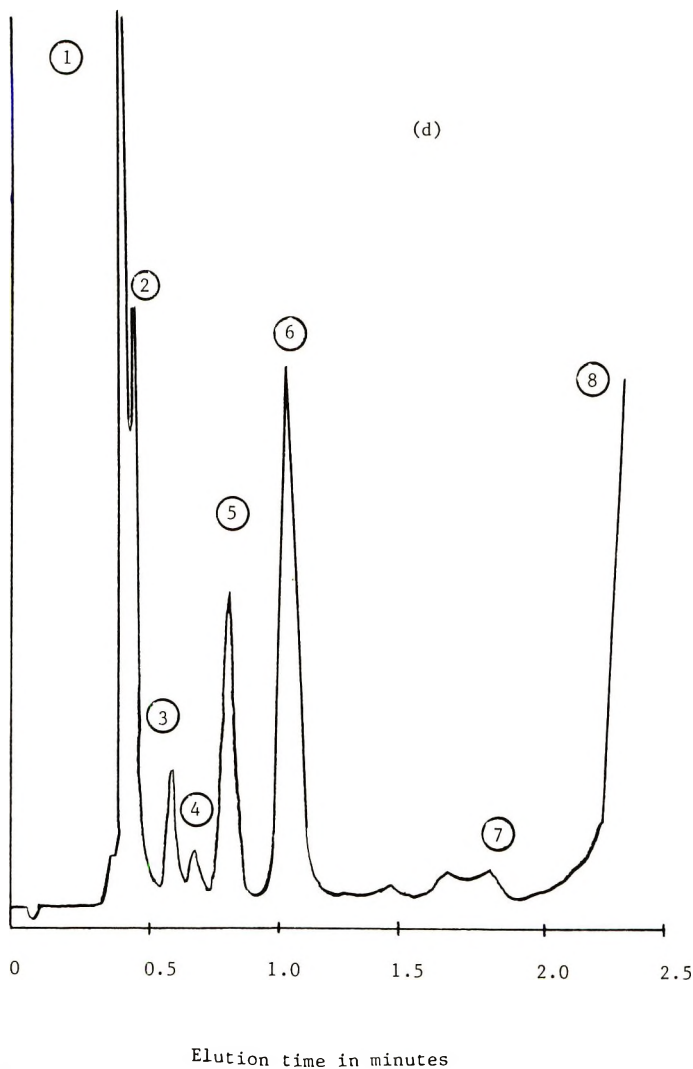


Fig. 4 (continued)

Liquid products identified from the oxidation of dithiaoctane at 150°C are acetaldehyde, ethanethiol, diethyl monosulfide, ethyl vinyl sulfide, 3-thiapentanaldehyde, diethyl disulfide.

Water could not be definitely identified; it may be present in the infrared spectrum of the liquid phase, absorbing weakly. The analytical techniques supporting these identifications are listed in Table II.

Gaseous Products of Oxidation of Dithiaoctane. Oxidation of dithiaoctane in the gas buret apparatus, in the absence of molecular sieves, was extended by repeated additions of O₂ upon its depletion, for the specific purpose of accumulating a large amount of gaseous products for analysis

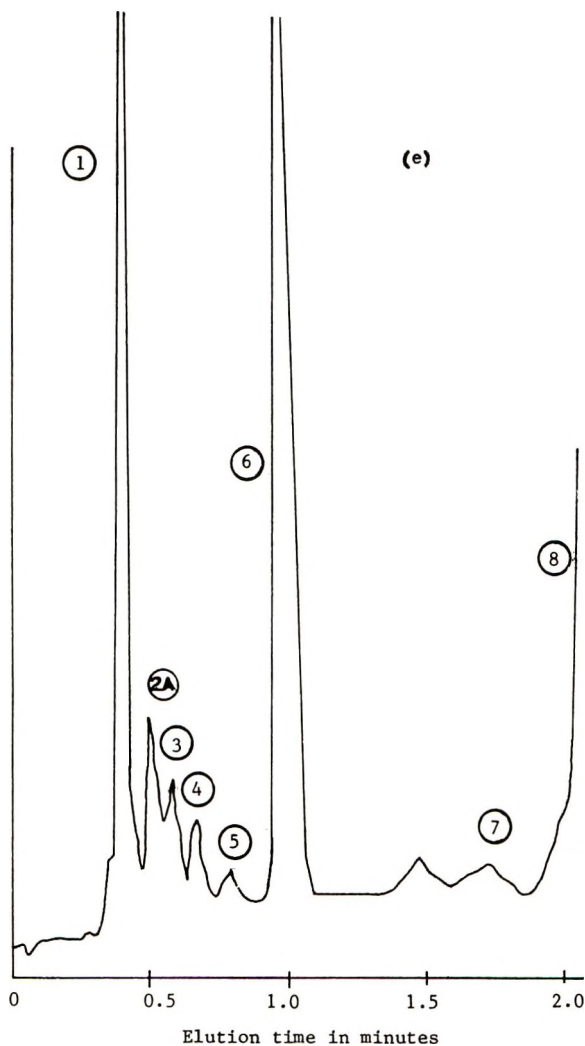


Fig. 4. Partial gas chromatograms of the liquid phase of 3,6-dithiaoctane oxidized at 150°C in O₂ pressure bombs for varying lengths of time for (a) dithiaoctane before oxidation, attenuation 1×; (b) 1 hr oxidation, attenuation 1×; (c) 2-hr oxidation, attenuation 1×; (d) 4 hr oxidation, attenuation 2×; (e) 21 hr oxidation, attenuation 2× except for peak 6, attenuation 4×. Identification of peaks: (1) acetaldehyde; (2) ethanethiol; (2A) unidentified; (3) ethyl vinyl sulfide and diethyl monosulfide; (4) unidentified; (5) 3-thiapentanaldehyde; (6) diethyl disulfide; (7) dithiaoctane impurity; (8) 3,6-dithiaoctane.

by infrared spectroscopy. Reaction was for 18 hours at one atmosphere pressure. Because of a bath malfunction, the temperature was not known, but was believed to be between 120 and 150°C. The same gases were found to be the products of oxidation by pressure bombs at 150°C, by infrared analyses. A facsimile of the spectrum is depicted in Figure 6a.

TABLE II
Analytical Techniques Identifying the Oxidation
Products of Dithiaoctane

GC peak (Fig. 4)	Compound	Identified by
1	Acetaldehyde (CH_3CHO)	Mass spectrometry Comparison with IR of known compound (characteristic band at 1730 cm^{-1} for carbonyl) Comparison with GC of known compound
2	Ethanethiol ($\text{CH}_3\text{CH}_2\text{SH}$)	Mass spectrometry Comparison with GC of known compound
3	Ethyl vinyl sulfide ($\text{CH}_3\text{CH}_2\text{SCH}=\text{CH}_2$)	Mass spectrometry and analogy with ethyl vinyl ether fragmentation IR with characteristic bands at 1590 cm^{-1}
3	Diethyl monosulfide ($\text{CH}_3\text{CH}_2\text{SCH}_2\text{CH}_3$)	Mass spectrometry Comparison with GC of known compound
5	3-Thiapentanaldehyde ($\text{CH}_3\text{CH}_2\text{SCH}_2\text{CHO}$)	Mass Spectrometry 1715 cm^{-1} peak in IR
6	Diethyl disulfide ($\text{CH}_3\text{CH}_2\text{SSCH}_2\text{CH}_3$)	Mass spectrometry Comparison with IR and GC of known compound Elemental analysis

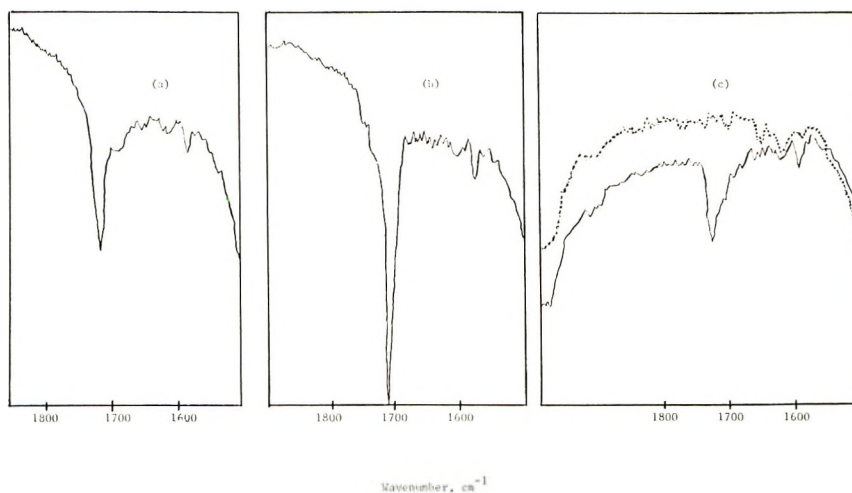


Fig. 5. Partial infrared spectra of oxidized poly(ethylene sulfide) and model compounds: (a) liquid phase of 3,6-dithiaoctane oxidized 4 hr at 150°C in 1 atm O_2 ; (b) liquid phase of 3,6,9-trithiaundecane oxidized 4 hr at 150°C in 1 atm O_2 ; (c) poly(ethylene sulfide) compression-molded film, (\cdots) unaged and (---) aged in air, 16 hr at 150°C .

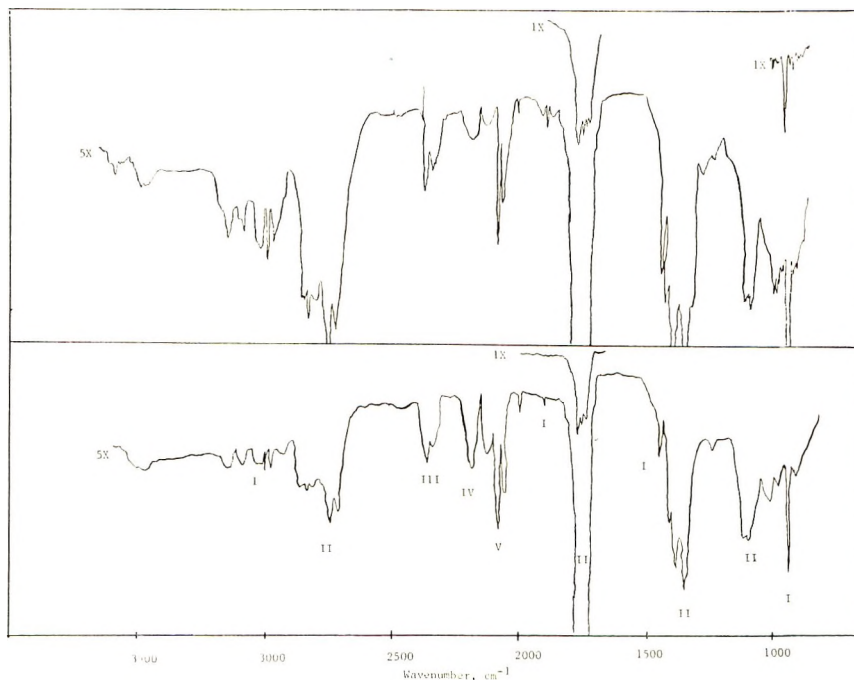


Fig. 6. Infrared spectra of gaseous products of oxidation of 3,6-dithiaoctane (top) and poly(ethylene sulfide) (bottom) at 150°C in 1 atm O_2 . Identification of peaks: (I) ethylene; (II) acetaldehyde; (III) CO_2 ; (IV) CO; (V) COS. 1X and 5X represent extent of scale expansion.

Identifications were assigned by comparison with reference spectra of the known gases.

Gasueous oxidation products of dithiaoctane are acetaldehyde, carbon dioxide, carbon monoxide, ethylene, and carbonyl sulfide. No absorptions due to water are evident in the spectrum.

OXIDATION OF POLY(ETHYLENE SULFIDE) AT HIGH TEMPERATURES

Rate of Oxidation

The rate of oxidation of poly(ethylene sulfide) at an oxygen pressure of 1 atm, in moles of oxygen consumed per unit ethylene sulfide per hour, was found to be 1.4×10^{-4} for polymer powder and 1.6×10^{-4} for polymer film having thicknesses of about 0.1 mm or less at the same temperature. This agreement suggests that the thickness of both powder and films used are within the limits of diffusability of oxygen. Again, due to a malfunction in the temperature control, the exact bath temperature was not known but was believed to be between 120 and 150°C.

Under identical temperature conditions, the rate of oxidation of dithiaoctane was found to be 6.3×10^{-4} mole oxygen consumed per mole of model compound per hour. Considering dithiaoctane to correspond to two

repeat units in the polymer, the rate of oxidation becomes 3.15×10^{-4} mole of oxygen consumed per unit of ethylene sulfide per hour. Thus the rate of oxygen uptake per ethylene sulfide repeat unit is only two times as great for the model compound as for the high molecular weight polymer. This is considered to be fairly good agreement, especially since the model compound is a liquid and the polymer is in the form of solid powder or film.

The similarity of oxidation rates between model and polymer suggests that the degradation mechanisms are similar as will be confirmed by analysis of the oxidation products.

Identification of the Oxidation Products of Poly(ethylene Sulfide)

Gaseous Products of Oxidation. Polymer and model compound were oxidized in parallel experiments in gas buret assemblies under the same conditions of temperature and pressure, for extended periods of time, and in the absence of molecular sieves, in order to accumulate gaseous products. Their infrared spectra are shown in Figure 6.

The same gaseous breakdown products are found in both spectra, further supporting the similarity of oxidation mechanism in polymer and model; they are acetaldehyde, carbon dioxide, carbon monoxide, ethylene, and carbonyl sulfide.

Solid Products of Oxidation. Due to the intractability of the polymer, it was impossible to isolate breakdown products due to oxidation. Detection of breakdown products in the molded polymer was therefore limited to the interpretation of consistent infrared absorptions by the polymer film.

The most characteristic absorption reflecting oxidation was at 1715 cm^{-1} . This was postulated to be due to the formation of a terminal carbonyl β to a sulfur atom ($\sim\text{CH}_2\text{CH}_2\text{SCH}_2\text{CHO}$). A 1590 cm^{-1} absorption, less strong, was equally characteristic and was considered due to terminal unsaturation also β to a sulfur ($\sim\text{CH}_2\text{CH}_2\text{—S—CH=CH}_2$) (Fig. 5c).

The 1715 cm^{-1} and 1590 cm^{-1} absorptions were similarly found in the spectra of the liquid phase of oxidized trithiaundecane, as shown in Fig. 5b. In dithiaoctane, the 1590 cm^{-1} peak is seen (Fig. 5a), but the carbonyl absorption is strong at 1730 cm^{-1} (which has been identified as due to acetaldehyde), as well as at 1715 cm^{-1} . The probable identity of the species absorbing at 1715 cm^{-1} among the liquid breakdown products of trithiaundecane is 3-thiapentanaldehyde, ($\text{H}_3\text{CCH}_2\text{SCH}_2\text{CHO}$). It seems reasonable to suspect a β -sulfur of being responsible for the small shift to a longer wavelength. Such a small shift was observed in comparing the carbonyl absorptions of acetic acid and ethylthioacetic acid.

MECHANISM OF OXIDATION

The products identified from the thermo-oxidative breakdown of the poly(ethylene sulfide) structure are consistent with the products one would anticipate from a free-radical oxidation in which the hydroperoxide is

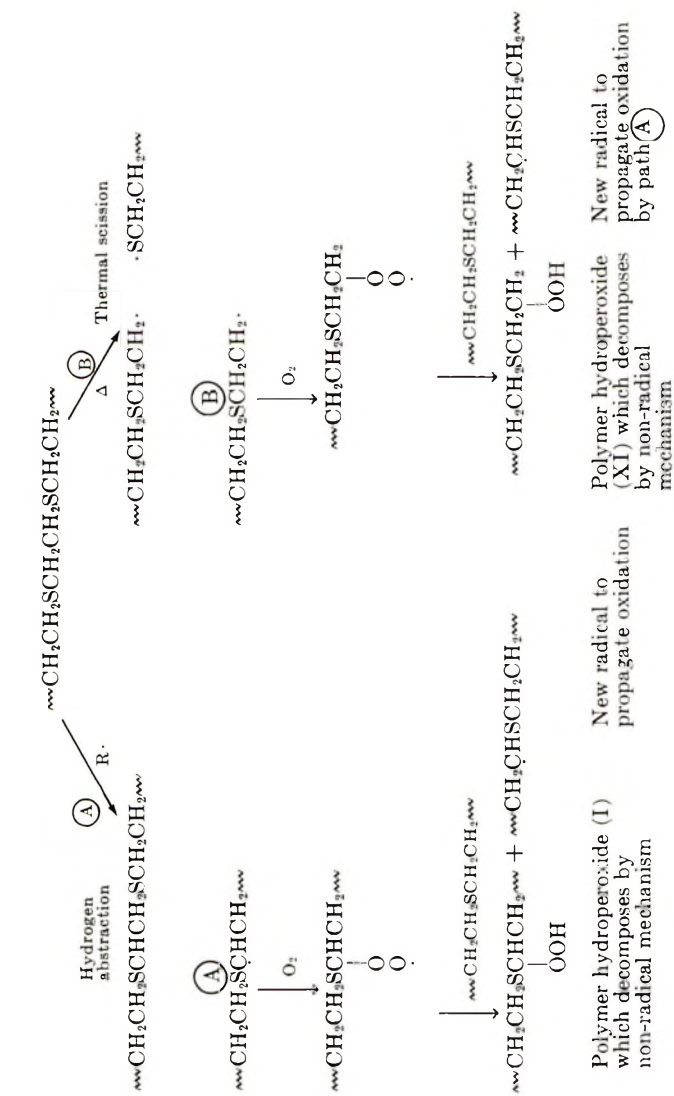


Fig. 7. Proposed scheme for oxidation of poly(ethylene sulfide).

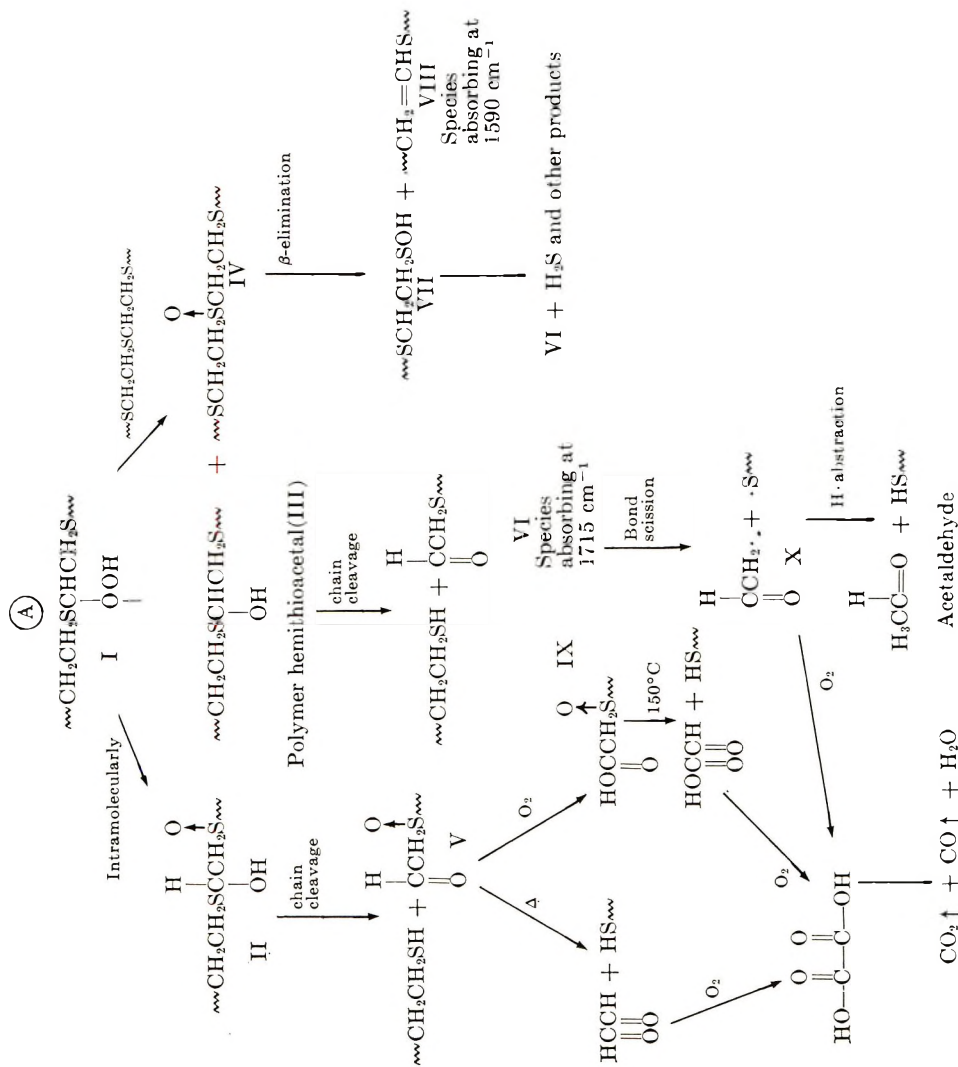
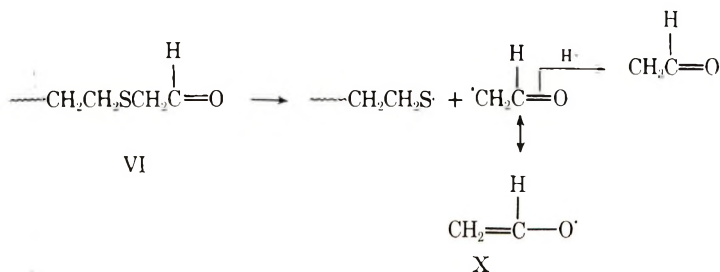


Fig. 8. Proposed scheme for hydroperoxide decomposition.

decomposed to nonradical fragments. Such a scheme was specifically outlined by Bateman et al.,⁸ and the general form of this scheme was also described by Barnard et al.⁹ Our proposed mechanism for the oxidation of poly(ethylene sulfide) is outlined in Figure 7. The decomposition of the hydroperoxide is outlined in Figure 8. The sulfoxide (IV) is decomposed by β elimination (Fig. 8) according to the scheme of Carruthers et al.¹⁰

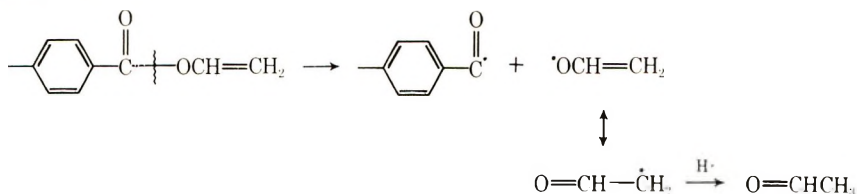
The oxidation products obtained in the liquid phase from the breakdown of dithiaoctane, are, in general, models of the polymer chain terminals that are formed by oxidative scission. Thus ethyl vinyl sulfide is the model for terminal unsaturation (VIII). Since the products are chain terminals frozen in a solid polymer, one cannot expect them to react with each other, as do the small molecules in the liquid dithiaoctane: e.g., an exceptionally prominent accumulation of diethyl disulfide was found to result from oxidation of dithiaoctane, but the coupling of polymeric sulfenyl radicals or the oxidation of mercaptan terminals to form a disulfide linkage is much less probable. Similarly, acetaldehyde and 3-thiapentanaldehyde are each predictable from the oxidation of dithiaoctane, depending on where the hydroperoxide forms; but both serve as the model for the same polymeric aldehyde terminal, $\sim\text{SCH}_2\text{CH}_2\text{SCH}_2\text{CHO}$ (VI), absorbing in the infrared at 1715 cm^{-1} .

The discovery of acetaldehyde as a gaseous oxidation product of the polymer itself requires some rationalization. The most reasonable explanation is that acetaldehyde is a secondary breakdown product, resulting from a homolytic scission of the polymeric aldehyde (VI) at the C—S bond β to the carbonyl.



The driving force for the formation of acetaldehyde is based on the relative stability of both radicals formed by the scission: the stability of the sulfenyl radical is well-known, and the vinyloxy radical (X) can exhibit resonance stabilization until it abstracts hydrogen to form acetaldehyde.

Such an argument was presented by Grassie¹¹ to explain the observed formation of acetaldehyde in the thermal breakdown of poly(ethylene terephthalate):



The two-step mechanism of acetaldehyde generation from the polymer can also explain why the carbonyl absorption at 1715 cm^{-1} characteristically reaches a limiting level: the formation of an aldehydic chain terminal approaches a rate equilibrium with the subsequent scission reaction generating acetaldehyde.

As indicated in Figure 8, the vinyloxy radical, in the presence of O_2 , could well be the precursor of an oxalic acid moiety, which would yield CO on dehydration. Another source of oxalic acid could conceivably be the thionylacetaldehyde endgroup (V) postulated as one result of intramolecular hydroperoxide decomposition. Szmant^{12a} cites the decomposition of phenylthionylacetic acid at $130\text{--}150^\circ\text{C}$ to form benzenethiol and glyoxalic acid. That a large part of the polymer hydroperoxide (I) may decompose intramolecularly to provide the thionylacetaldehyde (V) is suggested by Szmant's conclusion,^{12b} from the findings of Kharasch et al.,¹³ Szmant and Lapinski,¹⁴ and Oswald,¹⁵ that a β -hydroperoxide sulfide can give a quantitative yield of the corresponding β -hydroxy sulfoxide (our compound II, which is a hemithioacetal).

One obvious shortcoming of this oxidation mechanism is its failure to account for COS. The entity —S—C—O— is present in several of the intermediates, e.g., I, II, and III, but it is not obvious how any of these would decompose to release COS.

STABILIZATION

Before the inception of the fundamental studies on poly(ethylene sulfide) oxidation, exhaustive screening studies had been carried out involving all classes of antioxidants. Poly(ethylene sulfide) was found to be totally unresponsive to conventional antioxidants. Only the dithiocarbamates, particularly lead *N,N*-dimethyldithiocarbamate, and the chalcocyanates, especially KSeCN , prevented the rapid failure in properties that was shown in Table I. Data from some stabilization studies are given in Table III.^{15,17}

In the light of the fundamental work, the reason for resistance to stabilization by additives is clear: the polymer is self-stabilized; hydroperoxides are decomposed and oxidation never is permitted to attain the rate acceleration typical of uninhibited radical oxidations. The basic problem, resulting in deterioration of properties, is that the stabilizer is the polymer itself; and a fundamental part of the stabilization mechanism is the subsequent scission of chains. The antioxidant required, therefore, to stabilize the poly(ethylene sulfide) structure against oxidation must be even more efficient than the polymer itself, and preferably more reactive toward the initiating species than is oxygen.

Antioxidant effectiveness in preventing oxidation of the polymer was followed in two ways: (1) by infrared analysis of air-aged compression molded polymer film containing the antioxidant; (2) by measurement of the Izod impact strength of air-aged molded testpieces containing the antioxidant. Although measurement of a physical property is the closest

TABLE III
Effect of Additives on Notched Izod Impact Strength during Air Aging at 121°C

phr	Additive		Notched Izod impact strength, ft-lb./in. of notch ^a													
	Type		0	1 day	3 days	4 days	5 days	7 days	10 days	14 days	18 days	21 days	28 days			
	None	Control	1.11	0.44	—	0.19	—	0.05	—	0.02	—	—	0.08			
1	KSCN		1.12	1.06	—	0.94	—	1.00	—	0.61	—	—	0.27			
1	K ₂ CN		1.16	1.115	—	0.98	—	0.92	—	1.22	—	—	0.50			
2	ZnB ₂ DTC ^b		1.34	—	0.62	—	0.52	0.32	0.25	0.06	—	—	—			
2	ZnMe ₂ DTC ^c		0.89	—	0.52	—	0.45	0.70	0.40	0.31	—	—	—			
2	BiMe ₂ DTC		0.83	—	0.35	—	0.61	0.29	—	—	—	—	—			
2	NiB ₁₂ DTC ^d		1.06	—	0.76	—	0.25	0.18	—	—	—	—	—			
2	CuMe ₂ DTC		0.82	—	0.36	—	0.06	0.03	—	—	—	—	—			
2	PbMe ₂ DTC		1.18	—	1.20	—	1.16	0.75	—	0.77	0.80	0.25	—			

^a For samples air-aged at 121°C for various periods.

^b Dibenzylidithiocarbamate.

^c Dimethyldithiocarbamate.

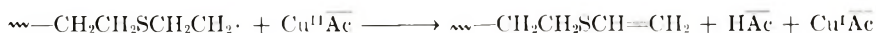
^d Dibutyldithiocarbamate.

indication of actual performance of the molded resin, the use of infrared scanning of a film was equally useful to the screening of antioxidants, in that sample preparation of films was more economical in both time and material required for an extensive aging study. Since the thermal stabilizers⁵ were normally omitted from the films (to simplify the spectra), a more straightforward approach to the oxidation reactions was achieved, also.

As described earlier, the 1715 and 1590 cm^{-1} infrared absorptions were characteristically prominent following the air-aging at 150°C for 16 hr of poly(ethylene sulfide) having no additives. Both oxidation peaks were absent, under these aging conditions, when the following additives were present: 2 phr cupric bromide, 2 phr cupric chloride, 1 phr mercuric chloride, 1 phr stannic chloride, or 1 phr bismuth trichloride. When the polymer film was similarly aged in presence of 2 phr cupric acetate or 2 phr cupric butyl phthalate, the 1715 cm^{-1} absorption was either absent or much diminished, while the 1590 cm^{-1} absorption was present. Films containing 1 phr lead dimethyldithiocarbamate or KSeCN also developed the 1590 cm^{-1} absorption on aging, with the 1715 cm^{-1} absorption absent or much diminished.

The possible reactions of a reducible cation with an alkyl radical have been outlined by Kochi.¹⁸ In his reaction schemes, electron transfer produces terminal unsaturation, whereas ligand transfer produces no unsaturation. If the predominant means of radical generation, initiating the oxidation reaction, is due to the slow thermal scission of the C—S bond,³ the resulting alkyl fragment would be the active initiating species.

Following Kochi, if a salt capable of electron transfer (e.g., salts of organic acids) were present, the alkyl radical fragment would be deactivated:



The resulting structure with terminal unsaturation should absorb at 1590 cm^{-1} . However if the salt of the reducible cation were a halide or pseudo-halide, ligand transfer would take place:



In this case, neither the carbonyl nor unsaturation absorptions would be evident.

We are indebted to the Dunlop Research Centres, Sheridan Park, Ontario, Canada and Birmingham, England for extensive discussions of this work. We also wish to acknowledge the many contributions of our present and former colleagues at Thiokol Chemical Corporation, in particular M. B. Berenbaum, S. W. Osborn, S. M. Ellerstein, G. F. Bulbenko, and R. Isaac as well as I. L. Dewitt of the Elkton Division, who performed the GC-MS analyses and assisted in their interpretation.

References

1. P. Sigwalt, *Chim. Ind.-Genie Chim.*, **96**, 909 (1966).
2. R. H. Gobran and S. W. Osborn (to Thiokol Chemical Corp.), U.S. Pats. 3,365,429 and 3,365,431 (Jan. 23, 1968).
3. R. H. Gobran, in *Encyclopedia of Polymer Science and Technology*, Vol. 10, Wiley, New York, 1969, p. 324.
4. R. H. Gobran and R. Larsen, *J. Polym. Sci. C*, **31**, 77 (1971), paper I.
5. E. H. Catsiff, M. N. Gillis, and R. H. Gobran, *J. Polym. Sci. A-1*, **9**, 1271 (1971).
6. F. Fehér and K. Vogelbruch, *Chem. Ber.*, **91**, 996 (1958).
7. L. Bateman and J. I. Cunneen, *J. Chem. Soc.*, **1955**, 1596.
8. L. Bateman, J. I. Cunneen, and J. Ford, *J. Chem. Soc.*, **1956**, 3056.
9. D. Barnard, L. Bateman, and J. I. Cunneen, in *Organic Sulfur Compounds*, Vol. 1, N. Kharasch, Ed., Pergamon Press, New York, 1961, Chap. 21.
10. W. Carruthers, I. D. Entwistle, R. A. W. Johnstone, and B. J. Millard, *Chem. Ind. (London)*, **1966**, 342.
11. N. Grassie, *Chemistry of High Polymer Degradation Processes*, Interscience, New York, 1956, p. 148.
12. H. H. Szmant in *Organic Sulfur Compounds*, Vol. I, N. Kharasch, Ed., Pergamon Press, New York, 1961, (a) p. 163; (b) p. 159.
13. M. S. Kharasch, W. Nudenberg, and G. J. Mantell, *J. Org. Chem.*, **16**, 524 (1951).
14. H. H. Szmant and R. L. Lapinski, *J. Org. Chem.*, **21**, 847 (1956).
15. A. A. Oswald, *J. Org. Chem.*, **24**, 443 (1959).
16. French Pat. 1,576,906 (to Thiokol Chemical Corp.) (June 23, 1969).
17. French Pat. 1,584,134 (to Thiokol Chemical Corp.) (Nov. 3, 1969).
18. J. K. Kochi, *Science*, **155**, 415 (1967).

Received June 30, 1970

Revised September 3, 1970

Dissociation-Association Sorption on Ion Exchangers.

I. Experimental Study of Dependence of Equilibrium Function of Acidity in Ion Exchanger on Activity of Hydrogen Ions in Aqueous Phase

MILAN NOVÁK, *Nuclear Research Institute,
The Czechoslovak Academy of Sciences, Řež, Prague, Czechoslovakia*

Synopsis

Equilibrium coloring of crystal violet, methyl violet, and dimethyl yellow sorbed on ion exchanger Dowex-50-WX4 was studied by a spectrophotometric method as a function of the pH of the aqueous phase. From the data obtained, the function of acidity in a ion exchanger was calculated corresponding to individual equilibria of the exchange reaction. A simple relationship between \bar{H}_0' in a ion exchanger and the pH of the aqueous phase was found.

The regularities of ion exchange have been studied by means of indicators sorbed on ion exchangers only rarely.

Nys and Savickaja¹ worked on a spectrophotometric determination of the ionization constant of *m*-nitroaniline sorbed on Dowex 50-X1. The value of the constant was found to be 2.75 ± 0.15 . Savickaja et al.² determined by another method the ionization constant of sorbed *m*-nitroaniline to be 2.6 ± 0.2 . In the aqueous phase, the same constant had been found by Paul and Long³ to be 2.5. These data show that no appreciable change of the ionization constant occurs.

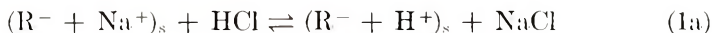
Surkova et al.⁴ compared the catalytic activity of hydrogen ions present in an ion exchanger, Dowex 50, with their activity in aqueous solutions of sulfuric acid in connection with the dehydration of tetracyclene. When *p*-nitroaniline was used as indicator, the pH values calculated by means of the Henderson-Hasselbach's equation for hydrogen ions in the ion exchanger which had been in equilibrium with 0.2–3.5*N* sulfuric acid were found to be practically the same as the values found for hydrogen ions in an aqueous solution of sulfuric acid of the same concentration. This result was verified by studying the kinetics of dehydration of tetracyclene in a sulfuric acid medium, the ion exchanger being in the form of hydrogen ions.

At the sulfuric acid concentrations used in the cited work, the ion exchanger was essentially in the form of hydrogen ions. When the regularities of the ion exchange are studied, it is this region of acidities, in which the

ion exchanger turns from one form of some ion into another ion form that is practically important.

THEORETICAL

The most simple system was chosen for the examination of the dependence of the dissociated hydrogen ions activity in the ion exchanger on their activity in the external solution. The following exchange reactions are supposed:



where R designates the functional ion exchanger group and *s* the ion exchanger phase.

We suppose that the sodium counterions remain fully dissociated in the ion exchanger phase, while the hydrogen counterions are forming uncharged ionic associates with the functional groups. The experimental study of eq. (1a) is presented in this paper. The generalization of results and description of the equilibrium state will be given in another paper. Under the equilibrium conditions expressed by eq. (1a), the activity of the hydrogen ions in the aqueous solutions may be experimentally determined by a glass electrode and the activity of dissociated hydrogen ions spectrophotometrically by help of acid-base indicators sorbed on the ion exchanger.

The spectrophotometric measurement of the color of sorbed indicators is rather complicated. In order to make it possible to investigate quantitatively the acidic and basic forms of acid-base indicators in the sorbed state, the validity of the Lambert-Beer law had to be verified. In spite of the fact that in an aqueous solution the indicator may be converted under some conditions practically completely into either acid or basic form it was found that, after the sorption under these conditions, the acidic form of the sorbed indicator contained such a portion of the basic form which cannot be neglected. An analogous phenomenon was found when the basic form of the indicator was sorbed. Therefore, only total amounts of the indicator sorbed are really known, not the individual amounts of the acidic and basic forms.

In order to determine the individual amounts of the indicators, the method of corresponding solutions suggested by Bjerrum³ was modified. The adopted method permits one to calculate the unknown concentrations of the colored component of the given compound if its total concentration in two different solutions and the corresponding hydrogen ions concentrations are known. The given quantities may be of different values. The extinctions of absorption bands of colored components in the solutions must be of the same value and so the concentrations of the colored components are equal. The counterions of the functional groups of swelled ion exchanger may be supposed, at least for the first approach, to be a solution which we shall call the intra-ion-exchange solution. Then the sorbed indicator might

be also regarded as a part of the intra-ion-exchange solution. For the corresponding solutions the following equation is valid:

$$\bar{c}_B = (\bar{c}_i)_1 - (\bar{c}_H)_1 \frac{(\bar{c}_i)_1 - (\bar{c}_i)_2}{(\bar{c}_H)_1 - (\bar{c}_H)_2} \quad (2)$$

where \bar{c}_B is the concentration of the basic component of the indicator, $(\bar{c}_i)_1$ and $(\bar{c}_i)_2$ are the total concentrations of the indicator at a constant \bar{c}_B concentration, and $(\bar{c}_H)_1$ and $(\bar{c}_H)_2$ are the total concentrations of hydrogen ions. The bar above the symbol indicates a quantity of the intra-ion-exchange solution.

The method of corresponding solutions may be used only when the absorption bands of the acidic and basic components are sufficiently separated.

If the absorption bands partly overlap, the concentrations of both colored components of the indicator may be calculated from relations presented by West:⁶

$$\bar{c}_B = \frac{\bar{\epsilon}_A'' E' - \bar{\epsilon}_A' E''}{d(\bar{\epsilon}_B' \bar{\epsilon}_A'' - \bar{\epsilon}_A' \bar{\epsilon}_B'')} \quad (3)$$

$$\bar{c}_A = \frac{\bar{\epsilon}_B'' E' - \bar{\epsilon}_B' E''}{d(\bar{\epsilon}_B' \bar{\epsilon}_A' - \bar{\epsilon}_A'' \bar{\epsilon}_B')} \quad (4)$$

where E' and E'' are the measured extinctions of the colored components B and A at the wavelengths λ' and λ'' , respectively, \bar{c}_A and \bar{c}_B are the concentrations of the colored components, respectively, $\bar{\epsilon}_A'$ and $\bar{\epsilon}_A''$ are the molar extinction coefficients of component A at the wavelengths λ' and λ'' , respectively; $\bar{\epsilon}_B''$ and $\bar{\epsilon}_B'$ are the analogous coefficients of component B, and d is the thickness of the absorbing layer.

The measurement of absorption spectra of sorbed indicators was performed in dispersed light. For optical reasons, this disadvantage might be improved by replacing the external equilibrium solution, among the ion exchanger beads, by another compound which has the same index of refraction for all wavelengths of visible spectrum, as the ion exchanger beads. Such a treatment is impossible, however, because of the influence on the physicochemical properties of the intra-ion-exchange solution by this compound. The only solution of these difficulties is probably associated with the quality of the spectrophotometer used, with the maximal sensitivity of the detector (photomultiplier), and with the calculation of extinctions of sorbed indicators by applying a system of corrections for light dispersion. The intensity of the monochromatic beam is weakened by the absorption in the colored indicator in the ion-exchanger phase, dispersion, and by the absorption, which corresponds to the light absorption by a neutral tone filter of distinct transparency. Spectrophotometric measurements were performed in such a way that quantitative data of colored absorption and dispersion were obtained. The absorption equivalent to the neutral tone filter was compensated by a standard sample. The extinctions for the individual

wavelengths of the absorption bands may be calculated according to the expression:

$$(E)_\lambda = (E_c - E_0 - E_H)_\lambda \quad (5)$$

where E_e is the experimentally measured extinction value, E_0 is the background of the measurement, and E_H is a correction factor covering the acidity of the equilibrium intra-ion-exchange, or external solutions, and is identical with the correction for light dispersion at wavelength λ .

The pH of the intra-ion-exchange solution might be calculated by means of the Henderson-Hasselbach's equation if the physicochemical properties of the intra-ion-exchange solution approach the properties of the aqueous solution:

$$\overline{\text{pH}} = \overline{\text{pK}}_i + \log(\bar{c}_B/\bar{c}_A) + \log(\bar{\gamma}_B/\bar{\gamma}_A) \quad (6)$$

where \bar{K}_i is the apparent dissociation constant of the indicator and $\bar{\gamma}_A$, $\bar{\gamma}_B$ are the activity coefficients of acid and basic indicator forms.

This would mean that the sorbed ions, e.g., hydrogen ions, would form a discrete solution inside the ion exchanger which would be minimally affected by the organic skeleton and would prove sufficiently polar properties. The fact that the ionization constant of *m*-nitroaniline is practically invariant¹⁻³ when *m*-nitroaniline is sorbed seems to give evidence for the existence of the above-mentioned state inside the ion exchanger. However, this conclusion cannot be generalized because similar quantitative data have not appeared frequently in the literature. Therefore, we have to measure either the ionization constants of the sorbed indicators or to express the acidity of the intra-ion-exchange solution by an equation in which the acidity does not depend on the nature of the solvent. Such conditions are satisfied by the Hammett equation:

$$\overline{H}_0 = (\text{pK}_i)_w + \log(\bar{c}_B/\bar{c}_A) = -\log a_{\text{H}^+} - \log(d_B/d_A)_s^w \quad (7)$$

where the subscript *w* denotes the indicator constant related to the aqueous solution as the standard state; the thermodynamic distribution coefficients of the acid and basic form d_A and d_B , respectively, define the distribution of the species between the aqueous and solid phases. According to the original Hammett assumption, the distribution coefficients ratio is of stable value and independent of the properties of the indicator.^{7a} A dependence of of this ratio on the nature of the indicator⁸ was found for nonpolar solvents. By applying the Hammett equation, some inaccuracy concerning the indicators used in this paper is introduced, because the equation was derived for the indicator base and its conjugate acid. The nature of ionization of the indicators used is more complicated. The ionization of triarylcannabinols in H_2SO_4 solutions was described by Gold and Hawes,⁹ and the acidity function J_0 for indicators, as secondary bases, was defined as:

$$J_0 = \text{pK}_i + \log(c_B/c_A) = H_0 + \log a_{\text{H}_2\text{O}} \quad (8)$$

The water activity in this solvent was determined by vapor-pressure measurements. The values of H_0 and J_0 were compared for 5–95% solutions of sulfuric acid. By increasing the H_2SO_4 concentration, the differences between H_0 and J_0 were enhanced also. For 40% H_2SO_4 , this difference was $\sim 10\%$.

The vapor tension of water over the ion exchanger was not measured under the given conditions. The intra-ion-exchanger solution of Dowex 50 may be supposed to constitute of a 40% solution of sulfonic acid. On comparison with the solution of sulfuric acid, we may expect that differences between H_0 and J_0 will lie in the range of experimental errors. From these reasons we have chosen the Hammett equation for the calculation of the intra-ion-exchanger acidity. Owing to the secondary base character of the indicators examined, we denoted this acidity H_0' .

On determining experimentally the pH values of the external solutions which are in equilibrium with the intra-ion-exchange solutions, the acidity of which has been calculated, the dependence of H_0' on the pH may be found.

EXPERIMENTAL

Stock solutions of crystal violet (hexamethyl-*p*-rosaniline chlorohydrate) and methyl violet 6 R (pentamethyl-*p*-rosaniline chlorohydrate) having a concentration of 0.1% were prepared using redistilled water. Dimethyl yellow (dimethyl aminoazobenzene) was dissolved in 40% ethyl alcohol solution in such a way that a saturated solution of the indicator resulted. The excess of undissolved dimethyl yellow was filtered off, dried, and weighed.

Sorption of Indicators on the Ion Exchanger

Before use, 0.500 ± 0.001 g of Dowex 50-WX4 having the grain size of 200–400 mesh was weighed, the ion exchanger being in the Na form. It was transferred alternatively into H and Na forms and thoroughly washed with redistilled water to the end. A 50-ml portion of redistilled water was added to each ion-exchange sample together with a corresponding amount of acid–base indicator. The sorption of the indicators was practically quantitatively complete within about 10 min because the aqueous solution decolorized. After decoloration of the solution, the sorption time was extended for about 30 min in order to achieve equilibrium. During the sorption, the sample was stirred. The individual samples were then filtered and transferred into Erlenmeyer flasks, in which the equilibrium experiments were made.

Equilibrium Experiments

The effect of varying amount of hydrogen ions in the intra-ion-exchange solution and in the external solution on the light dispersion was studied experimentally. Samples containing 0.500 ± 0.001 g of Dowex 50-WX4

in the Na form, having a grain size of 200–400 mesh, were brought under vigorous stirring into contact with 50 ml of hydrochloric acid of various concentrations; the contact time was 72 hr. With the equilibrium external solution, the pH was measured and the acid concentration was determined by titration.

In order to verify the Lambert-Beer law, the experiments were so arranged that an exchange reaction proceeded between the Na form of the ion exchanger and the hydrogen ions in the external solution at constant equilibrium activity of H^+ ions and varying amount of the sorbed indicator. The volume of the aqueous solution was 50 ml. With sorption of crystal violet and methyl violet 6R, the acidity of the aqueous phase was maintained constant by means of a phosphate-citrate buffer; similarly, with sorption of dimethyl yellow, the pH of 9.13 was maintained by means of a 0.1*N* borax solution. The equilibrium state was being established for about 72 hr with continuous shaking of samples. The acidity of the equilibrium external solution was checked by measuring the pH or by titrating.

When changes in color of the sorbed acid-base indicator were studied in dependence on the pH of the external solution, samples of ion exchanger on which a constant amount of the indicator was sorbed were brought into contact with 50 ml of hydrochloric acid of various concentrations. Then 0.1 or 1.0 ml. of crystal violet, 0.08 ml. of methyl violet, or 1.0 ml. of dimethyl yellow solution was sorbed on the ion exchanger. The samples were stirred and, after about 15 min. the acidity of the external solution was checked and adjusted by adding acid. The adjustment of the pH was accomplished only by adding hydrochloric acid because, in the external solution, only sodium ions from the exchange reaction were to be present. The pH of the external solution was adjusted several times as needed. The samples were shaken for about 72 hr; then the pH of the equilibrium external solution was measured, or the equilibrium acid was titrated. The pH was measured by means of a pH meter 22 (Radiometer Co.) using a glass electrode, which was calibrated with the use of buffer solutions. In case the equilibrium concentration of hydrochloric acid was too high for direct measurement of the pH, the solution was titrated. The corresponding activity coefficients of hydrochloric acid were found and the pH was calculated. In the calculation of activities, the influence of sodium chloride transferred into the equilibrium solution in the exchange reaction was neglected. In these cases the sodium chloride concentrations in the equilibrium solution were about 0.05*N*, while the hydrochloric acid concentration was higher than 0.5*N*.

Spectrophotometric Measurements

The variation of color of the sorbed acid-base indicators was investigated by means of a Unicam-SP-700 spectral photometer. The ion exchanger, together with the equilibrium solution, was put in 2-mm measuring cells, in which the exchanger grains sedimented freely for 15 min. The reproducibility of the results obtained in this way was satisfactory, which fol-

lows from the determination of the mean-square error of the measurement. Samples prepared by the same procedure, containing Dowex 50-WX4 in the Na form in redistilled water, served as the comparison samples. The same comparison sample was used during the whole series of a measurement. Before and after each series, the E_0 values were measured and, when evaluating the spectra, their arithmetic mean was used. The function of the spectral photometer was verified before every measurement. The base of the measurement was checked as well as the line of the 100% absorption. The photometer function was checked so that the absorption of air, or of an opaque filter, was measured against air. In individual cases, the base value varied within less than 1%.

The spectrophotometric measurements of light dispersion were made in the same way as in cases in which the indicator was sorbed on the ion exchanger. From the results of the experiments, corrections were determined which were used when evaluating the spectra.

The concentrations in the intra-ion-exchange solution were obtained so that the number of moles, or the number of gram-ions of the substance present in the exchanger, was divided by the exchange volume. The exchange volume, in which the space between the beads was not involved, was determined experimentally by using a method which will be described elsewhere in this report.

Each experiment was made at the room temperature, which varied in the range 20–25°C.

RESULTS AND DISCUSSION

The acid–base indicators were chosen according to their ability to be sorbed on the ion exchanger in the Na form. By a mechanism of ion exchange, such indicators may be sorbed on the exchanger, the chromogenous component of which is the cation of the indicator dye. The amounts of indicators used for the sorption were such that the indicator occupies less than 1% of the total number of functional groups. Under these conditions, the effect of indicator on the equilibrium of the exchange reaction was assumed to be negligible.

The pH range of the acid–base indicators sorbed on the exchanger by the ion-exchange mechanism should not change because the pH range for indicators does not depend on the types of ions which make up the charges of the chromogenous component. The compensating ions are, after the sorption, the functional groups of the exchanger.

Correction for Light Scattering

Separately, the absorption spectra of the ion exchanger in equilibrium with various hydrochloric acid concentrations were measured; in this exchanger, the concentration of hydrogen ions also varied. The absorption spectra of Dowex 50-WX4 are shown in Figure 1 as function of some equilibrium acidities of the external solution. The color of Dowex 50-WX4 in the Na forms is bright cream. Negligible changes of coloring occur on

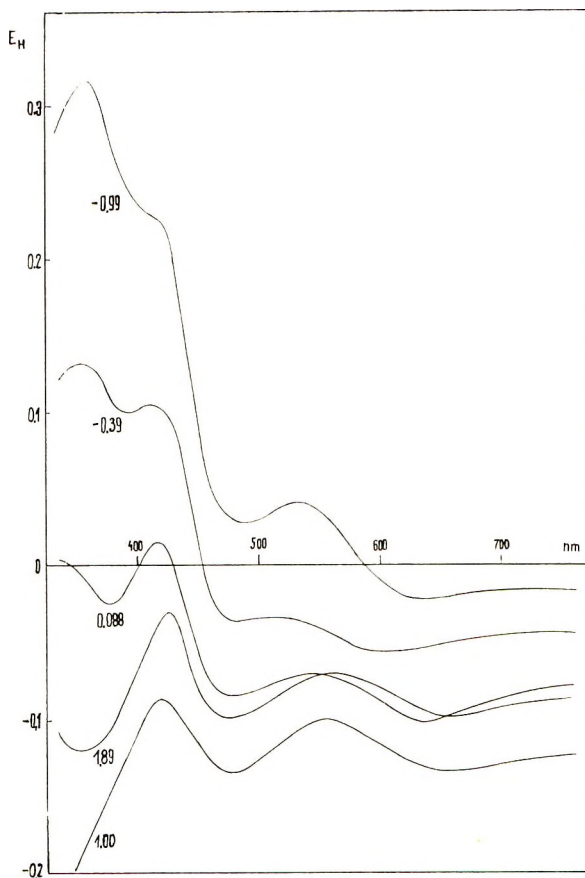


Fig. 1. Absorption spectra of Dowex 50-WX4 at equilibrium with external solutions of various acidity. The number on the curve indicates the equilibrium pH for the external solution.

changes in the concentration of hydrogen ions, and therefore the changes in extinction should be much smaller than those measured because they should correspond to the change of color. This discrepancy may be the result of the fact that the matter in question is not a simple absorption. In the presence of the exchanger, the absorption spectra are taken in scattered light. If the beads of ion exchanger could be regarded as optically homogeneous, the light scattering would be caused only by the difference in the index of refraction of the light rays in the exchanger and in the external equilibrium solution. It has been found that the equilibrium aqueous phase containing hydrochloric acid or sodium chloride involved immersion in the presence of an exchanger of the Dowex 50 type, the grain size of which was 0.5–1.0 mm.¹ Our results obtained with a finer exchanger do not confirm this experience. They show that the indices of refraction of the exchanger beads and the equilibrium solution differ from each other and that they depend on the hydrogen-ion concentration. Then, considerable changes of extinc-

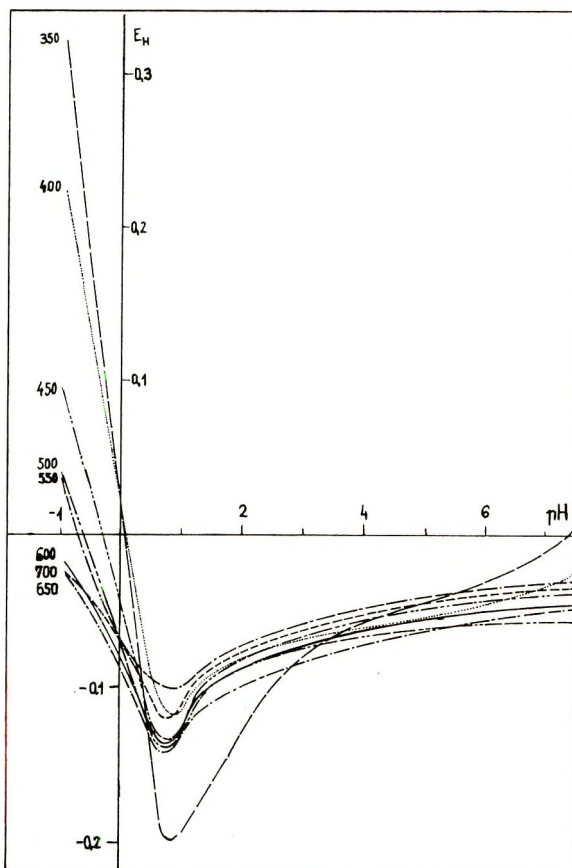


Fig. 2. Correction nomogram for the light dispersion. The numbers on the curves indicate the wavelengths (in nm).

tions with the samples (Fig. 1) with which palpable change of coloring did not occur might be explained by the change of the light scattering.

Figure 2 shows the nomogram of corrections for different wave lengths in dependence on the pH of the external equilibrium solution. For simplicity, the corrections are shown at intervals of 50 nm. The working graphs were made at intervals of 10 nm and in the needed range of the pH. From the values of the corrections it follows that directly measured extinctions of the sorbed indicators will be higher in strongly acidic and basic region than they would be if they corresponded only to the indicator concentration in the intra-ion-exchange solution, while within these limits the measured extinctions will be lower than those corresponding to the indicator concentration.

Qualitative Comparison of Absorption Spectra of Sorbed and Dissolved Indicators

With the indicator sorbed on the exchanger, the form of absorption spectra of the acidic and basic form might change when compared with the spectra of aqueous solution.

Therefore, the absorption spectra of indicators in aqueous solutions at different concentrations and acidities were measured. Conditions were so chosen that the indicators occurred preferably in the acidic or basic forms. The results were compared with the absorption spectra of indicators in external solutions at different pH values. We have found that practically congruent spectra were obtained. Maxima of the absorption bands of the sorbed indicators shifted only about 20 nm to the higher wavelengths. The acidities of the external and aqueous solutions differed substantially, however, in both cases.

Determination of the Molar Extinction Coefficients of the Sorbed Indicators

The results of experimental verification of the Lambert-Beer law for the acid-base indicators sorbed on the exchanger are presented in Figures 3-5. After the interfering influence of hydrogen ions on the form of the indicator spectra has been eliminated, the linear part of the dependence of extinction on the amount of indicator sorbed crosses the origin. As the equilibrium pH of the external solutions was constant in all cases, possible inaccuracy in the correction value does not affect the slope of the straight line. The acidities of the external equilibrium solutions were so chosen that the indicator dyes were not subject to the extreme conditions.

The straight lines connecting the experimental results in Figure 3a were drawn with regard to the location of points corresponding to 0-0.1 ml of the

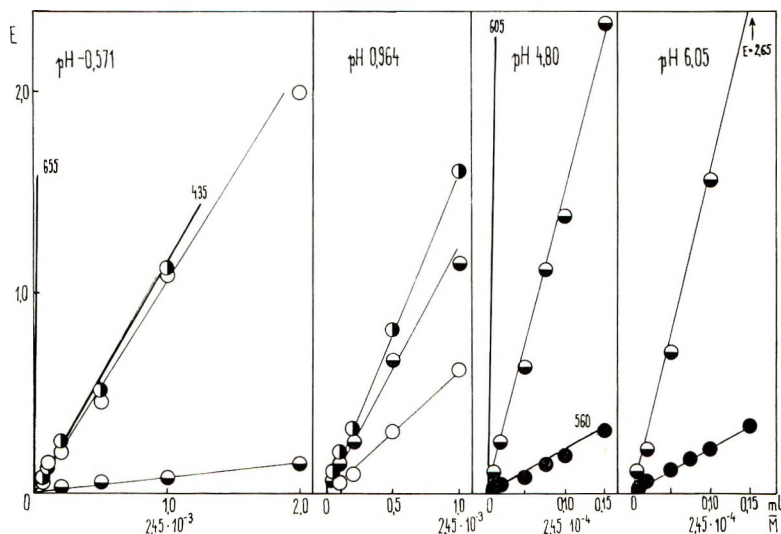


Fig. 3. Dependence of extinction of sorbed crystal violet on its amount in the intra-ion-exchange solution. Abscissa: amount of sorbed stock solution of the indicator, or the molarity of the crystal violet in the intra-ion-exchange solution after the sorption. (○) extinction at 435 nm (experimental); (◐) extinction at 655 nm (experimental); (◑) extinction at 605 nm (experimental); (●) extinction at 560 nm (experimental). Solid lines designate the calculated values for pure form.

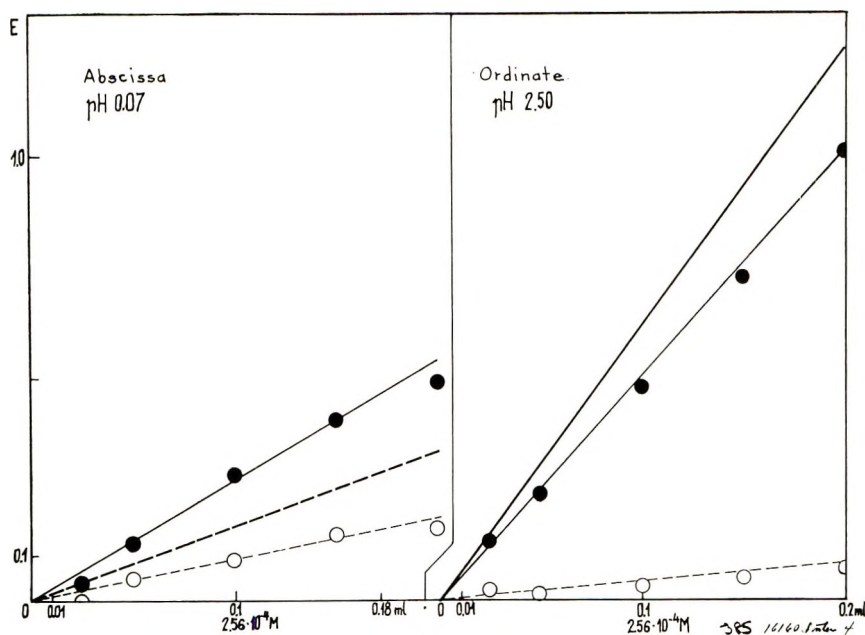


Fig. 4. Dependence of extinction of sorbed methyl violet 6R on its amount in intra-ion-exchange solution. Abscissa: amount of sorbed stock solution of the indicator or the molarity of methyl violet in the intra-ion-exchange solution after the sorption: (O) extinctions at 420 nm (experimental); (●) extinctions at 640 nm (experimental); (—) calculated dependence of the extinction of pure acidic or basic form on their actual concentrations in the intra-ion-exchange solution.

TABLE I
Molar Extinction Coefficients of Sorbed Indicators

Indicator	Coefficients in the maximum of absorption bands							
	nm	ϵ	nm	ϵ	nm	ϵ	nm	ϵ
Crystal violet	435	2.19×10^3	560	4.46×10^2	605	4.49×10^5	655	2.62×10^5
Methyl violet 6R	420	3.28×10^3					640	1.22×10^4
Dimethyl yellow	538	1.36×10^4	455	1.05×10^4				
Coefficients at the foot (λ_n) of the absorption band which has a maximum absorption at λ								
	λ/λ_n	ϵ	λ/λ_n	ϵ	λ/λ_n	ϵ	λ/λ_n	ϵ
Crystal violet	605/	2.46×10^5	605/	5.14×10^4	655/	2.83×10^4	560/	≈ 0
	560		655		605		605	
Dimethyl yellow	455/	1.18×10^5	538/	8.95×10^2				
	538		455					

sorbed indicator. On using the scale of Figure 3, the points close to each other hand, therefore, the plot seems to be inaccurate.

In Figures 3 and 4, the solid line represents the calculated dependence of extinction on the real amount of the basic or acidic form sorbed on the exchanger. The calculation was made by using the method of corresponding solutions. When this method is used, the total concentrations of hydrogen ions in the intra-ion-exchange solution must be known. The total analytical concentration is known from experiments. In the calculation, the concentration of hydrogen ions was replaced by their analytical concentrations.

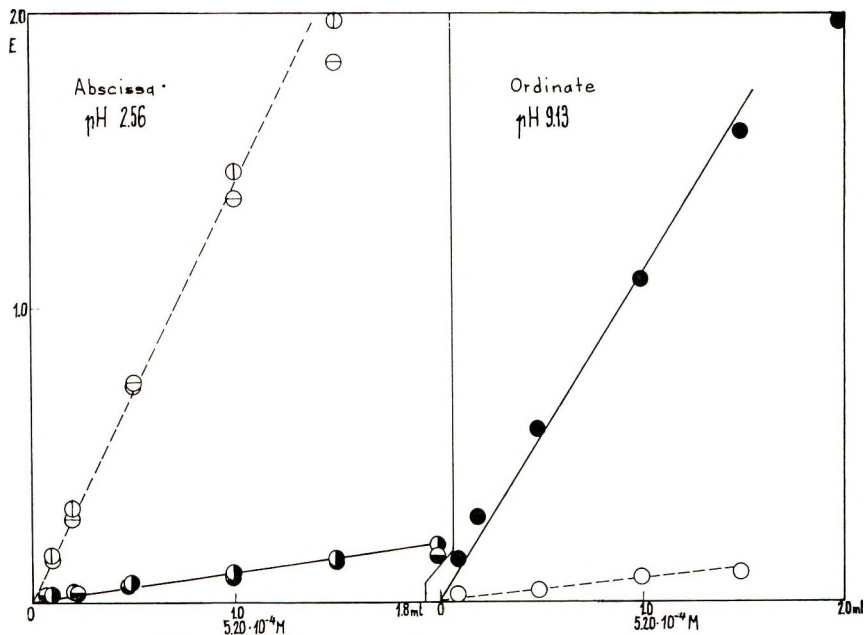


Fig. 5. Dependence of extinction of sorbed dimethyl yellow on its amount in intra-ion-exchange solution. Abscissa: amount of sorbed stock solution of the indicator or the molarity of dimethyl yellow in the intra-ion-exchange solution after the sorption: (⊕) extinctions at 538 nm in hydrochloric acid medium; (⊖) extinctions at 538 nm in the acetic acid medium (the pH was the same in both cases); (●) extinctions at 455 nm in the hydrochloric acid medium; (⊖) extinction at 455 nm in the acetic acid medium; (○) extinctions at 538 nm in sodium chloride medium of the concentration resulting from the exchange reaction; (●) extinctions in NaCl at 455 nm.

By means of the dependences found, the molar extinction coefficients of sorbed indicators were calculated. The molar extinction coefficients are presented in Table I. In the acidic form of dimethyl yellow, no basic component was found (Fig. 5). Similarly, no acidic component was found in the basic form. The pH range of this indicator made it possible to use acidities at which the concentrations of the components were negligible, the equilibrium solutions being not too acidic or basic due to the stability of the dye.

Measurement of c_B/c_A Ratio

Figure 6 shows the peaks of adsorption bands reflecting the change of the amount of the basic form of the sorbed crystal violet at different acidities of the external equilibrium solutions. That part of the spectrum corresponding to the absorption band of the acidic form of the crystal violet is not shown in the figure because in this region the results were not fully reproducible. This failure is caused by two reasons. The first is the great difference in the values of molar extinction coefficients of the two forms of crystal violet. Therefore, if the values of extinctions of the basic form are to lie in a convenient range, some amount of the indicator must be sorbed on the exchanger. However, then the values of extinctions of the acidic form are too low. The second reason is the fact that the maximum of the absorption of the hydrogen form of the exchanger lies in the range of the absorption bands of the acidic form of crystal violet. Therefore, the corrections for this range are relatively high and they are somewhat inaccurate. These inaccuracies, due to low values of the extinctions of the acidic form, cause considerable errors.

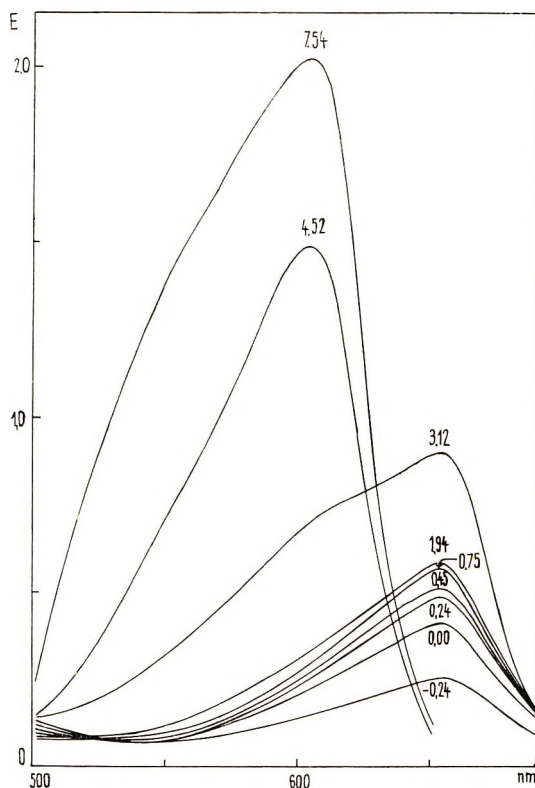


Fig. 6. Change of absorption maxima of basic form of sorbed crystal violet at various acidities of external solutions. The numbers on curves denote the equilibrium pH's of the external solutions.

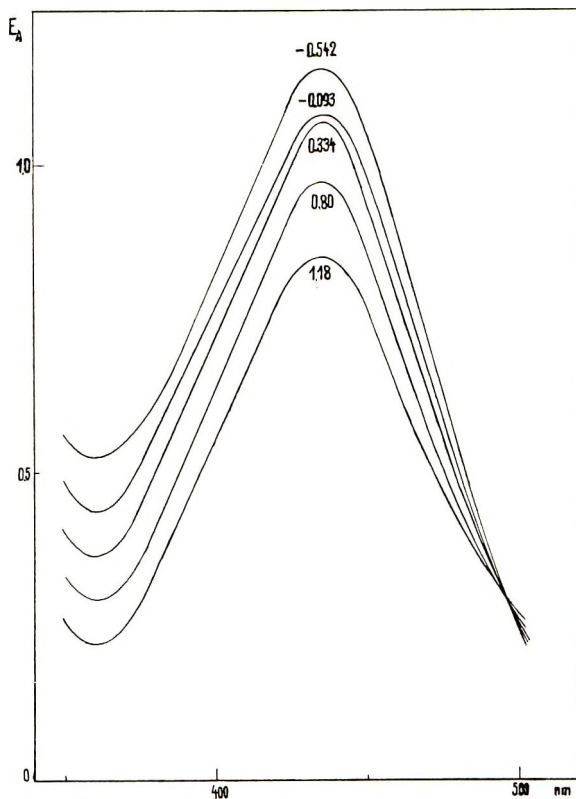


Fig. 7. Change of absorption maxima of acidic form of sorbed crystal violet at various acidities of external solutions. The numbers on curves indicate the equilibrium pH's of the external solutions.

In Figure 7 are shown sections of spectra with the absorption bands of the acidic form of the crystal violet in equilibrium with strongly acidic external solutions. The amount of sorbed indicator was ten times as high as it was with the experiments the results of which are presented in Figure 6. Under these conditions, the mentioned deficiencies do not appear and the results are reproducible. The absorption bands of the basic form are not shown in the figure because they reach (except those of the highest acidity, i.e., pH-0.542) 100% absorption.

From the experimental results it follows that crystal violet as well as methyl violet 6R is not a very convenient indicator for the given purpose even though it is usable in some range of acidity. Moreover, it is inconvenient also because it has too complicated a spectrum which cannot be evaluated directly over the whole range (three color changes occur). Therefore, Figure 8 shows the sections of spectra corresponding to the absorption bands of the basic form of the sorbed methyl violet, the last spectrum being that obtained with the indicator in external solution having a pH 3.96. The last spectrum cannot be evaluated at all because of the

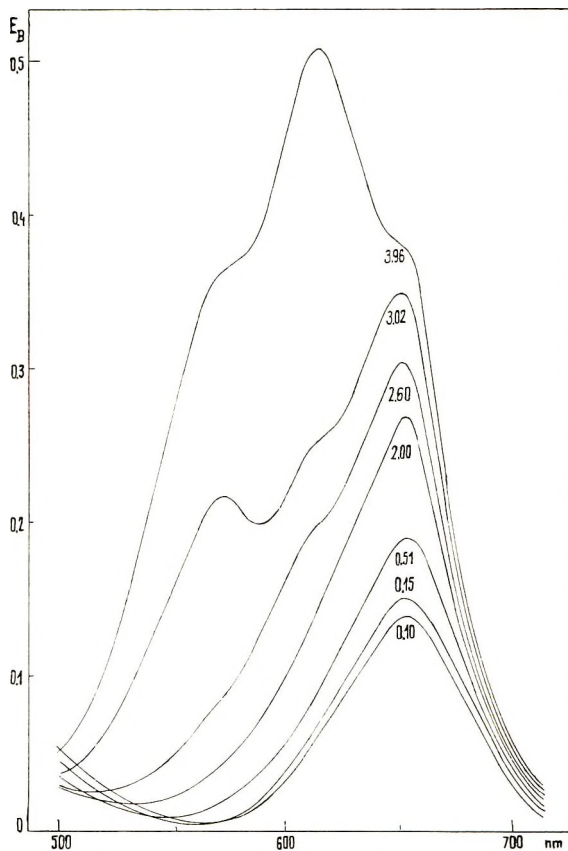


Fig. 8. Change of absorption maxima of basic form of sorbed methyl violet 6R at various acidities of external solutions. The numbers on curves indicate the equilibrium pH's of the external solutions.

presence of three overlapping absorption bands, all of comparable intensity and none of which may be neglected. The same holds with the spectrum of the acidic form of methyl violet as with the crystal violet.

In Figure 9, the spectra of sorbed dimethyl yellow are shown. The molar extinction coefficients of the acidic and basic forms do not differ too much from each other. At the equilibrium acidity, the correction values were lower than they were with the acidic media of the crystal violet and methyl violet. Therefore, with a single sample, the values of absorption of the acidic and basic forms could be obtained, the change of color of the indicator being well distinguishable from the curves.

Acidity Function \bar{H}_0'

The calculated values of the equilibrium functions of acidities of the intra-ion-exchange are shown in Fig. 10 as a function of the equilibrium values of pH in the external solution. The acidity functions were calculated for

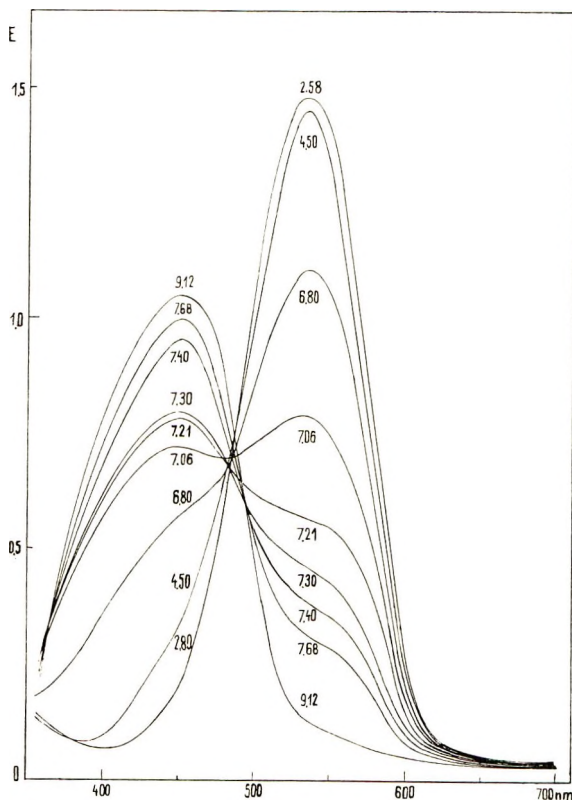


Fig. 9. Change of spectra of sorbed dimethyl yellow at various acidities of external solutions. The numbers on curves indicate the equilibrium pH's of the external solution.

the crystal violet from three different color changes of this indicator. In the most acidic region, the color change was experimentally determined for only one form of the indicator. The concentration of the second form was calculated from the difference between the total amount of the indicator and the experimentally determined concentration of the first form. For the two other color changes, the concentrations of acidic and base forms were determined by help of eqs. (3) and (4), because their adsorption bands were partially overlapped. Only one color change, occurring in the most acidic region, was used for the calculation of the acidity function of methyl violet 6R. The concentration of one form was thus experimentally determined, while the concentration of the other one was found by calculation. The color changes of both forms of dimethyl yellow were measured in the more acidic region. Their absorption bands are partially overlapped and therefore their concentrations were calculated according to the eqs. (3) and (4).

The values of indicator constants, which were determined for aqueous solutions, were used for Hammett's equation for the calculation of the acidity function in the intra-ion-exchange solution. The spectropho-

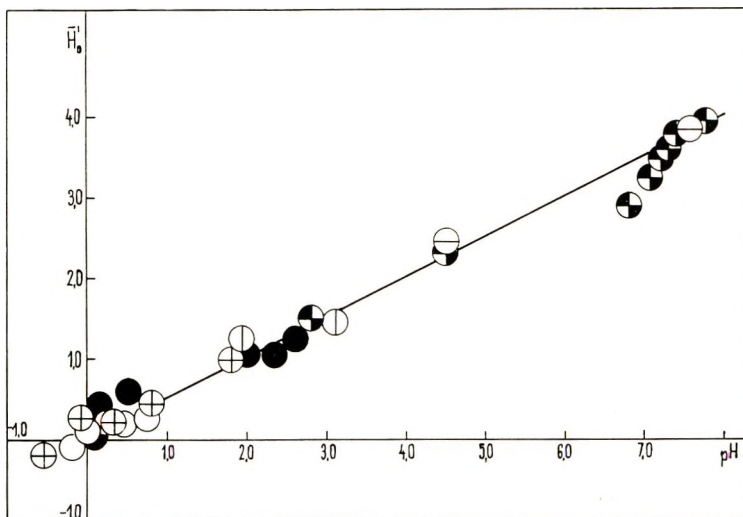


Fig. 10. Dependence of the acidity function of the intra-ion-exchange solution on the equilibrium pH of the external solution: (○) the values of \bar{H}_0' calculated by help of crystal violet from the spectra of its form having maximum absorption at 655 nm and a color change at 435 nm/655 nm, (⊕) the same values for maximum absorption at 435 nm and a color change at 435 nm/655 nm, (⊗) the values of \bar{H}_0' from spectra of crystal violet at a color change 655 nm/605 nm, (⊖) the same for the color change 605 nm/560 nm; (●) the values of \bar{H}_0' calculated by help of methyl violet 6R from spectra of its form having maximum absorption at 640 nm and a color change at 420 nm/640 nm; (★) the values of \bar{H}_0' calculated from the spectra of dimethyl yellow at a color change 538 nm/455 nm.

metric method was applied for the measurements and the values of constants were calculated by help of the Henderson-Hasselbach equation.¹⁰ The values found are listed in Table II. The comparison of determined pK_1 values with published data was possible only for dimethyl yellow. The value of 3.25 is given for the only one color change at 431 nm/515 nm.⁷ The difference between the amount of color changes presented in Table II and in data in the literature resulted probably from the fact that these basic studies on acido-basic indicators are relatively older. The studies were at that time performed visually or potentiometrically and thus the color changes which occurred in the region outside the eye sensitivity were unregistered or the color changes which are closed one to the other splitted into one color change.

The calculated values of the equilibrium \bar{H}_0' are in a simple relationship with the equilibrium pH in the external solution. Individual points lie acceptably on a straight line, expressed by

$$\bar{H}_0' = 0.5 \text{ pH} \quad (6)$$

when the pH varies in the range of eight orders.

The methodical error of the procedure suggested cannot be evaluated because no exact method and no theoretical relation are known by means of

TABLE II
Apparent Dissociation Constants of Indicators in Aqueous Solutions at 25°C^a

Indicator	1. Color change	2. Color change	3. Color change
Crystal violet	$p/K_1/637 = 1.60$ 433	$p/K_2/595 = 1.79$ 637	$p/K_3/545 = 2.50$ 595
Methyl violet 6R	$p/K_1/633 = 1.11$ 431	$p/K_2/562 = 2.28$ 633	$p/K_3/543 = 3.27$ 592
Dimethyl yellow	$p/K_1/431 = 3.14$ 515	$p/K_2/365 = 4.77$ 431	

^a Indices designate maxima of wavelengths p/K_i per basic or acidic form.

which the activity of dissociated hydrogen ions in the intra-ion-exchange solution could be found when associated ions are also present in the solution. The magnitude of the systematic error depends also on the choice of convenient acid-base indicators to be sorbed on the exchanger. The condition that the indicators should sorb on the exchanger by the mechanism of ion exchange makes the choice of convenient indicators quite narrow. Therefore, triphenylmethane dyes had to be used in spite of their poorer stability in acidic media. The decrease in the intensity of color in the acid form is a source of error in all calculations in which the values obtained with the acidic form are used. Further irregularities arise during establishment of the equilibrium of the exchange reaction, chiefly as a result of the variation of temperature, etc.

When calculating the errors, especially those arising during photometry, i.e. when preparing the samples, were taken into account. On the basis of experience one may expect that these errors will be decisive. The identical sample of sorbed crystal violet in equilibrium with the external solution was inserted nine times into the same cell and photometered. The mean square error of this measurement attained $\pm 0.15 \bar{H}_0'$. In Figure 10, the error is illustrated by the size of the points under the assumption that this value does not depend on the quality of the indicator nor on the acidity of the external solution.

On the basis of the experiments, one cannot decide whether the dependence of \bar{H}_0' on the pH found is true only for hydrogen ions or whether it illustrates a more general regularity. Therefore, this problem will be the subject of further work.

The author wishes to thank Mrs. L. Šourková, Mrs. E. Štěpanková, and Mr. A. Havel for their technical assistance.

References

1. P. S. Nys and E. M. Savickaja, *Dokl. Akad. Nauk SSSR*, **176**, 873 (1967).
2. E. M. Savickaja, P. S. Nys, and B. P. Bruns, *Dokl. Akad. Nauk SSSR*, **164**, 378 (1965).
3. M. A. Paul and F. A. Long, *Chem. Rev.*, **57**, 1 (1957).
4. K. I. Surkova, E. M. Savickaja, and B. P. Bruns, *Dokl. Akad. Nauk SSSR*, **160**, 402 (1965).

5. G. Charlot and R. Gaugin, *Les Méthodes d'Analyse des Réactions en Solution*, Masson, Paris, 1951, p. 92.
6. W. West, in *Physical Methods of Organic Chemistry*, Vol. I, Part II, A. Weissberger, Ed., Interscience, New York, 1949, p. 1430.
7. I. M. Kolthoff and S. Bruckenstein, *Acid-Bases in Analytical Chemistry*, Interscience, New York, 1959, (a) p. 497; (b) p. 519.
8. D. S. Noyce and W. A. Pryor, *J. Amer. Chem. Soc.*, **77**, 1397 (1955).
9. V. Gold and B. W. V. Hawes, *J. Chem. Soc.*, **1951**, 2102.
10. M. Novák and A. Havel, to be published in *Chem. Listy*.

Received February 26, 1970

Revised July 15, 1970

Organometal-Initiated Polymerization of Vinyl Ketones. III. Polymerization of Methyl Isopropenyl Ketone Initiated by the Triethylaluminum–Methyl Isopropenyl Ketone Complex

A. R. LYONS* and E. CATTERALL,† *Department of Chemistry and Metallurgy, Lanchester Polytechnic, Coventry, CV1 5FB, England*

Synopsis

The kinetics and mechanism of the triethylaluminum–methyl isopropenyl ketone complex-initiated polymerization of methyl isopropenyl ketone (3-methyl-3-butene-2-one) in toluene have been studied over a range of temperature. Equimolar quantities of monomer and triethylaluminum were premixed to form the initiator species prior to the addition of the excess monomer for polymerization. Initial and overall reaction rates indicate a first-order dependence on monomer and initiator concentrations. The overall activation energy for the polymerization is 52 ± 3 kJ/mole. Molecular weight distributions were bimodal, with peaks corresponding to the trimer and high molecular weight material. The kinetic data are consistent with a coordinate polymerization mechanism.

INTRODUCTION

We previously reported the kinetics and mechanism of the triethylaluminum initiated polymerization of methyl isopropenyl ketone, for the case of the rapid mixing of the total quantity of monomer with the triethylaluminum.¹ This paper reports the large effect on the kinetics of premixing equimolar quantities of methyl isopropenyl ketone and triethylaluminum to preform the initiator species, followed by the addition of excess monomer for polymerization.

EXPERIMENTAL

All reagents were prepared, purified, and dispensed by high-vacuum techniques as described previously.¹⁻³ Benzylidene acetone was dried by stirring a solution in toluene over calcium hydride.

To prepare the initiator complex, equimolar quantities of triethylaluminum and monomer were cooled to -20°C and mixed. After stand-

* Present address: Department of Chemistry, University of Leicester, Leicester LE1 7RH, England.

† To whom all communications should be addressed.

ing at 0°C for 1 hr under constant illumination (100-W tungsten lamp), the mixture was recooled to -20°C for the addition of the excess monomer for polymerization. The polymerization rates were determined dilatometrically and gravimetrically as previously described.^{1,2} The reactions were terminated after a polymerization time of 24 hr and the polymeric products recovered.

Molecular weight distributions were determined on a Waters gel permeation chromatograph as described previously.²

RESULTS

Rate Measurements

The effect of initial monomer concentration $[M]_0$, initial triethylaluminum-methyl isopropenyl ketone complex concentration $[I]_0$, and temperature on initial and overall polymerization rates were studied.

In all polymerizations, the reaction between triethylaluminum and monomer gave an intense yellow which faded during the premixing period. The addition of further monomer after 1 hr reintensified the yellow, but this again faded rapidly and the pale straw solutions became heterogeneous with the production of white poly(methyl isopropenyl ketone).

Figure 1 shows that the rate of polymerization is proportional to $[M]_0$ at constant $[I]_0$. Figure 2 shows that at constant $[M]_0$ the polymerization rate increases with $[I]_0$.

The effect of polymerization temperature is shown in Figure 3.

First-order rate plots with respect to monomer for the overall reaction are virtually linear, as shown in Figure 4.

Initial rates are directly proportional to both initial monomer and triethylaluminum-methyl isopropenyl ketone concentrations (Fig. 5).

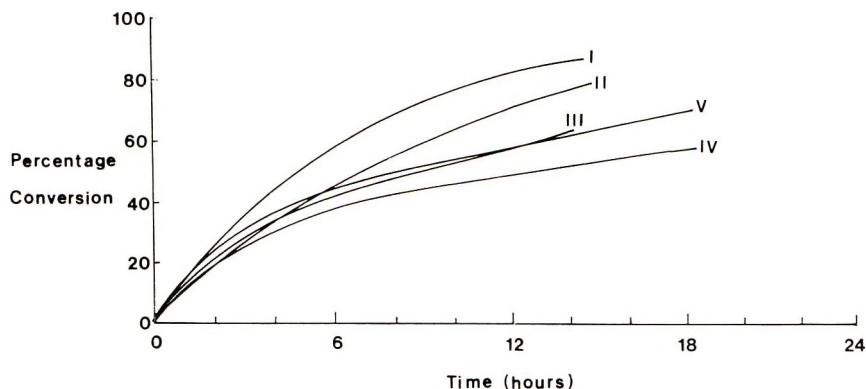


Fig. 1. Effect of initial monomer concentration on the rate of polymerization at various $[M]_0$: (I) = 1.0 mole/l.; (II) = 2.0 mole/l.; (III) = 3.0 mole/l.; (IV) = 4.0 mole/l.; (V) = 5.0 mole/l. Toluene solvent; 0°C; $[I]_0 = 0.10$ mole/l.

The overall and initial rate constants for the reaction, first order with respect to both monomer and triethylaluminum–methyl isopropenyl ketone complex are tabulated in Table I.

Activation energies for the overall and initial reactions, calculated from Arrhenius plots, are 52 ± 3 and 64 ± 2 kJ/mole, respectively.

TABLE I
Overall and Initial Rate Constant Data

$[I]_0$, mole/l.	$[M]_0$, mole/l.	Polymerization temp, °C	Overall rate constant $k_2 \times 10^2$, l./mole-min	Initial rate constant $k_2' \times 10^2$, l./mole-min
0.1	1.0	0.0	2.44	2.01
"	2.0	"	1.82	1.44
"	3.0	"	1.28	1.77
"	4.0	"	1.37	1.97
"	5.0	"	1.08	1.78
			Mean	1.79
0.05	2.0	0.0	1.27	1.68
0.075	"	"	1.76	1.55
0.10	"	"	1.82	1.44
0.15	"	"	2.00 ^a	1.47
0.20	"	"	2.08 ^a	1.77
			Mean	1.58
0.1	2.0	0.0	1.82	1.44
"	"	7.5	6.07	4.11
"	"	15.0	7.13	4.78
"	"	20.0	8.50	13.80
"	"	25.0	12.66	17.90

^a Estimated values.

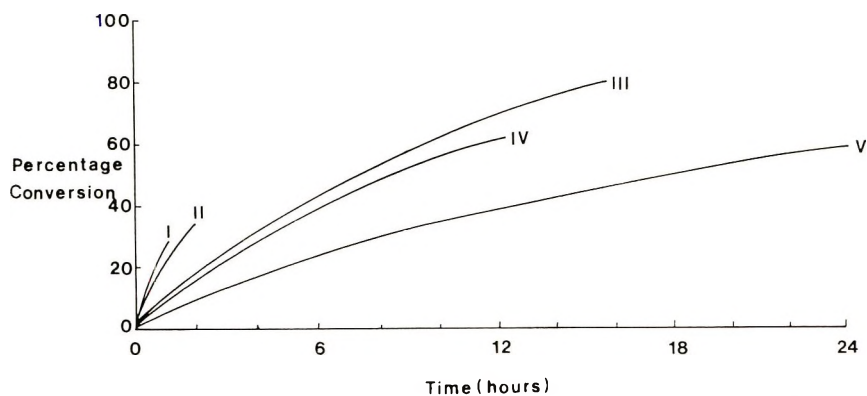


Fig. 2. Effect of initial triethylaluminum–methyl isopropenyl ketone complex concentration on the rate of polymerization at various $[I]_0$: (I) = 0.20 mole/l.; (II) = 0.15 mole/l.; (III) = 0.10 mole/l.; (IV) = 0.075 mole/l.; (V) = 0.05 mole/l. Toluene solvent; 0°C; $[M]_0 = 2.0$ mole/l.

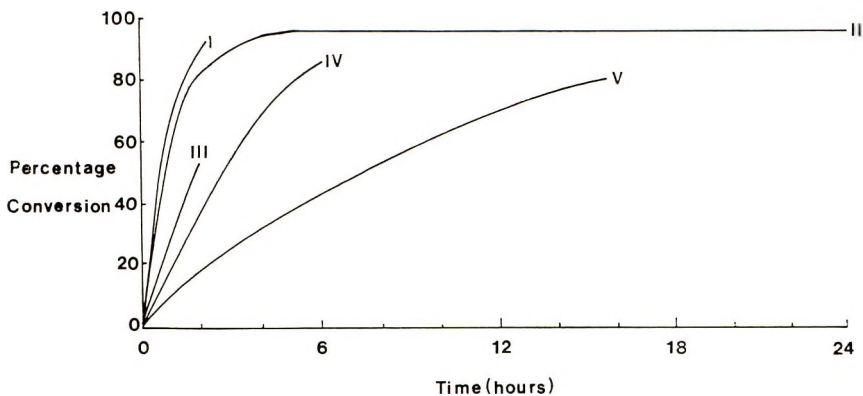


Fig. 3. Effect of temperature on the rate of polymerization: (I) = 25.0°C; (II) = 20.0°C; (III) = 15.0°C; (IV) = 7.5°C; (V) = 0.0°C. Toluene solvent; $[I]_0 = 0.10$ mole/l.; $[M]_0 = 2.0$ mole/l.

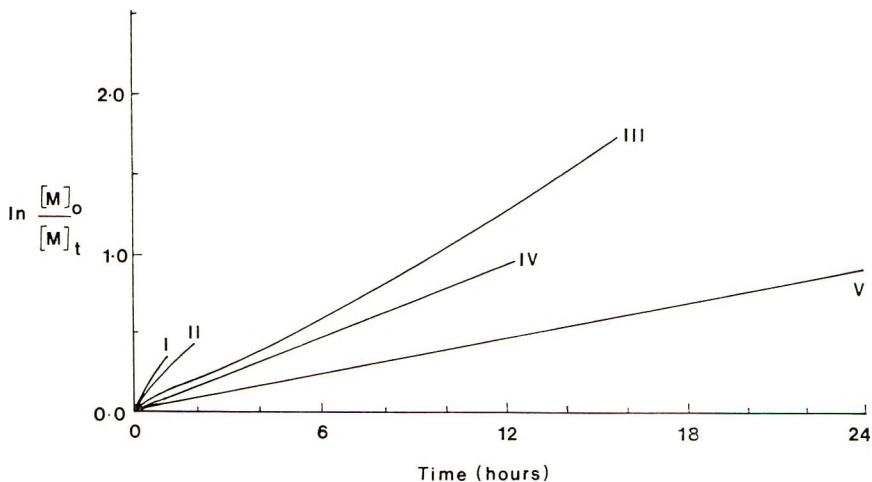


Fig. 4. First-order rate dependence on monomer concentration, effect of initial triethylaluminum-methyl isopropenyl ketone complex concentration $[I]_0$: (I) = 0.20 mole/l.; (II) = 0.15 mole/l.; (III) = 0.10 mole/l.; (IV) = 0.075 mole/l.; (V) = 0.05 mole/l. Toluene solvent; 0°C; $[M]_0 = 2.0$ mole/l.

Polymer Molecular Weights

Molecular size distributions of the polymeric products were bimodal. The broad higher molecular weight part of the distribution was asymmetric, and in some cases bimodal (Fig. 6).

Number-average molecular weights were calculated from the gel permeation molecular size distributions. The peak \bar{M}_n of the oligomer was limited to the very narrow molecular weight range (234–241); the peak \bar{M}_n of the higher molecular weight fraction ranged from 2650 to 17500.

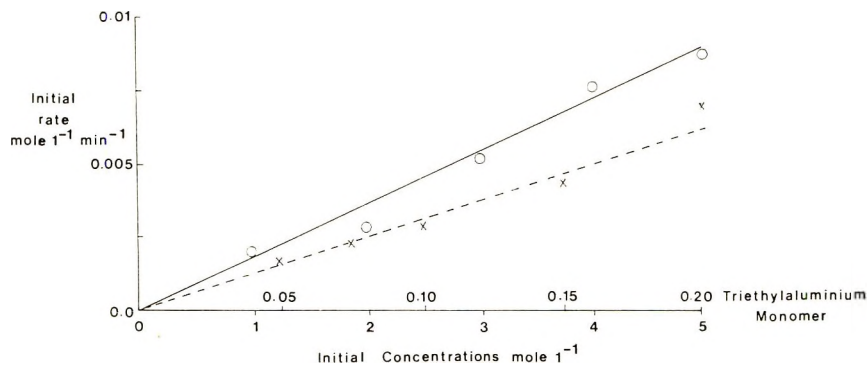


Fig. 5. Effect of monomer and triethylaluminum–methyl isopropenyl ketone complex on the initial rate of polymerization: (—) effect of monomer concentration at $[I]_0 = 0.10$ mole/l; (---) effect of initiator concentration at $[M]_0 = 2.0$ mole/l. Toluene, 0°C .

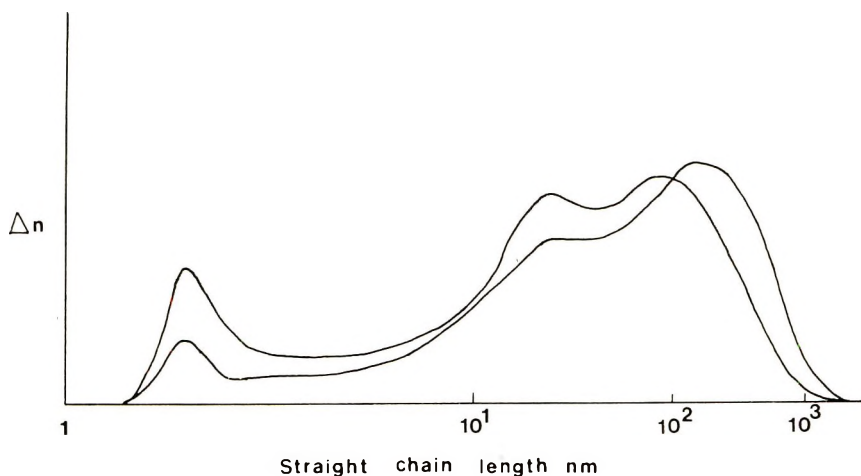


Fig. 6. Typical molecular size distributions. (Δn = refractive index difference between solvent and polymer solutions, arbitrary units.)

At constant $[I]_0$ the overall \bar{M}_n increased by a factor of 2.2 for a fivefold increase in $[M]_0$, neglecting the small variations in percentage conversion after 24 hr. However, this was largely attributed to an increase in the proportion, rather than the molecular weight, of the high molecular weight material. Similarly, at constant $[M]_0$ the overall \bar{M}_n only varied with $[I]_0$ by virtue of the variation in relative amounts of the high polymer and oligomer. Polymerization temperature had virtually no effect on the overall molecular size distributions.

Addition of further monomer after 24 hr to a polymerizing mixture at high conversion did not affect the pale straw color of the heterogeneous system. The added monomer polymerized slowly, but the overall \bar{M}_n was not increased significantly. The high molecular weight distribution broadened, while the oligomer peak remained narrow.

Initiation with the Triethylaluminum–Benzylidene Acetone Complex

The polymerization was also initiated with the triethylaluminum–benzylidene acetone complex. A pale yellow solution of benzylidene acetone in toluene and triethylaluminum solution were premixed to give a deep burgandy red. After 2 hr at 0°C no fading of the color was detected, and the excess monomer was added. The solution turned to the normal yellow produced from the reaction of triethylaluminum with methyl isopropenyl ketone. The subsequent polymerization rate, measured dilatometrically, was approximately 15% slower than for the equivalent system with methyl isopropenyl ketone complex initiation. Infrared absorption spectra of the oligomer indicated the incorporation of aromatic nuclei, however, because of the small effect of the end group in the high molecular weight fraction, no aromatic absorption could be detected.

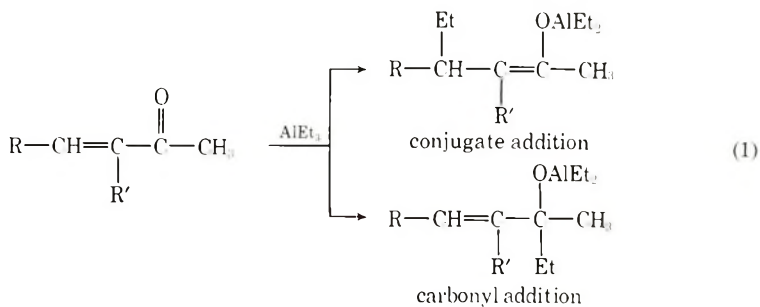
DISCUSSION

The overall and initial rate kinetic data indicate a first-order dependence on monomer and triethylaluminum concentrations. This is consistent with the coordinate mechanism proposed for the polymerization initiated by triethylaluminum.^{1,2} The overall activation energy, 52 ± 3 kJ/mole, is similar to that obtained by Wexler⁴ (54 kJ/mole) for the triethylaluminum-initiated polymerization of methyl methacrylate, in which a coordinate non-free-radical mechanism was also proposed.

Unlike polymerizations in which all the monomer and triethylaluminum were mixed rapidly giving rise to widely differing proportions of active centers, due to side reactions, the premixing technique ensures that a virtually constant proportion of the triethylaluminum is used in the formation of the active centers. The decrease in overall rate constant with increasing monomer concentration, and the small increase in overall rate constant with increasing initiator concentration (Table I) are both indicative of a decreasing production of active centers with increasing $[M]_0/[I]_0$ ratio. This trend is an order of magnitude larger when the premixing technique is not employed¹ and suggests that, here, the effect is due to incomplete initiator formation prior to the addition of further monomer for polymerization. The reappearance of the yellow color upon addition of monomer to the preformed initiator complex is in accord with this postulate.

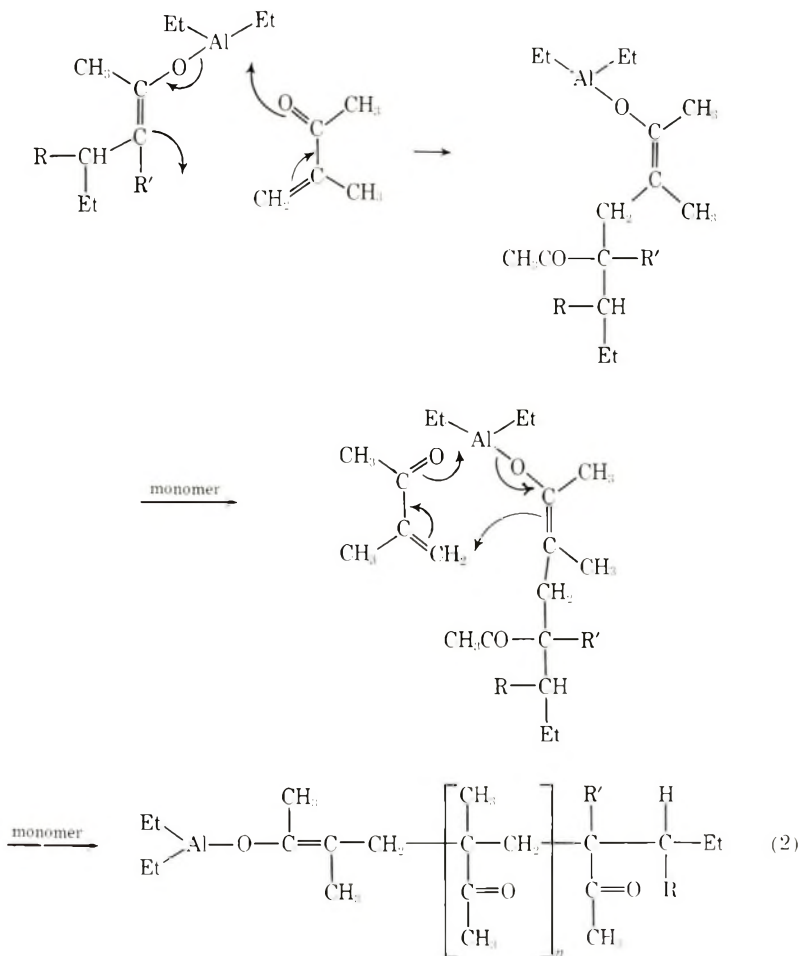
Initiation with benzylidene acetone and triethylaluminum gives rise to a different proportion of active centers compared to premixing with methyl isopropenyl ketone. This probably accounts for the slightly slower polymerization rate.

Baba⁵ reports that at room temperature the major product for benzylidene acetone is the carbonyl adduct, as we have shown for methyl isopropenyl ketone at room temperature.⁶ However, a high proportion of the conjugate adduct is produced at lower temperatures.⁷ The conjugate adduct acts as the active center in the generalized polymerization scheme [eqs. (2)].



R = C₆H₅; R' = H; benzylidene acetone
 R = H, R' = CH₃; methyl isopropenyl ketone

Molecular weights and molecular weight distributions are consistent with the previously proposed pseudotermination process for the trimer, and for a chain-transfer step with a low rate constant.¹



Kinetic Scheme

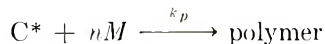
A kinetic scheme can be written.

Initiation:



where C* denotes active centers and X denotes inactive centers.

Propagation:



$$\ln [M]_0/[M] = k_p[\text{C}^*]t$$

Since graphs of $\ln [M]_0/[M]$ versus t are linear, the reaction is first-order with respect to monomer, and $[\text{C}^*]$ is constant within a given polymerization. As it is not possible to estimate the proportion of active centers, the absolute value of the propagation rate constant cannot be determined. However, the average value of $k_p x$, where x is the fraction of triethylaluminum giving rise to active centers is given by eq. (3):

$$k_p x = 1.7 \times 10^{-2} \text{ l./mole-min at } 0^\circ\text{C, } x = [\text{C}^*]/[\text{I}]_0$$

(calculated from initial rate data) (3)

CONCLUSIONS

The kinetics of the triethylaluminum–methyl isopropenyl ketone complex-initiated polymerization of methyl isopropenyl ketone indicate a first-order dependence on both monomer and initiator concentrations. The activation energy for the polymerization, over the temperature range 0–25°C, is 52 ± 3 kJ/mole, consistent with a coordinate mechanism. Molecular size distributions of the polymeric products are bimodal. Initiation with the triethylaluminum–benzylidene acetone complex produces poly(methyl isopropenyl ketone) with aromatic groups incorporated in the oligomer.

The authors wish to thank Professor M. C. R. Symons (University of Leicester) for helpful advice and discussions.

References

1. A. R. Lyons and E. Catterall, *Europ. Polym. J.*, in press.
2. A. R. Lyons and E. Catterall, *Europ. Polym. J.*, in press.
3. A. R. Lyons and E. Catterall, paper presented at IUPAC Symposium on Macromolecular Chemistry, Budapest, 1969, paper 3/04.
4. H. Wexler and J. A. Manson, *J. Polym. Sci. A*, **3**, 2903 (1965).
5. Y. Baba, *Bull. Chem. Soc. Japan*, **41**, 928 (1968).
6. A. R. Lyons and E. Catterall, *J. Organometal. Chem.*, **25**, 351 (1970).
7. S. Patai and Z. Rappoport, *The Chemistry of the Alkenes*, S. Patai, Ed., Interscience, New York–London, 1964, p. 501.

Received November 17, 1970

Revised December 29, 1970

Soluble Imide-Quinoxaline Copolymers

JOSEPH M. AUGL and JAMES V. DUFFY,

U.S. Naval Ordnance Laboratory, White Oak, Silver Spring, Maryland 20910

Synopsis

Eight new phenylated imide-quinoxaline ordered copolymers were prepared. The synthesis consisted of one-step solution condensations of aromatic bis(*o*-diamines) with *N,N'*-bis(benzilyl)benzophenoneimide and *N,N'*-bis(benzilyl)tetrahydrofuranimide respectively. The polymers were all of high molecular weight and were soluble in a number of different solvents. Thermal gravimetric analysis showed that the aromatic benzophenoneimide-quinoxalines (decomposing between 490 and 530°C) were considerably more stable than the aliphatic tetrahydrofuranimide-quinoxalines (decomposing between 290 and 320°C). All polymers gave tough films which could be cast from solution.

INTRODUCTION

The syntheses of polyquinoxalines,¹⁻¹⁰ polyphenylquinoxalines,¹¹⁻¹⁵ and polyimides¹⁶⁻¹⁹ have been reported by a number of investigators. The phenylated polyquinoxalines have thermal and oxidative stabilities comparable to the aromatic polyimides. Most aromatic polyimides, however, are intractable in their final state and can be processed only through their soluble amic-acid prepolymers, while the phenylated polyquinoxalines have good solubility in a number of phenolic and halogenated solvents.

In a previous publication²⁰ it was shown that soluble, ordered imide-quinoxaline copolymers of high molecular weight were obtained by reacting bisbenzilylpyromellitimide with aromatic tetraamines. Since one of the monomers contained preformed imide rings, it was possible to obtain the final copolymers in a one-step reaction without preparing the poly(amic acid) intermediate. Since the stability of the quinoxaline moiety is of the same magnitude as the best aromatic imides, no loss in thermal and oxidative stability of these copolymers is evident. It was anticipated that this synthetic route should easily lead to other soluble polyimides, and, in the following, a comparison is made between polymers containing an aliphatic (tetrahydrofuran) and an aromatic (benzophenone) imide moiety.

EXPERIMENTAL

Monomers

***N,N'*-Bis(4-benzilyl)-3,3',4,4'-benzophenonetetracarboxylimide (IX).** A mixture of 4 g of 4-aminobenzil,²⁰ 2.87 g of 3,3',4,4'-benzophenone-tetracarboxylic dianhydride, and 50 ml of dimethylacetamide was stirred

under nitrogen for 16 hr at room temperature. At this point, 8 ml of acetic anhydride and 2 ml of pyridine were added, and the mixture was then refluxed for 8 hr. After the first 5 hr of reflux, 2 ml more of pyridine were added. A light yellow solid precipitated, which was filtered and washed with a 1:1 mixture of hexane-acetone. The yield was 4.0 g (63%); mp 281°C.

N,N'-Bis(4-benzilyl)tetrahydrofurantetracarboxylimide (X). A mixture of 4.0 g of 4-aminobenzil, 1.89 g of tetrahydrofurantetracarboxylic dianhydride, and 50 ml of dimethylacetamide was stirred under nitrogen for 16 hr at room temperature; 8 ml of acetic anhydride and 2 ml of pyridine were then added, and the temperature was maintained between 75–80°C for 4 hr. After cooling, the solution was poured into 400 ml of water to give a bright lemon-yellow solid. The yield was 2 g; mp 280°C.

The elemental analyses of compounds IX and X are given in Table I.

TABLE I
Elemental Analyses of Monomers and Model Compounds

Compound	Mp, °C	Formula	Elemental analyses					
			Calculated			Found		
			C, %	H, %	N, %	C, %	H, %	N, %
IX	281	C ₄₃ H ₂₄ O ₉ N ₂	73.37	3.28	3.80	73.39	3.37	3.82
X	280	C ₃₆ H ₂₂ O ₉ N ₂	69.01	3.54	4.47	69.03	3.53	4.37
XI	345	C ₅₇ H ₃₂ O ₅ N ₆	77.72	3.66	9.54	77.59	3.72	9.16
XII	377	C ₄₈ H ₃₀ O ₅ N ₆	74.80	3.92	10.90	74.63	3.96	10.73

(dec.)

Model Compounds

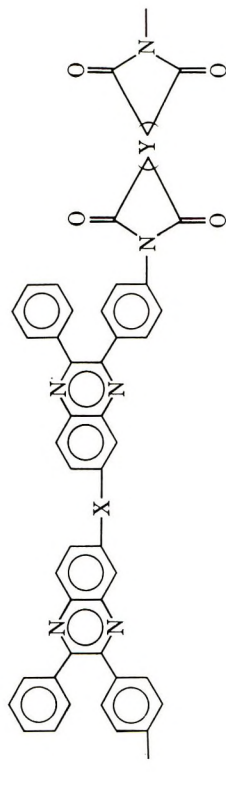
N,N'-Bis{1,4-[2-(3-Phenylquinoxaliny)]phenylene}benzophenonetetracarboxylimide (XI). A stirred mixture of 0.1081 g (0.001 mole) of *o*-phenylenediamine, 0.3683 g (0.0005 mole) of *N,N'*-bis(4-benzilyl)benzophenonetetracarboxylimide, and 19 ml of *m*-cresol was kept under nitrogen first for 3 hr at 100°C and then for 3 hr at reflux. Addition of methanol gave a white precipitate which was filtered and washed with acetone. The yield was 0.3 g (75%); mp 345°C.

N,N' - Bis{1,4 - [2 - (3 - phenylquinoxaliny)]phenylene} tetrahydrofuran-tetracarboxylimide (XII). This compound was prepared by reacting *N,N'*-bis(4-benzilyl)-tetrahydrofurantetracarboxylimide with *o*-phenylenediamine in a molar ratio of 1:2 under similar conditions as described for compound XI.

The elemental analyses for compounds XI and XII are given in Table I.

Polymer Synthesis

The polymers were prepared by the following general procedure. A three-necked flask fitted with stirrer, nitrogen inlet, and reflux condenser

TABLE II
 Characterization of Imide-Quinoxaline Copolymers


Polymer	X	Y	Inherent viscosity, dl/g ^a	T_g^b , °C ^b	PDT, °C ^c	Elemental analyses, Found (calcd) ^d		
						C, %	H, %	N, %
I	Nil		1.54	260	530	77.67 (77.90)	3.58 (3.44)	9.33 (9.56)
II	CO	"	0.78	255	525	75.85 (76.81)	3.32 (3.33)	9.10 (9.27)
III	SO ₂	"	0.62	240	490	72.57 (72.60)	3.20 (3.21)	8.69 (8.91)
IV	O	"	1.09	254	515	75.60 (76.50)	3.98 (3.38)	9.01 (9.39)
V	Nil		2.07	230	290	72.00 (74.99)	3.45 (3.67)	9.51 (10.93)
VI	CO	"	1.02	255	310	72.55 (73.86)	3.66 (3.54)	9.69 (10.55)
VII	SO ₂	"	1.24	---	300	68.95 (69.22)	3.59 (3.39)	9.75 (10.09)
VIII	O	"	2.11	(310) ^e	320	71.26 (73.46)	3.92 (3.60)	10.71 (9.90)

^a Determined in *m*-cresol at 30°C (0.5 g in 100 ml).

^b Measured by dielectric loss as a function of temperature at a heating rate of 5°C/min.

^c Polymer decomposition temperature (PDT) determined from TGA data in a vacuum at a heating rate of 5°C/min.

^d Calculated values are shown in parenthesis.

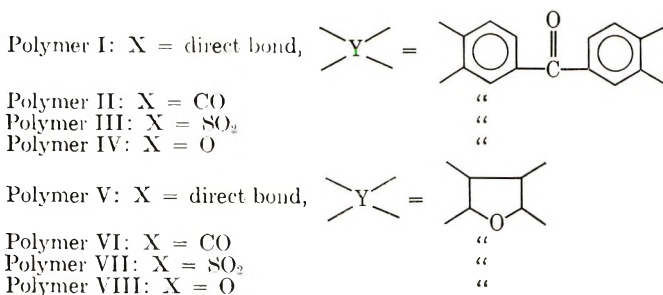
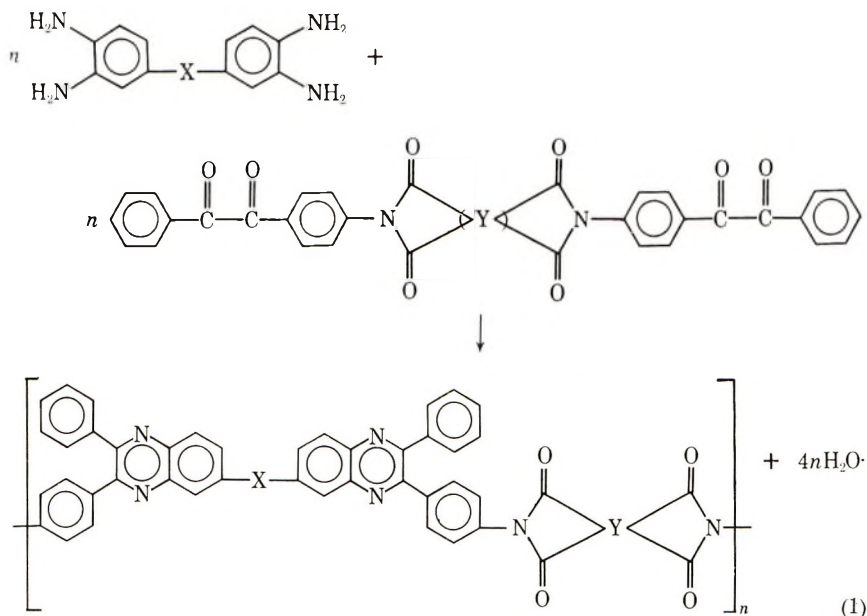
^e This T_g value is perhaps not reliable since at this temperature thermal decomposition may have started.

was charged with equimolar amounts of bisbenzilylimides IX or X and the aromatic tetraamine. Freshly distilled *m*-cresol was added to give an approximately 10% polymer solution. Nitrogen was slowly passed through the flask while the stirred mixture was kept at 90–100°C for 3 hr. Finally the solution was refluxed for 20 min to remove the water formed during the reaction. The polymers were precipitated by slowly pouring the polymer solution into strongly stirred methanol in a Waring Blender. All polymers were of high molecular weight and formed tough films. The properties of the polymers are given in Table II.

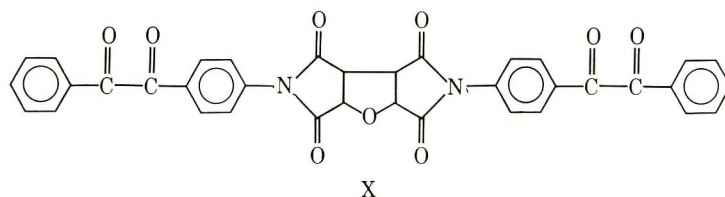
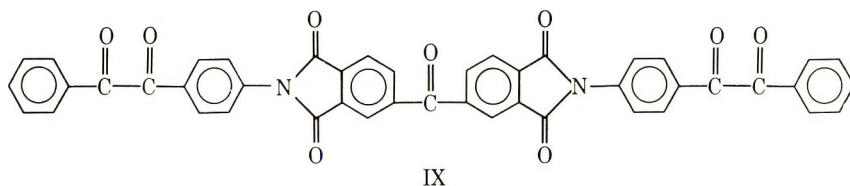
RESULTS AND DISCUSSION

Synthesis

Eight new ordered imide-quinoxaline copolymers were synthesized by a one-step solution condensation of aromatic bis(*o*-diamines) with *N,N'*-bis(benzilyl)imides [eq. (1)].



The two monomers *N,N'*-bis(4-benzyl)benzophenonetetracarboxylimide (IX) and *N,N'*-bis(4-benzyl)tetrahydrofuran-tetracarboxylimide (X) were prepared by reacting 4-aminobenzil²⁰ with 3,3',4,4'-benzophenonetetracarboxylic dianhydride and tetrahydrofuran-tetracarboxylic dianhydride.



The polymerization was carried out in *m*-cresol at temperatures between 90 and 100°C. All polymers were of high molecular weight, as indicated by their inherent viscosities, which ranged from 0.6 to 2.1 dl/g (Table I).

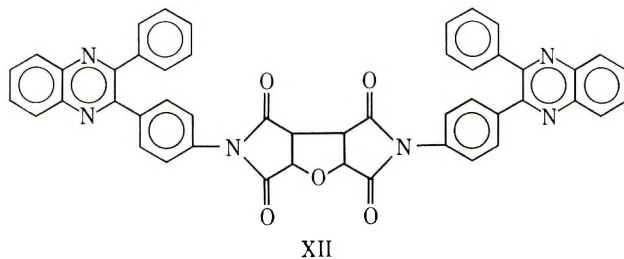
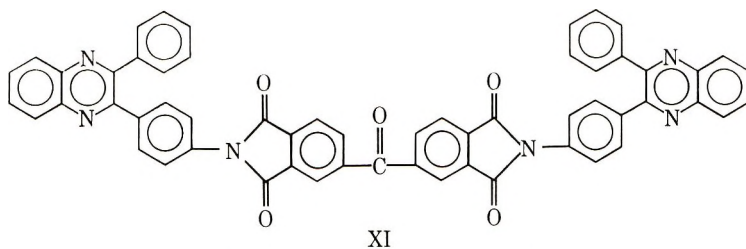
Several other solvents have been found to dissolve the polymers. Table III lists a number of solvents that dissolve some or all of the polymers at room temperature over a period of 24 hr without continued agitation.

Two models, XI and XII, were prepared by condensation of *o*-phenylenediamine with compounds IX and X, respectively, under conditions similar to those used for the polymerization.

TABLE III
Solubilities of Imide-Quinoxaline Copolymers

Solvent	Solubility ^a							
	Poly-	Poly-	Poly-	Poly-	Poly-	Poly-	Poly-	Poly-
	mer	mer	mer	mer	mer	mer	mer	mer
	I	II	III	IV	V	VI	VII	VIII
<i>m</i> -Cresol	+	+	+	+	+	+	+	+
<i>m</i> -Methoxyphenol	+	+	+	+	+	+	+	-
Tetrachloroethane	+	+	+	+	-	+	+	-
Chloroform	-	+	+	+	-	-	+	-
Dimethylacetamide	-	-	+	+	-	+	-	+
<i>N</i> -Methylpyrrolidone	-	+	+	+	+	+	+	+
Hexafluoroacetone	+	+	+	+	+	+	+	+
Hexafluoroisopropanol	+	+	+	+	+	+	+	+
Nitrobenzene	-	+	+	-	-	+	+	+
Pyridine	-	+	+	+	-	+	+	+
Sulfuric acid	+	+	+	+	+	+	+	+

^a The solubilities were qualitatively determined by letting the polymers dissolve at room temperature without continued mechanical agitation: (+) soluble; (-) insoluble.



The syntheses of other models concerning the quinoxaline moiety in the polymer chain have been reported previously.^{15,20} All absorptions found in the infra-red spectra of the polymers could be accounted for from the spectra of the models.

Thermal Properties

Thermogravimetric analysis (TGA) was performed on powdered samples of the polymers. The decomposition was carried out by using an Ainsworth vacuum balance programmed at a heating rate of 5°/min. The polymer decomposition temperature (PDT) is defined as the intersection of the

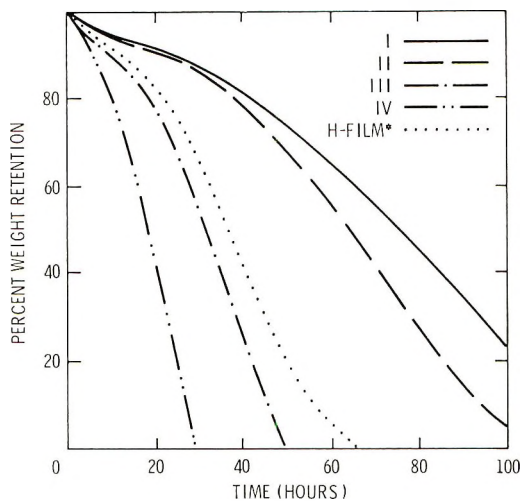


Fig. 1. Isothermal weight loss of polybenzophenoneimide-quinoxalines at 400°C in static air.

100% weight retention line with a line drawn tangent to the TGA curve at the first decomposition maximum.

As expected, the aromatic benzophenonetetracarboxylimide-quinoxalines (I-IV) are considerably more stable (PDT = 490–530°C) than their aliphatic tetrahydrofuranimide-quinoxaline analogs (V-VIII) which decompose at 290–320°C (Table II).

Isothermal weight loss measurements were carried out on powdered samples at 400°C in static air. To keep errors at a minimum in comparing oxidative stabilities of the polymers, all samples were placed simultaneously into a muffle furnace lined with aluminum foil. H-film [poly-*N,N'*-(4,4'-oxydiphenyl)-pyromellitimide] was included for comparison. Under these particular isothermal weight loss conditions (400°C, static air), the measurements show that the oxygen link in the chain decreases oxidative stability as compared to carbonyl, sulfonyl or direct carbon-carbon linkages. This observation was confirmed in our earlier work.^{15,20–22}

The weight loss curves of polymers I-IV are shown in Figure 1. The stability of H-film lies somewhere between polymer II and III. As anticipated, the aliphatic tetrahydrofuranimide-quinoxaline copolymers (V-VIII) have a very short lifetime at 400°C. They showed 100% weight loss in less than 20 hr.

Glass transition temperatures T_g were obtained from thin films by means of dielectric loss measurements in an apparatus described previously²¹ (Table II).

The validity of the T_g values of polymers V-VIII is uncertain, since the measurement temperature approaches their decomposition temperatures and part of the dielectric loss may be due to onset of decomposition.

The copolymer effect and true linearity of the polymers account for the lower T_g values as compared to pure polyimides.

CONCLUSIONS

Aromatic imide-quinoxaline ordered copolymers show good thermal and oxidative stability. They are prepared in a one-step condensation reaction leading to high molecular weight polymers, and due to their solubility in a variety of solvents they are easily processable.

References

1. G. P. de Gaudemaris and B. J. Sillion, *J. Polym. Sci. B*, **2**, 203 (1964).
2. J. K. Stille and J. R. Williamson, *J. Polym. Sci. A*, **2**, 3867 (1964); *J. Polym. Sci. B*, **2**, 209 (1964).
3. G. P. de Gaudemaris, B. J. Sillion, and J. Preve, *Bull. Soc. Chim. France*, **1964**, 1793.
4. P. M. Hergenrother, J. J. Wrasidlo, and H. H. Levine, Narmco Research and Development Div., "High Temperature Structural Adhesives," Final Summary Report, U. S. Navy Bureau of Naval Weapons Contract NOW 63-0420-c, San Diego, California, April 1964.
5. J. K. Stille, J. R. Williamson, and F. E. Arnold, *J. Polym. Sci. A*, **3**, 1013 (1965).
6. J. K. Stille and F. E. Arnold, *J. Polym. Sci. A-1*, **4**, 551 (1966).

7. J. K. Stille and E. Mainen, *J. Polym. Sci. B*, **4**, 39 (1966); *ibid.*, **5**, 665 (1967).
8. H. Jadamus, F. De Schryver, W. De Winter, and C. S. Marvel, *J. Polym. Sci. A-1*, **4**, 2831 (1966).
9. F. De Schryver and C. S. Marvel, *J. Polym. Sci. A-1*, **5**, 545 (1967).
10. J. K. Stille and M. E. Freeburger, *J. Polym. Sci. B*, **5**, 989 (1967).
11. P. M. Hergenrother and H. H. Levine, *J. Polym. Sci. A-1*, **5**, 1453 (1967).
12. P. M. Hergenrother, *J. Polym. Sci. A-1*, **6**, 3170 (1968).
13. W. Wrasidlo and J. M. Augl, *J. Polym. Sci. B*, **7**, 281 (1969).
14. W. Wrasidlo and J. M. Augl, *J. Polym. Sci. A-1*, **7**, 3393 (1969).
15. W. Wrasidlo and J. M. Augl, *Macromolecules*, **3**, 544 (1970).
16. E. C. Srogg, in *Macromolecular Chemistry, Prague 1965 (J. Polym. Sci. C, 16)*, O. Wichterle and B. Sedláček, Eds., Interscience, New York, 1967, p. 1191.
17. B. Vollmert, *Kunststoffe*, **56**, 680 (1966).
18. M. M. Coton, N. A. Adrowa, M. I. Bessonow, L. A. Lajus, A. P. Rudakow, and F. S. Florinskij, *Plaste Kautschuk*, **14**, 730 (1967).
19. A. H. Frazer, *High Temperature Resistant Polymers (Polymer Reviews, Vol. 17)*, Interscience, New York, 1968.
20. J. M. Augl, *J. Polym. Sci. A-1*, **8**, 3145 (1970).
21. W. Wrasidlo and J. M. Augl, *J. Polym. Sci. A-1*, **7**, 1589 (1969).
22. W. Wrasidlo and J. M. Augl, paper presented at American Chemical Society Meeting, Sept. 1969; *Polym. Preprints*, **10**, No. 2, 1353 (1969).

Received December 7, 1970

Revised January 8, 1971

Polymerization of Acrylamide and Acrylic Acid Photoinitiated by Diazidotetramminecobalt(III) Azide

H. KOTHANDARAMAN and M. SANTAPPA, *Department of Physical
Chemistry, University of Madras, Madras 25, India*

Synopsis

The kinetics of polymerization of acrylamide and acrylic acid in aqueous solution photoinitiated by the complex, diazidotetramminecobalt(III) was systematically studied at 35°C and pH = 3. Monochromatic radiation at $\lambda = 365, 405, \text{ and } 435 \text{ m}\mu$ was employed. The kinetics of polymerization were followed by measurements of the rates of monomer disappearance (bromometrically) and complex disappearance (spectrophotometrically) and the chainlengths of the polymers formed (viscometrically). The dependences of the rate of polymerization on variables like light intensity, light absorption by the complex, wavelength, monomer concentration, and hydrogen ion concentration were studied. The rates of polymerization of acrylamide and acrylic acid were found to be proportional to the square of the monomer concentration and to the first power of light absorption fraction k_a and light intensity I . A kinetic scheme is proposed in the light of experimental results involving (1) a primary photochemical act of excitation of the complex, followed by the dark reaction of electron transfer within the complex producing the azide radical; (2) initiation of polymerization by the azide radical; (3) termination of the chain process by the complex molecule.

INTRODUCTION

While the photochemistry of coordination compounds was known for a long time, quantitative interpretations are just emerging into view. Cobalt(III) forms a large number of diamagnetic hexacoordinate complexes which have been studied more thoroughly than any other class of coordination compounds.¹ The absorption spectra of complexes of the type $[\text{Co}(\text{NH}_3)_5\text{X}]^{2+}$ correlate well with the oxidizability of the ligand X. The charge transfer bands of the complexes with the easily oxidizable ligands I^- , N_3^- extend far into the visible, and on irradiation around $\lambda = 370 \text{ m}\mu$ redox photolysis occurs exclusively.² Irradiation of the ion-pair $\text{Fe}^{3+} \cdot \text{N}_3^-$ at $\lambda > 300 \text{ m}\mu$ caused electron transfer resulting in ferrous ion and azide radical which resulted in the initiation of polymerization of acrylonitrile, methyl methacrylate and methacrylic acid.³ The photoinitiation of vinyl monomers by azidopentamminecobalt(III) chloride was first reported by Santappa et al.⁴⁻⁶ Delzenne⁷ also observed photopolymerization of acrylamide by chloro- and aquo- pentamminecobalt(III) complexes. Studies on photolytic behavior including photoinitiated polymerization reactions in-

volving tetramminecobalt(III) complexes of the type $[\text{Co}(\text{NH}_3)_4\text{X}_2]^+$ have been few. In this paper we report a systematic kinetic study of polymerization of acrylamide and acrylic acid photosensitized by diazidotetramminecobalt(III)azide in aqueous solution at different wavelengths ($\lambda = 365, 405, \text{ and } 435 \text{ m}\mu$) at $T = 35 \pm 0.1^\circ\text{C}$ with a view to elucidate the nature of the primary process, subsequent dark reactions and initiation and termination of polymerization and to evaluate the various rate parameters.

EXPERIMENTAL

Optical Arrangement

Two types of light sources were used: a high-pressure mercury vapor lamp (250 W; Mazda ME/D box type fitted with glass windows, supplied by B.T.H. Co., U.K.) and a bulb-type ultraviolet lamp (125 W, Mazda MBW/W, also supplied by B.T.H. Co., purity of $365 \text{ m}\mu > 99\%$). The light from the lamp, condensed and rendered parallel by a biconvex lens, was allowed to pass through a series of filter combinations⁸ to isolate the required monochromatic wavelengths. To obtain light of $\lambda = 365 \text{ m}\mu$, the 125 W lamp (Mazda MBW/W) was used without any filters. The reaction cell (4.6 cm light path, 4.6 cm diameter) was a cylindrical vessel (capacity 75 ml) fused at both ends with flat, optically clear, quartz plates and had two outlet tubes of standard B-14 cones for deaeration of the system.

Preparation of the Complex

Diazidotetramminecobalt(III) azide prepared by the method of Linhard and Weigel⁹ was 99% pure as checked by spectrophotometry ($\log \epsilon = 4.15$ at $\lambda = 337 \text{ m}\mu$). The cobalt content of the complex as determined by the method of Schwarzenbach¹⁰ was 23.32% (theoretical 23.36%).

Reagents

Acrylamide (American Cyanamid Co., U.S.A.) recrystallized^{11,12} from warm chloroform solution was a white crystalline solid (mp 84.5°C). Acrylic acid¹³ was twice distilled under reduced pressure in an atmosphere of nitrogen, and the middle cuts (bp $48.5^\circ\text{C}/15 \text{ mm Hg}$) were used. Potassium ferrioxalate used for actinometry was prepared¹⁴ from potassium oxalate and ferric chloride and purified by recrystallization from water. Perchloric acid (E. Merck, G. R., ca. 60% HClO_4) was used to maintain pH. Solvents (methanol, ethanol, chloroform, acetone, etc.) were distilled immediately before use, and middle cuts were used. Nitrogen freed from traces of oxygen by Fieser's solution¹⁵ was passed through to deaerate the reaction system.

Estimations

The purity and concentrations of the monomer were estimated by bromometry.¹⁶ A typical experiment may be described as follows. The reac-

tion mixture containing the diazido complex (2×10^{-5} mole/l.), monomer (0.1 mole/l.), acid (HClO_4 , $\text{pH} \approx 3$), and neutral salt (0.1 mole/l. NaClO_4) was introduced in the reaction cell and deaerated for about 45 min in the dark. The reaction cell was then mounted in a thermostat at $35 \pm 0.01^\circ\text{C}$ (maintained by a toluene regulator and hot-wire vacuum switch relay, Gallenkamp) in the path of the monochromatic light and irradiated for 5–15 min, depending on the type and concentration of monomer. The rate of monomer disappearance was followed by determining the concentration of monomer (bromometrically) in the reaction solution before and after irradiation. The rate of disappearance of the diazido complex was followed by the change in absorbancy of the reaction solution (measured in an ultraviolet spectrophotometer, Hilger & Watts Unispek, H700) after irradiation and reference to a Beer's law calibration curve for the complex at $\lambda = 340 \text{ m}\mu$. The light intensity of the mercury vapor lamp was measured by potassium ferrioxalate actinometry.¹⁴ The polyacrylamide formed was precipitated by the addition of methanol and purified by reprecipitation. The viscosities of solutions of polyacrylamide in sodium nitrate (0.1% polymer in 1M sodium nitrate) were measured in an Ubbelohde viscometer (Polymer Consultants Corporation, U.K.) maintained at $30 \pm 0.01^\circ\text{C}$ in a thermostat for precision viscometry (Krebs Electrical and Manufacturing Co., New York). From the intrinsic viscosities $[\eta]$, the number-average molecular weight of the polymer \bar{M}_n was calculated by using the Mark-Houwink relationship:¹¹

$$[\eta] = 6.8 \times 10^{-4} \bar{M}_n^{0.66}$$

Similarly for poly(acrylic acid)¹² in dioxane at 30°C :

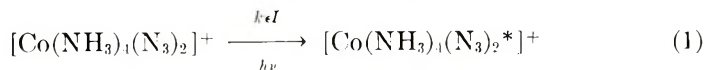
$$[\eta] = 7.4 \times 10^{-4} \bar{M}_n^{0.5}$$

was used.

KINETIC SCHEME

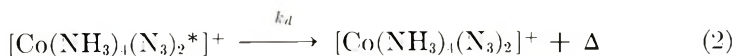
The kinetic scheme shown in eqs. (1)–(7) appears to explain most of the experimental results.

Light Absorption and Excitation of the Complex:



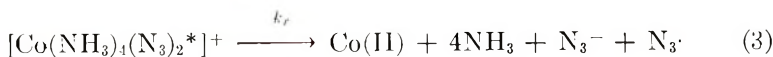
k_e is the light absorption fraction by the complex and I is the light intensity.

Dark Back Reaction:



Deactivation of the excited complex in the dark leads to the complex molecule in the ground state, the excess energy Δ being dissipated in the surrounding medium.

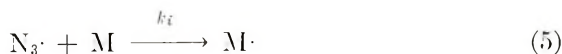
Redox Decomposition of the Excited Complex:



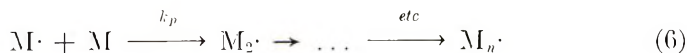
Radical Scavenging by the Complex Molecule:



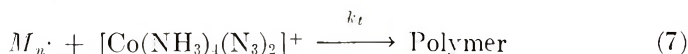
Initiation of Polymerization:



Propagation of Polymerization:



Termination by the Complex:



RESULTS AND DISCUSSION

The polymerization under deaerated conditions was only photochemical in nature, the thermal reaction being absent. The free-radical nature of the process was established by the observation of long induction periods (~ 20 min) in the presence of oxygen. The steady-state maximum rate was observed to be dependent on the type of monomer; monomer concentration, complex concentration, and wavelength of light. For acrylamide, the steady-state maximum rate was attained in about 5 min at $\lambda = 365$ and $435 \text{ m}\mu$, while at $\lambda = 405 \text{ m}\mu$ the time required was 10 min. For acrylic acid the steady-state maximum rate was reached in about 10 min for all the three wavelengths studied, i.e., 365, 405, and $435 \text{ m}\mu$. The percentage of acrylamide polymerization was kept below 35% and that of acrylic acid was below 10%. The conversion of the complex was about 40%. A $\text{pH} \approx 3$ was maintained in all the polymerization experiments to avoid precipitation of cobaltic hydroxide. All the experiments were conducted under deaerated conditions and at constant ionic strength ($\mu = 0.1$). The effects of variation of light absorption fraction, light intensity, monomer concentration, hydrogen ion concentration, wavelength of light, ionic strength, etc., on the measurables, rates of monomer and complex disappearance, chain length of polymer were studied in detail.

Rate of Monomer Disappearance ($-d[\text{M}]/dt$)

On making the usual assumptions for stationary-state kinetics for micro and macro radicals and nonvariation of propagation and termination constants with chain length and on the basis of initiation by azide radicals and termination by the complex:

$$-d[\text{M}]/dt = k_p k_i k_r k_i I [\text{M}]^2 / (k_t [\text{C}]) (k_d + k_r) \{ k_i [\text{M}] + k_2 [\text{C}] \} \quad (8)$$

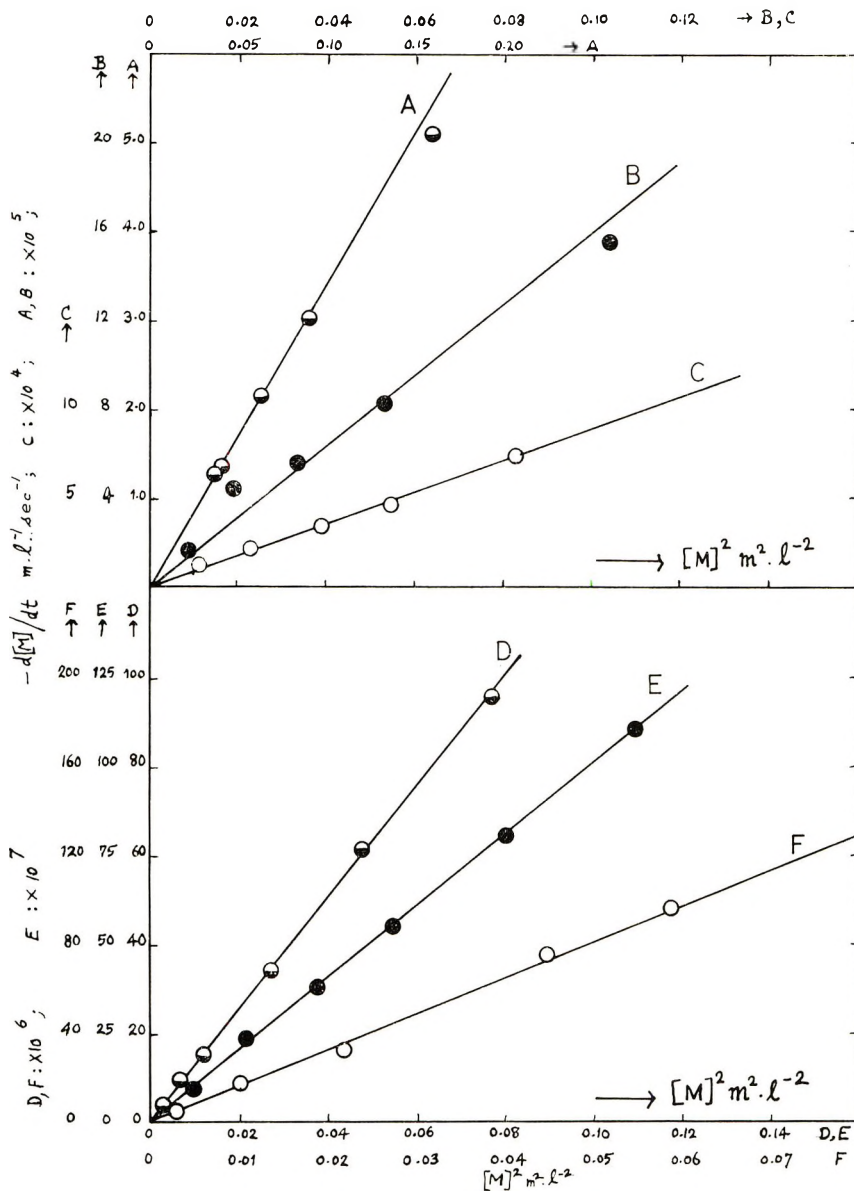


Fig. 1. Plots of $-d[M]/dt$ vs. $[M]^2$: (A) acrylamide, 365 $\mu\mu$; (B) acrylamide, 405 $\mu\mu$; (C) acrylamide, 435 $\mu\mu$; (D) acrylic acid, 365 $\mu\mu$; (E) acrylic acid, 405 $\mu\mu$; (F) acrylic acid, 435 $\mu\mu$.

The rate of monomer disappearance was found to be dependent on the square of the monomer concentration $[M]^2$ (Fig. 1), the first power of the light absorption fraction k_e (Fig. 2) and the first power of light intensity I (Fig. 3) in the case of both acrylamide and acrylic acid polymerizations. These observations support the postulation of termination by the complex.

If termination was by mutual combination the rate of monomer disappearance would have been dependent on $[M]^{3/2}$, $k_t^{1/2}$ and $I^{1/2}$. If termination by azide radicals were considered, the dependence would have been on $[M]^2$ only, k_t and I having no effect. Delzenne⁷ also observed a second-order dependence of the rate of acrylamide polymerization on monomer concentra-

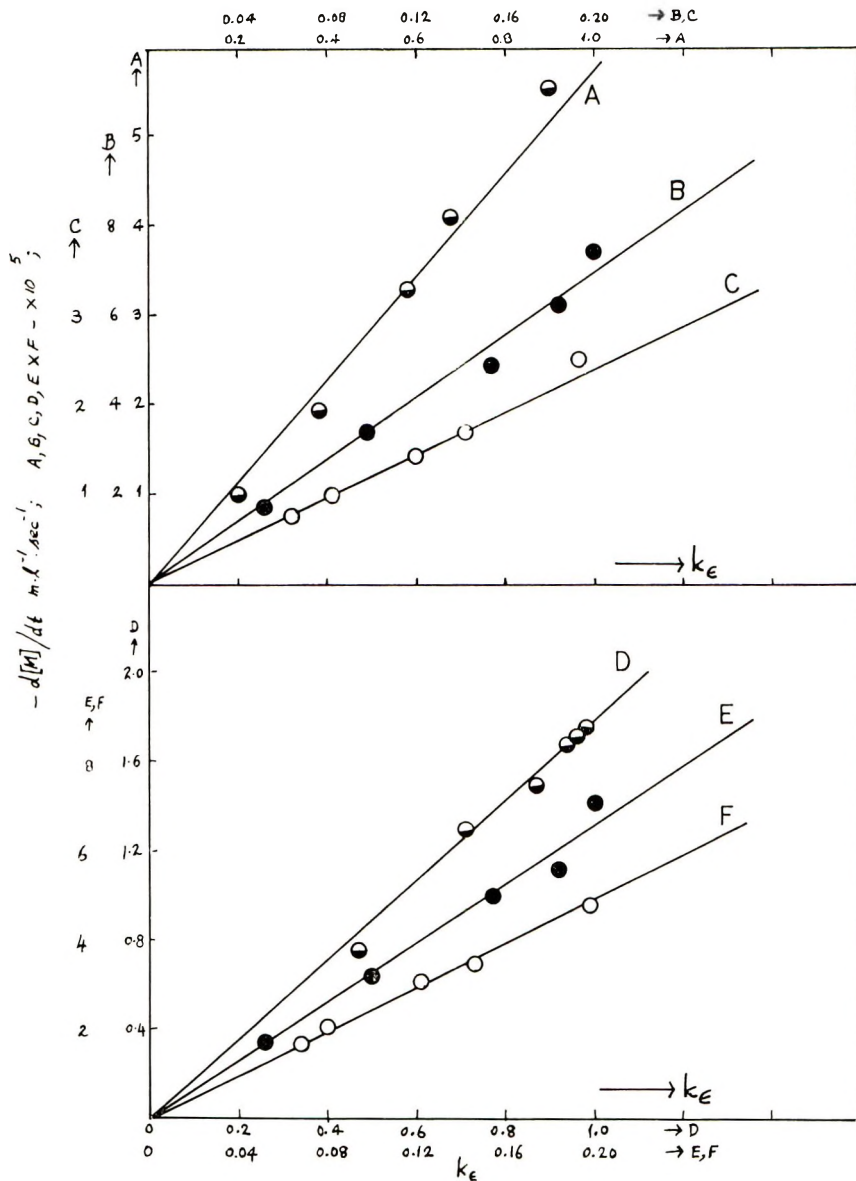


Fig. 2. Plots of $-d[M]/dt$ vs. k_t : (A) acrylamide, 365 μM ; (B) acrylamide, 405 μM ; (C) acrylamide, 435 μM ; (D) acrylic acid, 365 μM ; (E) acrylic acid, 405 μM ; (F) acrylic acid, 435 μM .

tion with aquopentamminecobalt(III) complex as the initiator and explained this on the basis of termination by the latter. Delzenne suggested participation of the monomer in the formation of the initiating radicals through a reversible substitution of the coordinatively bonded water molecule by acrylamide (analogous to the substitution of a ligand by *N*-

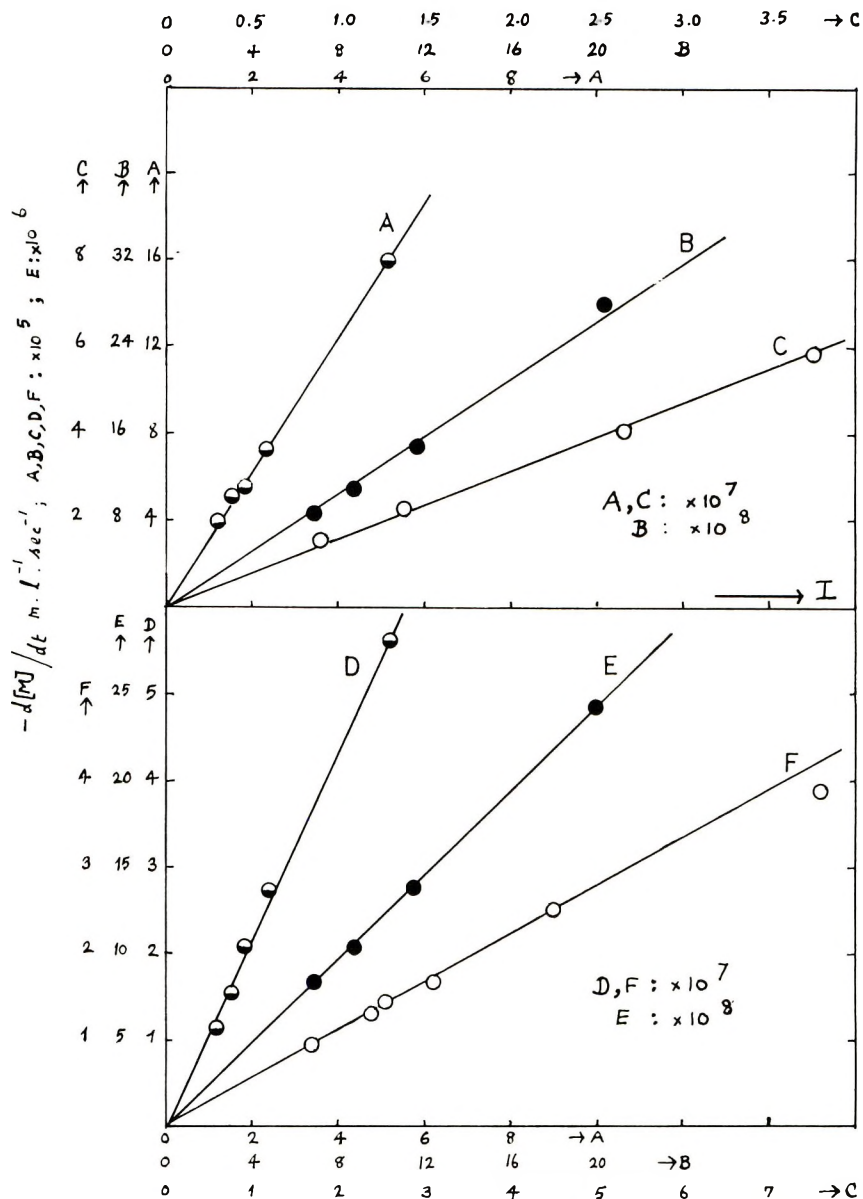
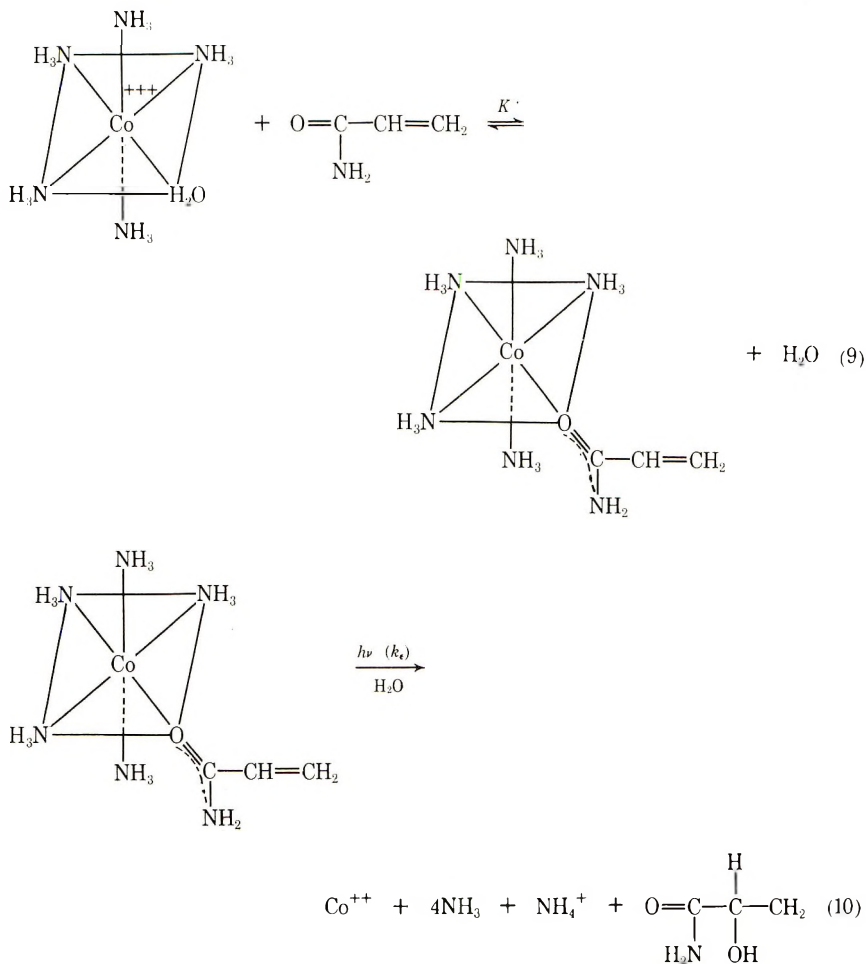


Fig. 3. Plots of $-d[M]/dt$ vs. I : (A) acrylamide, 365 $\mu\mu$; (B) acrylamide, 405 $\mu\mu$; (C) acrylamide, 435 $\mu\mu$; (D) acrylic acid, 365 $\mu\mu$; (E) acrylic acid, 405 $\mu\mu$; (F) acrylic acid, 435 $\mu\mu$.

methylacetamide¹⁷ in $[\text{Co}(\text{en})_2\text{X}_2]\text{X}$ followed by photochemically induced electron transfer within the intermediate complex.



The analogy cited by Delzenne may be somewhat inappropriate. In the case of substitution of H_2O by *N*-methylacetamide in the complex there was a distinct change of color on mixing *N*-methylacetamide and solution of the complex and the shifts in λ_{max} values were also reported. But in the case of the aquopentamminecobalt(III) complex no such color change or change in optical density measurements was reported. Complexation between azidopentamminecobalt(III) complex and acrylamide was discounted by Natarajan and Santappa.⁴ In the case of diazidotetramminecobalt(III) azide also there was no significant change in the spectrum of the complex on addition of acrylamide, the $\log \epsilon$ (4.15) remaining the same at the maxima which proved to a first approximation that no complexation by substitution was involved. By increasing the concentration of chloropentamminecobalt(III) complex (from 5×10^{-4} to 1×10^{-2} mole/l.),

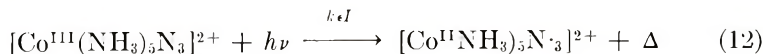
Delzenne⁷ observed a fall from 0.5 for the exponent of the complex concentration in the latter's dependence on the rate of polymerization. Also a decrease in the rate of polymerization with increase in the concentration of the complex was observed, and this was explained by the oxidative termination of polymer radicals by complex molecules. In the present study the rate of acrylamide disappearance increased with the concentration of the complex (1×10^{-5} mole/l.) at first (k_e increasing with [C]), reached a maximum value (at [complex] = 5×10^{-4} mole/l.); then on further increase of complex concentration (up to 2.5×10^{-3} mole/l.) a sharp decrease in rate was observed which may be due to the term [C] in the denominator in (8) becoming significant at high complex concentrations (due to increased termination by the complex). This was similar to the maximum rate observed in the case of the photopolymerization of acrylonitrile^{17,18} in dimethylformamide initiated by FeCl_3 at a concentration of the metal ion of $10^{-3} M$.

Rate of Complex Disappearance ($-d[\text{C}]/dt$)

The expression for the rate of complex disappearance on the basis of initiation by azide radical and termination by the complex molecule would be:

$$-d[\text{C}]/dt = [2k_t/(k_a + k_r)]k_e I \quad (11)$$

The net quantum yield for complex disappearance ϕ_b would be equal to $2k_t/(k_a + k_r)$. The rate of complex disappearance was found to be proportional to the first powers of k_e or [C] (Fig. 4) and I (Fig. 5) and independent of monomer concentration and wavelength for both acrylamide and acrylic acid polymerization. The primary photochemical act we postulate is excitation of the complex. The excited complex can in the dark undergo redox decomposition giving azide radicals or undergo de-excitation. For the photolysis of chloropentamminecobalt(III) complex, Delzenne⁷ had suggested that redox decomposition occurs giving the chlorine radical (the primary photochemical act) in a single step. For the photopolymerization involving aquopentamminecobalt(III) complex, Delzenne suggested complex formation with acrylamide in the dark, which then underwent photo-redox decomposition (which was the primary photochemical act) giving the radical. Natarajan and Santappa⁴ suggested the following primary step for the photolysis of azidopentamminecobalt(III)chloride:



Our suggestion of an excited state prior to the many possible reaction pathways like redox decomposition, deactivation, combination with polymer radicals etc., is supported by the conclusions of Valentine¹⁹ that electronically excited states of moderately long lifetime—able to undergo internal conversion before reactive deactivation—are intermediates in photochemical reactions of most cobalt(III) and other d^6 coordination complexes. He

further concluded that inefficiencies observed in the photoaquation and photoreduction of these systems are the result of competing reactions of their electronically excited states and not of recombination of radicals formed by primary homolytic cobalt-ligand bond fission as proposed by Adamson^{20,21} and Wehry.²²

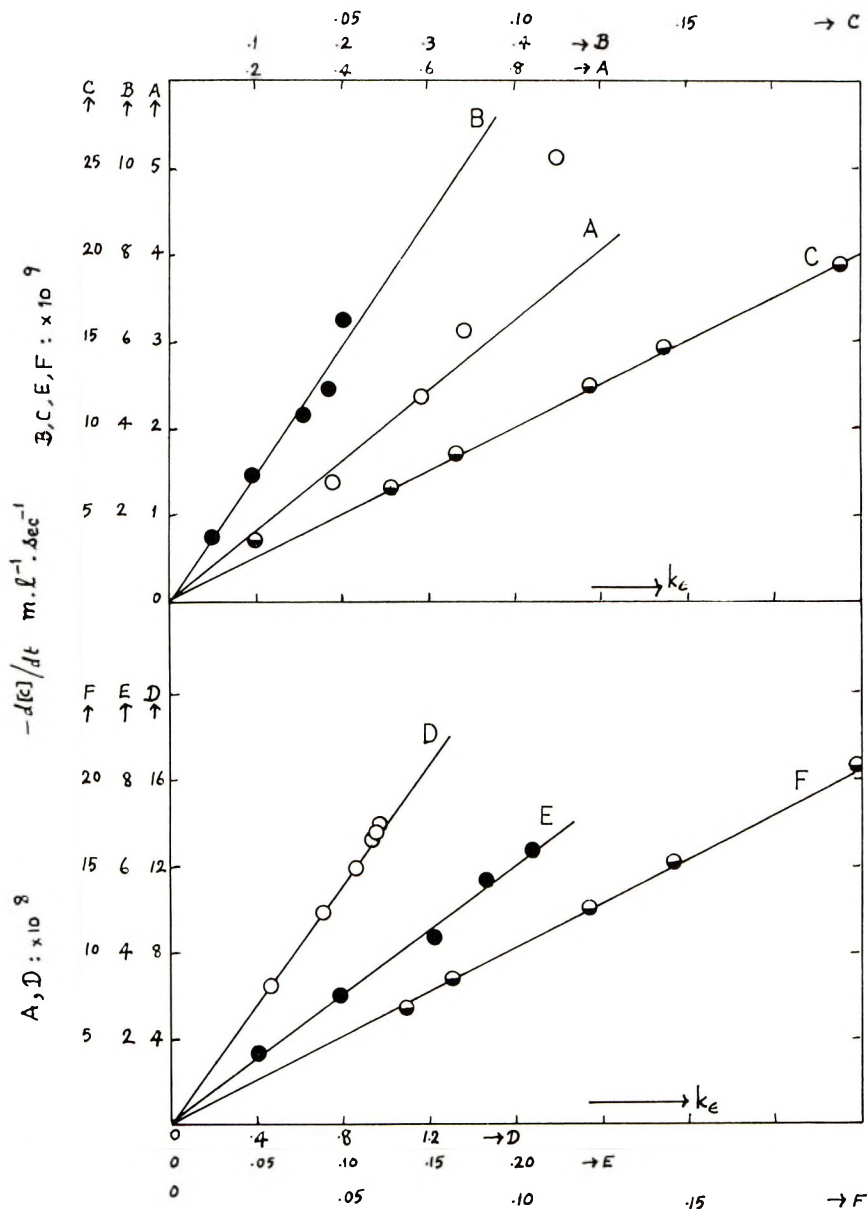


Fig. 4. Plots of $-d[C]/dt$ vs. k_e : (A) acrylamide, 365 $m\mu$; (B) acrylamide, 405 $m\mu$; (C) acrylamide, 435 $m\mu$; (D) acrylic acid, 365 $m\mu$; (E) acrylic acid, 405 $m\mu$; (F) acrylic acid, 435 $m\mu$.

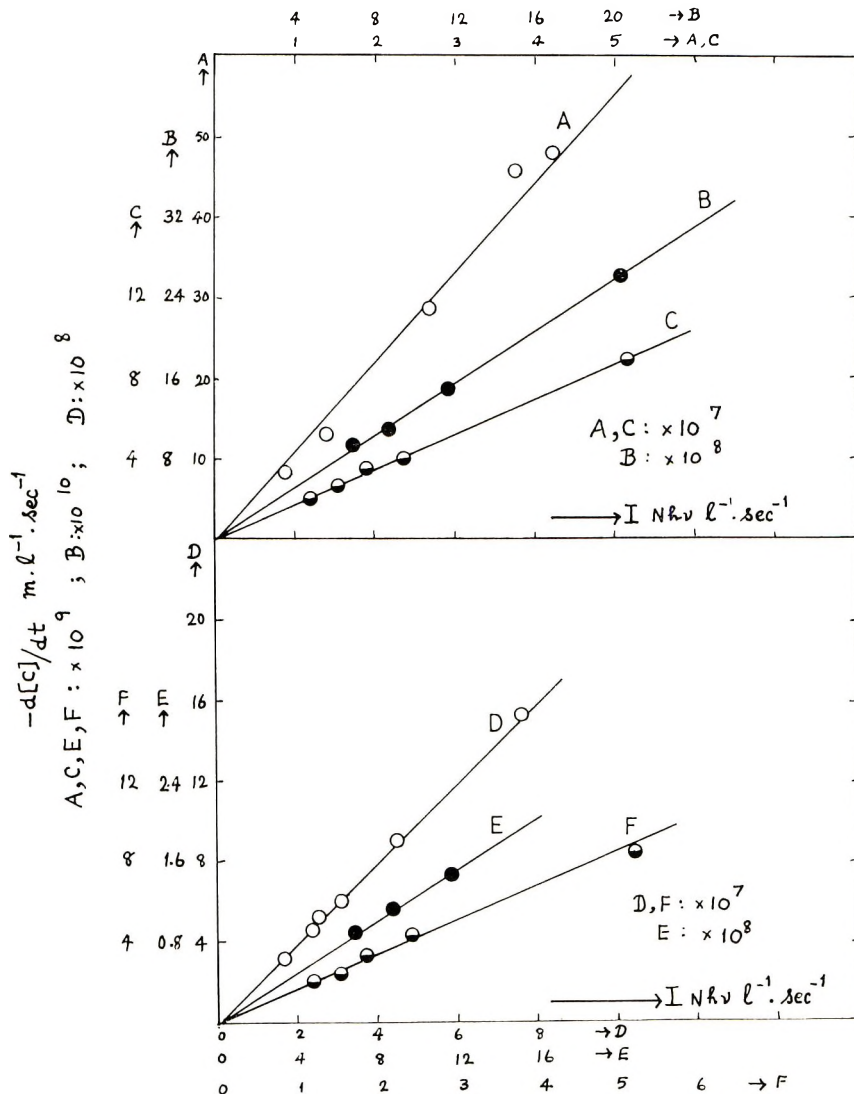


Fig. 5. Plots of $-d[C]/dt$ vs. I : (A) acrylamide, 365 μ ; (B) acrylamide, 405 μ ; (C) acrylamide, 435 μ ; (D) acrylic acid, 365 μ ; (E) acrylic acid, 405 μ ; (F) acrylic acid, 435 μ .

Quantum Yields, ϕ_c

The primary photochemical act is the excitation of the complex molecule followed by the dark reaction, i.e., homolytic fission of the cobalt-azide bond to produce the azide radical. The formation of the azide radical is evident from the evolution of nitrogen observed by us in the absence of any monomer.



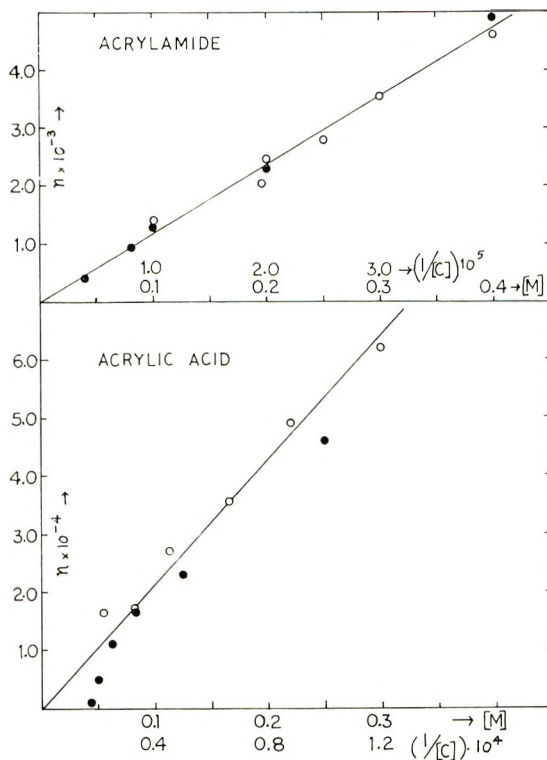


Fig. 6. Plots of chainlength vs. variables at 365 $m\mu$: (O) n vs. $[M]$; (●) n vs. $(1/[C])$.

Quantitative measurements of the nitrogen evolution were made by us²⁴ for the photolysis of azidopentamminecobalt(III)chloride. The decreasing quantum yields with increasing wavelength ($\phi_c = 0.27$ to 0.20; Table I)

TABLE I
Rate Constants

Monomer	Wavelength		k_p/k_t	k_d/k_r	ϕ_c
	λ , $m\mu$				
Acrylamide	365		21.18	6.408	0.27
Acrylic acid	"		28.74	"	"
Acrylamide	405		21.31	8.523	0.21
Acrylic acid	"		28.93	"	"
Acrylamide	435		21.24	9.0	0.20
Acrylic acid	"		28.81	"	"

reveal the operation of the Franck-Rabinowitch²⁴ cage effect in preventing the separation of the fragments with decreasing energy of radiation and that the dark back-reaction (k_d) becomes more and more important while the redox decomposition (k_r) becomes comparably less significant. (Table

I for k_d/k_t) Natarajan and Santappa⁴ reported the value of ϕ_c for azidopentamminecobalt complex to be 0.18 (at $\lambda = 365 \text{ m}\mu$).

Chain Lengths n

On the basis of initiation by the primary radical and termination by the complex, the expression for chain length would be:

$$n = (k_p/k_t)[M]/[C] \quad (14)$$

Chain lengths were found to be proportional to the first power of monomer concentration and inversely to the complex concentration both in the case of acrylamide and acrylic acid polymerizations (Fig. 6). Termination by the azide radical would reveal the chainlengths to be inversely dependent on k_t and I , while termination by mutual combination would require dependence on $[M]^{1/2}$, $k_t^{-1/2}$ and $I^{-1/2}$.

Rate Constants (k_p/k_t)

The rate constants k_p/k_t were evaluated from slopes of the plots of $[M]^2/R_p$ versus $[M]$ and assuming $2k_t/(k_d + k_t) = \phi_c = (-d[C]/dt)/k_t I$. The values were almost constant for different wavelengths studied (Table I). The values of k_p/k_t from Figure 6 involving chainlengths were 21.78 ± 2.0 for acrylamide polymerization and 36.05 ± 4.8 for acrylic acid polymerization, the error limits having been evaluated by the method of least squares. Natarajan and Santappa⁴ reported the values of $k_p/k_t^{1/2} \approx 1.83$ for acrylamide polymerization with azidopentamminecobalt(III)chloride as initiator. Dainton and Tordoff¹¹ reported a value of 4.2 for the hydrogen peroxide photosensitized polymerization of acrylamide. In a subsequent paper, Dainton and Tordoff¹² reported the rate constants for the polymerization of acrylamide photosensitized by ferric ion. For this system they have postulated linear termination by the ferric ion (k_4) and the ferric ion pair (k_5) and $k_p/k_4 \approx 8.0$ and $k_p/k_5 \approx 1.3$ and a comparison of these values with our $k_p/k_t \approx 21$ for the same monomer indicates that diazidotetramminecobalt complex terminates more slowly than Fe^{3+} or $\text{Fe}^{3+} \cdot \text{OH}^-$. The rate constants for acrylic acid polymerization with the use of any type of initiator are being reported for the first time.

We thank Dr. K. Venkatarao, formerly of this laboratory for helpful discussions.

References

1. F. A. Cotton and G. Wilkinson, "Advanced Inorganic Chemistry," 2nd Ed., Interscience, New York, 1965.
2. A. W. Adamson, W. L. Waltz, Q. Zinato, D. W. Watts, F. D. Fleischauer, and R. D. Lindholm, *Chem. Rev.*, **68**, 541 (1968).
3. M. G. Evans, M. Santappa, and N. Uri, *J. Polym. Sci.*, **7**, 243 (1951).
4. L. V. Natarajan and M. Santappa, *J. Polym. Sci. A-1*, **6**, 3245 (1968).
5. L. V. Natarajan and M. Santappa, *J. Polym. Sci. B*, **5**, 357 (1967).
6. M. Santappa and L. V. Natarajan, *Proc. Indian Acad. Sci. A*, **69**, 284 (1969).

7. G. A. Delzenne, in *Macromolecular Chemistry Prague 1965* (*J. Polym. Sci. C*, **16**) O. Wichterle and Q. Sedláček, Eds., Interscience, New York, 1967, p. 1027.
8. E. J. Bowen, *Chemical Aspects of Light*, Oxford Univ. Press, London, 1946, p. 279.
9. M. Linhard, M. Weigel, and M. Flygare, *Z. Anorg. Allgem. Chem.*, **263**, 233 (1951).
10. G. Schwarzenbach, *Complexometric Titrations* (transl. by H. Irving), Methuen London, 1957, p. 78.
11. F. S. Dainton and M. Tordoff, *Trans. Faraday Soc.*, **53**, 499 (1957).
12. F. S. Dainton and M. Tordoff, *Trans. Faraday Soc.*, **53**, 666 (1957).
13. P. J. Flory, S. Newman, W. R. Krigbaum, and C. Laugier, *J. Polym. Sci.*, **14**, 451 (1954).
14. C. A. Parker and C. G. Hatchard, *Proc. Roy. Soc. (London)*, **A235**, 518 (1956).
15. L. F. Fieser, *J. Amer. Chem. Soc.*, **46**, 2639 (1924).
16. G. Mino and S. Kaizermann, *J. Polym. Sci.*, **38**, 393 (1959).
17. W. I. Bengough, S. A. MacIntosh, and I. C. Ross, *Nature*, **200**, 567 (1963).
18. W. I. Bengough and I. C. Ross, *Trans. Faraday Soc.*, **62**, 2251 (1966).
19. D. Valentine, Jr., *Advances in Photochemistry, Vol. 6* (Noyes, Hammond, and Pitto, Eds.), Interscience, New York, 1968, p. 123.
20. A. W. Adamson and A. H. Sporer, *J. Amer. Chem. Soc.*, **80**, 3865 (1958).
21. A. W. Adamson, *Discussions Faraday Soc.*, **29**, 153 (1960).
22. E. L. Wehry, *Quart. Rev.*, **28**, 251 (1967).
23. H. Kothandaraman and M. Santappa, unpublished results.
24. H. Franck and E. Rabinowitch, *Trans. Faraday Soc.*, **30**, 120 (1934).

Received September 21, 1970

Revised November 12, 1970

Polymerization of Aminoalkyl Methacrylates in a Thin Layer in the Presence of Atmospheric Oxygen*

V. I. JELISEJEVA and E. M. MOROZOVA, *Institute of Physical Chemistry, U.S.S.R. Academy of Sciences, Moscow, U.S.S.R.*

Synopsis

Chemically initiated monomer polymerization in a thin layer in air has been studied. Under these conditions the process is intensively inhibited by oxygen. Aminoalkyl methacrylates characterized by low volatility and high reactivity were used as monomers. Conditions ensuring a high degree of conversion, control of the process have been found determined. Monomer structurization by an active filler such as carbon black and redox initiation with peroxides and copper salts were found to be the main factors diminishing the induction period and increasing rate of polymerization of the aminoalkyl methacrylates.

INTRODUCTION

Direct conversion of monomers to polymers is one of the urgent problems of polymer production. The production of coatings in which there is monomer polymerization without solvents is the subject of considerable attention at the present time. However, this problem has been studied inadequately, since the initiation of the process is rather difficult owing to the increased inhibiting action of atmospheric oxygen in a thin layer. Most publications in this field have been devoted to the study of direct film formation from monomers under the action of slow discharge¹⁻³ and electronic beams.^{4,5} These methods involving the use of complex equipment were employed to coat small simple articles with polymeric films.

It seemed plausible to obtain monomer coatings by chemical initiation in air. This would expand the application of the method by avoiding the use of complex equipment.

Coating via chemically initiated polymerization of monomers in air requires the study of kinetics of the process with regard to specificity in polymerization in the bulk, as air may display an inhibiting effect and cause possible oxidation. Since the process may be thought effective only if no monomer is lost, the induction period and the rate of polymerization at moderate temperatures are of prime significance.†

* Paper presented at the International Symposium on Macromolecular Chemistry, Budapest, 1969.

† There is no need to increase temperature under the conditions studied, in view of the greater monomer losses and the need for thermal devices.

The polymerization rate and induction period are influenced by a decrease in activation energy which can be varied by selecting the corresponding air-active initiators, and by the viscosity of the polymerized system hindering the diffusion of oxygen. In the case of polymer coatings, a certain viscosity of the polymerizing system is also necessary to avoid its flow from the bed.

The effects of different initiators, accelerators, and thickening, structuring, and crosslinking agents on the rate of polymerization and induction period were investigated. The polymerization kinetics has been studied for aminoalkyl methacrylates, which are advantageous owing to the presence of amino groups in the polymer for high adhesion of coatings to the surface. Monomers containing amino groups were assumed to participate in the redox initiating systems with peroxides and atmospheric oxygen, decreasing the inhibition effect of the latter.^{6,7} Besides, the low vapor pressure of these monomers decreases their losses during polymerization.

Azobisisobutyronitrile (AIBN), benzoyl peroxide (BP), and *tert*-butyl (TBP) peroxides were used as initiators. AIBN was studied, with consideration of the reported data^{8,9} concerning the optimal initiating effect of azo compounds on aminoalkyl methacrylate polymerization. Peroxide initiation was studied because the peroxides may react with given monomers in the redox initiating systems which are of special interest: the activation energy of initiation is low, and thus a fast polymerization is possible at moderate temperatures. The effect of transition metal and its salts on the redox system in aminoalkyl methacrylate polymerization initiated by peroxides was also studied. Use was made of copper and copper stearate.

EXPERIMENTAL

Reagents

The monomers were free from inhibitors by double distillation under low pressures. Their characteristics are given in Table I.

The following initiators and accelerators of polymerization were investigated: benzoyl peroxide (BP) and azobisisobutyronitrile (AIBN), doubly recrystallized; *tert*-butyl peroxide (TBP), distilled under low pressure; copper stearate (CS), analyzed as chemically pure; copper in the form of finely dispersed powder or copper foil turnings.

Acrylic telomer (molecular weight 3000) was used as a thickening agent. Triethanolamine trimethacrylate (TMTEA) was employed as a cross-linking reagent; its properties are given in Table I. Pure acetylene black with a surface of 99 m²/g was used as an active filler.

Kinetic Investigations

The polymerization kinetics was studied by the thermometrical method in view of its applicability to any degree of conversion. A special apparatus¹⁰ was designed for studying polymerization. It is shown schematically in Figure 1. This apparatus is a duplex compensation calorimeter with

TABLE I
Characteristics of Monomers

Monomer	Symbol	Structural formula	Bp, °C/mm Hg	n_D^{20}	d_4^{20} , g/cc
β -Diethyl-aminoethyl methacrylate	DEAMA	$\begin{array}{c} \text{CH}_3 \\ \\ \text{CH}_2=\text{C}-\text{COOCH}_2\text{CH}_2\text{N}(\text{C}_2\text{H}_5)_2 \\ \\ \text{CH}_3 \end{array}$	89/9	1.4445	0.9206
β -(N-piperidyl)ethyl methacrylate	PEMA	$\begin{array}{c} \text{CH}_2 \\ / \quad \backslash \\ \text{CH}_2-\text{CH}_2 \\ \quad \quad \\ \text{CH}_2-\text{CH}_2 \end{array}$ $\begin{array}{c} \text{CH}_2 \\ \\ \text{CH}_2=\text{C}-\text{COOCH}_2\text{CH}_2\text{N} \\ \\ \text{CH}_2-\text{CH}_2 \end{array}$	112/6	1.4692	0.9806
Triethanolamine trimethacrylate	TMTEA	$\begin{array}{c} \text{CH}_3 \\ \\ (\text{CH}_2=\text{C}-\text{COOCH}_2\text{CH}_2)_3\text{N} \end{array}$	170/0.7	1.4782	1.0762

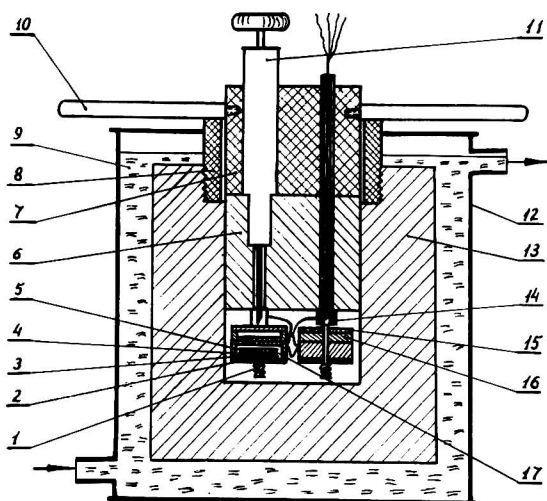


Fig. 1. Schematic view of the calometric apparatus for studying kinetics of polymerization in a thin layer: (1) spring; (2) cap of thermobattery; (3) body of thermobattery; (4) electric heater; (5) thermocouple; (6, 7) cap of calorimeter, (8) bushing; (9) heat carrier; (10) handle; (11) microsyringe; (12) vessel; (13) calorimeter walls; (14) heat insulator, (15) cell cap; (16) cell; (17) thermocouple.

continuous automatic recording of the heat liberated in the course of polymerization. The sensitivity was not less than 5×10^{-5} joule/sec.

The thickness of monomer layer in the reaction cell varied in the range 50–100 μ . The accuracy was $\pm 5\%$.

Investigation of kinetics by the apparatus described was carried out as follows: 0.05–0.1 g of monomer was placed into the cell; when the pre-set temperature was stable, an exact amount of an initiator dissolved in benzene was injected into the cell with a microsyringe.

The time dependence of the rate of heat liberation recorded by the apparatus was data obtained; the conversion, the polymerization rate, and the induction period were calculated from these data.

The activation energy for monomer polymerization was calculated from the plot of the logarithm of rate of heat liberation versus reciprocal temperature.

RESULTS AND DISCUSSION

The values of activation energy for polymerization of aminoalkyl methacrylates with various initiating systems are given in Table II.

Table II shows that initiation by the azo compounds recommended in the literature for aminoalkyl methacrylate polymerization in bulk^{8,9} leads to polymerization in a thin layer in air with a high activation energy, and thus polymerization with such initiators cannot be conducted below 50°C.¹¹ It also follows from Table II that PEMA polymerization initiated by peroxides (BP and TBP) occurs at a low activation energy (9–10 kcal/-

TABLE II
Activation Energy for Polymerization of Aminoalkyl
Methacrylates with Various Initiators

Monomer	Initiator	Activation energy, kcal/mole
PEMA	Azobisisobutyronitrile (0.5 mole-%)	19.6
PEMA	Benzoyl peroxide (0.5 mole-%)	9.0
PEMA	<i>Tert</i> -Butyl peroxide (0.5 mole-%)	10.2
PEMA	Azobisisobutyronitrile (0.5 mole-%) and copper	13.9
PEMA	Copper	14.5
PEMA	Copper stearate (0.3%)	14.3
DEAMA	Azobisisobutyronitrile (0.5 mole-%)	21

mole). This indicates a redox mechanism of the initiation. The mechanism is confirmed by the absence of active thermal decomposition of TBP at 25–80°C. Thus its initiating effect can be explained solely by its participation in the redox process.

The data in Table II show that both metallic copper and copper stearate exert a considerable effect on the course of PEMA polymerization in a thin layer in air, thus reducing the activation energy. Figure 2 show kinetic curves of polymerization of PEMA at 43°C in the presence of copper, copper stearate, or no admixtures; the accelerating effect of copper is evident even in the absence of initiators. The copper seems to affect the redox processes which initiate the polymerization catalytically. It may be suggested that in this case the atmospheric oxygen plays the part of oxidizers when aminoalkyl methacrylates are polymerized in the absence of the peroxides.

TABLE III
Induction Periods for PEMA Polymerization

Initiator	Temperature, °C	Additive	Induction period, min
Benzoyl peroxide (0.5 mole %)	36	—	19
"	43	—	14
"	58	—	10
"	65	—	4
None	43	—	100
"	"	Metallic copper	45
"	"	Copper stearate (0.3%)	7.5

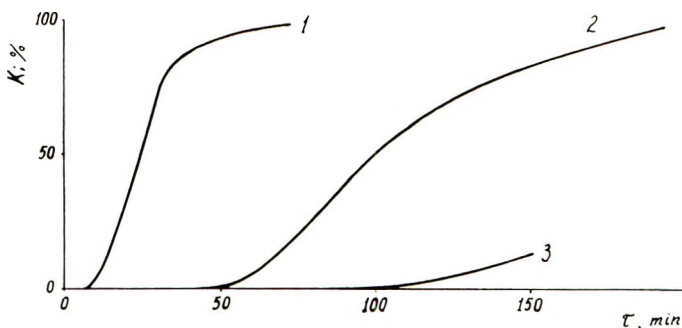


Fig. 2. Kinetics of PEMA polymerization at 43°C: (1) with copper stearate; (2) with metallic copper; (3) without additives.

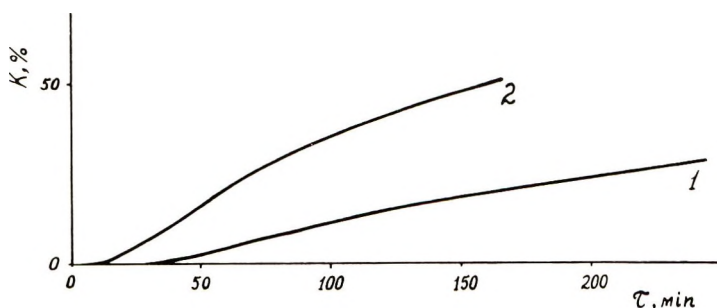


Fig. 3. Kinetics of PEMA polymerization at 36°C with BP in the presence of TMTEA: (1) 0% TMTEA; (2) 5.3% TMTEA.

Despite the low activation energy, polymerization of aminoalkyl methacrylates was not observed at room temperature for the initiators studied; this was attributed to the strong inhibiting effect of oxygen on polymerization in a thin layer. The values for induction periods of PEMA polymerization in the presence or absence of BP are shown in Table III.

To carry out the process at a room temperature, the redox treatment may be applied to the system whose viscosity was increased by the structurization, which would protect the polymerizing layer from the action of oxygen. The structurization of the polymerizing system can be attained by chemical and physicochemical techniques, i.e., by addition of a multifunctional copolymerizing monomer or of an active filler inducing the formation of a thixotropic system.

A multifunctional amino-containing monomer, TMTEA, was used for structurization of the system by formation of chemical bonds. Experiments have shown that addition of TMTEA to PEMA decreases the inhibiting action of atmospheric oxygen. This can be seen from the kinetic curves in Figure 3. This effect seems to be accounted for by an increase in viscosity of the system due to the fact that the three-dimensional structure forms as soon as the polymerization has begun. Thus, introduction of TMTEA has a positive effect essentially during the earlier steps of the

TABLE IV
Effect of TMTEA Addition on the Induction
Period for PEMA Polymerization with BP

Temperature, °C	TMTEA % based on PEMA	Induction period, min
36	0	19
36	5	15
43	0	14
43	5	11

TABLE V
Effect of Carbon Black on the Induction Period of
PEMA Polymerization at 28°C

Initiator ^a	Carbon black, % based on PEMA	Induction period, min
Benzoyl peroxide	0	No polymerization
Benzoyl peroxide and copper stearate	0	65
Benzoyl peroxide	10	6
Benzoyl peroxide and copper stearate	10	2

^a Benzoyl peroxide was 0.5 mole-% based on monomer; copper stearate was 0.3%.

polymerization, but it affects the induction period just slightly as may be seen from Table IV.

Introduction of an active filler, such as acetylene carbon black with a surface of 99 m²/g, had a great effect on the polymerization of aminoalkyl methacrylate. As shown by experiments, introduction of 10% carbon black results in formation of a thixotropic system. The effect of carbon black on the induction period is illustrated by Table V.

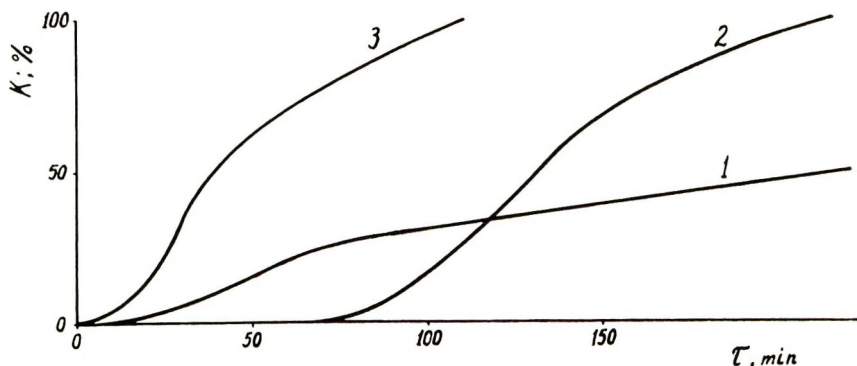


Fig. 4. Kinetics of PEMA polymerization at 28°C with benzoyl peroxide as initiator: (1) with carbon black; (2) with copper stearate; (3) with carbon black and copper stearate.

The observed effect of carbon black seems to be accounted for by its structurizing effect on the monomer owing to intermolecular forces. This would decrease oxygen diffusion into the monomer layer, thus reducing the induction period and favoring an increase in the polymerization rate at small conversions (Fig. 4). It follows from Table V and Figure 4 that the effect of carbon black on the rate of PEMA polymerization is particularly marked in the presence of copper stearate. A system consisting of the amino-containing monomer, the structurizing agent, benzoyl peroxide, and copper stearate is completely polymerized without monomer losses in 30–40 min at room temperature.

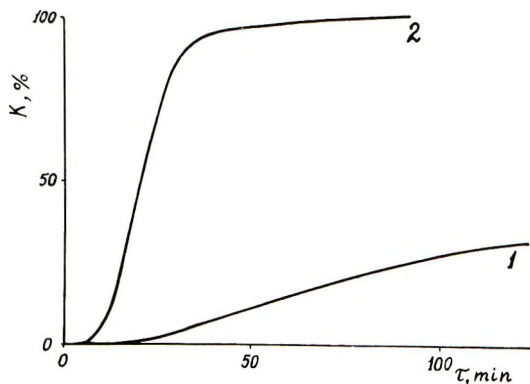


Fig. 5. Kinetics of PEMA polymerization at 43°C with benzoyl peroxide as initiator, acrylic telomer added: (1) 0% acrylic telomer; (2) 10.5% acrylic telomer.

The induction period may be affected considerably by a polymeric thickening agent which raises the viscosity of the system. An acrylic telomer (molecular weight, 3000) was used. When the telomer was introduced into PEMA in a concentration of 10.5%, the induction period dropped from 14 min to 4 min at 43°C (Fig. 5). It may be suggested that this effect, the same as in the case of carbon black, is accounted for by decrease in diffusion of atmospheric oxygen to the monomer layer because of the increase in the viscosity of the layer.

CONCLUSION

The results presented in this paper allow us to propose that two conditions must be fulfilled for the chemically initiated polymerization of monomers at moderate temperature in a thin layer in air: the polymerization activation energy should be lowered by use of redox initiating systems while the polymerizing layer should be made more viscous to prevent the diffusion of oxygen. The most logical method of thickening appears to be the introduction of an active filler into the monomer.

References

1. L. Morris, *Industrie-Lackier-Betrieb*, **36**, No. 4, 143 (1968).
2. T. Williams and M. W. Hayes, *Nature*, **216**, 614 (1967).
3. L. S. Tusov, A. B. Gil'man, A. N. Shurov, and V. M. Kolotyркин, *Vysokomol. Soedin. A*, **9**, 2414 (1967).
4. W. Brenner and W. Oliver, *SPE J.*, **23**, No. 4, 33 (1967).
5. F. L. Dalton, *Surface Coat*, **3**, No. 7-8, 193, 240 (1967).
6. S. D. Stavrova, G. V. Peregodov, and M. F. Margaritova, *Dokl. Akad. Nauk SSSR*, **157**, 636 (1964).
7. S. N. Trubitsyna, M. F. Margaritova, and S. S. Medvedev, *Vysokomol. Soedin.*, **7**, 1973 (1965).
8. P. Longi, E. Pellino, F. Greco, and R. Mazzocchi, *Chim. Ind. (Milan)*, **46**, 156 (1964).
9. H. Sims, P. L. Benneville, and A. J. Kreyge, *J. Org. Chem.*, **22**, 787 (1957).
10. E. M. Morozova, A. S. Morozov, and V. I. Jelisejeva, *Zh. Fiz. Khim.*, **42**, 297 (1968).
11. Kh. S. Bagdasaryan, *Theory of Radical Polymerization*, Nauka, Moscow, 1966 (in Russian).

Received May 15, 1970

Revised August 7, 1970

Electroinitiated Polymerization of Vinylic Monomers in Polar Systems. I. Contribution of the Electrolysis of Methanol to Free-Radical Polymerization

M. ALBECK, M. KÖNIGSBUCH, and J. RELIS, *Chemistry Department, Bar-Ilan University, Ramat-Gan, Israel*

Synopsis

Electrolytic polymerization of acrylates and methacrylates in methanol solution containing lithium acetate as electrolyte was investigated under currents ranging from 10 to 100 mA. Polymer yield increases up to a limiting current value, beyond which it decreases. This abnormal behavior is discussed. A free-radical mechanism is suggested.

INTRODUCTION

Polymerization initiated by electrolysis has been reported by some investigators.¹⁻⁶ It is accomplished in solutions containing a monomer and an electrolyte dissolved in a suitable polar solvent. Upon passing a direct electric current through such a solution, polymerization is initiated. The polymer yield is usually linearly dependent on the current employed. The mechanism may be free-radical, anionic, or cationic, depending on the solvents and the salts employed.

Methanol is generally used to precipitate the polymer obtained and as a polymerization suppressor. In this work the electroinitiation of polymerization of acrylates and methacrylates in methanol solution is discussed. This system behaved differently from those previously mentioned in that the polymer yield was not simply related to the electrolytic current. For this reason voltage-current measurements were conducted in order to clarify the polymerization mechanism. These measurements, together with conclusions based upon them, are presented in this paper.

EXPERIMENTAL

Materials

Methanol (Frutarom Lab. Chemicals, Israel) analytical grade was kept over Mg for 24 hr and then distilled. Only the middle fraction was used, bp 65°C.

The monomers (Fluka, Swiss) were washed with 5% NaOH and then with 5% H₃PO₄. They were dried under anhydrous Na₂SO₄ (24 hr) and

distilled under reduced pressure (1 mm Hg). The middle fraction was used. They were stored at -30°C .

Lithium acetate (Schuchardt, Munich), analytical grade, was used without further treatment.

Polymerization by Electrolysis at Constant Current

Electrolysis was performed in solution of the monomer in a polarizing solvent. Lithium acetate in methanol was employed for this purpose. The monomer was mixed with this solution in a 1:1 ratio.

A 30-ml portion of the mixture was electrolyzed between two flat carbon electrodes of surface area 24.3 cm^2 , held 0.5 cm apart by Teflon spacers. The cell was thermostatted at $40.0 \pm 0.1^{\circ}\text{C}$.

The electrolysis was conducted at constant current provided by a Kepco potentiostat Model HB 525M (General Electric Co. U.S.A.) in constant current mode. The polarity of the electrodes was periodically (5 min) reversed, as this was found to result in more highly reproducible yields by clearing the surface of the electrodes from polymer deposit.

After 18 hr of electrolysis the polymer was precipitated by further dilution with methanol, washed and dried *in vacuo* at 50°C .

Voltage-Current Measurements

The voltage between the electrodes in the cell (E_c) was measured at a number of current values by increasing the current stepwise from 5 mA to 100 mA. The conductivity of each monomer mixture was measured with the same electrodes previously described, and the cell resistance was calculated.

The measured cell voltage is the sum of two potentials: (1) the IR-(current-resistance) potential drop and (2) the electrode reaction potential (E_r).

The E_c was measured 1 min after switching on the electrolysis current. The specific electrode reaction potentials were found by subtracting the IR-(current-resistance) gradient from these values. The data are given in Tables I and II.

Polarography

Under polarographic conditions, a direct relationship between current and electrode reaction potential exists. A dropping mercury electrode was employed as indicator electrode and a graphite one served as a reference electrode. The temperature was 27°C . The voltage was scanned from 0 to 5 V (with reference to the graphite electrode) by use of an Electroscan 30 polarograph (Beckman Co., U.S.A.). Before starting the polarographic measurements, the solution was purged with dry hydrogen until no oxygen reduction wave was observed. The ratio of methanol to monomer was 10:1.

TABLE I
Potential-Current Data of Solutions of Acrylates at 40°C

Current, mA	Methyl acrylate, $\Omega = 8.2$ ohm			Ethyl acrylate, $\Omega = 8.85$ ohm			Butyl acrylate, $\Omega = 10.0$ ohm		
	E_c, V	IR, V	E_n, V	E_c, V	IR, V	E_n, V	E_c, V	IR, V	E_n, V
2	—	—	—	—	—	—	1.63	0.03	1.60
3	—	—	—	1.38	0.03	1.35	1.86	0.03	1.83
4	1.70	0.040	1.66	1.73	0.04	1.69	1.95	0.04	1.91
5	1.91	0.040	1.87	—	—	—	2.00	0.05	1.95
6	—	—	—	1.89	0.05	1.84	—	—	—
10	2.40	0.083	2.32	2.17	0.09	2.08	2.50	0.10	2.40
15	2.72	0.130	2.59	2.47	0.13	2.34	2.83	0.15	2.68
20	2.90	0.166	2.73	2.77	0.18	2.59	3.11	0.20	2.91
30	3.08	0.249	2.83	3.07	0.27	2.80	3.32	0.30	3.02
40	3.20	0.332	2.87	3.22	0.35	2.87	3.51	0.40	3.11
50	3.30	0.410	2.89	3.36	0.44	2.92	3.68	0.50	3.18
60	3.42	0.50	2.92	3.51	0.53	2.98	3.85	0.60	3.25
70	3.53	0.58	2.95	3.62	0.62	3.00	4.05	0.70	3.35
80	3.65	0.66	2.99	3.75	0.71	3.04	4.24	0.80	3.44
90	3.76	0.75	3.01	3.88	0.80	3.08	4.43	0.90	3.53
100	3.88	0.83	3.05	4.01	0.89	3.11	4.63	1.00	3.63

TABLE II
Potential-Current Data of Solutions of Methacrylates at 40°C

Current, mA	Methyl methacrylate, $\Omega = 8.2$ ohm			Ethyl methacrylate, $\Omega = 10$ ohm			Butyl methacrylate, $\Omega = 10.5$ ohm		
	E_0, V	IR, V	E_T, V	E_0, V	IR, V	E_T, V	E_0, V	IR, V	E_T, V
3	—	—	—	1.41	0.03	1.38	—	—	—
5	1.70	0.04	1.64	1.61	0.05	1.56	1.81	0.05	1.76
10	2.05	0.08	1.93	1.99	0.10	1.89	2.12	0.11	2.01
15	2.50	0.12	2.38	2.55	0.15	2.40	—	—	—
20	2.91	0.16	2.75	2.90	0.20	2.70	2.70	0.21	2.49
30	3.10	0.25	2.85	3.10	0.30	2.80	3.07	0.31	2.76
40	3.23	0.33	2.90	3.26	0.40	2.86	3.30	0.42	2.88
50	3.38	0.41	2.97	3.40	0.50	2.90	3.42	0.53	2.89
60	3.49	0.49	3.00	3.55	0.60	2.95	3.57	0.63	2.94
70	3.59	0.58	3.01	3.70	0.70	3.00	3.72	0.74	2.98
80	3.70	0.66	3.04	3.80	0.80	3.00	3.86	0.84	3.02
90	3.80	0.74	3.06	3.90	0.90	3.00	4.00	0.95	3.05
100	3.89	0.82	3.07	4.01	1.00	3.01	4.13	1.05	3.08

Variation of H₂ Volume with Current

The hydrogen evolved in the electrolysis of a methanol-lithium-acetate solution at currents between 10 and 100 mA, in the procedure described, was collected and measured in a gas buret.

The volume of hydrogen which evolved during a minute at each given current strength, was calculated from the experimental results.

pH Measurements

For pH measurements the two graphite electrodes were dipped into a methanol-lithium acetate solution. Glass and calomel electrodes were so inserted that the glass electrode was fixed near one of the graphite electrodes. By reversing the polarity of the electric field between the graphite electrodes, the glass electrode indicated the pH at the anode or cathode as a function of current.

RESULTS AND DISCUSSION

Experimental studies showed¹⁻⁶ a direct proportionality between current and polymer yield in electroinitiated polymerization. But the decrease in yield exhibited above certain current values in our work, requires explanation. The graphs in Figures 1 and 2 illustrate that the polymer yield increases with current rising to a definite value, beyond which further current increase causes decreased yields. For acrylates this maximum is between 20 and 40 mA, whereas for methacrylates it occurs in the 55-65 mA range.

An anionic mechanism may be excluded *prima facie* because of the methanol solvent used. Funt and Bhadani⁴ found that methanol is a chain-stopping agent in anionic polymerizations. They conducted polymerizations on a styrene solution containing 0.493*M* methanol and employed a 100 mA current. Although, in the presence of methanol no polymer was produced even after a period of 4 hr, conversion of greater than 60% was obtained in the absence of methanol under otherwise identical conditions.

A free-radical mechanism for the polymerizations may be tested by adding a free radical quencher and noting the effect produced by a current, which would in the absence of quencher give an optimum polymer yield.

We added *p*-benzoquinone to an ethyl acrylate solution and passed a 50 mA current for 18 hr. The conversion for this time was 3.6%, as compared to 40% conversion achieved under identical experimental conditions without *p*-benzoquinone (see Fig. 1). When oxygen was bubbled through the mixture and a current applied, the polymer yield decreased to 9% of the amount obtained at conditions where no oxygen was present. Also, when LiNO₃ was used as electrolyte, the yield was very low. (The polarographic measurements with this electrolyte showed the presence of oxygen). It is thus evident that in our system the polymerization is initiated by free radicals. These radicals are, in fact, Li atoms, formed at the cathode by electrolysis, in the reaction



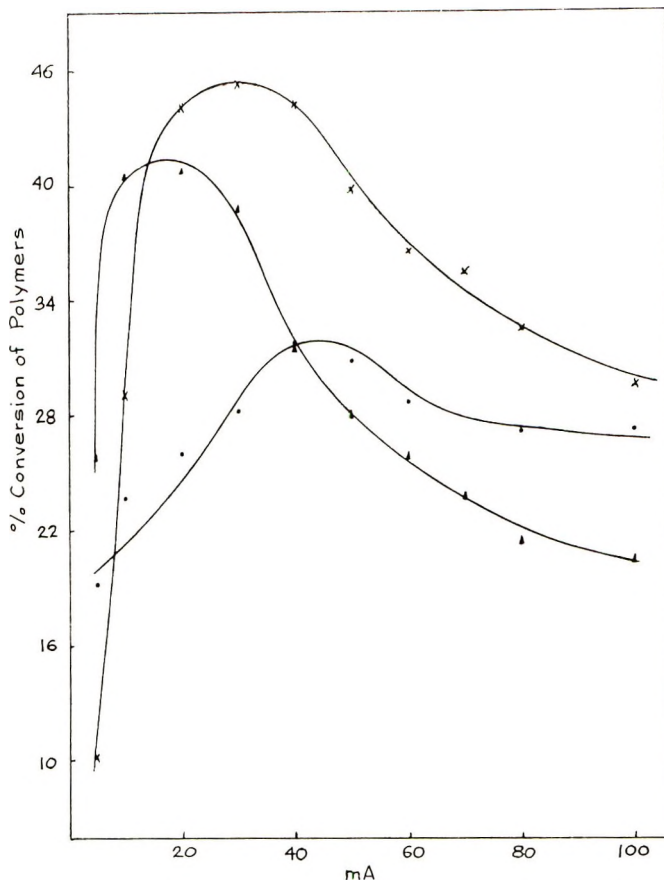


Fig. 1. Conversion of acrylates as a function of current: (▲) butyl acrylate; (×) ethyl acrylate; (●) methyl acrylate. Temperature $40.0 \pm 0.1^\circ\text{C}$.

The decrease in yield, occurring after a certain current value is exceeded, should be the result of the production of a free radical suppressor by the electrolysis process.

In polarography of a methanol-lithium acetate solution, two waves develop. The first wave, which begins at -1.95 V , shows the reduction of Li^+ ions. After this, at about -3 V , the solvent begins to decompose and there is a steep rise of the current. Since there are no other species in the solution which can undergo reduction at this potential, we assume that this wave is due to the decomposition of the solvent, reduction at the cathode and oxidation at the anode [see eqs. (1)-(7)]. This decomposition potential is about 50-100 mV lower for a mixture containing a monomer. Data of these potentials are given in Table III. Thus, two concurrent reactions occur, from which the first extends through the whole potential range investigated, while the second begins only at -3 V . The first wave exhibits a low current due to the low lithium concentration ($0.05M$), while the

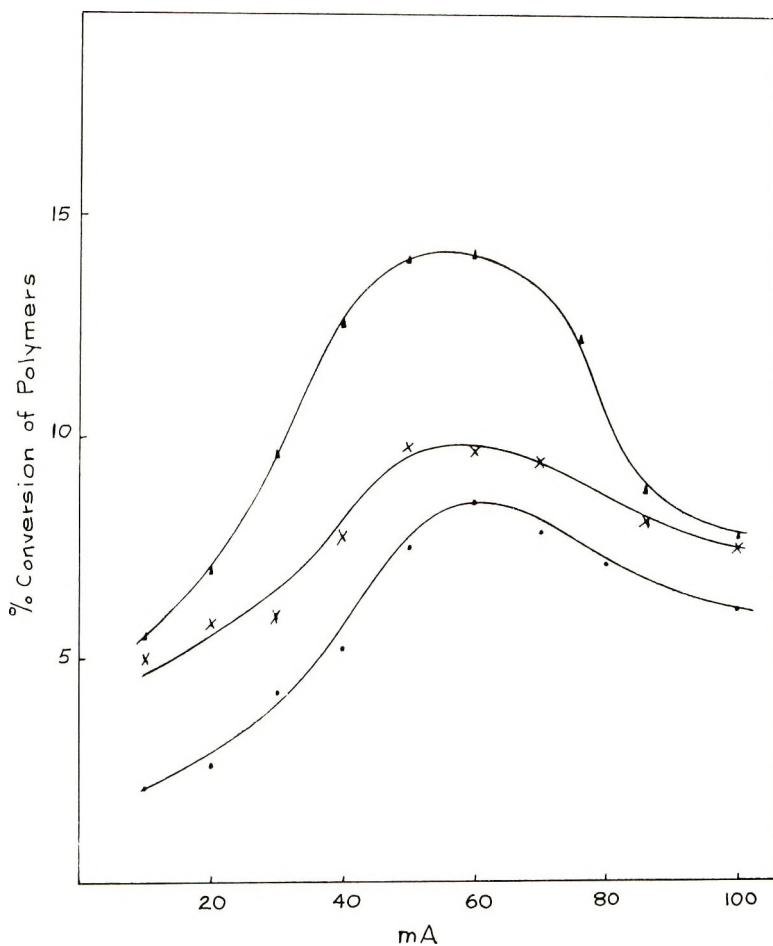
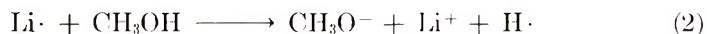


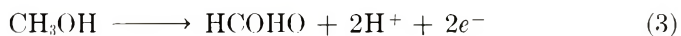
Fig. 2. Conversion of methacrylates as a function of current: (▲) butyl methacrylate; (×) ethyl methacrylate; (●) methyl methacrylate. Temperature $40.0 \pm 0.1^\circ\text{C}$.

second is of high current due to the high solvent concentration ($15M$). The reactions at the electrode may be as shown in eqs. (1)–(7):

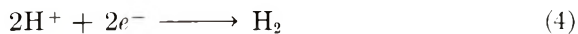
At the cathode:



At the anode:



At the cathode:



At the anode:

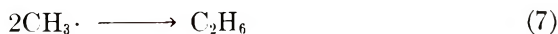


TABLE III
Reduction Potentials of Acrylate and Methacrylate Solutions Obtained by Polarography^a

Solvent	Monomer	First reduction potential, V	Second reduction potential, V
Methanol	—	-2.05	-3.30
"	MMA	-1.93	-3.00
"	EtMA	-1.90	-2.95
"	BuMA	-1.95	-2.95
"	MAc	-1.85	-2.85
"	EtAc	-1.85	-2.85
"	BuAc	-1.90	-2.93

^a Ratio of methanol to monomer = 10:1; 27°C.

CO₂ was not found (by GLC on silica gel column with a standard CO₂ as a reference) after polymerization, thus it may be assumed that, at the current densities employed, reactions (5), (6), and (7) do not take place. H₂ was evolved at the cathode throughout the polymerization, while formal-

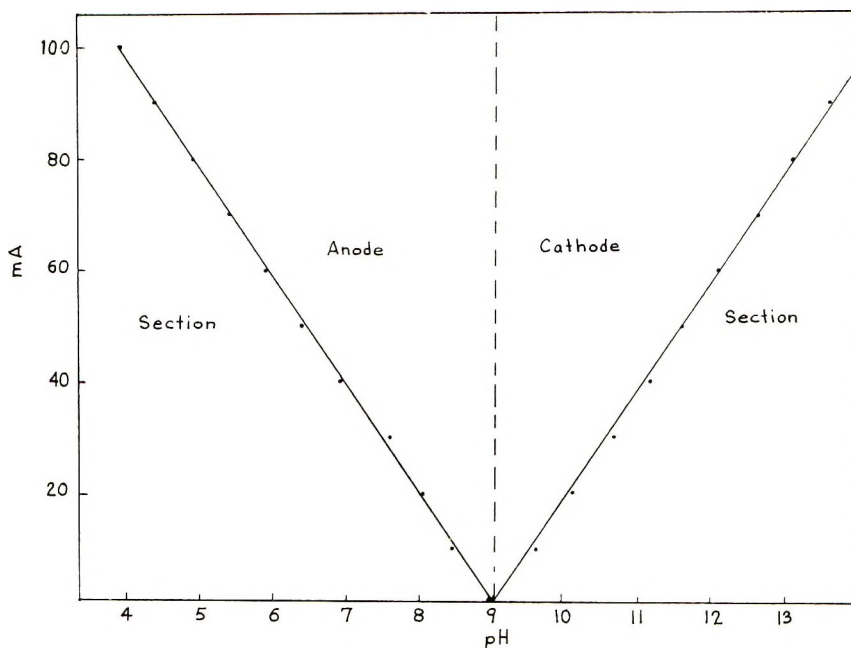


Fig. 3. Variation of pH with current in the anode and cathode sections, 27°C.

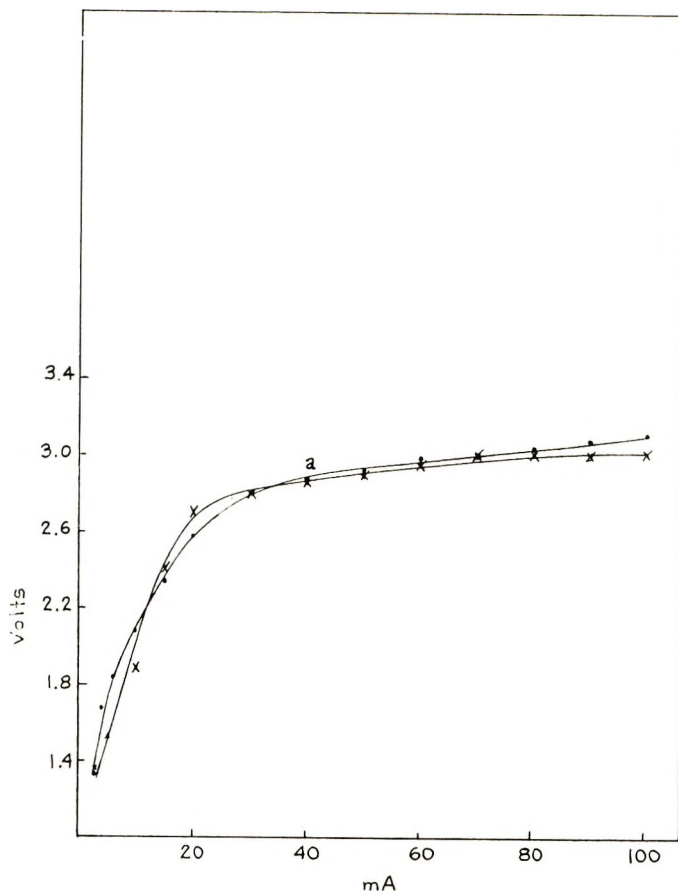


Fig. 4. Variation of the reaction potential E_r with current: (●) ethyl acrylate; (×) ethyl methacrylate.

dehyde was found in the reaction mixture. The presence of formaldehyde was confirmed by two methods: (1) GLC (a 15% Carbowax 20M on Chromosorb W (50–80 mesh) and (2) polarography against a standard solution of formaldehyde.

pH measurements demonstrated the presence of H^+ in the vicinity of the anode. The H^+ concentration increased with increasing current. In contrast, the solution of the cathode section was strongly basic (see Fig. 3).

In current–voltage (current scanning) measurements (Fig. 4), two current ranges, similar to the two potential ranges in polarography, are observed which indicate the existence of the two reactions. In the lower current range, up to point *a*, the voltage E_r rises steeply with relatively small current changes, according to reaction (1). From this point on, only small voltage changes occur with increasing current, according to reactions (3) and (4). (E_r is slightly different from the potential values in polarography because a different electrode pair is used). Experiments showed clearly

that the polymerization occurs at the cathode. Only the radicals $\text{H}\cdot$ and $\text{Li}\cdot$ are present, according to the reactions:



Some investigators believe that the hydrogen radicals initiate polymerization. Kern and Quast⁷ claim that the electrolytic polymerization of an aqueous acidic solution of MMA is initiated by hydrogen atoms, which are formed at the cathode. They found also that the hydrogen activity was a function of the electrode material and decreased in the order Hg, Pb, Fe, Pt. Generally, however, the opposite order is known about the catalytic activity of hydrogen at metal electrodes. Thus Liebafsky and Cairns⁸ showed that the electrode activity for hydrogen adsorption and evolution decreases from Pt through Pd, W, Fe, Cr, Ag, Cu, Pb, Hg. Also Federova et al.⁹ showed that it is not the hydrogen atoms that initiate polymerization at a Pb cathode. Polymerization occurs at the reduction potentials

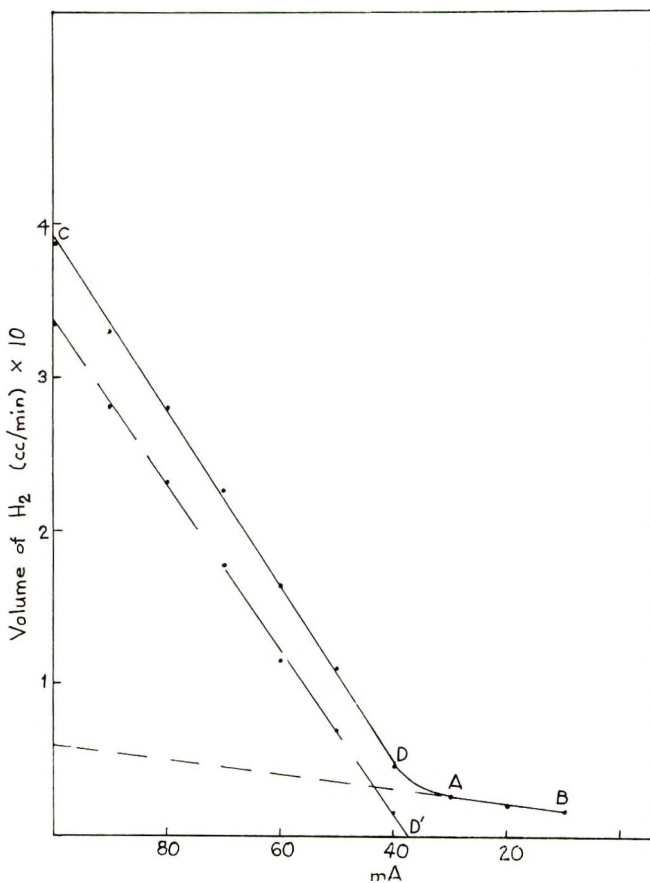
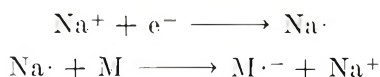


Fig. 5. Volume of H_2 evolved at different currents, 27°C .

of hydrogen ions only in presence of peroxy compounds in the monomer. In agreement with these findings, it is not surprising that Oplatka et al.¹⁰ found that the presence of Hg alone (not as electrode) initiates the polymerization of acrylonitrile.

Parravano¹¹ found that metals loaded with hydrogen, either electrolytically or by processes of chemisorption, initiate polymerization of aqueous solutions of MMA, but the efficiency is low compared with the total hydrogen released by electrolysis or present in the chemisorbed state. Bhadani and Parravano¹² performed electrolytic polymerization of 4-vinylpyridine, and in their opinion initiation occurs by direct electron transfer from cathode to monomer, but other possible mechanisms, such as



are not excluded.

Considering the possibility of initiation by hydrogen atoms in our system we introduced gaseous HCl into the solution instead of Li acetate, and passed an electric current for 12 hr (as mentioned above). The only result was a slight turbidity of the solution in contrast to about 3 g of polymer obtained when Li acetate was used as electrolyte.

Thus we assume that the main initiators in our system are the Li atoms and the mechanism is as follows. The H^+ ions migrate to the cathode and react quickly with a part of the Li atoms to give $\text{Li}^+ + \text{H}\cdot$ according to eqs. (8) and (9). This reaction is much faster than a free-radical reaction between Li atoms and the monomer at high concentrations of H^+ . Thus most of the Li free radicals are neutralized at currents above point *a* and a low conversion results. H^+ is present at low concentrations at low currents and do not quench the polymerization to an appreciable degree.

Measurements of the volume of hydrogen evolved, as described by eqs. (2) and (4) at various current densities, confirms the existence of these reactions and affords a means of studying the effect of the H^+ -ions on polymer conversion. The curve illustrated in Figure 5 comprises two different linear portions, indicating two electrochemical reactions. The curve would be linear throughout the range if reactions of one type only were occurring. The range *A-B* gives the amount of hydrogen resulting from reaction (2). By extrapolation, the volume of hydrogen which would be evolved at various current densities in absence of the other reaction may be obtained. Subtraction of the curve obtained by extrapolation from the experimental curve yields the hydrogen evolved for any given current, according to the reaction described by eq. (4). Section *C-D* in Figure 5 illustrates these results. The current at the point *D'* of zero evolution of hydrogen (extrapolated from the *C-D* line, Fig. 5) is theoretically the lowest value where reaction (4) can take place. This value agrees with that found by the methods already described above, and this further substantiates the validity of our conclusions.

This work is taken in part from the Ph.D. thesis of J. Relis.

References

1. J. W. Breitenbach, C. H. Srua, and O. F. Alaj, *Makromol. Chem.*, **42**, 171 (1960).
2. B. L. Funt and F. D. Williams, *J. Polym. Sci. A*, **2**, 865 (1964).
3. B. L. Funt and K. C. Yu, *J. Polym. Sci.*, **62**, 359 (1962).
4. B. L. Funt and S. N. Bhadani, *Can. J. Chem.*, **42**, 2733 (1964).
5. B. L. Funt and D. G. Gray, *J. Macromol. Chem.*, **1**, 625 (1964).
6. N. Yamazaki, I. Tanaka, and S. Nakahama, *J. Macromol. Sci. Chem. A*, **2**, 1121 (1968).
7. W. Kern and H. Quast, *Makromol. Chem.*, **10**, 202 (1953).
8. H. A. Liebafsky and E. J. Cairns, *Fuel Cells and Fuel Batteries*, Wiley, New York, 1938, p. 155.
9. A. I. Federova, L. Kuo-Tung, and I. V. Shelepin, *Russ. J. Phys. Chem.*, **38**, 921 (1964).
10. A. Oplatka, M. Königsbuch, and N. Shavit, in *Macromolecular Chemistry, Prague 1965* (*J. Polym. Sci. C*, **16**), O. Wichterle and B. Sedláček, Eds., Interscience, New York, 1967, p. 2795.
11. G. Parravano, *J. Amer. Chem. Soc.*, **72**, 628 (1951).
12. S. N. Bhadani and G. Parravano, *J. Polym. Sci. A-1*, **8**, 225 (1970).

Received September 1, 1970

Revised November 23, 1970

Pyrolysis-Gas Chromatographic Analysis of Poly(vinyl Chloride). II. *In Situ* Absorption of HCl during Pyrolysis and Combustion of PVC

MICHAEL M. O'MARA, *B. F. Goodrich Chemical Company, Avon Lake, Ohio 44012*

Synopsis

A pyrolysis-gas chromatographic technique for measuring the amount of hydrogen chloride released during the high temperature pyrolysis of poly(vinyl chloride) resins, plastisols, copolymers and compounds containing inert fillers has been developed. The technique, which is also applicable to the analysis of chlorinated polyethylene and chlorinated poly(vinyl chloride), is based on the use of a standard precursor of HCl, poly(vinyl chloride) homopolymer. The analysis has been successfully used to measure the degree of *in situ* absorption of HCl during pyrolysis by certain basic fillers [K_2CO_3 , $CaCO_3$, CaO , MgO , $Al(OH)_3$, Na_2CO_3 , Al_2O_3 and $LiOH$] dispersed in a poly(vinyl chloride)-*o*-dioctyl phthalate matrix. Combustion of a number of combustion residues (chloride determination) revealed that the amount of HCl absorbed by the basic filler was independent of the method of degradation (pyrolysis or combustion). Flammability measurements of those matrices having the same composition indicate that *in situ* absorption of HCl during combustion has little effect on the overall flammability of these materials.

INTRODUCTION

Pyrolysis of poly(vinyl chloride) in a radiant-heated quartz tube at 600°C under a helium atmosphere results in the formation of a series of aliphatic and aromatic (major) hydrocarbons. In addition, a quantitative recovery of HCl and a chlorine-free carbonaceous ash are also obtained. These analyses and a detailed description of the basic apparatus (pyrolysis chamber, gas chromatograph and mass spectrometer) have previously been described.¹

During the initial phases of this work, a pyrolysis-gas chromatographic technique was developed for determining the amount of HCl evolved from PVC resin, compounds, copolymers, and other chlorinated polymers during thermal degradation. As a result of this capability, an investigation has been carried out on the absorption of HCl by inorganic fillers in PVC compounds during pyrolysis and combustion processes.

The role of metal salts in PVC stabilization has been widely studied. Frye et al., in a series of papers on the stabilization of PVC by organotin

esters,² has shown that the ester moiety enters the polymer backbone during thermal (175°C) stabilization with the formation of organotin chlorides. Earlier work by Frye and Horst³ had shown that barium, cadmium, and zinc 2-ethylhexanoates undergo a similar interaction with PVC during stabilization.

Certain inorganic fillers in PVC compounds can act as HCl absorbers during low temperature stabilization and high temperature combustion processes. For example, calcium carbonate, a typical filler in PVC wire formulations might be expected to absorb a stoichiometric equivalent of HCl when the wire is burned. As shown later, this does not occur.

Little has been reported on the reaction of this and other inorganic metal oxides, carbonates and hydroxides with HCl during the high-temperature degradation of PVC. Chaleroix⁴ has shown that in a closed system containing HCl, the oxides of Mg, Ca, Ni, Co, Cr, and Al react with HCl, the completeness of reaction being a function of reaction temperature (18–650°C). Some metal oxides (Cu, Pb, Ag, Zn, and Sn) exhibit an inverse relationship between the degree of reaction and temperature while others (Cd, Hg and Fe⁺³) exhibit a maximum followed by a minimum conversion as temperature is increased.

It was of interest to investigate these reactions when applied to high temperature processes (pyrolysis and combustion) of PVC. To accomplish this, a series of inorganic fillers were dispersed in a PVC–dioctyl phthalate plastisol and fused at 150°C. HCl evolution from these matrices during pyrolysis at 600°C and during combustion was measured. In addition, the effect of HCl absorption on the flammability of each of the various matrices was also investigated.

EXPERIMENTAL

Apparatus

A pyrolysis unit consisting of a quartz tube with a volume of 23 ml, a tube furnace with capabilities to 1000°C, a F & M gas sampling valve, and a heated stainless steel line was placed on line with an F & M Model 700 gas chromatograph. On-line or off-line operation of the pyrolysis chamber was afforded by means of the gas sampling valve (see reference 1 for experimental detail).

A stainless steel union tee (Swagelok) was placed in the carrier gas line immediately before the quartz pyrolysis chamber. The tee was sealed with a standard nut containing a rubber septum. The purpose of this was to permit the injection of gaseous HCl into the pyrolysis unit for pre-conditioning the system.

Materials

The poly(vinyl chloride) used throughout this work was a commercial PVC homopolymer containing 56.7% chlorine. Plastisols were prepared by fusing the homopolymer with a commercial dioctyl phthalate at 170°C

for 5 min. This same procedure was used in preparing plastisols containing various inorganic fillers. The fillers (CaO , CaCO_3 , MgO , etc.) were dispersed in the plasticizer in a micro-pulverised form. Those materials not commercially available in this form were prepared from normal particle-sized samples.

Chromatographic Parameters

All HCl Analyses were performed on a 10 ft \times $\frac{3}{16}$ in. stainless steel column packed with 10% SE52 on CHRW, AG; carrier gas, helium; gas flow, 50 ml/min; oven temperature, ambient; pyrolysis effluent line, ambient; bridge current, 150 mA. Peak areas were measured by disk integration; areas reported are the product of disk count and attenuation $\times 10^{-2}$.

Chromatographic Analysis of HCl

The pyrogram (gas chromatogram of the pyrolysis products) of PVC consists of an intense peak with a retention time equal to the dead time of the column and a series of smaller peaks with retention times ranging from 18 to 35 min. The initial peak corresponds to the elution of HCl; the other components are the various hydrocarbons that are formed from the thermal collapse of the dehydrochlorinated PVC backbone.

In a series of pyrolysis experiments with PVC resin, it was found that a linear relationship existed between the amount of resin degraded (10–20 mg) and the area under the HCl peak. For a typical run, five samples of resin were weighed to ± 0.01 mg into $10 \times 6 \times 5$ mm porcelain boats. The pyrolysis chamber was brought up to temperature (600°C) and one of the boats was introduced into the cold zone of the pyrolyzer. The gas sampling valve was then positioned such that the pyrolysis chamber was on-line with the chromatograph. After a 5-min carrier gas purge, the boat was moved into the hot zone with the aid of a magnet. Immediately after the HCl chromatographic peak was recorded, the gas sampling valve was positioned for off-line operation. The pyrolysis chamber was opened, the previous sample boat removed and a new sample was introduced. This same operation was again repeated for each of the remaining samples. Upon completion of the analysis, the effluent line and chromatograph were heated to 150°C in order to drive off the condensed hydrocarbons resulting from the five pyrolysis experiments. Actually 6–7 runs could be made in this way before accumulated benzene, the primary organic pyrolysis product from PVC, began to bleed from the column.

The relationship between the amount of resin pyrolyzed and the chromatographic area of the HCl peak was linear. It was noted that the first run of the series did not correlate with the remaining runs.¹ This was attributed to the fact that the first run of HCl through the effluent and chromatographic lines conditions the apparatus for subsequent analyses. To test this, a second injection port in the form of a Swagelok tee with a rubber septum was added to the carrier gas line. In this way, once the first sample

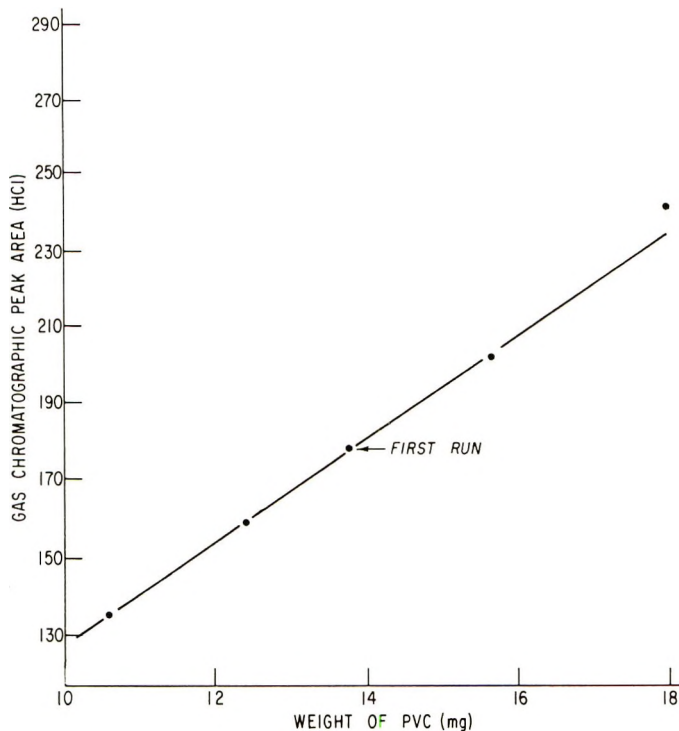


Fig. 1. Relationship of HCl chromatographic peak area and amount of PVC pyrolyzed at 600°C.

of PVC was introduced into the unit and the unit purged of air, a portion of HCl (4 ml) could be injected into the line for purposes of preconditioning. It was found that once this preconditioning step was taken, the first run of the series correlated with the remaining runs (Fig. 1).

The results from a typical run of 5 samples are summarized in Table I. These include the weight of homopolymer pyrolyzed, the area of the HCl peak (disk integration count \times attenuation) and the ratio of area to weight. The data are also plotted in Figure 1.

TABLE I
Relationship of Sample Size with Chromatographic Area of HCl

Run	Weight of PVC, mg	Gas chromatographic area of HCl	HCl area
			Wt. of PVC
1	13.61	176.6	13.0
2	17.80	243.2	13.7
3	10.49	134.4	12.8
4	15.53	202.2	13.0
5	12.30	160.8	13.1

Analysis of PVC Compounds

The amount of HCl that is released from PVC compounds which contain various levels of plasticizer, inert fillers, etc. can easily be determined by pyrolysis if PVC homopolymer is used as a standard precursor of HCl (58.3%). The following empirical formula has been devised for this purpose. If an equivalent of Cl in PVC produces an equivalent of HCl as a result of high temperature pyrolysis, then

$$\frac{(\text{Wt. HCl})_{\text{ref}}}{(\text{G.C. Area HCl})_{\text{ref}}} = \frac{(\text{Wt. HCl})_A}{(\text{G.C. Area HCl})_A} \quad (1)$$

where (Wt. HCl) is the amount of HCl formed and (G.C. Area HCl) is the corresponding gas chromatographic peak area of that component. Subscripts "ref" and "A" refer to the reference sample (PVC homopolymer) and to the PVC compound under investigation, respectively. Substituting the following relationship (2) into eq. (1)

$$\text{Wt. HCl} = \% \text{ HCl} \times \text{Wt. of sample} \quad (2)$$

results in eq. (3):

$$\frac{(\% \text{ HCl} \times \text{Wt.})_{\text{ref}}}{(\text{G.C. Area HCl})_{\text{ref}}} = \frac{(\% \text{ HCl} \times \text{Wt.})_A}{(\text{G.C. Area HCl})_A} \quad (3)$$

On solving eq. (3) for $(\% \text{ HCl})_A$ and substituting the theoretical amount of HCl contained in the PVC homopolymer, i.e., 58.3%, for the quantity $(\% \text{ HCl})_{\text{ref}}$, the final form of the equation becomes

$$(\% \text{ HCl})_A = \frac{(58.3)(\text{Wt.})_{\text{ref}} (\text{G.C. Area HCl})_A}{(\text{G.C. Area HCl})_{\text{ref}} (\text{Wt.})_A} \quad (4)$$

The amount of HCl released from a PVC compound during high temperature pyrolysis can thus be calculated by pyrolyzing known quantities of both the unknown compound and the reference (PVC homopolymer) and measuring the gas chromatographic areas of the resulting HCl peaks. In a typical experiment, three samples of the PVC compound to be analyzed and two samples of the reference are precisely weighed and pyrolyzed in a series of experiments analogous to that previously described.

In order to test this approach, a number of PVC compounds of known composition* were analyzed. A summary of the compounds studied, the per cent HCl found, and the theoretical HCl content is contained in Table II. This analysis has been extended to chlorinated polyethylenes and chlorinated poly(vinyl chloride) (CPVC). It is noted that the % theoretical and the found HCl contents for the CPVC samples are not the same. The reason for this is that the hydrocarbon fraction from CPVC contains a series of chlorinated hydrocarbons;⁵ therefore a quantitative yield of HCl is not realized for these polymers. The remaining analyses in Table II are within 0.6% of the theoretical value in every case but one.

* Cl analysis by Schöniger method.

TABLE II
 Pyrolytic Analysis of HCl from PVC Compounds,
 Chlorinated Polyethylene and Chlorinated Poly(vinyl Chloride)

Sample type	% HCl (found)	% HCl (theoretical)
PVC plastisol	30.1	29.1
"	37.0	37.3
"	44.7	44.5
PVC-Vinyl acetate copolymer	53.5	52.9
" "	46.3	46.3
PVC compound	38.5	38.6
PVC compound	47.5	47.7
Chlorinated polyethylene	34.9	34.3
" "	40.7	41.1
Chlorinated poly(vinyl chloride)	63.9	69.2
" "	68.5	71.5

Gross amounts of C_2-H_4 hydrocarbons in the pyrolyzate would seriously interfere with the described analysis due to the elution of these gases with HCl. For that reason, PVC plasticizers containing these structural moieties were not used.

In Situ Absorption of HCl

Many PVC compounds contain various levels of inorganic fillers which are typical HCl absorbers i.e., $CaCO_3$, $Pb(OH)_2$, etc. It might be expected that during pyrolysis and combustion a certain amount of the HCl evolved from the PVC matrix would react with these fillers in a typical acid-base reaction. The amount of HCl absorbed should be a function of the amount and of the equivalent weight of the particular filler. A series of compounds were prepared in which various levels of $CaCO_3$ in one set, and K_2CO_3 in another, were added to a PVC-dioctyl phthalate plastisol (50/50, w/w). Once these inorganic bases were dispersed in the plasticizer, the mixture was fused at $150^\circ C$. Chlorine analyses were obtained by ashing the samples in a Schoniger flask, addition of a greater than equivalent amount of silver nitrate (10-20% excess) and an atomic absorption analysis of excess silver ion.¹³ These analyses were cross-checked through x-ray fluorescence analyses. In all cases, the Cl analyses were equivalent to theoretical. A list of the compounds prepared, their compositions and the Cl analyses (atomic absorption, x-ray fluorescence and theoretical) are listed in Table III. The checking was done only for those PVC compounds containing K_2CO_3 .

Each of the compounds listed in Table III was pyrolyzed at $600^\circ C$ in a series of experiments aimed at determining the amount of HCl evolved during thermolysis. PVC homopolymer was used as a standard, and the determination was carried out in a manner analogous to that previously described. The results of these determinations are summarized in Table IV. For each compound analyzed, the theoretical amount of HCl evolved

(assuming no absorption), the actual amount of HCl evolved, and the molar absorption efficiency (MAE) of K_2CO_3 and $CaCO_3$ for each of the samples is given. The MAE value is defined as the amount of HCl absorbed by the particular base divided by the amount of HCl which theoretically could be absorbed (on a stoichiometric basis) times 100. This latter quantity is based on the equivalent weight and on the amount of the

TABLE III
Composition of PVC Plastisols Containing
Various Levels of $CaCO_3$ or K_2CO_3

Component	Amount g	Com- pound no.	Cl, %		
			Atomic Abs.	X-ray ^a	Theoretical
PVC	100	1	27.35	27.24	27.24
DOP	100				
K_2CO_3	0				
PVC	100	2	23.26	23.42	23.09
DOP	100				
K_2CO_3	36				
PVC	100	3	20.42	20.82	20.84
DOP	100				
K_2CO_3	61.5				
PVC	100	4	17.33	18.18	17.69
DOP	100				
K_2CO_3	108				
PVC	100	1	27.35	27.24	27.24
DOP	100				
$CaCO_3$	0				
PVC	100	5	—	—	24.78
DOP	100				
$CaCO_3$	20				
PVC	100	6	—	—	22.71
DOP	100				
$CaCO_3$	40				
PVC	100	7	—	—	19.46
DOP	100				
$CaCO_3$	80				

^a Matrix-corrected.

particular base in the matrix. For example, if one mole of $CaCO_3$ absorbed two moles of HCl during pyrolysis, the MAE value of $CaCO_3$ would be 100%.

These data reveal that on this basis, the basic salts absorbed only part of the evolved HCl. Potassium carbonate is more efficient in removing HCl than is calcium carbonate. It is apparent that the efficiency in this case is not influenced by the actual level of base present. For example, K_2CO_3 has a molar efficiency of 84%, whether it is present in 36 parts or 61.5 parts.

TABLE IV
Evolution of HCl from PVC Compounds Containing K_2CO_3 and $CaCO_3$

Compound ^a	Theoretical HCl evolved, %	HCl evolved (Found), %	HCl absorbed, %	MAE, %
1	28.0	28.1	—	—
2	23.9	17.1	6.8	84.2
3	21.4	11.1	10.3	83.1
4	18.2	2.9	15.3	87.7
5	25.5	22.1	3.4	53.6
6	23.4	17.1	6.3	51.3
7	20.0	11.7	8.3	40.0

^a See Table III for compound identifications.

Material Balance of Chloride

In order to cross-check the HCl evolution determination in the preceding section, a material balance of chloride in one of the above experiments (compound 3) was carried out. Evolution data indicated that of the 21.4% available HCl in that sample, approximately one-half (11.1%) was evolved. This coupled with a chloride analysis of the ash would yield a material balance calculation.

Equation (5) relates the amount of chloride in the original polymer to the amounts of chloride in the ash and in the gas phase after pyrolysis.

$$\frac{\text{Original sample}}{\% \text{ Cl} \times \text{Wt.}} = \frac{\text{HCl}}{\% \text{ Cl} \times \text{Wt.}} + \frac{\text{Ash}}{\% \text{ Cl} \times \text{Wt.}} + \frac{\text{Hydrocarbon}^*}{\% \text{ Cl} \times \text{Wt.}} \quad (5)$$

The results in Tables III and IV for compound 3 reveal that the chloride content in the original sample was 20.8% and that 11.1% of the total polymer is converted to evolved HCl. The chloride content of the ash was obtained by pyrolyzing 89.1 mg of the original sample, extracting the precisely weighed ash with a 10.00-ml aliquot of water, and determining the chloride content of an aliquot of that solution by an atomic absorption analysis of Ag^+ (after titration of Cl^- with an excess of silver nitrate). It was found that the ash contained 38.4% chloride. When these values are substituted into the material balance equation, the following is obtained:

$$\begin{aligned} \frac{\text{Original Sample}}{\% \text{ Cl} \times \text{Wt.}} &= \frac{\text{HCl}}{\% \text{ Cl} \times \text{Wt.}} + \frac{\text{Ash}}{\% \text{ Cl} \times \text{Wt.}} \\ (20.8)(89.05) &= (97.5)(9.88 \text{ mg}) + (38.4)(22.44 \text{ mg}) \\ 1852 &= 963 + 862 \\ 1852 &= 1825 \end{aligned}$$

* This quantity is zero.

In other words, the original 89.1 mg of sample which contained 18.5 mg of chloride, 18.2 mg of chloride (or 98.4%) could be accounted for in the gas phase as HCl and in the ash as KCl. Similar analyses were repeated for matrices containing lithium hydroxide and magnesium oxide, and in each case the material balance of chloride was excellent. Experiments with the lithium hydroxide matrix including the material balance are discussed below.

MAE Values of Typical Inorganic Fillers

A number of PVC compounds containing other typical HCl absorbers were also analyzed in a manner analogous to that just described. These compounds each contained one of the following fillers: aluminum oxide, calcium oxide, magnesium oxide, sodium carbonate, aluminum hydroxide, and lithium hydroxide. The molar absorption efficiencies (MAE) of these components along with those values previously found for CaCO_3 and K_2CO_3 are summarized in Table V.

A number of the basic fillers in Table VI caused the PVC matrix to discolor, and this was attributed to an initial dehydrochlorination with the formation of a conjugated polyene chain.

Some of the values reported in Table V are restated in Table VI in terms of actual percentage HCl absorbed. The level of each of the inorganic fillers in the matrix, except lithium hydroxide, is 23.6 wt-%; the remaining 76.4% consists of PVC and dioctyl phthalate.

TABLE V
Molar Absorption Efficiencies of PVC Fillers (Approximate)

Filler	MAE, %
CaCO_3	48
K_2CO_3	86
CaO	48
MgO	43
$\text{Al}(\text{OH})_3$	18
Na_2CO_3	37
Al_2O_3	0
LiOH	100

TABLE VI
Percentage (of Total) HCl Absorbed during Pyrolysis at 600°C

Filler	% HCl absorbed by ash
CaO	53.5
$\text{Al}(\text{OH})_3$	23.6
Na_2CO_3	21.8
MgO	67.6
Al_2O_3	0.0
LiOH	84.4

Thus a PVC compound containing 23.6 parts of MgO will absorb $\sim 68\%$ of the evolved HCl when thermally degraded at high temperatures. The deleterious effect of large amounts of this oxide on the PVC matrix unfortunately rules it out as an "acceptable" filler.

A matrix containing hydrated lithium hydroxide was also investigated. The composition in this case was 47% PVC, 24% DOP, and 28% LiOH·H₂O. It was assumed that during the fusion step at 150°C all of the water of hydration was vaporized from the sample. A thermogravimetric analysis at 5°C/min showed that all of the water of hydration in LiOH·H₂O is vaporized at temperatures below 100°C. Based on this assumption of a total water loss during fusion, the composition changes to 54% PVC, 28% DOP, and 18% LiOH. A theoretical chlorine content for this composition is 30.5%; we found $30.7 \pm 0.3\%$. When the sample was pyrolyzed at 600°C, $5.1 \pm 0.5\%$ HCl was found in the pyrolyzate. A chloride analysis of the ash after pyrolysis gave $25.9 \pm 0.4\%$, relative to the original weight of the sample. Thus the material balance of chloride in this experiment was:

$$\begin{aligned} \text{Cl, original sample} &= \text{Cl, ash} + \text{Cl, HCl} \\ 30.7\% &= 25.9\% + 5.0\% \\ 30.7\% &= 30.9\% \end{aligned}$$

Based on these values, the amount of HCl that is absorbed by the ash during pyrolysis is $\sim 85\%$ of the available HCl in the matrix.

The magnitude of each of the molar absorption efficiencies reported in Table V is dependent upon a number of variables. For the samples investigated in this study, an "intimate mixture" of PVC and filler has been achieved. Under conditions where the mixing is less homogeneous, the efficiency would be expected to be less than reported in Table V. A similar situation would also arise for mixtures which contained larger particle sized fillers.

The near 50% efficiency reported for calcium carbonate and oxide and magnesium oxide suggest that an intermediate calcium oxychloride (CaOCl) or magnesium oxychloride which is impervious to further HCl attack is formed at these high temperatures. The high efficiency of the strong base, lithium hydroxide, and the low efficiency of the weak base, aluminum hydroxide toward HCl absorption was expected. The low efficiency reported for sodium carbonate is surprising and may be in error, especially in view of the high efficiency of the potassium carbonate filler.

Relationship of Pyrolysis to Combustion

It was of considerable interest to determine the degree of HCl absorption under actual burning conditions. A number of samples of the PVC compound containing K₂CO₃ (Table III, compound 3) in the range of 80–170 mg were thermally degraded under pyrolytic and combustion conditions. The pyrolyzed samples were degraded at 600°C in a helium atmosphere

TABLE VII
Summary of Combustion (C) and Pyrolysis (P)
Data for PVC Matrix Containing K_2CO_3

Sample size, mg	Cl content of ash, mg	Method of degradation
96.13	9.72	C
166.02	17.24	C
117.35	11.91	P
83.72	8.21	P
89.05	8.61	P
136.79	14.13	C
105.90	10.72	C
154.15	16.55	P

inside the pyrolysis unit. The samples degraded under combustion conditions were placed in a porcelain boat and ignited with the aid of a Meeker burner. Once ignition took place, the samples were removed from the flame until the samples self extinguished. At this point, the residues were returned to the flame for a few seconds to insure complete combustion. The ashes which resulted from the two experiments were then analyzed for chloride by the atomic absorption method previously described. The data

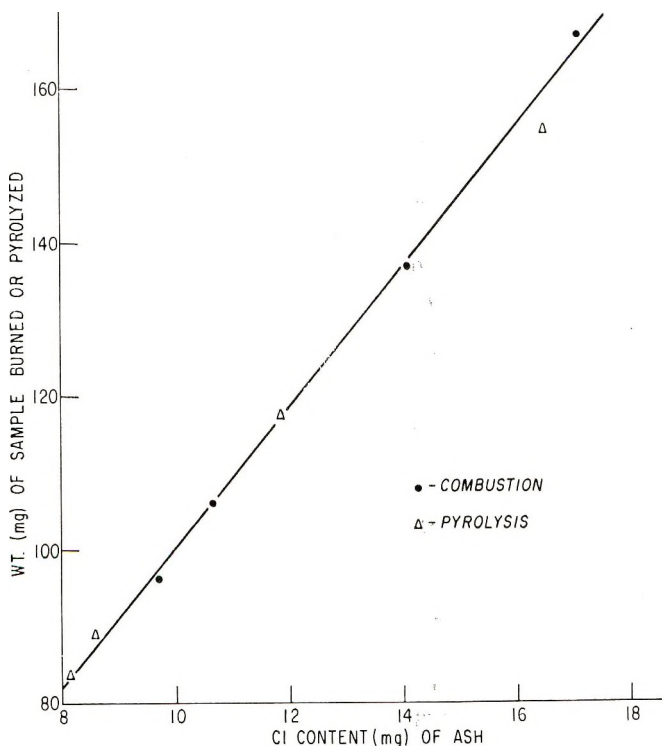


Fig. 2. Effect of pyrolysis and combustion on HCl absorption.

from these experiments are summarized in Table VII and shown graphically in Figure 2.

It is obvious that the same amount of HCl is absorbed by the K_2CO_3 , regardless of the method of degradation (pyrolysis or combustion). This supports the contention that the pyrolysis experiments reflect actual combustion processes in so far as HCl absorption is concerned. Similar experiments with the PVC matrix containing magnesium oxide provided analogous results.

It was found that the PVC-lithium hydroxide matrix absorbed more HCl under combustion conditions than under pyrolysis conditions, although this difference was small. For example after pyrolysis, $25.9 \pm 0.4\%$ chloride remained in the ash; after combustion $26.9 \pm 0.2\%$ remained. This amount of HCl absorbed during combustion corresponds to a molar efficiency of 100% for lithium hydroxide.

Effect of HCl Absorption on Flammability

The flammability of chlorinated polymers has been discussed by a number of authors. Basic studies by Fenimore and Martin⁶ have shown that as the chlorine content in a series of chlorinated polyethylene increases, the limiting oxygen indices (LOI) increase from 17.4 for polyethylene to ~ 60 for poly(vinylidene chloride). Additional experiments involving the burning of polyethylene in atmospheres containing HCl indicated that the increase in LOI for the above series was a result of changes in the pyrolysis reactions which were caused by the increasing chlorine contents of the polymers. There was no indication that the HCl released during combustion altered the gas phase flame reaction to any appreciable extent.

The pyrolysis products from the chlorinated polyethylenes and poly(vinyl chlorides) listed in Table II were investigated. Basically, this study showed that as the chlorine content of the polymer increased, the pyrolysis products changed from low-boiling aliphatics (methane, ethane, propane, etc.) to higher-boiling aromatics (benzene, chlorobenzene, dichlorobenzenes, etc.) These findings were in general agreement with those of Tsuge.^{5,7} In addition, we found that as the chlorine content of the polymer increased, the amount of carbonaceous ash increased from $<1\%$ for the chlorinated polyethylenes to 26% for the chlorinated poly(vinyl chlorides). Thus by increasing the chlorine content of the polymer, the pyrolysis products undergo a qualitative change to less flammable fuels. In addition, cross-linking in the polymer during thermal degradation is greatly increased in the higher chlorinated polymers which results in the formation of greater amounts of carbonaceous ash. Both of these changes in the degradation profile account for the higher degree of flame retardancy in the chlorinated polyvinyl chlorides.

The PVC matrices which contain the five different inorganic fillers (Table VI) provide an interesting case of flammability. Each of the matrices contain the same amount of PVC and plasticizer, yet each differs with respect to the amount of HCl which is evolved during combustion.

TABLE VIII
Oxygen Indices of PVC Matrices Containing 23.6% Inorganic Filler

Matrix filler	Oxygen index	% of HCl in matrix evolved
MgO	22.6	32.4
Na ₂ CO ₃	23.4	78.2
Al ₂ O ₃	24.4	100.0
CaO	21.8	46.5
MgO (11.8%), clay (11.8%)	23.5	60.9
Al(OH) ₃	26.1	76.4

Of the available HCl in each matrix (27.5%), the degree of HCl evolution during combustion ranges from 100% (Al₂O₃) to 32% (MgO). It might be expected that if hydrogen chloride is grossly affecting the gas-phase flame reactions, the flammability of these matrices should be quite different. Along these lines, the flammability of each matrix as defined by the Oxygen Index was recorded. Indices were measured on the General Electric FL-101 flammability tester; samples were in the form of 4 × 1/4 × 1/4 in. sticks. The results of these determinations are summarized in Table VIII; the amount of the available HCl which is evolved during combustion is also included.

The oxygen indices of the six matrices which are identical in composition reveal that there is no real relationship between the index and the amount of HCl evolved during combustion. There is little change in flammability over the entire range of HCl evolution which may indicate the relatively minor role of this gas in flame retardation. Unfortunately a matrix capable of total HCl absorption is not in hand at this time. Thus the above observation may not hold over the entire range (0-100%) of HCl absorption. For example, the effect of HCl on flammability may be drastic from 100 to 90% absorption and level off after that point. However, for the range investigated in the present study, it is evident that there is little change in the flammability of the matrices tested.

The matrix exhibiting maximum flame retardation is that one which contains the aluminum hydroxide filler. Considering that during thermal degradation this filler is converted to the oxide with the subsequent release of water suggests that the gross quantity of diluent water in the gas phase has the greatest influence on the overall flammability of the matrix. The absorption of HCl by this matrix calls to mind another possible explanation for the higher degree of flame retardancy. The formation and volatilization of aluminum (III) chloride may contribute to flame retardation in a manner analogous to that reported for antimony chloride.^{8,9} Although the direct formation of the trichloride is unlikely, the oxychloride is a precursor of the trichloride at elevated (600-700°C) temperatures.^{10,11} A similar, though more detailed transformation has recently been reported for antimony oxychloride.¹²

Whether aluminum (III) chloride plays a role in flame retardation or not, the results of this study show that HCl over a wide, but not inclusive, range plays a minor role in flame retardation.

The author wishes to acknowledge the helpful suggestions of L. B. Crider and M. L. Dannis during the course of this work, the atomic absorption analyses by Mrs. E. D. Truscott, and the x-ray fluorescence analyses by R. A. Yount.

References

1. M. M. O'Mara, *J. Polym. Sci. A-1*, **7**, 1887 (1970).
2. A. H. Frye, R. W. Horst, and M. A. Paliobagix, *J. Polym. Sci. A*, **2**, 1801 (1964) and references therein.
3. A. H. Frye and R. W. Horst, *J. Polym. Sci.*, **45**, 1 (1960).
4. C. Chaleroux, *Ann. Chim.*, **5**, 1069 (1960).
5. S. Tsuge, T. Okumoto, and T. Takeuchi, *Macromolecules*, **2**, 277 (1969).
6. C. P. Fenimore and F. J. Martin, *Combustion Flame*, **10**, 135 (1966).
7. S. Tsuge, T. Okumoto, and T. Takeuchi, *Macromolecules*, **2**, 200 (1969).
8. J. A. Rhys, *Chem. Ind. (London)*, **1969**, 187.
9. C. P. Fenimore and G. W. Jones, *Combustion Flame*, **10**, 295 (1966).
10. H. Schafer, C. Göser, and L. Bayer, *Z. Anorg. Chem.*, **263**, 87 (1950).
11. P. Hagenmuller, J. Rouxel, J. David, A. Colin, and B. Le Neindre, *Z. Anorg. Allgem. Chem.*, **323**, 1 (1963).
12. J. J. Pitts, P. H. Scott, and D. G. Powell, *J. Cell. Plast.*, **6**, 35 (1970).
13. E. D. Truscott, *Anal. Chem.*, **42**, 1657 (1970).

Received September 1, 1970

Revised November 18, 1970

Polymerizations with Hydrido and Alkyl Transition Metal Complexes in Aqueous Media

H. L. LENTZNER and H. E. DE LA MARE, *Shell Development Company, Emeryville, California 94608*

Synopsis

Hydrido pentacyanocobaltate(III) and alkyl pentacyanocobaltate(III) have been studied as initiators for the polymerization of isoprene and butadiene in aqueous emulsion systems. The microstructure of the polymers is consistent with a free radical process. Other transition metal hydrides are relatively ineffective as polymerization initiators or act as inhibitors for the radical polymerization of the same dienes.

INTRODUCTION

During the last decade, a variety of stereospecific and nonstereospecific polymerizations have been reported in water or other polar media^{1,2} by using transition metal complexes as catalysts. In several cases, sodium borohydride, hydrogen, or other reducing agents were found to be effective cocatalysts.³⁻⁷ These latter observations suggested the examination of complex transition metal hydrides *per se* in aqueous polymerizations. Accordingly, we now report our studies with several complex metal hydrides in the emulsion polymerization of isoprene and butadiene. Much of our work has utilized the well-known pentacyanocobalt hydride, but several complex hydrides of other metals were also tested. Independently, Takahashi⁷ has communicated his results with the cobalt cyanide-hydrogen complex, demonstrating that such a system was active for polymerizing various polar monomers, styrene, and butadiene. However, no structural determinations were made on the polymers.

In addition to the hydrido complexes, we have also examined the alkyl-pentacyanocobaltate complexes as initiators in the emulsion polymerization of butadiene and isoprene. Recently, Aoki, et al.⁸ have also reported on the use of the pentacyanobenzylcobaltate (III) as an initiator for the polymerization of methyl methacrylate, styrene, acrylonitrile, and vinyl acetate. The data reported in this paper for diene polymerizations are in accord with their findings with the polar vinyl monomers.

EXPERIMENTAL

Materials

Butadiene. Phillips high purity (99.5%) butadiene was used in all experiments.

Isoprene. Polymer grade (Shell Chemical) isoprene was distilled off sodium dispersion, stored over CaH_2 , and kept refrigerated when not in use.

Water. Distilled water was degassed by refluxing and storing under an argon sparge.

Sodium Borohydride. Sodium borohydride was obtained from Metal Hydride Corp. and used as received.

Sodium Dodecylbenzene Sulfonate. This was (Siponate DS-10) a product of the American Alcolac Corporation (abbreviated Na-p-DOBS). Attempts to limit the hydroperoxide contamination were made by storing the emulsifier in the dark and under an inert atmosphere, by extraction with methanol and by dry box storage and sampling. Batches of emulsifier were analyzed periodically for hydroperoxide content and those used normally had $<0.01\%$ w peroxide calculated as the hydroperoxide of the original emulsifier. An emulsifier which is peroxide-free should give no polymer with isoprene at 60°C in the standard emulsion system; this appears to be a good test for peroxide content.

Alkylpentacyanocobaltates. The K and Na complexes were prepared usually in water/methanol by the procedures suggested by Halpern.⁹

All other chemicals were standard reagent grade chemicals. The transition metal complexes were prepared by standard literature methods.

General Procedure

High Vacuum-Line Method. Weighed amounts of metal complex, reducing agent (*in situ* reductions), and solid emulsifier were placed in heavy-walled 25 ml ampoules and degassed on the high vacuum line until a pressure of 5×10^{-5} mm of mercury was attained.

The ampoules were then filled with a slightly positive pressure of argon. The ampoules were removed and quickly capped with rubber serum caps. Water and isoprene were added by syringe and the tubes immediately returned to the vacuum line and frozen in liquid nitrogen. Butadiene was condensed in the ampoule by distillation from a storage vessel on the high vacuum line. The vacuum line was pumped down to 5×10^{-5} mm. The contents of the ampoules were allowed to thaw and then refrozen and pumped down again. After this freeze-thaw degassing procedure was repeated, the ampoules were sealed off under vacuum with a torch.

The ampoules were placed in wire gauze wrappers and warmed in variable temperature water shaker baths.

At the termination of the polymerization period, the ampoules were broken open and their contents dumped into methanol containing Ionox 330[®] antioxidant.

Bottle Polymerizations. Bottle polymerizations were carried out in 8-oz hydrogen peroxide bottles equipped with self-sealing Hycar rubber gaskets and punched metal screw caps. Solid reactants were placed in the clean bottle and the bottles purged with argon or nitrogen prior to charging the other materials (water, isoprene, etc.) by standard syringe techniques. Gaseous butadiene was condensed into carefully cooled bottles ($\leq -35^\circ\text{C}$)

and the amount determined by weight. Unpenetrated rubber gaskets were exchanged for entry serum caps under vigorous inert gas purge prior to final capping. The bottles were placed in protective cages and tumbled in a controlled temperature water bath. The experiments of Tables II and IV were carried out in bottles. All other experiments were carried out by the vacuum-line technique.

Analyses

The microstructure of the polymers was determined by standard infrared (butadiene) and NMR techniques (isoprene) which are equivalent to published methods.^{10,11} In the case of high molecular weight or crosslinked polymers, particularly polyisoprene, samples were degraded by ultrasonic techniques to give benzene solutions ($\sim 5\%$ w) which were of suitable viscosity for analysis by NMR.

The hydroperoxide content of the emulsifier was determined by a spectrophotometric technique based on the oxidation of ferrous iron to $\text{Fe}(\text{SCN})_6^{+3}$ and determination of the latter species.

RESULTS AND DISCUSSION

Polymerization Studies with Hydrido Pentacyanocobaltates

Potassium Pentacyanocobalt Hydride [$\text{K}_3\text{Co}(\text{CN})_5\text{H}$]. Pentacyanocobaltate ion [$\text{Co}(\text{CN})_5^{-3}$] has long been known as the product obtained by the addition of cobaltous chloride to excess aqueous potassium cyanide.¹² Japanese workers first reported that the pentacyanocobaltate anion could be used as a hydrogenation catalyst.¹³ A subsequent investigation by King and Winfield pointed out that the active hydrogenation catalyst was the hydrido anion $\text{HCo}(\text{CN})_5^{-3}$.^{14,15} Kwiatek¹⁶ then reported the facile hydrogenation of conjugated diolefins to mono-olefins using this hydride anion. Because of the similarity involved in the first steps of hydrogenation and polymerization, it was attractive to study the polymerization activity of this cobalt hydride.

The hydrido pentacyanocobaltate(III) ion [$\text{HCo}(\text{CN})_5^{-3}$] can be prepared in various ways.^{14,15} Of the possible methods, the one which is simplest and gives the highest yield in hydride consists of treatment of the pentacyanocobaltate(II) anion with a ten molar excess of sodium borohydride. The hydrido complex has also been found to form via a disproportionation reaction of the pentacyanocobaltate(II) ion in water, a process referred to as "aging." This aging reaction can be accelerated by the addition of excess alkali cation, especially cesium. Both aging in water only and cesium-promoted aging give hydride concentrations of about 40% of the total cobalt. Borohydride reductions give essentially 100% hydride. In this study we have examined the hydride species from all three sources.

Isoprene Polymerization. In aqueous emulsion systems, potassium pentacyanocobaltate hydride was found to be active in the initiation of

TABLE I
Isoprene Polymerization with Potassium Pentacyanocobalt Hydride^a

Preparation	[Co], mmole/l.	Temp, °C	Time, hr	Conversion, %
NaBH ₄	0	0	53	0
	24	0	24	11
NaBH ₄	0	RT	120	0
	24	RT	"	72
	0	40	"	2.1
	24	40	"	94
	0	60	"	29 ^b
CsCl	24	60	"	83
	0	40	40	0
	24	40		82
	0	60		23 ^b
Aging	24	60		77
	0	40	17	0
	24	40	17	31

^a Conditions: 5 ml isoprene, 10 ml H₂O, 0.3 g Na-p-DOBS.

^b This activity at 60°C in the absence of catalyst must be due to traces of peroxide in the emulsifier.

TABLE II
Effect of Cobalt Concentration on Polymerization of Isoprene
with Hydrido Pentacyanocobaltate(III)^a

Catalyst	Preparation	[Co], mmole/l.	Conver- sion, %	Structure		
				<i>trans</i> , %	<i>cis</i> , %	1,2, % ^b
CoCl ₂	—	2.4	0	—	—	—
CoCl ₂	—	0.24	0	—	—	—
K ₃ Co(CN) ₅	Co ⁺² + 5 KCN	2.4	59	61.8	28.5	4.7
K ₃ Co(CN) ₅	Co ⁺² + 5 KCN	0.24	21	61.9	21.0	8.6
K ₃ Co(CN) ₅ -H	Co ^{+2c} + 10 BH ₄ ⁻	2.4	70	62.0	25.1	6.5
K ₃ Co(CN) ₅ -H	Co ⁺² + 10 BH ₄ ⁻	0.24	79	—	—	—

^a Conditions: 48 hr, 40°C; 1.5 g Na-p-DOBS, 50 ml H₂O; 25 ml isoprene.

^b The 3,4-structure content is usually about the same as that of 1,2.

^c As Co(CN)₅⁻³.

free radical polymerization of isoprene irrespective of the method of preparation.* The results of this study are summarized in Table I.

Further study of the effect of lower cobalt concentrations on the polymerization of isoprene was carried out in argon-sparged pressure bottles at 40°C (see Table II).

As shown in Table II, solutions of cobaltous chloride and emulsifier were completely ineffective in making polymer. This, in our opinion, is indica-

* This is an important observation because of the fact that borohydride and the emulsifier alone can be productive of radical polymerization.

tive of an essentially peroxide-free emulsifier.* However, the surprising result in Table II is the observation that $K_3Co(CN)_5$ and $K_3Co(CN)_5H$ are about equally effective in promoting the polymerization of isoprene at $[Co] = 2.4$ mmole/l., whereas at $[Co] = 0.24$ mmole/l., the hydrido species is about four times as effective. We presume that the reason $K_3Co(CN)_5$ is more effective at $[Co] = 2.4$ mmole/l. than at 0.24 mmole/l. is because of the relatively more rapid formation of the hydride itself by the *in situ* aging with water.^{14,15} In fact, it has been shown that the aging is at best very slow when the Co concentration is low (<100

TABLE III
Butadiene Polymerization with Pentacyanocobalt Hydride^a

[Co], mmole/l.	p-DOBS, g/10 ml	Conver- sion, %	Structure		
			<i>cis</i> , %	<i>trans</i> , %	1,2, %
2.4	0.03	26	30	52	18
2.4	0.03	24	25	56	19
2.4	0	0	—	—	—
2.4	0	1	—	—	—
2.4 ^b	0.03	25	39	42	19
2.4 ^b	0.03	25	33	49	18
24	0.03	49	27	51	22
24	0.3	100	26	53	21
24	(Makon NF-5) ^c 0.1	1	—	—	—
24	0.03	0	}	with 1-pentene	
24	0.3	0			
24	(Makon NF-5) ^c 0.1	0			
24	(Makon NF-5) ^c 0.1	0			

^a Conditions: 5 days, 40°C; 5.5 ml butadiene, 10 ml aqueous Co solution.

^b These experiments included some colloidal cobalt (?) which formed during the preparation of the hydride catalyst; all preparations were made by $NaBH_4$ reduction of $K_3Co(CN)_5$.

^c A nonionic emulsifier sold by Stepan Chemical Company.

mM).¹⁵ On the other hand, it will be noted that when one starts with the Co—H species (last two entries of Table II), there is experimentally little difference in the overall conversion to polymer at $[Co] = 2.4$ mmole/l. as compared to 0.24 mmole/l. This latter observation is consistent with the effective initiating capability of very low concentrations of the pure hydrido species.

Butadiene Polymerization. Similarly, potassium pentacyanocobalt hydride was found to be an effective catalyst for the emulsion (anionic emulsifier, sodium *p*-dodecylbenzene sulfonate) polymerization of butadiene; representative data are summarized in Table III.

The microstructure of the polybutadiene as determined by an infrared film analysis is also seen to be typically free radical in nature.

* However, in our experience, butadiene is much less susceptible to radical-producing impurities than is, e.g., isoprene.

In contrast to butadiene, no activity whatsoever was shown for a simple α -olefin, 1-pentene (see the last three entries). The failure of the catalyst to act in the presence of the nonionic emulsifier (Makon NF-5; a polyether) may reflect the fact that the latter is a good "radical trap" although this was not established.

Alkylpentacyanocobalt Complexes

The effective initiating capability of $\text{Co}(\text{CN})_5\text{H}^{-3}$ suggested to us the use of the alkyl complexes of cobalt, $\text{K}_3\text{Co}(\text{CN})_5\text{R}$, reported by Halpern.⁹ Solutions of the benzyl and allylpentacyanocobalt complexes were made *in situ* from $\text{K}_3\text{Co}(\text{CN})_5$ and the corresponding alkenyl bromide by Halpern's technique. The results of some representative experiments are shown in Table IV.

TABLE IV
Polymerization of Dienes with Alkylpentacyanocobaltate Complexes^a

Diene	Catalyst	[Co], mmole/l.	Conver- sion, %	Structure		
				<i>trans</i> , %	<i>cis</i> , %	1,2, %
Butadiene	—	0	0	—	—	—
Butadiene	$\text{K}_3\text{Co}(\text{CN})_5\text{-CH}_2\text{C}_6\text{H}_5$	24	94	50.8	27.1	22.1
Butadiene	$\text{K}_3\text{Co}(\text{CN})_5\text{-C}_3\text{H}_5$	24	82	58.4	21.8	19.8
Butadiene	$\text{K}_3\text{Co}(\text{CN})_5$	24	48	59.0	22.4	18.7
Isoprene	—	0	0	—	—	—
Isoprene	$\text{NaCo}(\text{CN})_5\text{-CH}_2\text{C}_6\text{H}_5$	48	>76 ^b	70.5 ^c	21.4	8.1
Isoprene	$\text{K}_3\text{Co}(\text{CN})_5\text{-C}_3\text{H}_5$	24	91	61.6	27.3	5.5

^a Conditions: 44 hr, 40°C; 1.5 g Na-p-DOBS, 50 ml; 25 ml isoprene or butadiene.

^b In 41 hr; structure shown was run on a sample made in another run at 0–5°C, 93% conversion to polymer in 2 days with no methanol present; 4 mmoles/l in Co.

^c Includes 3,4 structure.

Clearly these alkyl cobalt complexes are effective polymerization initiators for either butadiene or isoprene. In all probability, as with the hydrido species, they could be used at much lower concentrations; however, we have not attempted to study them extensively below 24 mmole/l. In every case, within experimental error of determination, the microstructure of the polymers is about that expected for typical free radical-initiated polydienes.

Miscellaneous Transition Metal Hydride Complexes

Several other stable hydrides and some presumably "transient" hydrides were examined for polymerization activity with isoprene (40–60°C). The list included those complexes listed in Table V.

In none of these cases was evidence found for significant polymerization activity with isoprene over and above that observed with controls. Surprisingly, the last two complexes even showed some inhibitory effects at higher catalyst concentrations (see Table VI).

TABLE V

Complex	Preparation
<i>trans</i> -(Et ₃ P) ₂ Pt(Cl)-H	Neat ¹⁶
H-Co[(C ₆ H ₅) ₂ P-CH ₂ -CH ₂ -P(C ₆ H ₅) ₂] ₂	Neat ¹⁷
Fe(C ₅ H ₅)(CO) ₂ Cl (+ NaBH ₄)	In situ ¹⁸
Ru[(C ₆ H ₅) ₂ P-CH ₂ -P(C ₆ H ₅) ₂] ₂ (Cl)-H	Neat ¹⁹
<i>trans</i> -[Co(en) ₂ Cl ₂]Cl (+ NaBH ₄)	In situ ²⁰

TABLE VI

Inhibition of Isoprene Polymerization by Transition Metal Complexes^a

Complex	[Complex], mmole/l.	Temp, °C	Time, hr	Conversion, %
Ru[(C ₆ H ₅) ₂ P-CH ₂ -P(C ₆ H ₅) ₂] ₂ (Cl)-H	0	40	26	0
	0.5			15
	0.9			10.7
	4.2			3.2
	10.2			3.8
	19.3			0.3
<i>trans</i> [Co(en) ₂ Cl ₂]Cl ^b	0	40	96	0
	10			0
	20			0
	0	60	96	25
	10			0
	10			0
	20			0

^a Conditions: 5 ml isoprene; 10 ml water; 0.3 g Na-p-DOBS.^b Wilkinson and Gillard²¹ have postulated a *trans*-to-*cis* isomerization via a hydride intermediate. They have found that NaBH₄ catalyzes this easily observed isomerization (green to pink). Although no NaBH₄ was present in the above example, the color change from green to pink was observed. In an experiment at 0°C in which NaBH₄ was present, the color change was also observed and again no polymer was formed.

Inhibition of Free Radical Polymerization by Transition Metal Complexes

Some complexes tested for catalytic activity actually exhibited inhibiting tendencies, reducing the yield of free radical product from that found in control runs. Clear examples of this behavior were found with *trans*-Ru[(C₆H₅)₂P-CH₂-P(C₆H₅)₂]₂(Cl)-H and *trans*-[Co(en)₂Cl₂]Cl (see Table VI). It should be noted that the free-radical emulsion polymerization of isoprene at 60°C in the absence of any catalyst is very difficult to suppress and must come from traces of peroxide in the emulsifier. Yet as seen in Table VI, a 10–20 mmole/l. solution of [Co(en)₂Cl₂]Cl appears to be very effective in inhibiting any radical polymerization.

Inhibition by transition metal compounds has been described in the literature in very similar emulsion polymerizations.^{22,23} A plausible mechanism for such a reaction entails ligand transfer from the transition metal to the free radical. Ligand transfer of halide specifically is a well-known reaction.^{24,25} Chloride "*trans*" to hydride would be expected to

undergo ligand transfer with ease; perhaps the inhibition with the Ru complex is an example of this.

Initiation with Borohydride and Emulsifier

In the course of this work on several occasions it was observed that combinations of sodium borohydride and anionic emulsifier (Na-p-DOBS) were effective free radical initiators for polyisoprene. Representative examples of these polymerizations are shown in Table VII where it is seen that use of a 240 mmole/l. NaBH_4 solution leads to low but significant yields of polymer in 48 hr at 40°C . Reasoning that this was due to the interaction of trace metal ions in the hydride and traces of peroxide in the emulsifier, an attempt was made to sequester these ions by adding tetramethylethylenediamine (TMED) and a Versene- Fe^{+3} solution. Neither

TABLE VII
Emulsion Polymerization of Isoprene with Sodium Borohydride^a

Diene	[NaBH_4], mmole/l.	Chelator	Conversion, %	Structure		
				<i>trans</i> , %	<i>cis</i> , %	1,2, %
Isoprene	0	—	0	—	—	—
Isoprene	240	Versene- Fe^{3+}	8	61.6	27.3	5.6
Isoprene	240	—	10	60.4	23.5	8.0
Isoprene	0	—	0			
Isoprene	240	TMED	25	Insoluble gel		
Isoprene	240	—	10	64.3	22.9	6.4

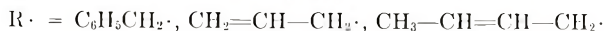
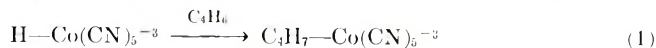
^a Conditions: ≤ 48 hr, 40°C .

of these chelators was effective in stopping polymerization, nor could we find evidence for any significant trace metal ions in the borohydride when it was subjected to analysis by emission spectroscopy. We have no definitive explanation for the borohydride activity at this time, but simply suggest that caution must be exercised in interpreting data where excess borohydride has been used to generate other species *in situ* in an emulsion polymerization system. Our data, however, show that this is not a complicating factor in our work with cobalt since borohydride-free, aged $\text{K}_3\text{Co}(\text{CN})_5\text{H}$ is similar to the $\text{K}_3\text{Co}(\text{CN})_5\text{H}$ prepared with borohydride.

CONCLUSIONS

We conclude that both $\text{HCo}(\text{CN})_5^{-3}$ and $\text{RCo}(\text{CN})_5^{-3}$ complexes are useful initiators for the polymerization of butadiene and isoprene in an aqueous emulsion system. However, the polydienes obtained have microstructures consistent only with free radical initiation and propagation. Therefore, it is suggested that the initiation step in the absence of oxygen is the homolytic cleavage of an $\text{R}-\text{Co}$ bond [eq. (2)]. In the case of the

hydrido complex, the alkylcobaltate complex is derived by reaction with the diene as suggested by Kwiatek²⁶ and shown for butadiene in eq. (1):



As reported above, unsuccessful attempts were made to polymerize isoprene with other hydrido complexes of Co, and complexes of Fe, Ru, and Pt. We can only presume in these cases that any alkyl-transition metal bonds which may have formed were relatively stable to homolytic cleavage at 40–60°C, the operating range of these experiments.

We also conclude as have others that certain halogen-containing transition metal complexes are relatively effective inhibitors for the free radical polymerization of dienes and, therefore, any initiating capacity may be masked by the ability of the complex to capture free radicals.

References

1. R. E. Reinhart, H. P. Smith, H. S. Witt, and H. Romeyn, Jr., *J. Amer. Chem. Soc.*, **83**, 4864 (1961).
2. R. S. Berger and E. A. Youngman, *J. Polym. Sci.*, **2**, 357 (1967).
3. L. B. Luttinger, *Chem. Ind.* (London), **1960**, 1135; *J. Org. Chem.*, **27**, 1591 (1962).
4. L. B. Luttinger and E. C. Colthup, *J. Org. Chem.*, **27**, 3752 (1962).
5. M. L. Green, M. Nehmé, and G. Wilkinson, *Chem. Ind.* (London), **1960**, 1136.
6. A. J. Canale, W. A. Hewett, T. M. Shryne, and E. A. Youngman, *Chem. Ind.* (London), **1962**, 1054.
7. M. Takahashi, *Bull. Chem. Soc. Japan*, **36**, 622 (1963).
8. S. Aoki, C. Shirafuji, and T. Otsu, *Makromol. Chem.*, **126**, 1 (1969).
9. J. Halpern and J. P. Maher, *J. Amer. Chem. Soc.*, **86**, 2311 (1964).
10. J. L. Binder, *Anal. Chem.*, **26**, 1877 (1954).
11. H.-Yu Chen, *Anal. Chem.*, **34**, 1793 (1962).
12. M. A. Descamps, *C. R. Acad. Sci. (Paris)*, **67**, 330 (1868).
13. M. Iguchi, *Kogyo Kagaku Zasshi*, **63**, 534 (1942).
14. N. K. King and M. E. Winfield, *J. Amer. Chem. Soc.*, **83**, 3366 (1961).
15. G. A. Mills, S. Weller, and A. Wheeler, *J. Phys. Chem.*, **63**, 403 (1959).
16. J. Kwiatek, I. Mador, and J. Seyler, *J. Amer. Chem. Soc.*, **84**, 304 (1962).
17. J. Chatt and B. L. Shaw, *J. Chem. Soc.*, **1962**, 5075.
18. F. Zingales, F. Canziani, and A. Chiesa, *Inorg. Chem.*, **2**, 1303 (1963).
19. T. S. Piper, F. A. Cotton, and G. Wilkinson, *J. Inorg. Nuc. Chem.*, **1**, 165 (1955).
20. J. Chatt and R. G. Hayter, *J. Chem. Soc.*, **1961**, 2605.
21. R. D. Gillard and G. Wilkinson, *J. Chem. Soc.*, **1963**, 3594.
22. R. E. Reinhart, H. P. Smith, H. S. Witt, and H. Romeyn, Jr., *J. Amer. Chem. Soc.*, **84**, 4145 (1962).
23. N. N. Dass and M. H. George, *J. Polym. Sci. A-1*, **7**, 269 (1969).
24. H. E. De La Mare, J. Kochi, and F. F. Rust, *J. Amer. Chem. Soc.*, **85**, 1437 (1963).
25. J. Kumamoto, H. E. De La Mare, and F. F. Rust, *J. Amer. Chem. Soc.*, **82**, 1935 (1964).
26. J. Kwiatek and J. Seyler, *J. Organomet. Chem.*, **3**, 421 (1965).

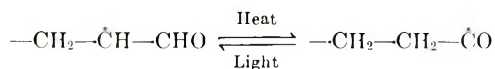
Received November 10, 1970

ESR Study of Free Radicals Produced in Polyethylene Irradiated by Ultraviolet Light

YOSHIMASA HAMA, KAZUYA HOSONO, YASURO FURUI, and KENICHI SHINOHARA, *Science and Engineering Research Laboratory, Waseda University, Tokyo, Japan*

Synopsis

ESR studies of ultraviolet-irradiated polyethylene (PE) were carried out. Irradiation effects different from those of high-energy radiation are observed. Ultraviolet radiation is absorbed selectively, and especially in carbonyl groups in PE produced by oxidation. Radicals produced were identified as $-\text{CH}_2-\dot{\text{C}}\text{H}-\text{CHO}$ and $-\text{CH}_2-\dot{\text{C}}\text{H}-\text{CH}_2-$. Some radicals giving a quintet signal stable at room temperature were also observed but remained unidentified. The radical $-\text{CH}_2-\dot{\text{C}}\text{H}-\text{CHO}$ undergoes a mutual conversion with the acyl radical:



INTRODUCTION

Electron spin resonance (ESR) studies of free radicals produced in irradiated high polymers have been reported by many authors. In most cases, free radicals were produced by high-energy radiation such as γ -rays, electron beams, or x-rays. There are, however, also some ESR studies on the effect of ultraviolet light on high polymers. Charlesby et al.¹ have made a comparison of the effect of ultraviolet and γ -radiation on poly-(methyl methacrylate). Browning et al.² have reported that alkyl radicals are produced in polyethylene in ESR study of ultraviolet-irradiated polyolefins. Rånby et al.³ made some observations on free radicals produced in ultraviolet-irradiated polyethylene. They also detected methyl radicals in ultraviolet-irradiated polypropylene.

In our recent ESR study of ultraviolet-irradiated polyethylene, it was found that major absorption of light occurs at oxidized segments in the sample and that the resulting acyl radicals $-\text{CH}_2-\text{CH}_2-\dot{\text{C}}\text{O}$ are converted by absorption of visible light to $-\text{CH}_2-\dot{\text{C}}\text{H}-\text{CHO}$.⁴

The present paper concerns a more detailed study of the ESR spectra produced by ultraviolet irradiation of polyethylene and the photoinduced isomerization of the resulting radicals.

EXPERIMENTAL

Materials

Polyethylene used in the present work was Hizex 1200J (high density) manufactured by Mitsui Toatsu Chemicals, Inc. The sample was purified first by dissolving in boiling xylene and precipitating by cooling and then was washed in *n*-hexane and acetone and dried at about 343°K in a vacuum oven. A rod-shaped sample, about 3.5 mm in diameter, was prepared from this purified polyethylene by extrusion through a nozzle at 403°K. It was sealed in Spectrosil tube after being evacuated in a vacuum of 10^{-4} – 10^{-5} torr for one day at room temperature. Oriented samples were prepared by stretching the rod-shaped sample up to about 1000% at room temperature.

Irradiation

Irradiation was carried out with ultraviolet light from a super high-pressure mercury lamp (USH-250D) and a low-pressure mercury lamp (UL2-1HQ), manufactured by Ushio Electric Co. Ltd. Predominant wavelengths of the super high pressure mercury lamp are 4358 Å, 3650 Å (strongest), 3132 Å, and a trace of 2537 Å; those of the low-pressure mercury lamp are 2537 Å and 1849 Å. In all cases of ultraviolet irradiation, the sample was kept in liquid nitrogen. In some cases, various color filters were used for selecting light of desired wavelengths from the lamp.

ESR Measurement

ESR measurements were carried out by using an X-band spectrometer manufactured by Japan Electron Optics Laboratory Co., Ltd., with 100 kHz field modulation. Measurements at 77°K were made by inserting a Dewar flask with a transparent cylindrical tip into the cavity. The sample was held in the Dewar flask filled with liquid nitrogen.

Heat treatment of the sample was carried out by keeping the sample in a liquid bath of a fixed temperature for 4 min and then returning it quickly into liquid nitrogen.

RESULTS

ESR Spectra of Ultraviolet-Irradiated Polyethylene

The ESR spectrum of polyethylene (PE) irradiated by ultraviolet light from the super high-pressure mercury lamp at 77°K and measured at 77°K immediately after irradiation is shown in Figure 1a. It consists of a superposition of a signal with hyperfine structure and a central broad singlet. The main feature of this hyperfine structure seems to be that of a sextet with an average hyperfine splitting of about 30 gauss, though the feature at the central part is masked by the broad singlet. It is well known that such a spectrum for PE is assigned to the alkyl radical $-\text{CH}_2-\dot{\text{C}}\text{H}-\text{CH}_2-$.⁵⁻⁷ Therefore, this hyperfine spectrum may also be attributed to

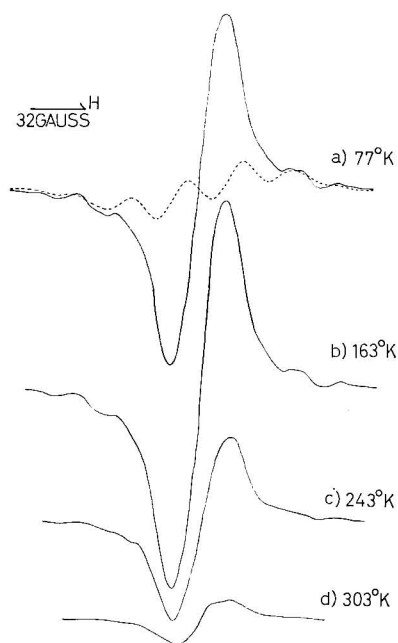


Fig. 1. ESR spectra of PE irradiated by ultraviolet light from super high-pressure mercury lamp: (a) observed immediately at 77°K after irradiation; (b), (c), (d) observed at 77°K after heat treatment of (a) at indicated temperatures; (---) theoretical curve for alkyl radical.

alkyl radicals. The spectrum calculated for alkyl radical is shown in Figure 1a by the broken line.

This interpretation that the hyperfine structure is given mostly by alkyl radicals was ascertained by using a stretched PE. The spectrum of the stretched PE irradiated by the super high-pressure mercury lamp and observed with the applied magnetic field perpendicular to the direction of stretch, is shown in Figure 2a. This spectrum is similar to that obtained by Libby et al.⁸ for a stretched PE by high energy radiation which is known to produce alkyl radicals.

ESR spectrum of PE irradiated with ultraviolet light from the low-pressure mercury lamp and observed at 77°K is shown in Figure 3a. Some differences from the ESR spectrum (shown in Fig. 1a) obtained by using the super high-pressure mercury lamp are observed in the central portion. This is due to more rich production, in Figure 3a, of alkyl-type free radicals which have an even number of hyperfine splittings. Since the ultraviolet light from the low-pressure mercury lamp contains a strong light of wavelength 2537 Å this suggests that the alkyl radicals are mainly produced by the light of this wavelength.

ESR spectra of PE irradiated by ultraviolet light filtered through UV-29 or UV-31 filters which cut out wavelengths below 2900 Å and 3100 Å, respectively, are shown in Figure 4. The two spectra look alike and do not

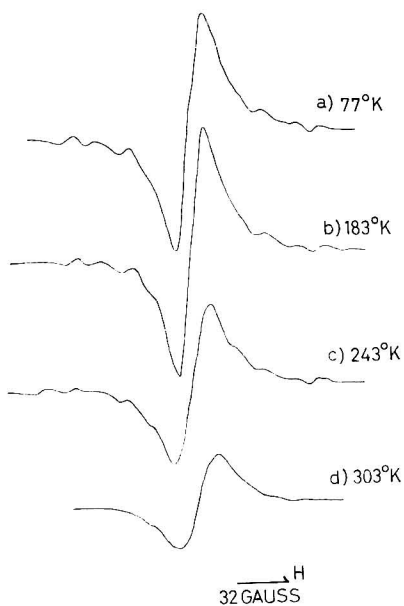


Fig. 2. ESR spectra of stretched PE, irradiated by super high-pressure mercury lamp, observed with applied magnetic field perpendicular to the direction of stretch: (a) observed immediately at 77°K after irradiation; (b), (c), (d) observed at 77°K after heat treatment of (a) at indicated temperatures.

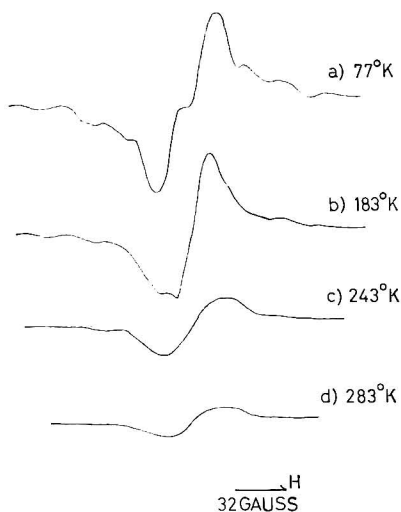


Fig. 3. ESR spectra of PE irradiated by low-pressure mercury lamp: (a) observed immediately at 77°K after irradiation; (b), (c), (d) observed at 77°K after heat treatment of (a) at indicated temperatures.

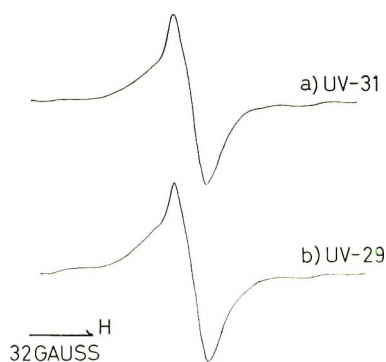


Fig. 4. ESR spectra of PE irradiated by using color filters UV-31 and UV-29.

contain hyperfine structure. The alkyl radicals giving the hyperfine structure are produced only by light of wavelength below 2900 Å.

Change of the Line Shape with the Temperature of Heat Treatment

Figs. 1b–1d show the change of the line shape of the spectrum observed at 77°K on heat treatment at various temperatures. The height of the central broad singlet begins to increase at about 163°K, as the temperature of heat treatment is raised, reaching a maximum at about 183°K. The shape of the broad singlet also changes to a sharp singlet during the course of this change and, as a result, the spectral intensity of the singlet does not noticeably change. The hyperfine spectrum, on the other hand, decreases gradually from about 163°K.

At temperatures above 183°K, the central singlet, too, decreases gradually and a weak broad singlet remains at 303°K. The line width between points of maximum slope ΔH_{msl} of this singlet was 24–30 gauss.

The ESR spectrum obtained by irradiation with ultraviolet light from the low-pressure mercury lamp also showed a similar change with the temperature of the heat treatment.

Irradiation of Oxidized PE

Browning et al.² noted that ultraviolet light tends to be selectively absorbed by impurities and chain imperfections (e.g., olefinic or oxidized segments), in the ESR study of ultraviolet-irradiated polyolefins. In the present work, it may be possible that the sample is oxidized slightly in the process of preparation and that ultraviolet light may be absorbed by the oxidized segment to produce free radicals.

In order to get some evidence on this matter, a measurement was carried out on PE oxidized by ultraviolet irradiation in air. The ESR spectra of such sample irradiated *in vacuo* at 77°K by the super high-pressure mercury lamp and observed at 77°K after heat treatment at various temperatures are shown in Figure 5. The efficiency of radical production was higher in the oxidized sample than in the unoxidized one. It is also seen

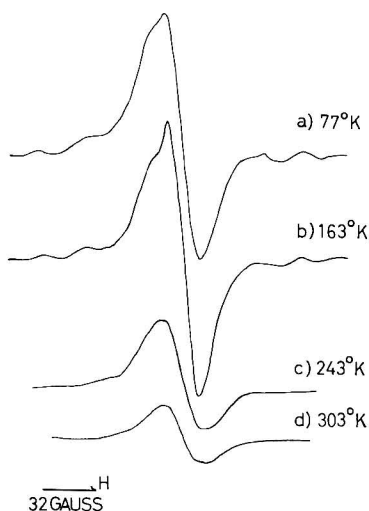


Fig. 5. ESR spectra of oxidized PE, irradiated by super high-pressure mercury lamp: (a) observed immediately at 77°K after irradiation; (b), (c), (d) observed at 77°K after heat treatment of (a) at indicated temperatures.

in Figure 5 that the central sharp singlet is more prominent. On heat treatment at temperatures above 183°K, the spectrum changes to one similar to that of the unoxidized sample, and a broad singlet spectrum remains at 303°K.

These results show that the broad singlet which is observed immediately after irradiation and changes to the sharp singlet by heat treatment at 163°K is most certainly related to oxidized segments in the main chain.

Effect of Visible Light on the ESR Spectra of Irradiated PE

The central broad singlet observed immediately after irradiation at 77°K increases in height on heat treatment at 183°K, as described above. When such PE is illuminated with visible light from a tungsten lamp at 77°K, the spectrum reverts back to the original spectrum before heat treatment. Heat treatment and illumination with visible light could be repeated for the spectrum reversibly and during the mutual conversion almost no change was observed in the spectral intensity.

The conversion was observed more clearly in the case of the oxidized sample.

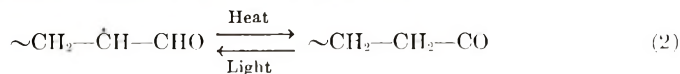
Stable Radicals at Room Temperature

It is shown above that a weak broad singlet with $\Delta H_{msl} = 24\text{--}30$ gauss is observed after heat treatment at 303°K, when the ESR observation is made at 77°K. The width at maximum slope is slightly different for the unoxidized, stretched, and oxidized samples.

When the ESR observation is at room temperature, the appearance of the spectrum is as shown in Figure 6. The spectra are probably a quintet and the splitting is about 11 gauss. The same spectrum is also observed at room temperature when the sample was irradiated with ultraviolet light,

after its formation, causes the migration of a hydrogen atom and a considerable part of the radical I changes to $\sim\text{CH}_2-\dot{\text{C}}\text{H}-\text{CHO}$ (hereafter referred to as radical III). Radical III is expected to give a hyperfine structure. In fact radical III produced in di-*n*-heptadecyl ketone gave a poorly resolvable hyperfine spectrum.⁹ Buley et al.¹¹ showed that the splitting $a_{\text{H}\alpha}$ due to the α -proton of the radical $\cdot\text{CH}_2-\text{CHO}$ is 19.0 gauss. In the present work, however, the radical III observed immediately after irradiation at 77°K seems to have an appearance of a broad singlet. This suggests that oxidized segments may be irregularly present in PE.

Heat treatment causes the radical III to return to the original acyl radical I and a sharp singlet makes its appearance. Mutual conversion between these two radicals can be written as in eq. (2):



Light of wavelength below 6500 Å was effective in the conversion of radical I to radical III.

Acyl radicals I may be produced by ultraviolet irradiation from carbonyl groups situated at chain ends or on some points along the chain. If the reaction occurs at a carbonyl group situated at a chain end, only acyl radical I produced by reaction (3) will be observed in ESR measurement.



The hydrogen atom will probably unite quickly with another hydrogen atom to become H_2 even at 77°K.

The observation shown in Figure 4, that ultraviolet light of wavelength above 2900 Å produces radicals giving only the singlet spectrum and no hyperfine structure in PE, indicates that such light reacts only with carbonyl groups at the chain end when PE is irradiated to produce acyl radicals.

Light of wavelength below 2900 Å, including that of 2537 Å, will react also with carbonyl groups situated at random points along the chain and produce radicals I and II as in eq. (1).

Radicals Giving Hyperfine Structure

An observation was made by Ohnishi et al.¹² that allyl radicals in PE are converted to alkyl radicals by illumination of light of 2537 Å. Radicals II and III, in our case, may be expected to undergo similar conversion by absorption of visible or ultraviolet light from the mercury lamp during the irradiation.

The fact that the major feature of the hyperfine spectrum is explained as a sextet arising from alkyl-type radicals suggests that most of the radicals II have converted to alkyl-type radicals to give the hyperfine structure.

Some of the radicals III, too, have probably changed to alkyl-type radicals during the irradiation because of the following reasons.

The irradiation of PE by unfiltered light from the super high-pressure mercury lamp causes scission of the main chain at carbonyl groups situated

at random on the chain to produce radicals II and III in equal quantities, in addition to the production of radicals III from carbonyl groups situated at chain ends. Therefore, the intensity of the singlet should exceed that of the hyperfine spectrum if no conversion of radicals III occurs.

The broad singlet due to radicals III and the hyperfine spectrum, however, were observed to appear in comparable intensities. This fact suggests that the conversion of radicals III to alkyl-type radicals is occurring during the irradiation. The result that only a singlet was observed in the irradiation by light of wavelength above 2900 Å shows that such conversion occurs by light of wavelength below 2900 Å.

Further, the observation that the irradiation by the low-pressure mercury lamp produces more abundant alkyl-type radicals than the irradiation by super high-pressure mercury lamp, probably, indicates that the light of 2537 Å is effective in causing the conversion.

Radicals Stable at Room Temperature

It is stated above that a weak broad singlet is observed at 77°K after heat treatment at 303°K and that this spectrum shows hyperfine structure when the measurement is done at room temperature.

Rånby et al.³ observed what was probably the same spectrum, and they attributed it to polyenyl type radicals which, they thought, are converted from radical II by dehydrogenation. Our observation that the radicals giving this weak singlet are also produced in liquid oxygen and that they are comparatively stable in air at room temperature shows that the radicals are probably related to oxidized sites in polyethylene. The identification of the radical responsible for the spectrum is not yet possible.

We wish to thank late Professor S. Okamoto for helpful discussions.

References

1. A. Charlesby and D. K. Thomas, *Proc. Roy. Soc. (London)*, **A269**, 104 (1962).
2. H. L. Browning, Jr., H. D. Ackermann, and H. W. Patton, *J. Polym. Sci. A-1*, **4**, 1433 (1966).
3. B. Rånby and H. Yoshida, in *Perspectives in Polymer Science (J. Polym. Sci. C, 12)*, E. S. Proskauer, E. H. Immergut, and C. G. Overberger, Eds., Interscience, New York, 1966, p. 263.
4. Y. Hama, Y. Furui, K. Hosono, and K. Shinohara, *Repts. Progr. Polym. Phys. Japan*, **12**, 481 (1969).
5. B. Smaller and M. S. Matheson, *J. Chem. Phys.*, **28**, 1169 (1958).
6. E. J. Lawton, J. S. Balwit, and R. S. Powell, *J. Chem. Phys.*, **33**, 395 (1960).
7. S. Ohnishi, Y. Ikeda, M. Kashiwagi, and I. Nitta, *Polymer*, **2**, 119 (1961).
8. S. Libby and M. G. Ormerod, *J. Phys. Chem. Solids*, **18**, 316 (1961).
9. Y. Hama and K. Shinohara, *Mol. Phys.*, **18**, 279 (1970).
10. S. Noda, K. Fueki, and Z. Kuri, *J. Chem. Phys.*, **49**, 3287 (1968).
11. A. L. Buley, R. O. C. Norman and R. J. Pritchett, *J. Chem. Soc. B*, **1966**, 849.
12. S. Ohnishi, S. Sugimoto, and I. Nitta, *J. Chem. Phys.*, **39**, 2467 (1963).

Received May 4, 1970

Revised July 1, 1970

Graft and Modified Polymers from Rubber Network.

I. Method of Obtaining Graft and Modified Polymers from Sulfur Vulcanizates with Dehydrogenated Raney Nickel and Raney Cobalt

P. D. NIKOLINSKI and V. V. MIRTSHEVA, *Department of Organic Synthesis, Institute of Chemical Technology, Sofia, Bulgaria*

Synopsis

The present paper reports on an investigation of eliminating sulfur from sulfur vulcanizates by using dehydrogenated Raney Ni (Raney Co). The dehydrogenated Raney metal eliminates the sulfur by forming free radicals which recombine with each other. The result is a heavily crosslinked product containing traces of sulfur. When applying dehydrogenated Raney metal in the presence of substances readily producing free radicals or monomers polymerizing by way of a free-radical mechanism, one obtains a modified or a grafted high molecular product.

By desulfurizing sulfur vulcanizates with dehydrogenated Raney nickel and Raney cobalt in the presence of monomers which are easily polymerized by a free-radical mechanism or of substances yielding free radicals, we obtained graft polymers and modified rubber products.

The use of dehydrogenated Raney nickel for the desulfurization of some organic sulfur compounds has been reported in the literature. Hauptmann and Wladislaw et al.^{1,2} have effected desulfurization of organic disulfides, ethyl and phenyl esters of thiobenzoic acid by employing partially dehydrogenated Raney nickel. The mechanism of desulfurization with Raney nickel may be outlined as follows.³ First, the sulfur chemisorbed on the Raney nickel surface combines with the nickel and forms a Ni-S bond; this is followed by breaking of the C-S bond resulting in the formation of free radicals and Ni sulfide. The hydrogen of the Raney Ni, if the latter contains any, combines with the free radicals. In case of lack of hydrogen the free radicals recombine. The radical hydrogenation and recombination processes develop simultaneously, their rate being dependent on the amount of hydrogen sorbed on the Raney nickel.



In case of hydrogen shortage in the Raney metal, a high yield of dimeric products is obtained and the C-S bond is replaced by a C-C bond. On

desulfurizing polycyclic sulfides, Birch⁴ has obtained olefins in about 60% yield. Desulfurization of sulfur-rubber networks with Raney metals rich in hydrogen (about 100 cm³ H₂/g metal) brings about decomposition of the network and replacement of C-S bonds by C-H bonds. The result is a product containing no sulfur and soluble in the usual organic solvents for natural rubber.^{5,6} Desulfurization with dehydrogenation Raney metal (containing about 5 cm³ H₂/g metal) results in a product containing traces of sulfur but insoluble in organic solvents (only swelling) and having a much higher degree of crosslinking than the initial sulfur vulcanizate. The probable explanation of this finding was given by us in a previous paper.⁷ We assume that the additional crosslinking is a result of recombination to C-C intermolecular bonds of radicals formed as a result of eliminating the intramolecularly combined sulfur from the Raney Ni. The recombination of the free radicals is somewhat hampered by the poor mobility of the rubber molecules fixed in the network of the vulcanizate. Due to the above, when desulfurization is carried out in the presence of monomers subject to ready free-radical polymerization, the radicals obtained by elimination of sulfur initiate polymerization, yielding graft polymers. Desulfurization of the vulcanizate with dehydrogenated Raney Ni in the presence of compounds yielding free radicals (benzoyl peroxide, triphenylchloromethane, etc.) results in modified products.

Experimental

For preparation of graft and modified polymers rubber networks obtained by the curing recipe of Table I were used.

Press curing was carried out at 100°C for 2 hr. The concentration of intermolecular chemical crosslinks, determined by the Flory and Rehner⁸ and Moore and Watson⁹ calibration was $0.32 \pm 0.01 \times 10^{-4}$ moles/cm³.

The vulcanizate was crumbed by means of rollers with 1:1.17 friction and the resulting rubber crumbs were sifted to 28 mesh and extracted with acetone. After complete removal of Captax and free sulfur, the rubber crumbs contained 2.4% sulfur. The analysis for sulfur content was carried out by burning the samples under oxygen flush, and the sulfuric acid was determined by titration.

The desulfurization of the rubber crumbs was by use of Raney Ni and Raney Co.

TABLE I

	Weight units
Natural rubber (white crepe)	100
Stearic acid	2
Zinc oxide	3
Captax	2
Neoson D	1
Sulfur	3

Preparation and dehydrogenation of the metals to Raney form was carried out as follows. A 50-g portion of alloy containing 50% Ni (Co) and 50% Al was treated with 26% solution of NaOH after Pavlik and Adkins.¹⁰ After being washed to neutrality, the Raney Ni (Co) was placed in a flask with two outlets and flushed with nitrogen. During that operation the Raney Ni (Raney Co) was kept on the bottom of the flask by means of a magnet. After that the flask with the Raney nickel (Raney Co) was treated under vacuum (5 mm Hg) and heated for 4 hr at 200°C. The flask with the dehydrogenated Ni or Co was cooled in nitrogen and the Raney nickel (Raney Co) kept submerged in toluene. The amount of hydrogen in the so obtained Raney Ni (Raney Co) was determined by hydrogenation of benzoquinone.¹¹

The desulfurization was carried out in glass ampoules with the vulcanizate network swelled in toluene in nitrogen medium. About 0.5 g of the rubber network was swelled in the material dissolved in toluene and readily yielding free radicals or in the solution of the monomer to be grafted. As substances readily yielding free radicals we used benzoyl peroxide and triphenylchloromethane; the monomers were styrene, methyl acrylate, and acrylonitrile. After 24 hours the ampoules were flushed with nitrogen, 2.5 g of the dehydrogenated Raney Ni (10–15 ml H₂/g metal) or Raney Co added, and the ampoules sealed. The desulfurization was carried out at room temperature for 90 min, with vigorous shaking of the ampoules.

The separation of the desulfurized product and the metal in Raney form was effected by means of a magnet centrifuge. The separated Raney metal is quite good for two more desulfurizations. The traces of Raney metal were removed by processing with 18% hydrochloric acid, after which the desulfurized product was washed with distilled water to neutral reaction and the product dried under vacuum to a constant weight.

To remove benzoyl peroxide the product was extracted with ethyl alcohol at boiling temperature. Every 4 hr the ethyl alcohol was changed and the presence of benzoyl peroxide in the extract checked by the conventional qualitative reactions.¹²

The styrene and polystyrene were removed by extraction with butanone at 50°C, the butanone being changed every 24 hr. This was repeated until styrene and polystyrene were removed completely.

To determine the quantity of sulfur removed by means of Raney Ni or Raney Co, an apparatus for decomposition the NiS with acid¹³ was used, the isolated H₂S being absorbed in 10% solution of Cd(CH₃COO)₂. The quantity of CdS was determined iodometrically.

The solubility of the resulting product was determined in toluene. The toluene was heated to 60°C and flushed for 30 min with nitrogen. A polyamide bag with an exactly weighed amount of desulfurized product was immersed in toluene and heated at same temperature for 6 hr. After that the bag with undissolved product was removed, washed twice with toluene, and dried to constant weight.

In cases when particles of undissolved product pass through the bags, the sol fraction was separated from the gel by centrifugation. Simultaneously and in the same way the solubility of the initial rubber crumb was also determined. The sol fraction was calculated by using the equation:

$$\text{Sol } \% = [(P_1 - P_2)/P_1] - [(P_1^0 - P_2^0)/P_1^0]$$

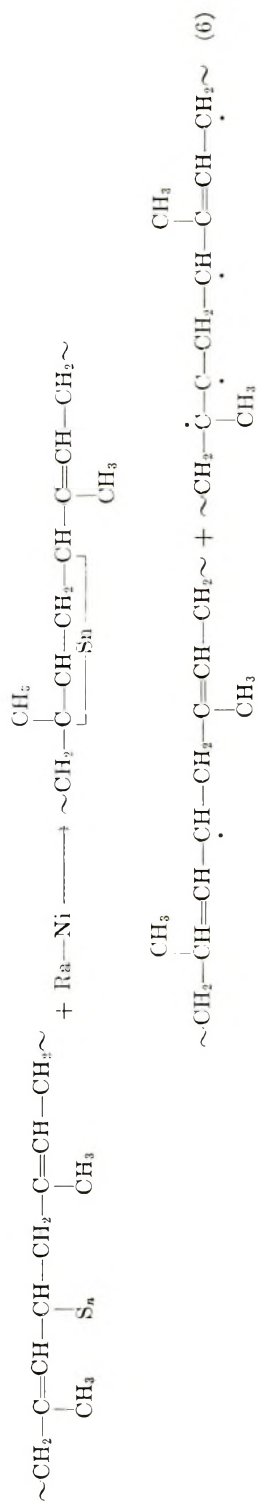
where P_1 and P_1^0 represent the initial weight of the resulting product and of the original vulcanizate, while P_2 and P_2^0 represent the insoluble part of the resulting product and of the original vulcanizate, respectively. We also obtained the infrared spectra of the products in a solution of tetrachloromethane. All experimental results are given in Table II.

TABLE II

Kind of modifying agent	Amount of modifying agent (g/g vulcanizate)	Conditions of reaction				Degree of sulfur removal (%)	Solubility	Proof of functional groups
		Temp. (°C)	Time (min)	Amount of dehydrogenated Ra-Ni	Amount of dehydrogenated Ra-Co			
None	—	20	90	2.5	—	72	Insoluble	—
Benzoyl peroxide	0.3	20	90	2.5	—	68.8	98.2	JR spectra
	0.3	80	90	2.5	—	62.5	69.4	max at 700,
	0.3	20	90	—	2.5	58.7	72.6	1500, 1600 and 3100 cm^{-1}
Triphenylchloromethane	0.5	20	90	2.5	—	56	52	Containing 1.8% chlorine
Styrene	0.5	20	90	2.5	—	78	78.0	JR spectra
	0.5	80	90	2.5	—	70	58.4	max at 700,
	0.5	20	90	—	2.5	65.4	68.3	3000–3100 cm^{-1}
Methylmethacrylate	0.5	20	90	2.5	—	71.4	70.3	—
Acrylonitrile	0.5	20	90	2.5	—	30	10	—

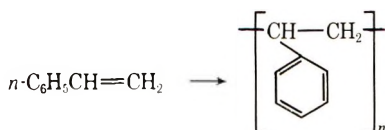
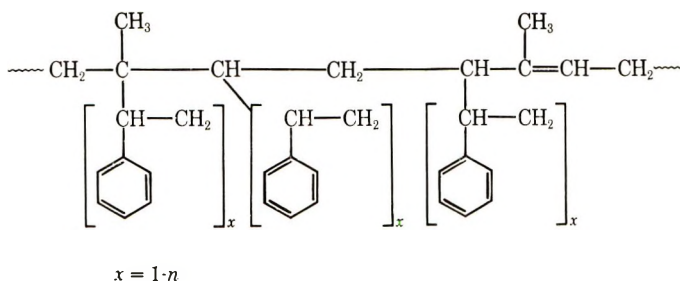
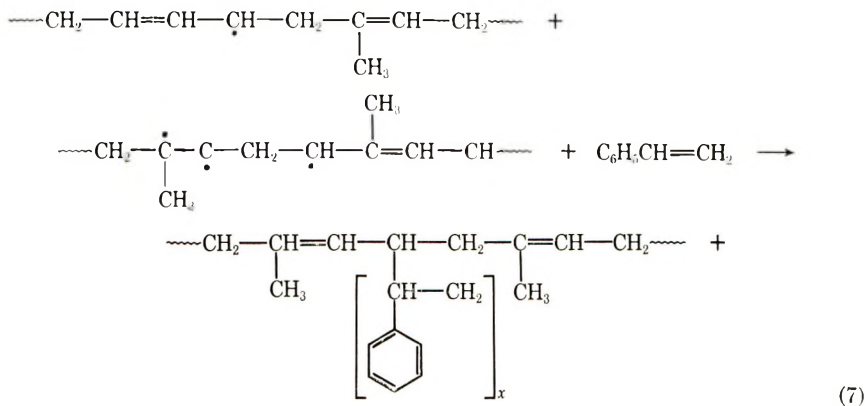
Results and Discussion

The results given in Table II show that by desulfurizing rubber crumb swelled in toluene with Raney Ni, poor in hydrogen, about 72% of the sulfur present in the vulcanizate is eliminated. The obtained product is insoluble in organic solvents of natural rubber and is much more cross-linked ($c = 0.62 \pm 0.01 \times 10^{-4}$ mole/ cm^3) than the original vulcanizate ($c = 0.32 \pm 0.01 \times 10^{-4}$ mole/ cm^3). In our opinion, the additional



Desulfurization in the presence of free radicals obtained from triphenylchloromethane yields a product containing 1.8% chlorine. Its solubility is 52%.

If desulfurization is carried out in the presence of a monomer readily polymerizing by way of a free-radical mechanism, the free radicals obtained upon the elimination of sulfur bring about its polymerization. Desulfurization in the presence of styrene, for instance, involves the process (6)–(8).



The grafts polymers are obtained by reaction (7).

The obtained product is about 78% soluble in toluene (Table II). The unreacted styrene and the polystyrene are eliminated by dissolving in butanone. The infrared spectra show maxima at 3000–3100 cm^{-1} which is characteristic of monoalkylbenzene and at 700 cm^{-1} , characteristic for the benzene nucleus.

When sulfur vulcanizates are desulfurized in the presence of methyl methacrylate by using dehydrogenated Raney Ni (Raney Co), the resulting product is about 70% soluble.

Desulfurization with acrylonitrile leads to the introduction of an insignificant quantity of CN groups into the obtained product. The solu-

bility of the resulting product in toluene is very low (10%), and the degree of sulfur removal is 30%. This is probably due, first, to the fact that the radical polymerization of the acrylonitrile yields crosslinked products and, secondly, to the deactivating effect of the CN group on the Raney Ni (Raney Co).

References

1. H. Hauptmann and B. Wladislaw, *J. Amer. Chem. Soc.*, **72**, 707 (1950).
2. H. Hauptmann, B. Wladislaw, Nazario, L. and W. F. Walter, *Ann*, **576**, 45 (1952).
3. R. G. Pettit and E. E. van Tamelen, *Organic Reactions*, Vol. 12, J Wiley, New York, 1962, pp. 356-529.
4. S. F. Birch, N. J. Hunter, and D. T. McAllan, *J. Org. Chem.*, **21**, 970 (1956).
5. P. D. Nicolinski, Ch. P. Ivanov, V. V. Mirtsheva, and M. A. Krestewa, *C.R. Acad. Bulg. Sci.*, **20**, p. 811 (1967).
6. P. D. Nicolinski and V. V. Mirtsheva, *Kautschuk Gummi, Kunststoffe*, **22**, No. 6, 298 (1969).
7. P. D. Nicolinski, and V. V. Mirtsheva, *Ann. Inst. Chem. Technol. (Sofia)*, **13**, No. 3, 153 (1966).
8. P. Flory and C. Rehner, *J. Chem. Phys.*, **11**, 521 (1943).
9. C. Q. Moore and W. F. Watson, *J. Polym. Sci.*, **19**, 237 (1956).
10. A. Pavlic and H. Adkins, *J. Amer. Chem. Soc.*, **68**, 1471 (1946).
11. O. V. Sokolski, *Akad. Nauk Kaz. S.U., Khim. Nauk*, **2**, 1 (1958).
12. F. Feigl, *Spot Tests in Organic Analysis*, G. Kh., I., Moscow, 1962.
13. A. Trifimov, Ch. Ivanov, and D. Pavlov, *C. R. Acad. Bulg. Sci.*, **7**, 1 (1954).

Received June 29, 1970

Availability and State of Order of Hydroxyl Groups on the Surfaces of Microstructural Units of Crystalline Cotton Cellulose

S. P. ROWLAND, E. J. ROBERTS, and J. L. BOSE, *Southern Utilization Research and Development Division, Agricultural Research Service, U. S. Department of Agriculture, New Orleans, Louisiana 70119*

Synopsis

The relative accessibilities of the hydroxyl groups of the D-glucopyranosyl units of hydrocellulose have been studied by means of the reaction of *N,N*-diethylaziridinium chloride, which produces 2-(diethylamino)ethyl cellulose. The deviation in the distribution of substituents among the 2-*O*-, 3-*O*-, and 6-*O*-positions of the D-glucopyranosyl residues in a hydrocellulose from that in a disordered cellulose in which the three types of hydroxyl groups are equally accessible is the basis for estimating the selective accessibilities of the hydroxyl groups in the crystalline cellulose. A particular hydrocellulose, lying within the range of leveling-off degree of polymerization, was studied in detail; this hydrocellulose, designated EHC ("Exemplar Hydrocellulose"), was formed from fibrous cotton by hydrolysis for 0.67 hr in 2.5*N* hydrochloric acid at reflux. EHC exhibited higher selective accessibility (larger deviation from equal accessibility) of the hydroxyl groups at C-2, C-3, and C-6, than samples of hydrocellulose formed in shorter or longer periods of hydrolysis. This selective accessibility is discussed in terms of intra- and intermolecular hydrogen bonding on the surfaces of crystalline microstructural units in EHC.

INTRODUCTION

Recently, Haworth et al.¹ interpreted the results of multiple methylations of cotton cellulose with dimethyl sulfate, dimethyl sulfoxide, and 2*N* sodium hydroxide to be consistent with a rapid reaction on the surfaces of crystalline elementary fibrils. This was accompanied by a slower reaction which was interpreted to involve penetration into the crystalline regions. From studies of reactions of *N,N*-diethylaziridinium chloride with cotton in solutions of sodium hydroxide ranging from 1*N* to 6*N*, Rowland et al.² found the hydroxyl groups of cotton cellulose to be selectively available or selectively accessible: for every hydroxyl group at C-2 that was accessible for reaction in 1*N* and 2*N* sodium hydroxide there were only approximately 0.75 hydroxyl group at C-6 and 0.30 hydroxyl group at C-3 which were accessible. This selective accessibility is interpreted as evidence that reactions occur, at least in part, with an ordered arrangement of hydroxyl groups on the surfaces of crystalline microstructural units.

The selective accessibilities of hydroxyl groups noted above are representative of the state of order among the hydroxyl groups in the readily

accessible regions of the cotton fiber. It appears reasonable to consider that the regions of lower accessibility (or of inaccessibility) in the cotton fiber might be characterized by a higher state of order of the hydroxyl groups on the surfaces of the crystalline regions. For this very reason, the highly ordered surfaces may be less accessible (or inaccessible) due to regular and strong hydrogen bonding between potential surfaces.

To assess the state of order of the hydroxyl groups on the surfaces of crystalline regions of low accessibility in the cotton fiber, samples of cotton fiber have been converted to hydrocellulose and these have been studied in reactions with *N,N*-diethylaziridinium chloride. A particular sample of hydrocellulose, which falls within the range of leveling-off degree of polymerization³ and which is designated "Exemplar Hydrocellulose" (EHC), has been selected for consideration in this report. The significance of the selective accessibility of hydroxyl groups in EHC is discussed relative to the microstructure of the cotton fiber.

EXPERIMENTAL

Materials

The cotton cellulose was the same as that employed in a preceding study:² i.e., desized, scoured, bleached 80 × 80 print cloth.

2-Chloroethyldiethylamine hydrochloride was the nominal reagent for the reactions yielding 2-diethylaminoethyl celluloses. The nominal reagent (17.2 g, 0.1 mole) was placed in a 100-ml volumetric flask and the volume was made up to the mark with 10% sodium hydroxide. 2-Chloroethyldiethylamine, as the free base, rose to the top of the flask. This layer was withdrawn immediately and dissolved in water, whereupon it was converted to the actual reagent, *N,N*-diethylaziridinium chloride.²

Preparation of Hydrocellulose

The procedure was that of Nelson and Tripp.³ Five gram samples of fibers (print cloth ground in a Wiley mill to pass a 20-mesh screen) were refluxed in 2.5*N* hydrochloric acid for a period of 0.67 hr. The samples were filtered, washed, and dried as already described.^{2,3}

Reaction of *N,N*-Diethylaziridinium Chloride with Hydrocellulose

Air-dried hydrocellulose (5 g) was suspended in 25 ml of 0.5*M* solution of *N,N*-diethylaziridinium chloride and subsequently filtered to remove solution from the hydrocellulose to the point that the filter cake contained equal weights of hydrocellulose and solution. The wet cake was suspended in 50 ml of sodium hydroxide of specific, selected normality, and reaction was allowed to take place for 45 min. The detail has been described earlier.²

Reaction of *N,N*-Diethylaziridinium Chloride with Disordered Celluloses

Samples of cellulose (from print cloth) were disordered by ball-milling and by regeneration from solution, and samples of cellulose acetate (from

yarns) were deacetylated as described earlier;² these were subjected to reactions with 0.5*M* and 1.0*M* *N,N*-diethylaziridinium chloride in the manner described for hydrocellulose.²

Hydrolysis of 2-Diethylaminoethyl Celluloses

The chemically modified cellulose was dissolved in 72% sulfuric acid and hydrolyzed during stepwise dilution of the acid. The method is described in detail by Rowland et al.⁴ The mixture of glucose and substituted glucoses was isolated as "anhydrous" freeze-dried solids.

Removal of Glucose from the 2-Diethylaminoethyl Glucoses

A 2-g portion of the mixture of glucose and substituted glucoses was dissolved and subjected to fermentation as described earlier.⁵ It is desirable that the fermentation be completed in 16–24 hr and be followed immediately by filtration (microporous filter, to remove the yeast) and by freeze-drying. Prolongation of the above steps or even storage of the solid product often resulted in a loss or disappearance of the α -anomer of 6-*O*-[2-(diethylamino)ethyl]-*D*-glucopyranose. The occurrence of such a case was signalled by the appearance of two new peaks just before and after that for the α -anomer of the 3-*O*-isomer and by the deviation of the α/β ratio of anomers of the 6-*O*-isomer from 43/57. It was found, by comparison of values obtained from reruns, that when this happened, the correct value for the distribution of substituents could be obtained by basing the calculation on the peak areas of the α -anomer of the 2-*O*-isomer, the α -anomer of the 3-*O*-isomer, the β -anomer of the 6-*O*-isomer, and the established ratios of the anomers⁵ (i.e., 37/63, 49/51, and 43/57, respectively). Generally, the replicabilities of the values for distributions in the 2-*O*- and 3-*O*-positions (relative to the 6-*O*-position) were better than $\pm 4\%$.

Distribution of Substituents in *O*-(2-Diethylaminoethyl)-*D*-glucoses

The solid product from above was taken up in 2 ml of dry pyridine and allowed to reach equilibrium between the anomeric forms in 4 to 20 hr. A portion ($1/2$) of the pyridine solution was withdrawn and silylated by the method of Sweeley et al.⁶ prior to gas-liquid chromatographic analysis as described by Roberts and Rowland.⁷ It was important that the sample be analyzed within 1–2 days. All steps from the beginning of the fermentation through gas-liquid chromatographic analysis were completed within periods indicated above in order to obtain satisfactory results (i.e., to avoid disappearance of the 6-*O*-isomer).

RESULTS

Distribution of 2-(Diethylamino)ethyl Substituents

The reactions of *N,N*-diethylaziridinium chloride with samples of cellulose were conducted, as in previous studies, in solutions of sodium hydrox-

ide of various normalities ranging from 0.5*N* to 6.0*N*. A desired, low degree of substitution results under the conditions employed; as a consequence, di- and trisubstitution of D-glucopyranosyl units of the cellulose chain are insignificant.

The ratio of 2-*O*- to 6-*O*-substitution in samples of hydrocellulose was found to be a function of the time involved in the hydrolysis of the fibrous cotton. The ratio reached a maximum for the hydrocellulose resulting from a 0.67-hr period of hydrolysis; 2.5*N* hydrochloric acid was employed at reflux, and samples were hydrolyzed for periods of 0.33, 0.67, 1, 2, 3, 4, and 5 hr. This report is concerned only with the hydrocellulose having the highest ratio of 2-*O*- to 6-*O*-substitution, i.e., the highest degree of selective accessibility. Throughout this report this hydrocellulose is referred to as EHC.

TABLE I
Distribution of Substituents Resulting from Reaction of EHC with
N,N-Diethylaziridinium Chloride in Various Normalities of Sodium Hydroxide^a

Base concn, <i>N</i>	<i>O</i> -(2-Diethylamino)ethyl hydrocelluloses				
	Nitrogen content ^b	2- <i>O</i> - ^c	3- <i>O</i> - ^c	6- <i>O</i> - ^d	3- <i>O</i> - ^d
0.5	0.10	3.80	0.41	0.26	0.11
1.0	0.10	3.11	0.32	0.32	0.10
2.0	0.09	2.79	0.36 ^e	0.36	0.13 ^e
4.0	0.22	1.82	0.31	0.55	0.17
6.0	0.16	1.68	0.32	0.60	0.19

^a EHC = hydrocellulose from 0.67 hr hydrolysis of cotton in 2.5*N* hydrochloric acid at reflux.

^b It has been shown that the distribution of substituents is independent of the extent of reaction (%*N*) or the repetition up to five reaction cycles.²

^c Relative to 1.00 for the 6-*O*-position.

^d Relative to 1.00 for the 2-*O*-position.

^e This experimental measurement was low in reliability.

The distributions of substituents that resulted from reactions of EHC with *N,N*-diethylaziridinium chloride in the various basic media are summarized in Table I. The distribution of substituents is shown in two ways: first, in the manner which has proven most useful for consideration of relative reactivities of the hydroxyl groups, i.e., 2-*O*-:3-*O*-:6-*O*-, where the 6-*O*-substitution is expressed as unity; and second, in the manner most appropriate for the subsequent calculation of the relative reactivities of the hydroxyl groups in view of the fact that the hydroxyl group at C-2 is most available, i.e., 6-*O*-:3-*O*-:2-*O*-, where the 2-*O*-substitution is the basis for comparison and is represented by unity. The significant differences in ratios of 2-*O*- to 6-*O*-substitution in EHC compared to those in fibrous cotton² (in print cloth) are obvious on comparison of curve *C* with curve *B* of Figure 1.

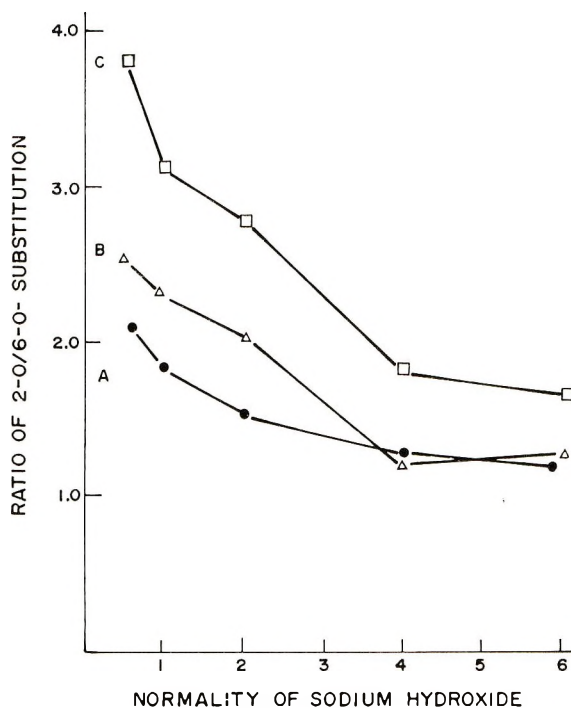


Fig. 1. Ratio of 2-*O*-/6-*O*-substitution resulting from reactions of *N,N*-diethylaziridinium chloride with samples of cellulose in various normalities of sodium hydroxide: (●) disordered cellulose; (Δ) cotton fibers; (□) EHC.

Relative Availabilities of Hydroxyl Groups on the Surfaces of EHC

The relative availabilities or relative accessibilities of the hydroxyl groups in a sample of crystalline cellulose may be calculated from the distribution of substituents at the 6-*O*-, 3-*O*-, and 2-*O*-positions (2-*O*-substitution as unity and the basis of comparison). Each of the numbers representing the distribution of substituents at a specific position is divided by the corresponding number which represents the relative reactivity of the hydroxyl group at that position. The relative reactivities of the hydroxyl groups at the C-6, C-3, and C-2 positions are obtained by conducting reactions of *N,N*-diethylaziridinium chloride with samples of cellulose in which the hydroxyl groups at C-6, C-3, and C-2 are equally available or equally accessible for the reaction. The relative reactivities of the hydroxyl groups have been shown to be dependent upon the concentration of base;^{2,8} this is evident in curve *A* of Figure 1; thus, it is essential that the relative availabilities of the hydroxyl groups be calculated from values of distribution of substituents in a crystalline cellulose and from relative reactivities in a disordered cellulose that result from reactions conducted under the same conditions, including the same normality of base.

The kinetic and mathematical justifications for calculation of relative availabilities of hydroxyl groups in samples of crystalline cellulose in the

manner indicated above are presented in an earlier paper.² It was shown that the relative accessibility of the hydroxyl group at C-6 compared to that at C-2 (i.e., $[O_6H]_a/[O_2H]_a$) is equal to the quotient of the ratio of 6-*O*- to 2-*O*-substitution in the crystalline cellulosic product (i.e., dP_{6x}/dP_{2x}) and the corresponding ratio representing relative reactivities of hydroxyl groups in the disordered cellulosic product (i.e., dP_{6d}/dP_{2d}). This corresponds to eq. (1),² in which the k are relative rate constants for the hydroxyl groups denoted by the subscripts.

$$\frac{[O_6H]_a}{[O_2H]_a} = \frac{k_2}{k_6} \frac{dP_6}{dP_2} = \frac{dP_{2d}}{dP_{6d}} \frac{dP_{6x}}{dP_{2x}} \quad (1)$$

Substantially greater difficulty has been encountered in the reproducible determination of the distributions of substituents resulting from reactions of disordered celluloses than from reactions of crystalline celluloses. For this reason, the results of reactions of disordered celluloses with *N,N*-diethylaziridinium chloride in 0.5*N*, 1*N*, and 2*N* sodium hydroxide, as reported earlier,² have been re-examined. In this case the aziridinium reagent was employed at 0.5*M* and at 1.0*M*. Again, considerable scatter in distribution of substituents was encountered; this is attributed to the tendency of disordered celluloses to regain some of their original crystallinity⁹ during the course of the reaction with *N,N*-diethylaziridinium chloride. The actual results were quite similar to those reported earlier;² the apparent best average values are summarized in Table II. In terms

TABLE II
Relative Reactivities of Hydroxyl Groups in Disordered Celluloses^a

Base concn, <i>N</i>	Relative substitution in <i>O</i> -(2-diethylamino)ethyl celluloses			
	2- <i>O</i> - ^b	3- <i>O</i> - ^b	6- <i>O</i> - ^c	3- <i>O</i> - ^c
0.5	2.10	0.81	0.48	0.38
1.0	1.75	0.64	0.57	0.37
2.0	1.48	0.46	0.68	0.31
4.0	1.29	0.34	0.78	0.26
6.0	1.24	0.32	0.81	0.26

^a From ball-milling or regeneration of cotton cellulose and from deacetylation of cellulose acetate.

^b Relative to 1.00 for the 6-*O*-position.

^c Relative to 1.00 for the 2-*O*-position.

of the ratio of 2-*O*- to 6-*O*-substitution, these values are shown in Figure 1 as curve *A*.

The relative accessibilities of the hydroxyl groups in EHC calculated from the distributions of substituents in EHC (Table I) and the relative reactivities of the hydroxyl groups in disordered celluloses (Table II) are listed in Table III. It is evident that the relative accessibility of the hydroxyl group at C-6 is substantially lower in EHC than it is in fibrous cotton. It is significant that for both EHC and fibrous cotton the selective

TABLE III
 Accessibilities of Hydroxyl Groups at C-6 and C-3 Relative
 to those at C-2 in EHC and Cotton Fibers

Cellulose	[O ₆ H] _a /[O ₂ H _a]			[O ₃ H] _a /[O ₂ H _a]		
	In 0.5 <i>N</i> base	In 1.0 <i>N</i> base	In 2.0 <i>N</i> base	In 0.5 <i>N</i> base	In 1.0 <i>N</i> base	In 2.0 <i>N</i> base
EHC	0.55	0.55	0.53	0.28	0.29	0.42 ^a
Fibrous ^a cotton	0.82	0.76	0.72	0.27	0.37	0.33

^a This experimental measurement was low in reliability.

^b These results are slightly different from those reported earlier² due to the use of revised values for relative reactivities of the hydroxyl groups at C-2, C-3, and C-6 (Table II).

accessibilities do not change (within experimental error) in basic media over the range from 0.5*N* to 2.0*N*.

DISCUSSION

Preliminary Explanation of Selective Accessibilities of Hydroxyl Groups in Crystalline Celluloses

The low accessibility of the hydroxyl group at C-3 relative to that at C-2 (i.e., 0.29) in EHC is considered to be evidence that the hydroxyl group at C-3 is hydrogen-bonded to the ring oxygen of the *D*-glucopyranosyl unit which is next in line in the cellulose chain. This hydrogen bond requires a bent conformation of the two glucopyranosyl groups that make up the cellobiose units in the cellulose chain. This hydrogen bonding and the bent conformation, as shown in Figure 2, have been proposed by Hermans¹⁰ and by Liang and Marchessault¹¹ from studies of the arrangements of units within the body of the crystalline cellulose: i.e., in the crystalline unit cell of cellulose (lattice I). It is to be expected, at least to first approximation, that the structure that they have attributed to cellulose in the body of the crystalline structure may also apply to the units on the surfaces of the crystalline regions.

The reduced accessibility of the hydroxyl group at C-6 relative to that at C-2 (i.e., 0.54) in EHC is attributed to hydrogen bonding of this hydroxyl group to the bridge oxygen (O₁) of an adjacent (antiparallel) molecular chain. This type of hydrogen bonding within the crystalline unit cell of cellulose was first proposed by Frey-Wyssling¹² and was later amplified by Liang and Marchessault;¹¹ it is illustrated in Figure 3, which is an extension of the unit cell of Frey-Wyssling which, in turn, is a slight modification of the unit cell proposed by Meyer and Misch.¹³ In this figure, the unit cell is that portion within the parallelogram. A portion of the upper surface of an elementary fibril may be visualized from the top-most plane in Figure 3; this is the 101 plane. The hydrogen atoms on the oxygens at C-6 are hydrogen-bonded back into the surface of the elementary fibril to the

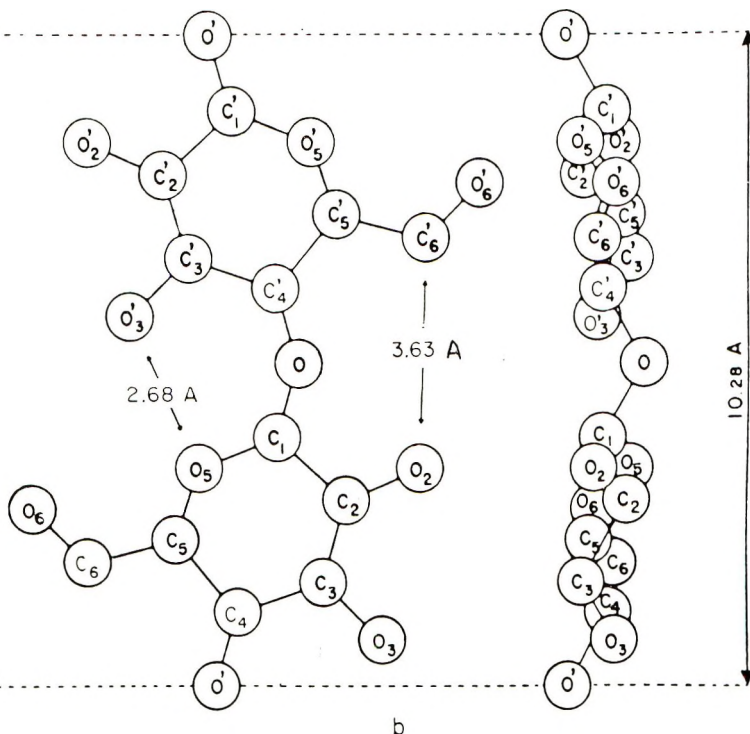


Fig. 2. Bent conformation of the cellobiose segment of the crystalline cellulose chain. The numbers identify the specific carbon and oxygen atoms in the cellobiose segment. This is reproduced from reference 14 with the permission of R. H. Marchessault and Academic Press.

bridge oxygens of adjacent molecular chains. Similar hydrogen bonds occur in the lateral surfaces, i.e., the $10\bar{1}$ planes as is illustrated on the left side of Figure 3. A difference in the $O_6 \dots O_1$ distance was indicated by Frey-Wyssling:¹² 2.54 Å for the distance in the 101 plane and 2.80 Å in the $10\bar{1}$ plane. The former distance is that for the stronger hydrogen bond. Liang and Marchessault¹¹ stated that the distances were only slightly altered when the chain units were bent to incorporate the intramolecular $O_3H \dots O_5$ bond as shown in Figure 2.

It is possible, therefore, that in the case of an elementary fibril having perfectly formed (and preserved) surfaces, such as those illustrated in the left and upper sides of Figure 3, the hydroxyl groups at C-6 in the $10\bar{1}$ planar surface may be dislodged from hydrogen bonds more readily than those in the 101 planar surface. This could account for the availability of hydroxyl groups at C-6 being approximately 50% of that of hydroxyl groups at C-2. However, another explanation appears equally acceptable at this time. From examination of models, it is evident that there may be a unique directional feature to each surface: i.e., the right side and the lower side (developed by an extension of Figure 3) may not be the simple inverted

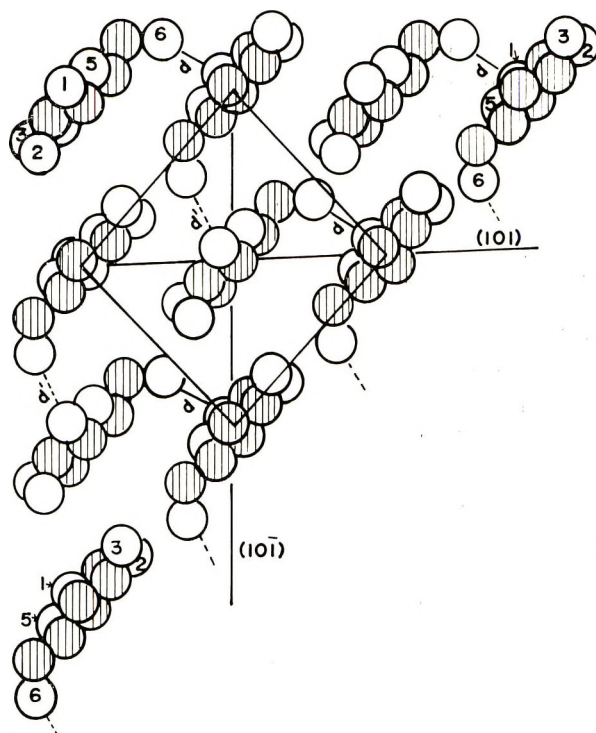


Fig. 3. Section of the upper left corner of an elementary fibril constructed by an extension of the unit cell of Meyer and Misch¹³ as modified by Frey-Wyssling.¹² The unit cell is shown by the parallelogram. The direction of the molecular chains (and the *b* axis) is perpendicular to the plane of the projection. The projection of the D-glucopyranosyl residues on the left side lie in the $10\bar{1}$ plane and those on the top surface lie in the 101 plane. Shaded circles designate carbon atoms and open circles designate oxygen atoms; the latter are numbered in representative cases. The $O_6 \dots O_1$ distances in the 101 planes (shown by *d* and solid lines) are approximately 2.5 Å and those in the $10\bar{1}$ planes (shown by *d'* and dotted lines) are approximately 2.8 Å.

analogs of the left and upper sides, respectively. Unless the conformations of the hydroxyl groups at C-6 in the right and lower surfaces are different from those throughout the rest of the model cross section of the elementary fibril, the hydroxyl groups on these surfaces will be extended outwards and will be readily available for reaction. These readily available hydroxyl groups at C-6 amount to about 50% of the total hydroxyl groups at C-6 on the surfaces and to about 50% of the available hydroxyl groups at C-2.

Haworth et al.,¹ in discussing the orientation of D-glucopyranosyl residues in the surfaces of crystalline elementary fibrils of cotton cellulose refer to "D-glucose residues lying mainly in the plane of the surface" on two sides of the elementary fibril and "those at right angles to the surface" on the other two sides. Our concept of the arrangement of D-glucopyranosyl (or cellobiose) segments of the cellulose chain on the surfaces of elementary fibrils is quite different, as discussed above and shown in part in Figure 3.

The concept presented here is consistent with the unit cell of Meyer and Misch¹³ (or a slight modification thereof^{12,14}), the Hermans conformation for the cellobiose units with intramolecular O₃H . . . O₅ bonds, and the intermolecular O₆H . . . O₁' bonds of Frey-Wyssling¹² and Liang and Marchessault.¹¹

SUMMARY

Both the exemplar hydrocellulose (EHC) and fibrous cotton show essentially constant selective accessibilities (within the range of experimental error) in basic media ranging from 0.5*N* to 2.0*N*. Under these non-decrystallizing conditions, the hydroxyl groups at C-6 and C-3 in EHC are approximately 54% and 29% as available for reactions as the hydroxyl group at C-2. Thus, EHC exhibits a substantially higher degree of selective accessibility than fibrous cotton, for which the hydroxyl groups at C-6 and C-3 have been found to be 77% and 32% as available as the hydroxyl group at C-2. The selective accessibilities of the hydroxyl groups of EHC, which is considered to be a highly crystalline cellulose, are indicative of the presence of highly ordered surfaces on crystalline elementary fibrils. The type and degree of selective accessibilities of EHC are consistent with the Meyer-Misch unit cell and with hydrogen bonding on the surfaces of crystalline microstructural units that is similar to the intramolecular O₃H . . . O₅ and intermolecular O₆H . . . O₁' bonding proposed by others to occur within the crystalline regions.

Appreciation is expressed to Verne W. Tripp for many helpful discussions and suggestions.

References

1. S. Haworth, D. M. Jones, J. G. Roberts, and B. F. Sagar, *Carbohydr. Res.*, **10**, 1 (1969).
2. S. P. Rowland, E. J. Roberts, and C. P. Wade, *Text. Res. J.*, **39**, 530 (1969).
3. M. L. Nelson and V. W. Tripp, *J. Polym. Sci.*, **10**, 577 (1953).
4. S. P. Rowland, V. O. Cirino, and A. L. Bullock, *Can. J. Chem.*, **44**, 1051 (1966).
5. E. J. Roberts and S. P. Rowland, *Can. J. Chem.*, **47**, 1571 (1969).
6. C. C. Sweeley, R. Bentley, M. M. Makita, and W. W. Wells, *J. Amer. Chem. Soc.*, **85**, 2497 (1963).
7. E. J. Roberts and S. P. Rowland, *Can. J. Chem.*, **45**, 261 (1967).
8. E. J. Roberts, C. P. Wade, and S. P. Rowland, *Carbohydr. Res.*, **17**, 393 (1971).
9. P. H. Hermans and A. Weidinger, *J. Amer. Chem. Soc.*, **68**, 2547 (1946).
10. P. H. Hermans, *Kolloid-Z.*, **102**, 169 (1943); *Physics and Chemistry of Cellulose Fibers*, Elsevier, New York, 1949, p. 13.
11. C. Y. Liang and R. H. Marchessault, *J. Polym. Sci.*, **37**, 385 (1959).
12. A. Frey-Wyssling, *Biochim. Biophys. Acta*, **18**, 166 (1955).
13. K. H. Meyer and L. Misch, *Helv. Chim. Acta*, **20**, 232 (1937).
14. R. H. Marchessault and A. Sarko, *Advan. Carbohydrate Chem.*, **22**, 421 (1967).

Received December 3, 1970

Electroinitiated Copolymerization Reactions with Donor-Acceptor Complexes. III. Copolymerization of Butadiene and Acrylonitrile with $ZnCl_2$ as Catalyst

B. LIONEL FUNT and JAROSLAV RYBICKY, *Department of Chemistry, Simon Fraser University, Vancouver, British Columbia, Canada*

Synopsis

The passage of an electrolytic current initiated polymerization of acrylonitrile with butadiene to form an alternating copolymer. The rate of polymerization increased with increase in current, but the copolymer composition was invariant with current and with degree of conversion. A mechanism is proposed based on donor-acceptor complexes. The formation of these is facilitated by the addition of $ZnCl_2$ which forms an initial complex with the acrylonitrile. Polymerization of the donor-acceptor complexes is initiated by electrochemically generated transient species whose rate of formation is dependent on the current.

Recent work has shown that, in the presence of suitable salts, pairs of polar monomers can be induced to undergo alternating copolymerization.¹⁻⁵ The characteristics of these polymerizations are extremely interesting. The rates of polymerization are greater than for free radical polymerizations conducted in the absence of salts; the molecular weights are high;⁶ the copolymer composition remains remarkably constant over a wide range of feed ratios.⁷

Gaylord and his co-workers have conducted intensive studies of these systems and have proposed an elegant mechanism, based upon donor-acceptor complexes, to account for the observed experimental behavior in these polymerizations.^{3,5,8-15} In essence, Gaylord proposed that an initial complex is formed between an electron-acceptor monomer, such as acrylonitrile (AN) and a metal halide. The electron-accepting tendency of the monomer is thus enhanced, and a donor-acceptor complex will be formed with an electron-donating monomer such as butadiene (BD). Spontaneous or radical-initiated polymerization of this donor-acceptor complex may then occur to form an alternating copolymer.

We were led to investigate the application of electrochemical initiation to such systems. With electrochemical techniques, it was considered possible to vary the rate of initiation of the donor-acceptor complexes without varying the temperature, and thus without shifting the equilibria which must exist. Whereas an increase in temperature enhances the reactivity of the donor-acceptor complexes, it could also presumably lead to a decrease

in the concentration of the complexes¹⁶ and thus produce a reduced rate of overall reaction. With electrochemical initiation, these effects can be investigated separately by varying the rate of attack on the complexes at constant temperature.

However, it cannot be presumed that the mechanisms in electrochemical polymerization will be identical to those in polymerizations initiated by other techniques. Differences in composition, microstructure, and mechanism have been observed in investigations of electrochemical polymerizations from those obtained in thermal polymer.^{17,18} We therefore undertook to explore the feasibility of initiating donor-acceptor complex polymerizations by electrochemical means and to determine the specific effects upon rate and on structure which resulted from variation in the impressed current.

Our preliminary studies of styrene-methyl methacrylate and of styrene-acrylonitrile have been reported.^{19,20}

EXPERIMENTAL

Materials

AN was dried over CaH_2 and vacuum distilled. BD, 99.6%, instrument grade was used without further purification. ZnCl_2 reagent grade was dried for 50 hr in a vacuum oven at 150°C and then stored under argon.

Polymerization

The apparatus shown in Figure 1 provided a constant pressure of butadiene regulated through solenoid C. The total system pressure was read on manometer B and the consumption of butadiene was monitored on manometer A. The reaction cell D contained two identical Pt electrodes, each 2.5×2.5 cm, separated by 1.0 cm. Polymerizations were performed at constant current.

The products were isolated at the conclusion of the polymerization by dilution with THF and precipitation in a large excess of acidified methanol.

TABLE I
Copolymer Formation in the Presence of ZnCl_2 ^a

PrN, g ^b	Feed		Current, mA	Time, min	Polymer formation
	AN, g	BD, g			
—	20	1.3	0	60	None
—	20	—	25	60	Homopolymer (AN)
20	—	1.3	25	60	None
—	20	1.3	25	60	Alternating copolymer

^a Conditions: 8.40 g ZnCl_2 , 45°C .

^b PrN = propionitrile.

The electrochemical control of the polymerization is evident from Table I. Solution of AN-BD-ZnCl₂ did not yield polymer unless current flowed. If BD was not introduced as a reactant, AN could be polymerized electrochemically to a homopolymer. On the other hand, the substitution of propionitrile (PrN) for (AN) did not produce polybutadiene. This in-

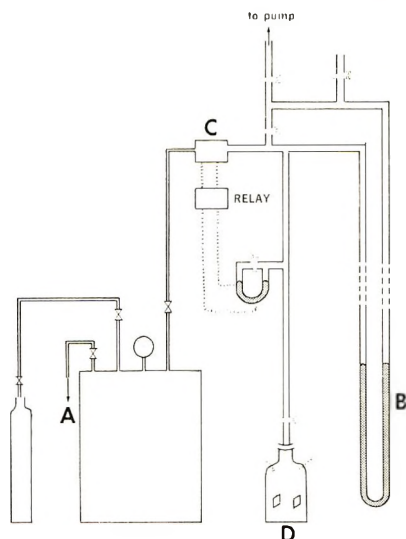


Fig. 1. Apparatus.

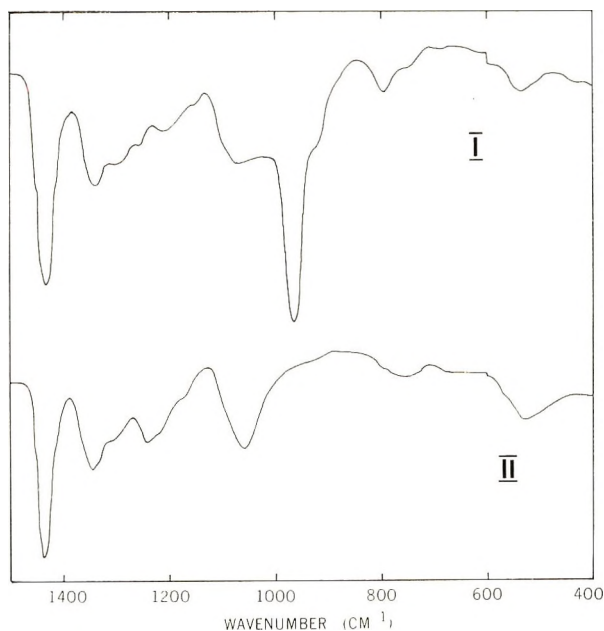


Fig. 2. Infrared spectra: (I) copolymer; (II) polyacrylonitrile formed under same conditions.

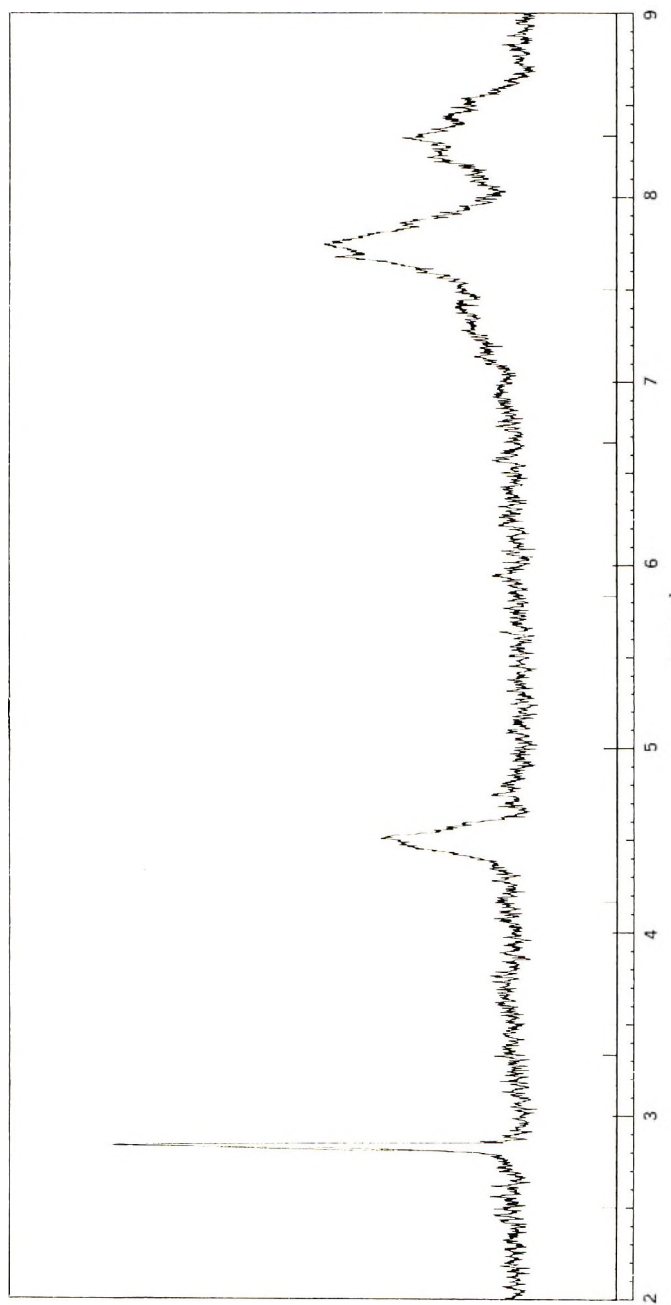


Fig. 3. NMR spectrum of copolymer.

indicates the absence of homopolymerization of BD in the AN-BD-ZnCl₂ system.

The observations were based on the appearance of the solution, the ability to isolate polymers, and the properties of the material isolated.

This circumstantial evidence is supported by direct analysis of the resultant products formed in the electrochemical polymerization. The infrared spectra are shown in Figure 2 for polyacrylonitrile and for the copolymer obtained in this work. The line at 966 cm⁻¹ indicates a double bond with 1,4-*trans* microstructure of BD units.

The NMR spectrum shown in Figure 3 also confirms the presence of copolymer. Further, the peak at 7.7 τ shows a BD-A unit sequence whereas the corresponding peak at 7.9 τ corresponding to BD-BD is not present.²¹ Elemental analysis indicates a molar composition corresponding to a 1:1 BD/AN mole ratio. This composition is essentially invariant with degree of conversion (Table II) and with rate of initiation (Table III).

The reaction profiles in the electroinitiated polymerizations are shown in Figure 4. Rates of polymerization increase with current, but are constant with time for the initial period of reaction. All the data at various currents and times are shown in Figure 5, which indicates that the total number of Faradays determines the polymer yield.

The ZnCl₂/AN ratio is a determinant factor in the polymerization, as shown in Figure 6. For the same time of polymerization, the yields of polymer are determined by the ZnCl₂ available for complex formation. However, the copolymer composition remains relatively constant with

TABLE II
Effect of Degree of Conversion on Composition^a

Yield, g	Composition, mole-% AN	$[\eta]$, dl/g
0.073	48.8	—
0.135	50.6	4.14
0.203	—	4.48
0.221	50.1	5.30
0.290	—	5.74

^a Conditions: 8.4 g ZnCl₂, 20 g AN, 1.3 g BD, 45°C, 25 mA.

TABLE III
Copolymer Composition as a Function of Rate of Initiation^a

Current, mA	Composition, mole-% AN
8	49.1
25	50.6
35	49.0
45	50.4

^a Conditions: 8.4 g ZnCl₂, 20 g AN, 1.3 g BD, 45°C; polymer yield, 0.13 g in all samples.

variation in rate of initiation as shown in Table III and with ZnCl_2 concentration as shown in Table IV.

The intrinsic viscosities of samples determined in THF are shown in Table II. The very high intrinsic viscosities are characteristic of donor-acceptor complex polymerizations. The gel-permeation chromatograms of the systems exhibited a very broad distribution of molecular weights. However, it was not possible to apply the Benoit universal calibration technique²² to obtain molecular weights, as the upper limits of the distribution fell significantly above the highest standard sample of polystyrene

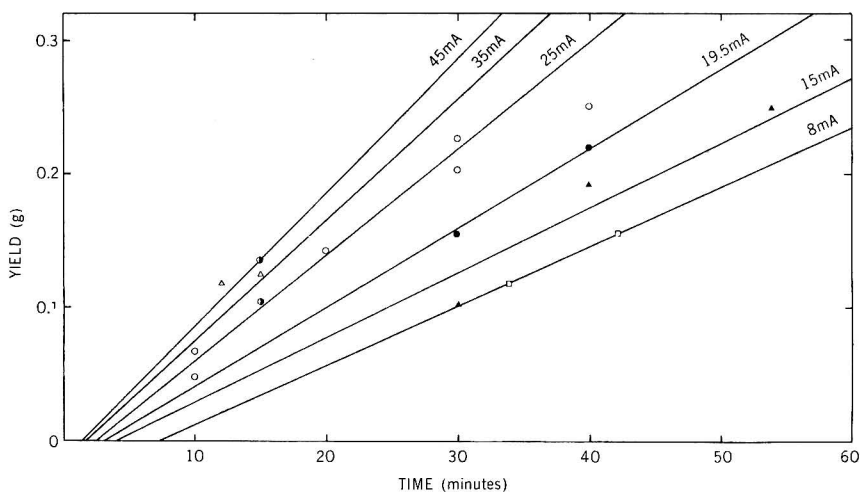


Fig. 4. Copolymer formation as a function of current and time.

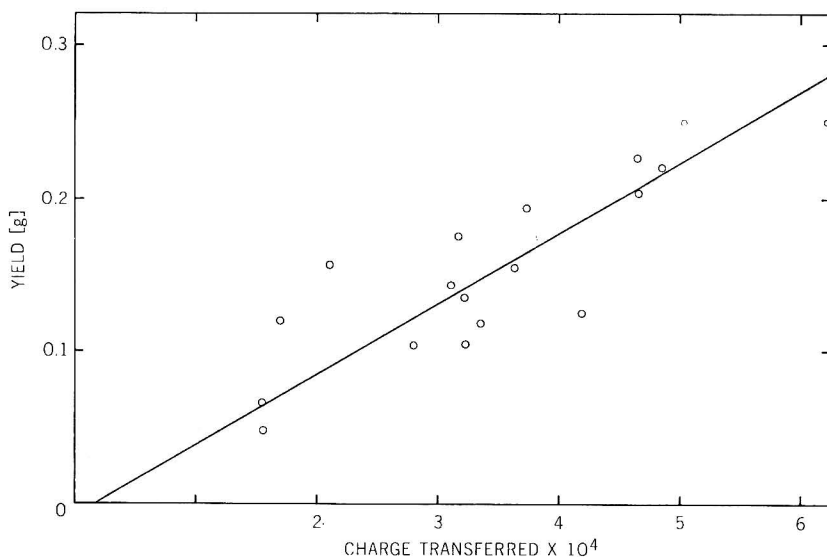


Fig. 5. Polymer formation as a function of charge transferred in Faradays.

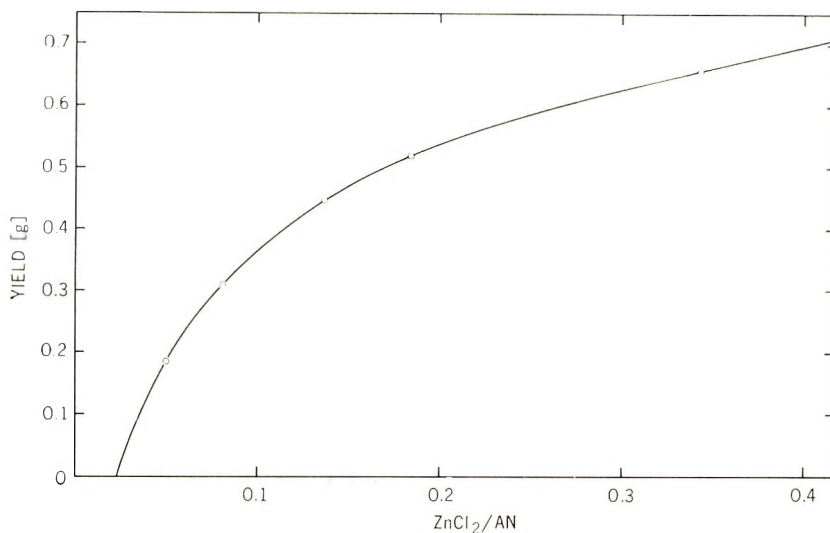


Fig. 6. Polymer formation at various mole ratios of ZnCl_2/AN .

employed (Water's #61970, peak molecular weight 1.987,000) and the calculation of molecular weight is quite sensitive to calibration in this region.

TABLE IV
Copolymer Composition as a Function of ZnCl_2/AN Ratio^a

ZnCl_2/AN , mole/mole	BD in feed, g	Copolymer composition, mole-% AN
0.05	1.33	47.2
0.08	1.28	47.8
0.14	1.19	48.3
0.19	1.23	51.3
0.34	0.69	50.9

^a Conditions: 20 g AN, 0.15 g $\text{Zn}(\text{OAc})_2$; 25 mA at 45°C, 1 hr.

DISCUSSION

A mechanism for donor-acceptor polymerization has been brilliantly enunciated by Gaylord and Takahashi.¹ Our results are interpreted on this basis.

The complexation of a polar monomer such as AN with ZnCl_2 increases its electrophilic character and facilitates complex formation with an electron-donating monomer such as BD. The electrophilicity of the metal halide determines whether a free-radical initiator is required to initiate polymerization or whether this will occur spontaneously for a given pair of monomers. Furukawa investigated a number of effective catalysts for the spontaneous polymerization of AN-BD.^{4,22}

A delicate balance exists in such systems determined by the equilibria. An increase in temperature decreases the concentration of complexes but increases their reactivity. With some metallic salt catalysts, increase in temperature will increase the rate of formation of alternating copolymer. With others the rate is decreased.

The conditions selected for this work are similar to those employed by Gaylord⁸ and presumably require activation by a free-radical initiator for the onset of polymerization. That this is the case is confirmed by the nonelectrolytic blank experiments and by the dependence of rate of copolymer formation on current.

The AN-BD complex may be viewed as a distinct chemical entity whose homopolymerization produces an alternating copolymer. The NMR data confirm BD-AN diad sequences from the 7.7 τ peak assigned to methylene groups. The absence of a peak at 7.9 τ shows that BD-BD sequences are not found and that the homopolymer is not formed in significant amounts.¹⁴ This conclusion is reinforced by the elemental analyses which also supports an equimolar copolymer composition.

The copolymer composition was unaffected by variations of the current passing through the solution, but was sensitive to variation of the ZnCl₂ mole ratios. On the mechanistic model proposed, the variation of current would change the rate of attack on the donor-acceptor complexes. However, the copolymer, though formed more quickly, would still be unaffected in composition. A lowering of the ZnCl₂ concentration should decrease the concentration of the donor-acceptor complexes, reduce the rate of polymerization of the complex, and increase the rate of homopolymerization of the individual monomers in the system. The change in copolymer composition is probably due to this effect. The invariability of composition with variation in temperature shows that the complexes are relatively stable over the range investigated. However, the control of the rate of polymerization by the current flowing through the solution demonstrates that electrochemical control can be employed by varying the rate of reaction, even when a greater degree of thermal dependence is met.

The authors thank the National Research Council of Canada for financial support.

References

1. N. G. Gaylord and A. Takahashi, *Adv. Chem.*, **91**, 94 (1969).
2. S. Okuzawa, H. Hirai, and S. Makishima, *J. Polym. Sci. A-1*, **7**, 1039 (1969).
3. A. Takahashi and N. G. Gaylord, *J. Macromol. Sci. Chem.*, **A4**, 127 (1970).
4. M. Taniguchi, A. Kawasaki, and J. Furukawa, *J. Polym. Sci. B*, **7**, 411 (1969).
5. N. G. Gaylord, B. Matzka, and B. Arnold, *J. Polym. Sci. B*, **8**, 235 (1970).
6. S. Yabumoto, K. Ishii, M. Kawamori, K. Arita, and H. Yano, *J. Polym. Sci. A-1*, **7**, 1683 (1969).
7. S. Yabumoto, K. Ishii, and K. Arita, *J. Polym. Sci. A-1*, **7**, 1577 (1969).
8. N. G. Gaylord and A. Takahashi, *J. Polym. Sci. B*, **7**, 443 (1969).
9. M. Hirooka, H. Yabuuchi, S. Morita, S. Kawasumi, and K. Nakaguchi, *J. Polym. Sci., B*, **5**, 47 (1967).
10. N. G. Gaylord and A. Takahashi, *J. Polym. Sci. B*, **6**, 749 (1968).

11. N. G. Gaylord and H. Antropiusova, *J. Polym. Sci. B*, **7**, 145 (1969).
12. N. G. Gaylord and H. Antropiusova, *Macromolecules*, **2**, 442 (1969).
13. H. Hirai, T. Ikegami, and S. Makishima, *J. Polym. Sci. A-1*, **7**, 2059 (1969).
14. B. Patnaik, A. Takahashi, and N. G. Gaylord, *J. Macromol. Sci. Chem.*, **A4**, 143 (1970).
15. N. G. Gaylord and H. Antropiusova, *J. Polym. Sci. B*, **8**, 183 (1970).
16. N. G. Gaylord, *J. Polym. Sci. B*, **8**, 411 (1970).
17. B. L. Funt and S. N. Bhadani, in *Macromolecular Chemistry, Tokyo-Kyoto 1966* (*J. Polym. Sci. C*, **23**), I. Sakurada and S. Okamura, Eds., Interscience, New York, 1968, p. 1.
18. B. L. Funt and D. G. Gray, *J. Macromol. Chem.*, **1**, 625 (1966).
19. B. L. Funt, I. McGregor, and J. Tanner, *J. Polym. Sci. B*, **8**, 695 (1970).
20. B. L. Funt, I. McGregor, and J. Tanner, *J. Polym. Sci. B*, **8**, 699 (1970).
21. J. Furukawa, Y. Iseda, K. Hagai, and N. Kataoka, *J. Polym. Sci. A-1*, **8**, 1189 (1970).
22. H. Benoit, Z. Grubisic, P. Rempp, D. Decker, and J. G. Zilliox, *J. Chim. Phys.*, **63**, 1507 (1966).

Received November 3, 1970

Revised December 4, 1970

Cationic Polymerization of Isobutene Initiated by Stannic Chloride and Phenols: Polymer Endgroup Studies*

R. F. BAUER† and K. E. RUSSELL, *Department of Chemistry, Queen's University Kingston, Ontario, Canada*

Synopsis

Low molecular weight polymers of isobutene produced with stannic chloride as catalyst and phenols as cocatalysts have been subjected to ultraviolet and NMR analysis. A high proportion of the endgroups are derived from the phenol cocatalyst when the concentration of free phenol in the reaction mixture at -78.5°C is fairly large. At low concentrations of free phenol, termination to give vinylidene endgroups becomes more significant. The results lend support to the suggestion that an important mode of termination in this polymerization system involves the reaction between a growing carbonium ion and the phenol cocatalyst.

INTRODUCTION

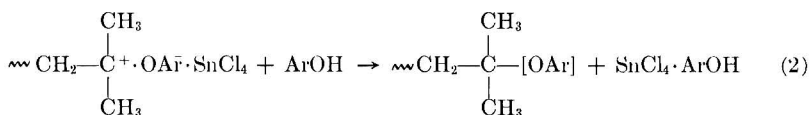
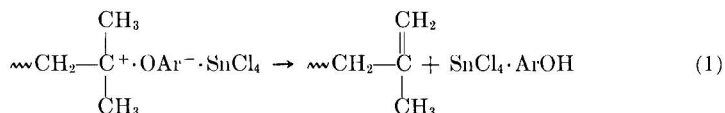
It has been recognized for some time that endgroup analysis can be an important aid in formulating detailed mechanisms of cationic polymerization. Pleschl¹ has shown that a large fraction of polystyrene molecules, prepared with titanium tetrachloride as catalyst, trichloroacetic acid as cocatalyst, and toluene as solvent, contain tolyl endgroups. Overberger and co-workers showed by chemical and infrared analysis that a wide variety of aromatic compounds function as transfer agents in the stannic chloride-catalyzed polymerization of styrene at 0°C .²⁻⁴ Transfer constants range from 0.002 for 1,4-di-*tert*-butylbenzene to 1.6 for anisole, and Overberger compared the attack of the growing polymer carbonium ion to that of the cation in Friedel-Crafts alkylation of aromatic compounds. Endgroups have also been identified⁵ in the room temperature polymerization of isobutene; the presence of *tert*-butyl and $-\text{C}(\text{CH}_3)=\text{CH}_2$ groups in the low polymer shows that proton transfer must be involved in both the initiation and chain-breaking steps in the polymerization catalyzed by boron trifluoride and water. Further information on these and other endgroup studies is contained in major reviews of cationic polymerization.⁶⁻¹⁰

* Presented at the Fifteenth Canadian High Polymer Forum, Kingston, Ontario, 1969.

† Present Address: Dunlop Research Centre, Sheridan Park, Ontario, Canada.

The low-temperature polymerization of isobutene generally gives rise to high molecular weight polymers, and accurate endgroup analysis is more difficult to perform. Nevertheless Plesch and co-workers^{11,12} have shown that terminal unsaturation is present in polyisobutene obtained when titanium tetrachloride acts as catalyst and water as cocatalyst and that with trichloroacetic acid as cocatalyst, trichloroacetate endgroups are present. Anisole is a chain-transfer agent and gives rise to 4-methoxyphenyl residues in the polymer.¹³ Kennedy and co-workers¹⁴ have used ¹⁴C techniques to investigate the role of the solvent, methyl chloride, in aluminum chloride-initiated polymerization.

In our studies of the cationic polymerization of isobutene by means of stannic chloride at -78.5°C , we investigated the effect of a variety of phenols as cocatalysts.¹⁵ The rate and molecular weight results were interpreted by a simplified mechanism which includes the steps (1) and (2).



The square brackets in the C—[OAr] endgroup indicate that the group may be attached through the oxygen or through a carbon-carbon bond to the aromatic ring. The main endgroups in the phenol-cocatalyzed polymerization have been identified through ultraviolet and NMR studies, and the results presented here shed further light on the proposed mechanism.

EXPERIMENTAL

Materials

Isobutene (99.6%, Phillips Petroleum Co.) and ethyl chloride (Ohio Chemical Co.) were subjected to 8–10 bulb-to-bulb distillations from -78.5°C to -196°C on the vacuum line. Stannic chloride was subjected to bulb-to-bulb distillation until a mixture of isobutene, ethyl chloride, and stannic chloride showed no observable polymerization over a period of 1 hr.

Phenols (Aldrich Chemical Co.) were used as received with the exception of 2,3,4,6-tetramethylphenol, which was recrystallized from an ethanol-water mixture and phenol which was pumped on at room temperature in order to remove traces of water.

Procedure

A known amount of phenol was introduced into the reaction tube of 10 mm bore and the tube evacuated while the phenol was cooled by means of

liquid nitrogen. Stannic chloride and ethyl chloride were added, and the mixture was warmed until mixing occurred. The mixture was refrozen, isobutene was added, and the tube sealed. The polymerization mixture was warmed and shaken and the tube immersed in a Dry Ice-acetone mixture. After about 20% of the monomer had reacted, the polymerization was stopped by the addition of ethanol. The precipitated polymer was washed with cold ethanol, dried in a vacuum oven, and stored in the dark.

The number-average molecular weights of the polymer samples were obtained by means of gel-permeation chromatography.¹⁵ The samples subjected to endgroup analysis all had a fairly narrow molecular weight distribution. In some cases the number-average molecular weights were checked by osmometry by means of a Hewlett-Packard Model 501 membrane osmometer.

Ultraviolet measurements were made with a Unicam SP800 spectrophotometer on 1% (w/v) solutions of polyisobutene in chloroform and with a 1 cm path length. Spectra of the parent phenols were taken at concentrations of $1.6-8 \times 10^{-4} M$ in chloroform.

NMR spectra were obtained by Mr. D. Wooden, Polymer Corporation Ltd., Sarnia, Ontario. They were time-averaged by means of a Varian CAT. All δ values are relative to the internal standard TMS; the solvent was carbon tetrachloride.

RESULTS

Ultraviolet Analysis of Polymers

Chloroform solutions of high molecular weight polyisobutene prepared using stannic chloride as catalyst and water as cocatalyst show no significant absorbance at wavelengths greater than $250 m\mu$. When phenol and alkylphenols are used as cocatalysts, the resulting polymers show characteristic absorptions in the $270-300 m\mu$ region. The ultraviolet spectra of two polymer samples in chloroform solution prepared with the use of 2-*sec*-butylphenol as cocatalyst are shown in Figure 1. The 2-*sec*-butylphenol at low concentration (ca. $5 \times 10^{-4} M$) possesses a similar absorption spectrum, except that the absorption maxima are better resolved and occur at slightly lower wavelengths than in the polymer samples. The results show that the polymer samples contain fragments derived from the phenol; it is probable that these fragments are substituted phenol endgroups. The extinction coefficient of each substituted phenol is not known, and the rough assumption is made that it is the same at the absorption maximum as that of the parent phenol. The proportions of endgroups in polymers obtained with the use of phenol, 2-*sec*-butylphenol, and 2,6-disopropylphenol are given in Table I. The estimates are probably not accurate to better than $\pm 20\%$ because of uncertainties in the molar extinction coefficients and the number average molecular weights. Some values are greater than 100%, and it may well be that all the experimental results are 10-20% too high. Separate gel-

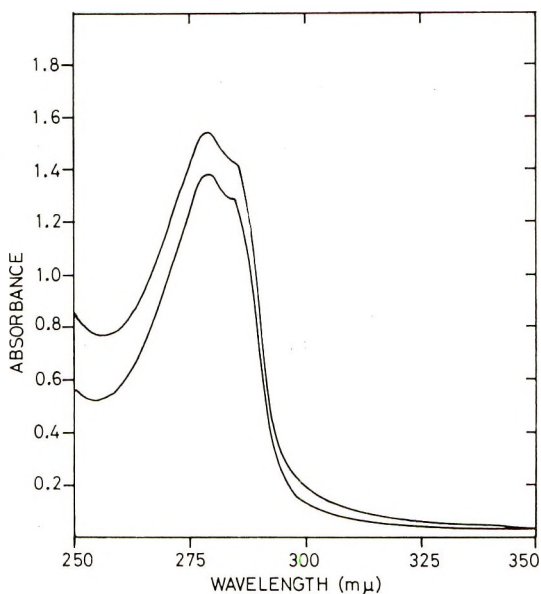


Fig. 1. Ultraviolet spectra of polyisobutene samples prepared with stannic chloride as catalyst and 2-*sec*-butylphenol as cocatalyst. Pathlength 1 cm.

permeation chromatography studies show that there is no measurable amount of free phenol in the polymer samples, so that the observed ultraviolet absorption must arise from phenol which is chemically bound to the polymer.

TABLE I
Endgroups in Polyisobutenes by Ultraviolet Analysis

Phenol	Phenol-concentration, M	Stannic chloride concentration, M	Monomer concentration, M	\bar{M}_n	% Polymer molecules with phenol endgroups
2- <i>sec</i> -butyl phenol	0.071	0.185	3.2	11,300	48
"	0.178	0.037	3.2	7,900	87
"	0.178	0.092	3.2	8,100	97
"	0.178	0.185	3.2	10,500	102
"	0.362	0.185	3.2	6,700	100
"	0.071	0.185	1.6	8,900	58
"	0.071	0.185	2.24	11,300	49
"	0.071	0.185	4.80	11,200	40
Phenol	0.062	0.185	3.2	8,200	25
2,6:Di-isopropyl-phenol	0.063	0.185	3.20	15,100	92
"	0.187	0.185	3.20	7,400	90
"	0.185	0.312	3.2	7,100	110
"	0.156	0.092	3.2	9,600	109

Ultraviolet evidence for the presence of phenol endgroups was also obtained when 2,3,4,6-tetramethylphenol and 2,6-dimethylphenol were used as cocatalysts. However, the polyisobutenes produced under the conditions of our experiments possessed number average molecular weights of the order of 100,000 and quantitative analysis was not practical. The high molecular weights arise largely because of low rate constants for reactions (1) and (2).

NMR Analysis of Polymers

The NMR spectra of two polymer samples produced with phenol and 2-*sec*-butylphenol as cocatalysts were time-averaged 240 and 500 times, respectively, in order to obtain detailed endgroup information. The first sample (phenol, 0.071*M*; stannic chloride, 0.185*M*; \bar{M}_n , 8200) gave an NMR spectrum having a weak absorption at $\delta = 7.1$ ppm due to aromatic protons and stronger absorptions at $\delta = 4.55$ and 4.75 ppm due to >C=CH_2 protons. This latter assignment is supported by the occurrence of resonances at $\delta = 4.60$ and 4.80 ppm in the model compound 2,2,4-trimethylpentene-1. Quantitative analysis by using the absorption at $\delta = 3.75$ ppm due to added 1,2-dichloroethane shows that the percentages of polymer molecules with phenol and vinylidene endgroups are approximately 7% and 60%, respectively. A similar analysis of the polymer produced with 2-*sec*-butylphenol as cocatalyst (2-*sec*-butylphenol, 0.362*M*; stannic chloride, 0.185*M*; \bar{M}_n , 6700) gave strong absorptions in the range $\delta = 6.45$ –7.05 ppm and only a weak absorption at $\delta = 4.6$ ppm (Fig. 2). The percentage of polymer molecules having phenol endgroups is estimated to be 89% on the assumption that the 2-*sec*-butylphenol undergoes Friedel

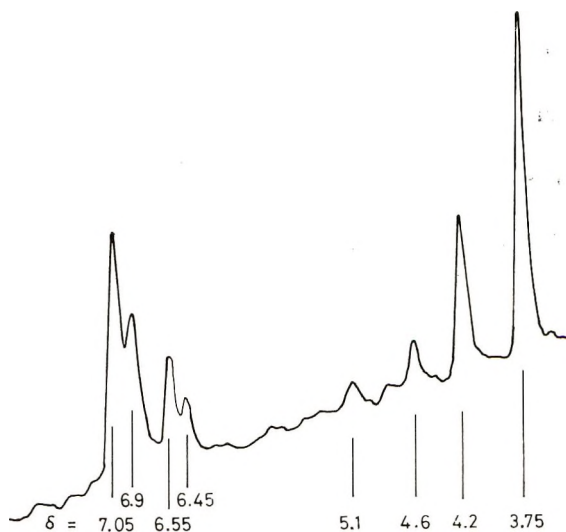


Fig. 2. NMR spectrum of polyisobutene prepared with stannic chloride as catalyst and 2-*sec*-butylphenol as cocatalyst.

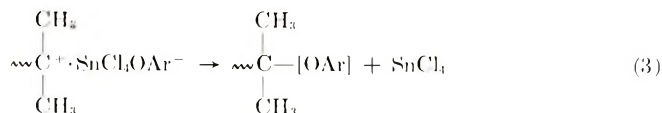
Crafts alkylation on the ring. Approximately 12% of the polymer molecules have $\diagdown \text{C}=\text{CH}_2$ endgroups.

The assignment of other resonances in the NMR spectra is less certain. The polymer from the 2-*sec*-butylphenol-cocatalyzed reaction gives small peaks at $\delta = 1.00$ ppm and $\delta = 5.10$ ppm and a stronger absorption at $\delta = 4.18$ ppm. The first peak may arise from *tert*-butyl groups at the head of the polymer and the second from $-\text{CH}=\text{C}(\text{CH}_3)_2$ endgroups. The absorption at $\delta = 4.18$ ppm has one third of the area of the aromatic complex at $\delta = 6.45\text{--}7.05$ ppm, and it disappears on treatment with heavy water. It may be due to the OH group of the phenol endgroup; it should be noted however that NMR studies¹⁵ suggest that the value of δ for the OH proton of such a disubstituted phenol should be closer to 4.4 ppm. Small peaks in the NMR spectra of the polymer from the phenol-cocatalyzed reaction at $\delta = 1.00$ ppm and $\delta = 5.0$ ppm are also tentatively assigned to *tert*-butyl and $-\text{CH}=\text{C}(\text{CH}_3)_2$ endgroups in the polymer.

DISCUSSION

Phenol Endgroups

Ultraviolet and NMR analysis demonstrate that polyisobutenes prepared by the stannic chloride-catalyzed polymerization of isobutene at -78.5°C contain fragments derived from the phenols which act as cocatalysts. It is highly probable that substituted phenols are present as endgroups in the polymer molecules and that they arise from the chain-breaking steps in the polymerization. In earlier studies¹⁵ it was shown that high concentrations of free phenol may be present in reaction solutions in addition to the 1:1 stannic chloride-phenol initiating complexes. It is frequently observed that addition of more cocatalyst actually retards the polymerization, and this is ascribed to the incidence of reaction (2) in which a growing polymer cation attacks a free (probably monomeric) phenol molecule. In keeping with this, it is found that a high proportion of polymer molecules contain phenolic endgroups when the concentration of free phenol is relatively large. For the system, stannic chloride, 0.185*M*, total 2-*sec*-butylphenol 0.362*M*, isobutene 3.2*M*, the free phenol concentration is 0.189*M* and the fraction of phenol endgroups is estimated to be 89–100%. On the other hand, for a low concentration of free unsubstituted phenol (0.008*M*), the proportion of phenolic endgroups is small (7–25%). A termination reaction of the type (3)



is not excluded, but the correlation between rate of reaction and concentration of free phenol is an indication that this is not a major mode of termination under our reaction conditions.

Vinylidene Endgroups

The other main endgroup in the polyisobutene samples subjected to NMR analysis is the vinylidene group $\diagup\text{C}=\text{CH}_2$. The proportion of vinylidene endgroups is high in the polymer prepared with a free phenol concentration of $0.008M$. Kinetic studies¹⁵ indicate that transfer to monomer proceeds at a very low rate at -78.5°C , and it therefore seems probable that the vinylidene endgroups are produced by termination reaction (1) in which a proton from the growing carbonium ion returns spontaneously to the gegenion. The alternative mode of termination to give a $-\text{CH}=\text{C}(\text{CH}_3)_2$ endgroup appears to be less favored.

tert-Butyl Endgroups

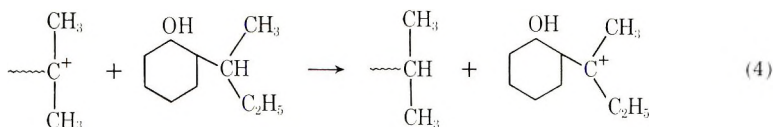
The weak resonance at $\delta = 1.00$ ppm probably arises from *tert*-butyl head groups formed during the proton transfer initiation process. Its area is difficult to estimate because of overlap with the very strong resonance at $\delta = 1.05$ ppm, but it is approximately correct for 9 *tert*-butyl protons per polymer molecule. The assignment is supported by the observation of a similar chemical shift for *tert*-butyl protons in model compounds such as 2,2,4-trimethylpentene-1.

General Comments on Mechanism

The present work provides strong evidence for termination reaction (2) in which a cocatalyst molecule becomes part of the terminated polymer molecule. It is likely that, as in the stannic chloride-catalyzed polymerization of styrene,²⁻⁴ the growing polymer attacks the nucleus of the phenol thus giving rise to a substituted phenol. The NMR result for polymer shaken with heavy water appears to support this conclusion, but further results are required for the isobutene polymerization in order to substantiate this mechanism.

The number of vinylidene endgroups relative to phenol endgroups can in principle be predicted from the relative rate constants for reactions (1) and (2) and the free phenol concentration. There is fair agreement between predicted and experimental results under the conditions reported in Table I. The termination mechanisms in their present form are, however, too oversimplified to take account of all the available experimental evidence. The estimated rate "constant" for reaction (1) appears to decrease significantly when extremely low phenol concentrations (ca. $0.001M$) are used. Part of the answer may lie in the complete neglect of solvation effects by phenol, monomer etc. in our simple theory.

A referee has suggested that 2-*sec*-butylphenol might undergo hydride transfer by reaction (4):



The cation produced could then reinitiate polymerization. Our results do not eliminate this suggestion, but such a mechanism cannot apply in the system involving phenol as cocatalyst and it is not therefore of general application. It is hoped to shed further light on the mechanism by end-group and rate studies with a wide range of substituted phenols as cocatalysts.

The authors are grateful to the Polymer Corporation Ltd., and the National Research Council of Canada for financial support of this work. They thank Mr. D. Wooden, Polymer Corporation for taking the NMR spectra of polyisobutene and Dr. G. Wilson and Mr. Wooden for helpful discussion.

References

1. P. H. Plesch, *J. Chem. Soc.*, **1953**, 1659.
2. C. G. Overberger and G. F. Endres, *J. Amer. Chem. Soc.*, **75**, 6349 (1953).
3. C. G. Overberger and G. F. Endres, *J. Polym. Sci.*, **16**, 283 (1955).
4. G. F. Endres and C. G. Overberger, *J. Amer. Chem. Soc.*, **77**, 2201 (1955).
5. F. S. Dainton and G. B. B. M. Sutherland, *J. Polym. Sci.*, **4**, 37 (1949).
6. P. H. Plesch, *The Chemistry of Cationic Polymerization*, MacMillan, New York, 1963.
7. P. H. Plesch, *Progress in High Polymers*, Vol. 2, J. G. Robb and F. W. Peaker, Eds., Heywood Books, London, 1968.
8. D. C. Pepper, *Friedel-Crafts and Related Reactions*, Vol. 2, G. A. Olah, Ed., Interscience, New York, 1964.
9. J. P. Kennedy and A. W. Langer, *Fortschr. Hochpolym.-Forsch.*, **3**, 508 (1964).
10. J. P. Kennedy, in *The Polymer Chemistry of Synthetic Elastomers (High Polymers, Vol. 23)*, Part 1, J. P. Kennedy and E. G. M. Tornquist, Eds., Interscience, New York, 1968, Chap. 5.
11. M. St. C. Flett and P. H. Plesch, *J. Chem. Soc.*, **1952**, 3355.
12. R. H. Biddulph, P. H. Plesch, and P. P. Rutherford, *J. Chem. Soc.*, **1965**, 275.
13. J. Penfold and P. H. Plesch, *Proc. Chem. Soc.*, **1961**, 311.
14. J. P. Kennedy, I. Kirshenbaum, R. M. Thomas, and D. C. Murray, *J. Polym. Sci. A*, **1**, 331 (1963).
15. R. F. Bauer, R. T. LaFlair, and K. E. Russell, *Can. J. Chem.*, **48**, 1252 (1970).

Received October 30, 1970

Revised December 4, 1970

NOTES

Radiational Grafting of Vinyl Fluoride to Some Natural and Synthetic Polymers

Due to the valuable physico-chemical properties and operations of polyvinyl fluoride (PVF), its grafting to natural and synthetic polymers with the aim of modifying these polymers has gained considerable interest. There is, however, very little data on this topic in the literature.

The current work is aimed at investigating the radiation-induced graft copolymerization of vinyl fluoride (VF) to cotton cellulose, cellulose hydrate, cellulose acetate, and also to polyvinyl chloride (PVC), polystyrene (PS), polytetrafluoroethylene (PTFE) and polymethylmethacrylate (PMMA) in both the presence and absence of various solvents.

The original cellulose was purified by Cores and Grey's method, and the synthetic polymers by extraction with methanol.

Particular attention was also paid to the purification of VF. On the basis of gas-liquid chromatographic data, the impurity content was not more than 1×10^{-4} weight-%. Grafting was γ -ray initiated in a Co^{60} source. Doses varied in an interval of 9–150 R/sec.

With the aim of establishing some general rules governing the radiation grafting of VF to the above mentioned polymers, dependence of the degree of grafting on the (polymer: monomer) ratio, the dosage and the integral value of the dosage and also on the nature of the polymer and solvent used were studied.

From the results of research done on the grafting of VF in the liquid phase to cellulose at various polymer—monomer ratios, in the absence of such substances which promote cellulose swelling (Fig. 1), it can be seen that although the degree of conversion and the original weight gained increased with increase in integral dosage, the PVF content in the grafted copolymer is insignificant and constitutes only 2–5%. It is important to note that increase in the (polymer: monomer) ratio from 0.65:1 to 1:3 leads only to a negligible increase of PVF content in the polymer. It can be concluded from this that the graft copolymer of cellulose and VF, just as in the case of grafting with other vinyl monomers, is formed to an insignificant degree in the absence of liquids promoting the swelling of cellulose.¹⁻² Similar phenomena are observed in the case of radiationally grafted VF to cellulose hydrate.

In order to obtain graft copolymers with large contents of PVF, grafting was carried out in the presence of dimethyl formamide, ethyl alcohol, and water, substances which evoke swelling in cellulose. VF dissolves well in dimethyl formamide and ethyl alcohol but badly in water. In the latter, however, cellulose swells well. Data given in Fig. 1 show that the presence of dimethyl formamide (10% in weight of cellulose) causes an increase in the degree of swelling. At a radiation dosage of 3 Mrad in the presence of dimethyl formamide, for example, PVF content in the graft copolymer is 26.6%, while in its absence this value is reduced to 4.1%. This is attributed to the good swelling capacity of cellulose in dimethyl formamide, a factor which facilitates the diffusion of the molecules of VF into cellulose.

In order to obtain homogeneous copolymers, from the point of view of their chemical content, grafting was done under homogeneous conditions in the presence of solvents which are common for both polymer and VF.

In all systems studied at the given dosage, the increase in the integral dosage has led to the amount of graft copolymer produced (Fig. 2). This quantity of graft copolymer

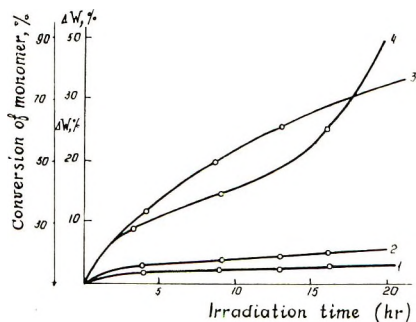


Fig. 1. Dependence of monomer conversion and of PVF weight gain on radiation time during graft copolymerization of VF with cellulose in the absence of solvent and at the polymer-monomer ratio 0.65: 1 (1), 1:3 (2), and in the presence of DMFA (3). (4) Monomer conversion. Dose rate: 70 r/sec.

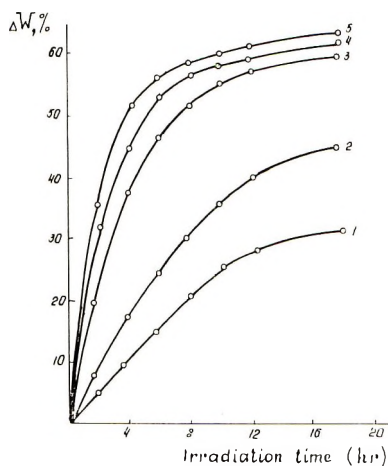


Fig. 2. Dependence of PVF weight gain on radiation time during graft copolymerization of VF with PVC in the presence of dichloroethane (1) 10 R/sec, (2) 20 R/sec, (3) 50 R/sec, (4) 100 R/sec, and (5) 150 R/sec.

produced is greatly influenced by the dosage value. At a constant integral dose, increase in the dosage leads mainly to a decrease in the amount of graft copolymer produced. This is explained by an increase in the rate of rapture of growing chains, since the concentration of free radicals is proportional to the dosage value.

The logarithmic dependence of the rate of grafting of VF to the above mentioned synthetic polymers on the dosage value is expressed by a straight line. The rate of grafting is proportional to the dosage to the 0.40–0.80 degree, dependent on the nature of the polymer and the solvent.

Calculated values of the radiational chemical output of systems studied amounted from 500 to 13600 molecules/ev., an indication that the process of graft copolymerization in these systems is of a chain nature.

Results of investigations into the influence of the nature of solvents on the process of VF to PVC grafting show that the highest reaction rate is observed when grafting is carried out in the presence of dichloroethane. For example, at a dosage of 10 R/sec and a radiation duration of 18 hours, in the presence of dichloroethane, PVF weight gain

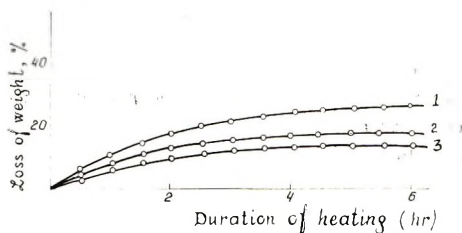


Fig. 3. Kinetics of weight loss of graft copolymers of PVC with PVF at 220°C in vacuo. (1) Original PVC; (2,3) graft copolymers containing 31.4 and 37.0% of PVF, respectively.

is 30.2%, while in the presence of dioxane this constitutes only 7.3%. Such an influence of the nature of solvents on the process of grafting is evidently due to the radiation stability of these solvents, a factor which determines the number of free radicals that are formed as a result of irradiation.

Study of the kinetics of graft copolymerization of VF to PVC, PS, and PMMA under similar conditions shows that the highest rate of grafting is observed in the PVC-VF system. At a dosage of 50 R/sec and a 10-hour irradiation duration, the rates of graft copolymerization of VF to PVC, PMMA, and PS are 5.56, 2.40, and 0.46%/hour, respectively. The relatively low VF-PS grafting rate, compared with the corresponding values for the other polymers, is effected by the high radiation stability of PS, hindering the formation of large numbers of macroradicals which initiate graft copolymerization.

PVC and PS copolymers do not dissolve in solvents in which the original polymers were soluble at room temperature, but they do swell in them well. PMMA graft copolymers containing up to 10% of PVF dissolve in acetone which is a characteristic solvent of the original PMMA. A study of the solubility of graft copolymers of viscose rayon with VF in concentrated sulphuric acid shows that the solubility of the copolymers decreases with increase in PVF content, and that starting from an 8.8% content value of PVF the copolymers lose their solubility in sulphuric acid completely. This is explained by the screening effect of PVF side groups. PVF, as we already know, is insoluble in sulphuric acid.

Investigation into kinetics of swelling of the graft copolymers of PVC and PS in cyclohexanone and toluene respectively, show that the degree of swelling of the graft copolymers is less than that of the original PVC and PS samples though more than the degree of swelling of PVF.

Grafting of VF to the polymers studied resulted in increasing the thermal stability of these polymers, evidence of which is given by experimental data on the thermal degradation of PVC graft copolymers carried out in an interval of 180–260°C in vacuum (Fig. 3). A comparative study of the thermal degradation of the original PVC and its graft copolymers at different temperatures indicates a considerable rise in the thermal stability of grafted copolymers obtained in comparison with the original PVC samples. This is caused by the presence in the grafted copolymer of PVF chains which are thermally more stable than PVC. At a temperature of 220°C, for example, the maximum weight lost in the graft copolymer containing 37.0% PVF was 14.0%, while PVC lost 26.0% of its original weight at the same temperature. Similar results were obtained for PS-VF systems.

Work done on the thermomechanical properties of PVC graft copolymers proved that the temperature of glass formation of the copolymers obtained is lower than that of the original PVC. The higher the content of PVF in the graft copolymer the lower the temperature of glass formation. The temperature of glass formation was lowered from 88° to 75°C while increasing the grafted PVF content from 0.0% to 34.2%. This lowering of the glass formation temperature is explained in the first place by the forma-

tion of branched structures in the polymer, and secondly by the plastifying action of the grafted PVF chains.

The grafting of PVF to cellulose and its derivatives greatly increases its rot resistance. An example of this is that viscose rayon loses its strength completely after 30 days in wet soil. Graft copolymers with PVF weight gains of 8.8% and 19% retain their strength after spending the same length of time in wet soil.

Conclusions

1. The graft copolymerization of VF with cellulose and its derivatives, and also with PVC, PS, PTFE, and PMMA at various radiation dosages and integral doses was studied.

2. It was shown that the grafting of PVF to the above-mentioned polymers decreases their solubilities in their respective solvents and increases their thermal stability and their resistance.

References

1. K. G. Huang, B. Immergut, E. H. Immergut, and W. H. Rapson, *J. Polym. Sci. A-1*, **1**, 257 (1963).
2. Kh. U. Usmanov, U. A. Azizov, and M. U. Sadikov, *Radiatsionaya Himiya Polimerov*, A. N. SSSR. M., 1968, p. 153.

KH. U. USMANOV
A. A. YULCHIBAEV
M. K. ASAMOV
A. VALEEV

Department of Chemistry
Tashkent State University
Vusgorodok Tashkent 95 U.S.S.R.

Received March 13, 1970
Revised November 5, 1970

Stereospecific Polymerization of Methacrylonitrile.
VII. Attempts of Molecular Weight Control

Molecular weight control in the polymerization by organometallic catalysts has been a problem of great interest to both scientific and industrial viewpoints. Stereospecific polymerization of methacrylonitrile has been developed in this laboratory;¹⁻¹¹ a useful method for controlling the molecular weight, however, has not been established so far. Some attempts to regulate molecular weight were made based on the fact that either the magnesium-carbon or magnesium-nitrogen bond in the organometallic compounds is capable of initiating stereospecific polymerization.^{2,7} The present note deals with these attempts, which were not successful. Unlike Ziegler-Natta catalyst, the organometallic catalysts effective for the stereospecific polymerization of methacrylonitrile seem to have an advantage for regulation of molecular weight control, since both metal-carbon and metal-nitrogen bond in the catalysts are able to effect the polymerization. For example, the organomagnesium compounds containing magnesium-nitrogen bond such as bis(pentamethylene imino)magnesium, ethyl(pentamethylene imino)magnesium, bis(diethylamino)magnesium, ethyl(diethylamino)magnesium, and bis(divinylene imino)magnesium have catalytic activities comparable or higher than that of diethylmagnesium.⁷

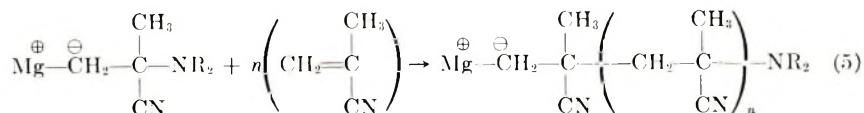
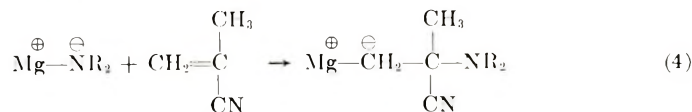
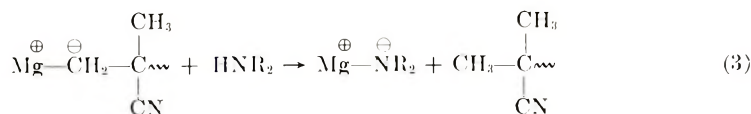
Diethylmagnesium can easily react with amines at room temperature to form magnesium amides with evolution of ethane:⁷⁻¹²



Regardless of whether a mono amide or disubstituted amide is used, the resulting magnesium amides have high catalytic activity in the stereospecific polymerization of methacrylonitrile.

The fact suggests that this reaction may be used for the regulation of molecular weight, since in the stereospecific polymerization of methacrylonitrile, the propagating chain end should be a magnesium-carbon linkage which is certainly polarized in the direction of the carbanion whether the polymerization is catalyzed with diethylmagnesium or magnesium amide derivatives, if the coordinated anionic mechanism is accepted.^{1,6,7,13}

On the basis of the above consideration, some experiments were undertaken, the polymerization of methacrylonitrile in the presence of secondary or primary amine being expected to yield polymers of lower molecular weight with a chain-breaking reaction at the magnesium-carbon linkage; the newly formed magnesium-nitrogen bond would again be able to initiate the polymerization in the same fashion as RMgNR_2 or R_2NMgNR_2 catalyst as indicated in eqs. (3)–(5).



Experimental

All the procedures, including purification of materials, preparation of initiator, and polymerization, were carried out in a nitrogen atmosphere. The preparation of catalyst and the purification of solvent and monomer are described elsewhere.^{6,7} Amines were dried over calcium hydride and fractionally distilled prior to use. Dimethyl sulfoxide was purified by distillation. Diethylmagnesium and bis(pentamethylene imino)magnesium were prepared by the same procedure described in other papers.^{1,6,7}


The polymerization equipment was the same described in another paper.^{6,7} First, the diethylmagnesium was placed in a polymerization reactor. For the preparation of bis(pentamethylene imino)magnesium, 2 mole-equivalents of piperidine were introduced to the suspension of diethyl magnesium in 20 ml of toluene and the mixture was allowed to react at its boiling temperature for a few minutes. Then a sufficient amount of toluene was added to this to make its total volume 180 ml. The polymerization was started by an introduction of methacrylonitrile mixed with a given amount of chain regulator such as amines or dimethyl sulfoxide. After being polymerized for 4 hr at 70°C, the polymer was precipitated by pouring the reaction mixture into an excess of acidic methanol, filtered, washed, dried, and weighed.



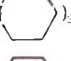
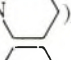
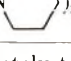
The solubility index was measured as the percentage of the acetone-insoluble fraction of total yield. The method is described in previous papers.^{6,7} Intrinsic viscosities were determined in dichloroacetic acid at 30°C in an Ubbelohde viscometer having a flow time for pure solvent of approximately 140 sec. The molecular weights were determined by Joh's relationship:⁷

$$[\eta] = 2.27 \times 10^{-4} M^{0.75}$$

Results and Discussion

Table I shows the results of polymerization of methacrylonitrile with piperidine as a chain regulator. The catalyst used was bis(pentamethylene imino)magnesium. Contrary to our expectation, the solubility index and the molecular weight of the resulting polymer were independent of the amount of piperidine used, while the conversion de-

TABLE I
Results of Polymerization of Methacrylonitrile by Mg (N )₂
with Piperidine as Chain Regulator^a

Catalyst	Toluene, ml	Piperidine, ml	Piperidine / catalyst ^a mole ratio	Conversion, %	Solubility index, %	$[\eta]$, dl/g ^b	Mol. wt. ^b $\times 10^{-5}$
Mg (N ) ₂	180	0	0	78.7	66.2	3.23	3.23
Mg (N ) ₂	180	0.8	2	76.8	70.2	3.18	3.15
Mg (N ) ₂	180	1.6	4	76.3	66.1	3.15	3.10
Mg (N ) ₂	180	4.0	10	73.7	65.1	3.27	3.28
Mg (N ) ₂	180	8.0	20	69.1	63.4	2.93	2.85

^a Catalyst: bis(pentamethylene imino)magnesium, 0.004 mole; monomer, methacrylonitrile, 20 ml; polymerization temperature, 70°C; polymerization time, 4 hr.

^b Measured for the acetone-insoluble fractions.

TABLE II
Results of Polymerization of Methacrylonitrile by MgEt_2
with Piperidine as Chain Regulator^a

Catalyst	Toluene, ml	Piperi- dine, ml	Piperi- dine/ catalyst, mole ratio	Conver- sion, %	Solu- bility index, %	$[\eta]$, dl/g ^b	Mol. wt. $\times 10^{-5}$
MgEt_2	180	0	0	51.0	68.8	2.02	1.74
MgEt_2	180	0.2	0.5	52.0	70.2	2.34	2.10
MgEt_2	180	0.4	1.0	54.1	71.7	2.18	1.92
MgEt_2	180	0.8	2.0	50.8	68.2	2.08	1.80
MgEt_2	180	1.6	4.0	47.3	69.8	2.12	1.85
MgEt_2	180	4.0	10.0	48.1	67.8	2.12	1.85
MgEt_2	180	8.0	20.0	53.0	64.7	2.37	2.15
MgEt_2	180	20.0	50.0	48.5	45.4	2.60	2.42

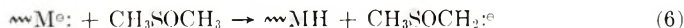
^a Catalyst, diethylmagnesium, 0.004 mole; monomer, 20 ml; polymerization temperature, 70°C; polymerization time, 4 hr.

^b Measured for the acetone-insoluble fractions.

creased very slightly with an increase of piperidine used. Table II shows the results of another experiment in which diethylmagnesium was used as catalyst. The results were quite similar to those obtained with bis(pentamethylene imino)magnesium. No tendency of decreasing molecular weight with increasing piperidine concentration was observed, which was quite contrary to our expectation.

Table III shows the results of polymerizations with diethylmagnesium with the use as chain regulators of primary amines, which are more reactive than secondary amines. Again, no tendency of decreasing molecular weight with an increase of primary amine concentration was observed. The conversion and the solubility index of the polymer decreased also with an increase of the primary amines used except in the case of *tert*-butylamine, which showed a different behavior, i.e., that the solubility index increased as the concentration of *tert*-butylamine increased.

Mulvaney et al.¹⁵ and more recently, Trossarelli et al.¹⁴ reported the anionic polymerization of acrylonitrile and other monomers by dimethylsodium, dimethylpotassium, or dimethyl lithium in dimethyl sulfoxide. The extreme low molecular weight of the polymers formed in dimethyl sulfoxide was explained in terms of chain transfer to dimethyl sulfoxide:¹⁴⁻¹⁶



If dimethyl sulfoxide is able to act as an effective chain transfer agent in the anionic polymerization, this may be utilized as a useful chain regulator.

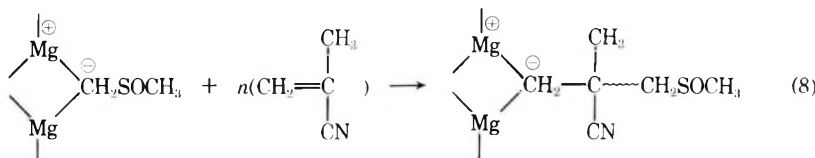
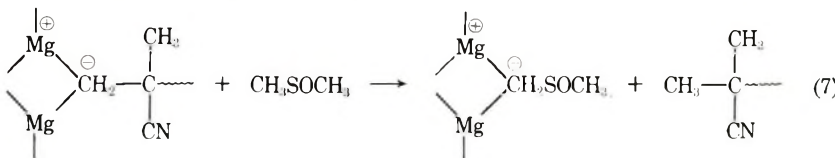


TABLE III
Results of Polymerization of Methacrylonitrile by $MgEt_2$ with
Various Primary Amines as Chain Regulator^a

Amine		Amine/ catalyst mole ratio	Conver- sion, %	Solu- bility index, %	$[\eta]$, dl/g ^b	Mol. wt. $\times 10^{-3}$
Type	Volume, ml					
None	0	0	49.1	73.9	2.16	1.90
<i>n</i> -Propylamine	0.16	0.5	40.0	72.3	1.93	1.64
<i>n</i> -Propylamine	0.33	1.0	37.5	66.3	2.02	1.73
<i>n</i> -Propylamine	0.66	2.0	33.1	62.7	2.05	1.78
<i>n</i> -Propylamine	3.28	10.0	30.4	29.8	2.45	2.22
Isopropylamine	0.16	0.5	44.5	75.4	2.40	2.18
Isopropylamine	0.33	1.0	43.6	74.8	2.44	2.23
Isopropylamine	0.66	2.0	39.9	71.3	2.47	2.26
Isopropylamine	3.28	10.0	33.1	56.8	2.87	2.75
<i>n</i> -Butylamine	0.195	0.5	39.2	69.0	2.05	1.75
<i>n</i> -Butylamine	0.39	1.0	36.8	64.3	2.17	1.90
<i>n</i> -Butylamine	0.78	2.0	32.8	52.5	2.16	1.90
<i>n</i> -Butylamine	3.9	10.0	28.2	20.8	2.09	1.82
Isobutylamine	0.21	0.5	36.8	75.3	2.43	2.21
Isobutylamine	0.42	1.0	35.8	73.3	2.62	2.45
Isobutylamine	0.84	2.0	34.9	68.3	2.97	2.80
Isobutylamine	4.2	10.0	28.6	42.6	3.30	3.35
<i>tert</i> -Butylamine	0.21	0.5	45.5	75.0	2.34	2.09
<i>tert</i> -Butylamine	0.42	1.0	47.0	74.6	2.30	2.06
<i>tert</i> -Butylamine	0.84	2.0	45.2	77.1	2.34	2.09
<i>tert</i> -Butylamine	4.18	10.0	44.4	82.3	2.65	2.48
Cyclohexylamine	0.46	1.0	35.0	73.2	2.56	2.37
Cyclohexylamine	0.92	2.0	41.9	73.1	2.86	2.75
Cyclohexylamine	4.6	10.0	36.5	60.5	3.44	3.50
Benzylamine	0.22	0.5	39.4	67.3	1.90	1.60
Benzylamine	0.44	1.0	40.2	65.8	2.11	1.85
Benzylamine	0.88	2.0	32.5	56.6	2.28	2.04
Benzylamine	4.40	10.0	22.9	38.8	2.79	2.66

^a Polymerization conditions: catalyst, $MgEt_2$, 0.004 mole; toluene, 180 ml; monomer, 20 ml; polymerization temperature, 70°C; polymerization time, 4 hr.

^b Measured for the acetone-insoluble fractions.

Table IV shows the results of polymerization of methacrylonitrile by bis(pentamethylene imino)magnesium in the mixed solvent comprising toluene and dimethyl sulfoxide at various ratios. Since diethylmagnesium reacts violently with dimethyl sulfoxide and loses its catalytic activity, it cannot be used for this experiment. Advantageously, magnesium amides with no Mg—C bond such as bis(pentamethylene imino)magnesium hardly react with dimethyl sulfoxide; therefore, they can be used as catalysts in the presence of dimethyl sulfoxide. The results in Table IV indicate that the molecular weight of the polymer obtained in the presence of dimethyl sulfoxide certainly decreased compared with that obtained in toluene. However, it should be noted that the solubility index markedly decreased as the concentration of dimethyl sulfoxide increased. This suggests that dimethyl sulfoxide destroys the coordinating type catalyst, and the catalyst changed to a different type which may act as rather conventional anionic catalyst.

The above results clearly indicate that the consideration of molecular weight control by the action of amines or dimethyl sulfoxide as a chain regulator is erroneous. This is

TABLE IV
Results of Polymerization of Methacrylonitrile in the Presence of Dimethyl Sulfoxide^a

Solvent, ml		Conversion, %	Solubility		Mol. wt.
Toluene	DMSO		index, %	$[\eta]$, dl/g ^b	
90	90	49.4	25.2	0.56	3.2×10^4
135	45	51.8	19.7	1.68	1.3×10^5
150	30	78.7	14.7	1.92	1.6×10^5
170	10	86.2	14.7	1.71	1.4×10^5
180	0	75.0	67.5	3.72	3.9×10^5

^a Catalyst: bis(pentamethylene imino)magnesium, 0.004 mole; monomer, methacrylonitrile, 20 ml; polymerization temperature, 70°C; polymerization time, 4 hr.

^b Measured for the acetone-insoluble fractions.

quite unanticipated and results from the fact that diethylmagnesium reacts with amines very violently at room temperature with evolution of ethane¹² to form magnesium amides, the substitution reaction being stoichiometric.

In view of the fact that most of the effective catalysts in the stereospecific polymerization of methacrylonitrile are composed of organobimetallic compounds like ate-complex or polymeric organometallic compounds as reported in other papers,^{12,18} the propagating chain end would probably be connected with two catalytic metals through two electron-deficient bonds in the same situation of diethylmagnesium.¹⁷

The extremely low reactivity to amines during the polymerization indicates that the situation of the catalyst must be essentially changed after the polymerization takes place. It is very difficult to explain the results that the monomer can react to polymerize and that amines or dimethyl sulfoxide are no longer able to react after polymerization occurs. It is speculated that the coordination of the nitrile in the ultimate unit of the growing chain to one of the metals in the catalyst must be related to this effect. The coordination seems reasonable, since it is geometrically possible to form a stable five-membered ring. The coordination would probably influence the bond energy of the electron-deficient bonds between the terminal methylene and two metals in the catalyst so that amines may be unable to react in substitution reaction. However, incoming monomers are able to release the coordination of nitrile of the growing chain by competitive coordination through the nitrile and the double bond; accordingly, they may be possible to polymerize.

This behavior may be closely related to the actual mechanism of the polymerization. The increased molecular weight with increasing amine concentration may be a result of the solvating effect of amines present in the reaction medium.

The authors wish gratefully to acknowledge the encouragement of Dr. T. Isoshima throughout the work and the diligent assistance of Mr. N. Kurashige in the performance of the technical work.

References

1. Y. Joh, T. Yoshihara, Y. Kotake, F. Ide, and K. Nakatsuka, *J. Polym. Sci. B*, **3**, 933 (1965).
2. Y. Joh, T. Yoshihara, Y. Kotake, F. Ide, and K. Nakatsuka, *J. Polym. Sci. B*, **4**, 673 (1966).
3. Y. Kotake, T. Yoshihara, H. Sato, N. Yamada, and Y. Joh, *J. Polym. Sci. B*, **5**, 163 (1967).
4. T. Yoshihara, Y. Kotake, and Y. Joh, *J. Polym. Sci. B*, **5**, 459 (1967).
5. Y. Joh, Y. Kotake, T. Yoshihara, F. Ide, and K. Nakatsuka, *J. Polym. Sci. A-1*, **5**, 593 (1967).

6. Y. Joh, Y. Kotake, T. Yoshihara, F. Ide, and K. Nakatsuka, *J. Polym. Sci. A-1*, **5**, 605 (1967).
7. Y. Joh, T. Yoshihara, Y. Kotake, Y. Imai, and S. Kurihara, *J. Polym. Sci. A-1*, **5**, 2503 (1967).
8. Y. Joh, T. Yoshihara, S. Kurihara, I. Tsukuma, and Y. Imai, *Makromol. Chem.*, **119**, 239 (1968).
9. Y. Joh, S. Kurihara, T. Sakurai, Y. Imai, T. Yoshihara, and T. Tomita, *J. Polym. Sci. A-1*, **8**, 377 (1970).
10. Y. Joh, T. Yoshihara, S. Kurihara, T. Sakurai, and T. Tomita, *J. Polym. Sci. A-1*, **8**, 1901 (1970).
11. Y. Joh, S. Kurihara, T. Sakurai, and T. Tomita, *J. Polym. Sci. A-1*, **8**, 2383 (1970).
12. Y. Joh and Y. Kotake, *Macromolecules*, **3**, 337 (1970).
13. G. Natta and G. Dall'Asta, *Chim. Ind. (Milan)*, **46**, 1429 (1964).
14. L. Trossarelli, M. Guaita, and A. Priola, *J. Polym. Sci. B*, **5**, 535 (1967).
15. J. E. Mulvaney and R. Markham, *J. Polym. Sci. B*, **4**, 343 (1966).
16. C. E. H. Bawn, A. Ledwith, and N. McFarlane, *Polymer*, **10**, 653 (1969).
17. E. Weiss, *J. Organometal. Chem.*, **4**, 101 (1965).
18. G. E. Coates and D. Ridley, *J. Chem. Soc. A*, **1967**, 56.

YASUSHI JOH*
SEIKI KURIHARA
TATSUNORI TOMITA

Research Laboratories
Mitsubishi Rayon Company, Ltd.
Otake City, Hiroshima, 739-06, Japan

Received October 6, 1970
Revised November 16, 1970

* Present address: Department of Chemistry, University of Michigan, Ann Arbor, Michigan 48104, U.S.A.

Contents (continued)

H. L. LENTZNER and H. E. DE LA MARE: Polymerizations with Hydrido and Alkyl Transition Metal Complexes in Aqueous Media	1401
Y. HAMA, K. HOSONO, Y. FURUI, and K. SHINOHARA: ESR Study of Free Radicals Produced in Polyethylene Irradiated by Ultraviolet Light.....	1411
P. D. NIKOLINSKI and V. V. MIRTSHEVA: Graft and Modified Polymers from Rubber Network. I. Method of Obtaining Graft and Modified Polymers from Sulfur Vulcanizates with Dehydrogenated Raney Nickel and Raney Cobalt..	1421
S. P. ROWLAND, E. J. ROBERTS, and J. L. BOSE: Availability and State of Order of Hydroxyl Groups on the Surfaces of Microstructural Units of Crystalline Cotton Cellulose.....	1431
B. LIONEL FUNT and J. RYBICKY: Electroinitiated Copolymerization Reactions with Donor-Acceptor Complexes. III. Copolymerization of Butadiene and Acrylonitrile with $ZnCl_2$ as Catalyst.	1441
R. F. BAUER and K. E. RUSSELL: Cationic Polymerization of Isobutene Initiated by Stannic Chloride and Phenols: Polymer Endgroup Studies.....	1451

NOTES

KH. U. USMANOV, A. A. YULCHIBAEV, M. K. ASAMOV, and A. VALIEV: Radiational Grafting of Vinyl Fluoride to Some Natural and Synthetic Polymers..	1459
Y. JOH, S. KURIHARA, and T. TOMITA: Stereospecific Polymerization of Methacrylonitrile. VII. Attempts of Molecular Weight Control.....	1463

The *Journal of Polymer Science* publishes results of fundamental research in all areas of high polymer chemistry and physics. The *Journal* is selective in accepting contributions on the basis of merit and originality. It is not intended as a repository for unevaluated data. Preference is given to contributions that offer new or more comprehensive concepts, interpretations, experimental approaches, and results. Part A-1 *Polymer Chemistry* is devoted to studies in general polymer chemistry and physical organic chemistry. Contributions in physics and physical chemistry appear in Part A-2 *Polymer Physics*. Contributions may be submitted as full-length papers or as "Notes." Notes are ordinarily to be considered as complete publications of limited scope.

Three copies of every manuscript are required. They may be submitted directly to the editor: For Part A-1, to C. G. Overberger, Department of Chemistry, University of Michigan, Ann Arbor, Michigan 48104; and for Part A-2, to T. G. Fox, Mellon Institute, Pittsburgh, Pennsylvania 15213. Three copies of a short but comprehensive synopsis are required with every paper; no synopsis is needed for notes. Books for review may also be sent to the appropriate editor. Alternatively, manuscripts may be submitted through the Editorial Office, c/o H. Mark, Polytechnic Institute of Brooklyn, 333 Jay Street, Brooklyn, New York 11201. All other correspondence is to be addressed to Periodicals Division, Interscience Publishers, a Division of John Wiley & Sons, Inc., 605 Third Avenue, New York, New York 10016.

Detailed instructions in preparation of manuscripts are given frequently in Parts A-1 and A-2 and may also be obtained from the publisher.

Coming soon from Wiley-Interscience—

The Second Edition of the Most Comprehensive Book in the Field of Polymer Science

TEXTBOOK OF POLYMER SCIENCE

Second Edition

By FRED W. BILLMEYER, JR., *Rensselaer Polytechnic Institute*

In the last 50 years, the field of polymer science has developed into a discipline essential to most aspects of our modern technology. Because this development has been so rapid, it has been difficult for educational systems and texts to keep pace. *Textbook of Polymer Science* was originally published in 1962 to help fill this gap, and this new Second Edition continues to supply up-to-date information on the field.

To up-date the original treatment of the theory and practice of all major phases of polymer science, engineering, and technology, the author has made extensive revisions and additions throughout the entire work.

Part I:

An introduction to concepts and characteristics of macromolecules, Part I now includes material on solubility parameters, free-volume theories of polymer solution thermodynamics, gel-permeation chromatography, vapor-phase osometry, and scanning electron microscopy.

Part II:

The advances gained from new data on the crystalline nature of polymers are now treated in a thorough discussion of the structure and properties of bulk polymers.

Part III:

The format and content of Part III, concerned with polymerization kinetics, have been revised to include recent advances and new references, as well as further data and explanations of recently discovered processes.

Part IV:

The material on commercially important polymers has been rearranged, and now includes information on aromatic heterochain, heterocyclic, ladder, and inorganic polymers.

Part V:

The comprehensive discussion of polymer processing in Part V now includes many new references for plastics, fiber, and elastomer technology.

1971 In Press

wiley 

WILEY-INTERSCIENCE

a division of JOHN WILEY & SONS, Inc.

605 Third Avenue, New York, New York 10016

In Canada: 22 Worcester Road, Rexdale, Ontario